1192

TRANSPORTATION RESEARCH RECORD

Soil Engineering

TRANSPORTATION RESEARCH BOARD
NATIONAL RESEARCH COUNCIL
WASHINGTON, D.C. 1988

Transportation Research Record 1192
Price: $15.50

modes
1 highway transportation
2 public transit
3 rail transportation
4 air transportation

subject areas
17 energy and environment
22 hydrology and hydraulics
33 construction
61 soil exploration and classification
63 soil and rock mechanics

Transportation Research Board publications are available by ordering directly from TRB. They may also be obtained on a regular basis through organizational or individual affiliation with TRB; affiliates or library subscribers are eligible for substantial discounts. For further information, write to the Transportation Research Board, National Research Council, 2101 Constitution Avenue, N.W., Washington, D.C. 20418.

Printed in the United States of America

Library of Congress Cataloging-in-Publication Data
National Research Council. Transportation Research Board.
Soil engineering.
p. cm. — (Transportation research record, ISSN 0361-1981 ; 1192)
ISBN 0-309-04770-6
1. Soil mechanics. 2. Soils—Testing. I. National Research Council (U.S.). Transportation Research Board. II. Series.
TE7.H5 no. 1192
[TA710]
380.5 s—dc20
[624.1'5136] 89-38438
CIP

Sponsorship of Transportation Research Record 1192

GROUP 2—DESIGN AND CONSTRUCTION OF TRANSPORTATION FACILITIES
Chairman: David S. Gedney, Harland Bartholomew & Associates

Soil Mechanics Section
Chairman: Raymond A. Forsyth, California Department of Transportation

Committee on Transportation Earthworks
Chairman: Robert D. Holtz, Purdue University
Mehmet C. Anday, Thomas A. Bellatty, William A. Cutter, Joseph D'Angelo, Jerome A. Dimaggio, Raymond L. Gemme, Wilbur M. Haas, William P. Hofmann, J. M. Hoover, Ilan Juran, James E. Kelly, Philip C. Lambe, Richard E. Landau, Robert M. Leary, Larry Lockett, Richard P. Long, C. William Lovell, Kenneth M. Miller, Lyle K. Moulton, Walter C. Waidelich, David E. Weatherby, William G. Weber, Gary C. Whited

Committee on Subsurface Drainage
Chairman: Gary L. Hoffman, Pennsylvania Department of Transportation
Robin Bresley, George R. Cochran, Barry J. Dempsey, Gregory A. Dolson, Ervin L. Dukatz, Jr., Wilbur M. Haas, Donald J. Janssen, Larry Lockett, Donald C. Long, Robert H. Manz, Vernon J. Marks, Charles D. Mills, Lyle K. Moulton, Edwin C. Novak, Jr., Willard G. Puffer, Georges Raimbault, Hallas H. Ridgeway, Emile A. Samara, L. David Suits, William D. Trolinger, Walter C. Waidelich, David C. Wyant, Thomas F. Zimmie

Geology and Properties of Earth Materials Section
Chairman: C. William Lovell, Purdue University

Committee on Soil and Rock Properties
Chairman: James J. Schnabel, Schnabel Engineering Associates
Robert C. Bachus, S. S. Bandyopadhyay, Robert K. Barrett, Roy H. Borden, Timothy Bowen, Carl D. Ealy, William H. Highter, Robert D. Holtz, Richard H. Howe, Robert B. Johnson, Ernest Jonas, C. William Lovell, Priscilla P. Nelson, Gerald P. Raymond, Surendra K. Saxena , J. Allan Tice, Mehmet T. Tumay, John L. Walkinshaw, Gary C. Whited

Committee on Physicochemical Phenomena in Soils
Chairman: Thomas F. Zimmie, Rensselaer Polytechnic Institute
John J. Bowders, John B. Heagler, Jr., Richard H. Howe, Joakim G. Laguros, C. William Lovell, Milton W. Meyer, Thomas M. Petry, Marion R. Scalf, Mumtaz A. Usmen, Anwar E. Z. Wissa

Committee on Engineering Geology
Chairman: A. Keith Turner, Colorado School of Mines
Robert K. Barrett, William D. Bingham, Robert C. Deen, Jerome V. Degraff, C. William Lovell, Stephen F. Obermeier, Rodney W. Prellwitz, Berke L. Thompson, J. Allan Tice, Duncan C. Wyllie

G. P. Jayaprakash, Transportation Research Board staff

Sponsorship is indicated by a footnote at the end of each paper. The organizational units, officers, and members are as of December 31, 1987.

NOTICE: The Transportation Research Board does not endorse products or manufacturers. Trade and manufacturers' names appear in this Record because they are considered essential to its object.

Transportation Research Record 1192

Contents

Simplification of Subgrade Resilient Modulus Testing

ROBERT P. ELLIOTT AND SAM I. THORNTON

The standard test method (AASHTO T274) for the resilient modulus of cohesive soils can be simplified without affecting the reliability of flexible pavement design by the AASHTO Guide. The traffic life prediction accuracy (standard deviation) of the AASHTO design equation is equivalent to a resilient modulus testing accuracy of about 30 percent. The overall prediction accuracy is not affected substantially as long as the testing error (standard deviation) is 15 percent or less. Three cohesive soils were tested to examine the effects of confining pressure, deviator stress, number of stress cycles, and compaction method. For routine design the standard method of test can be simplified by (1) reducing the number of confining pressures from three to one (3 psi is suggested); (2) reducing the number of deviator stress levels from five to one (8 psi is suggested); and (3) reducing the number of stress cycles from 200 to 50. With these test simplification measures, the time required for testing (excluding sample preparation and test setup) is reduced from 100 minutes per specimen to less than 2 minutes.

The 1986 AASHTO Guide for the Design of Pavement Structures is affecting the routine testing of soils for pavement design to a great extent. Under the previous Guide, soils were evaluated on an arbitrary "soil support" scale, which was not based on any particular method of test or evaluation. As a result, there was no universally accepted test method or relationship between test results and the soil support. Each highway agency adopted its own test and relationship.

The 1986 Guide uses resilient modulus as the method of test and evaluation for pavement subgrade support. Resilient modulus is a fundamental property that should be included in any rational pavement design procedure. The incorporation of resilient modulus by AASHTO represents a significant advance in pavement design practice. Nevertheless, adoption of resilient modulus created some legitimate concerns: most highway engineers were not familiar with the resilient modulus, nor did most state highway agencies have experience with the test. In addition, few agencies had the proper test equipment for this complex and time-consuming test.

The Arkansas State Highway and Transportation Department initiated a study at the University of Arkansas (*1*) to determine the resilient properties of typical Arkansas soils and to develop specific recommendations for routine resilient modulus testing. According to the study, the method of test for cohesive soils can be greatly simplified.

Department of Civil Engineering, University of Arkansas, Fayetteville, Ark. 72701.

STANDARD TEST REQUIREMENTS

The standard method for resilient modulus testing is AASHTO test method T274 (*2*). The objective of the test is to simulate the in-service behavior of the soil. The test specifications for compaction are intended to produce a test specimen that closely resembles the soil's in-service structure and moisture condition. Three methods of compaction are described: gyratory, kneading, and static. The method to be used depends upon the moisture conditions expected during construction and later in service.

The method of compaction is determined by the degree of saturation (Table 2). If field compaction will result in less than 80 percent and the moisture content is not expected to increase after construction, any method may be used. However, if the degree of saturation will later increase to more than 80 percent, the specimens are to be compacted at the in-service moisture content using the static method. Soils that will be field compacted to greater than 80 percent saturation are to be prepared by the kneading method.

The resilient modulus testing requirements were developed recognizing the stress-dependent nature of soil. Testing is done in a triaxial chamber so that lateral confining pressures can be applied. The standard test for cohesive soils requires three levels of confining pressure: 0, 3, and 6 psi. To simulate traffic loading, a vertical load (called the deviator stress) is applied for 0.1 second at a repeated interval of 1 to 3 seconds. Five levels of deviator stress are required: 1, 2, 4, 8, and 10 psi. Each deviator stress is repeated for 200 cycles at each of the three confining pressures. The resilient modulus is determined for each combination of deviator stress and confining pressure by the equation:

$$M_R = \theta_d/\varepsilon_r$$

in which

M_R = the resilient modulus
θ_d = the deviator stress
ε_r = the resilient (or recoverable) strain.

TABLE 1 ROUTINE SOIL PROPERTIES

	Jackport	Gallion	Sawyer	Clarksville	Leadvale
AASHTO T99					
Maximum Density (pcf)	94	94	96	109	99
Opt. Moisture (%)	20	25	23	15	22
Liquid Limit	55	68	48	24	38
Plast. Index	34	43	28	6	15
Gradation (% Passing)					
#4				100	
#10	100	100	100	93	100
#40	97	95	94	85	90
#80	92	88	88	84	89
#200	89	85	81	82	82
0.02 mm	70	73	66	49	61
0.002 mm	41	55	41	16	37
0.001 mm	38	54	36	13	36

With three levels of confining pressure and five levels of deviator stress, 15 M_R values are found for each test. Using 2 seconds between stress cycles, the testing time is 100 minutes, exclusive of sample preparation and conditioning.

Design Resilient Modulus

In addition to the 15 M_R values from a single test, the AASHTO Guide design procedure calls for testing at moisture contents that simulate the primary moisture seasons. Assuming four seasons, as many as 60 M_R values are determined. Nevertheless, a single M_R value must be selected as the effective roadbed resilient modulus to be used in the design procedure. The engineer is faced with (1) estimating seasonal moisture conditions, (2) testing at each of these moisture contents, (3) selecting a single M_R value from among the 15 test values for each moisture season, and (4) selecting the effective roadbed resilient modulus from an analysis of the seasonal values.

The AASHTO Guide provides a procedure for selecting the design M_R once the seasonal values are identified. The procedure is based on a relative damage concept. Relative damage factors are determined for the seasonal M_R's. From these, the annual average damage factor is calculated. The M_R value consistent with the average damage factor is identified as the effective roadbed resilient modulus that is used for design.

As an example of the AASHTO selection procedure, M_R tests were used to establish a relationship with subgrade moisture content (Figure 1). This relationship was then used with estimated monthly moisture contents to select an M_R for each month. The monthly M_R values were then used with the scale along the right side of Figure 1 to determine monthly relative damage factors. This scale was then used with the average of the monthly relative damage factors to determine the effective roadbed soil resilient modulus.

Required Testing Accuracy and Precision

From an analytical and conceptual point of view the testing and selection process is appealing. However for routine design, the "measure-with-a-micrometer, mark-with-a-grease-pencil, cut-with-an-ax" syndrome seems to be at work. The ability to predict traffic, moisture conditions, and pavement performance is currently much less precise than the sophistication required by AASHTO T274 and the M_R selection process would imply.

The sophistication required for routine testing depends on the accuracy and precision needed from the test. Three factors must be considered in determining the accuracy and precision required for subgrade resilient modulus testing: these are (1) the sensitivity of the design to the test parameter, (2) the capability to predict the in-service variables that affect the test result (i.e., moisture content and freeze-thaw), and (3) the accuracy of the prediction models used for design.

Design Sensitivity

The sensitivity of the design thickness to subgrade resilient modulus is illustrated in Figure 2. In practical terms, Figure 2 shows that a 30 percent change in the resilient modulus will result in a change in total asphalt thickness of 1 to 1.5 inches.

In-Service Variables

Figures 3 and 4 illustrate the moisture and freeze-thaw sensitivity of an Arkansas soil. Moisture and freeze-thaw significantly affect the subgrade support capability and should be considered. However, reliable procedures for predicting moisture and freeze-thaw cycles are not available. Until better methods are available for predicting seasonal moisture variation, testing at several moisture contents does not appear to be justified.

Month	Roadbed Soil Modulus, M_R (psi)	Relative Damage, u_f
Jan.	30,000	.005
Feb.	5,500	.25
Mar.	9,500	.070
Apr.	8,900	.081
May	8,600	.088
June	11,000	.050
July	12,700	.038
Aug.	13,000	.034
Sept.	13,100	.033
Oct.	12,800	.035
Nov.	12,700	.036
Dec.	12,300	.038
Summation: Σu_f =		.758

Average: $\bar{u}_f = \frac{\Sigma u_f}{n} = .063$

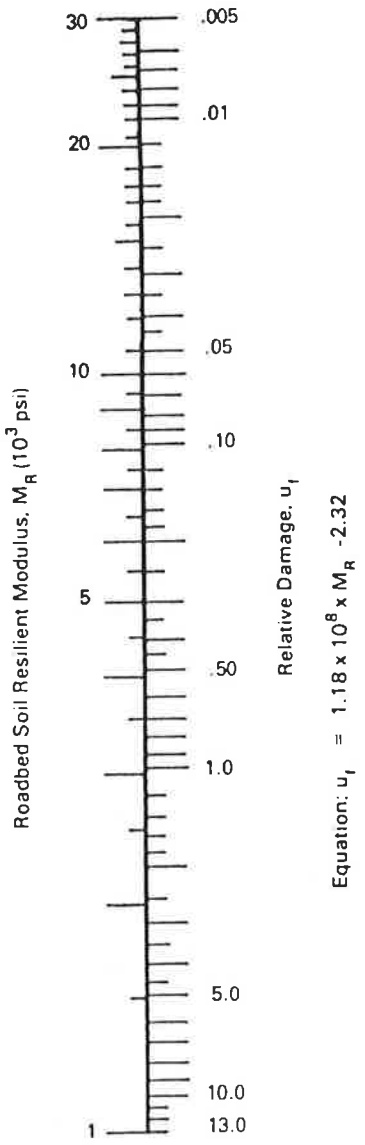

Effective Roadbed Soil Resilient Modulus, M_R (psi) = 9,900 (corresponds to $\bar{u}_f$)

FIGURE 1 Example determination of the effective roadbed resilient modulus.

For Arkansas, a moisture content of 120 percent of optimum has been identified as a reasonable estimate of in-service moisture content; and a 50 percent reduction in resilient modulus for one month in the spring is considered appropriate for the northern band of counties that experience some subgrade frost penetration (*3*).

Prediction Models

The prediction models used for design include traffic projection and the pavement performance equation. The inability to accurately predict future traffic is well recognized. Less well recognized is the inherent inaccuracy in the pavement performance equation.

The pavement performance equation is based on the AASHO Road Test (*4*). The basic equation, developed to predict the traffic life of the Road Test pavements, has a standard error of estimate of 0.31 on the logarithm of axle applications (log W). By the modified equation used in the AASHTO Guide, the 0.31 error in log W is equivalent to an error of about 30 percent in the subgrade resilient modulus. No amount of sophisticated testing can reduce the error or improve the inherent prediction accuracy.

The significance of accurate testing can be examined with regard to its effect on the overall standard deviation

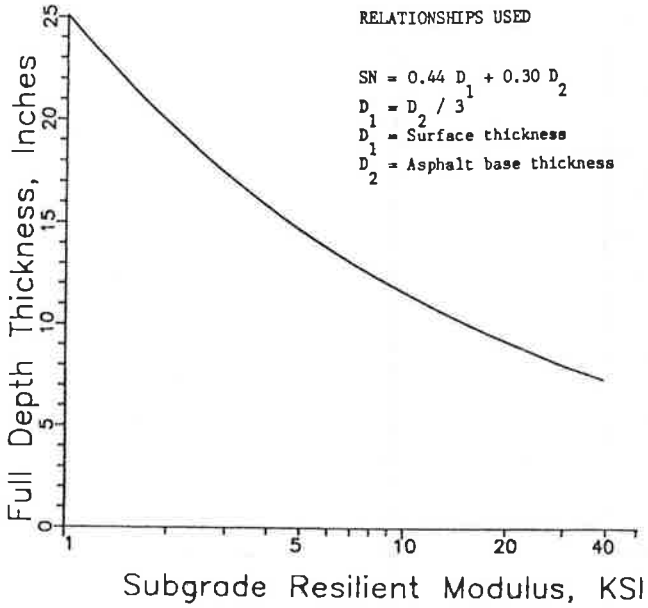

FIGURE 2 Effect of resilient modulus on design thickness.

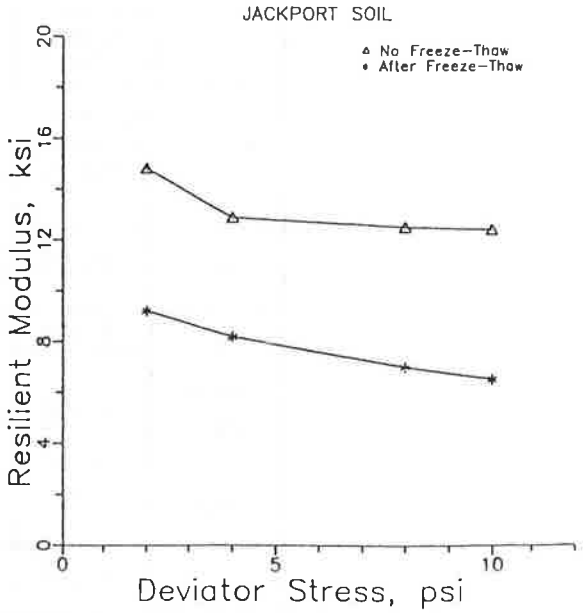

FIGURE 4 Effect of freeze-thaw on resilient modulus.

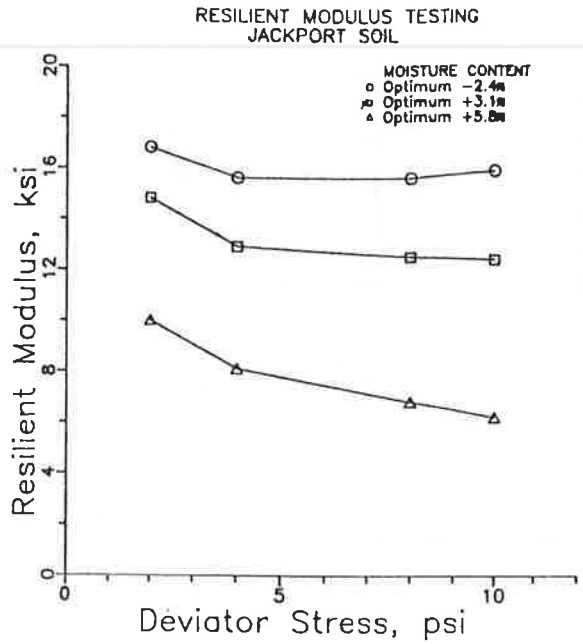

FIGURE 3 Effect of moisture content on resilient modulus.

of predicted pavement life (S_o). S_o, which is used with the design reliability concept of the AASHTO Guide, possesses two major components: (1) pavement performance prediction error, and (2) traffic usage prediction error. Any error in subgrade testing is reflected in S_o as an increase in the pavement performance prediction error.

The effect of testing error on S_R was examined for two levels of traffic prediction accuracy using the AASHT0 Guide design performance equation. With no traffic prediction error and no testing error, S_o is 0.31 (the standard error from the AASHO Road Test). With a traffic prediction error of 75 percent (standard deviation of log W = 0.24) and no testing error, S_o becomes 0.39. When testing error is added, S_o increases as shown in Figure 5. However, the testing error is seen to have little effect as long as the error remains below about 15 percent. (The change in S_o represents less than 0.25 inches in asphalt thickness.)

Test Simplification

To identify ways that the standard test requirements might be simplified, three typical Arkansas soils (Table 1) were tested extensively in accordance with AASHTO T274. The test data were analyzed to determine the relative effect of the various test requirements, including (1) the three confining pressures, (2) the five deviator stresses, (3) the 200 stress cycles, and (4) the compaction methods.

Confining Pressure

As a matter of routine there appears to be no reason for testing at more than one confining pressure. Ideally, that pressure would represent the confining pressure expected in the completed subgrade. Analysis using the ILLI-PAVE finite element model (*5*) indicates that the subgrade confining pressure is typically 2 to 3 psi.

Increasing confining pressure was found to increase the resilient modulus of the three Arkansas soils. Typical trends are shown in Figure 6. The increase from 0 to 3 psi was found to be greater than the increase from 3 to 6 psi. With increasing moisture content, however, the effect of

confining pressure was found to decrease. At 120 percent of optimum, which approximates the normally expected in-service moisture content, the difference between 0 and 3 psi ranged from none to about 15 percent.

Testing can normally be conducted at a single confining pressure. Because the effect of confining pressure is low at the expected in-service moisture content, unconfined testing (0 psi) might be considered. The unconfined test would be both somewhat conservative and easier to perform. However, testing at 3 psi is more consistent with the confining pressure expected in the field and more in keeping with the design reliability concept used in the AASHTO Guide. The reliability approach requires that average material property values be used in design. Any conservatism is to be incorporated into the reliability of the traffic life prediction (i.e., the probability of not failing early). The 3 psi confining pressure also provides the lateral support sometimes needed when testing low PI soils.

Deviator Stress

Five levels of deviator stress are used in AASHTO T274 to determine the stress-dependent nature of the soil. While stress dependency is a significant material property, it is not included in the current design methodology. Consequently, testing at five levels of deviator stress does not provide data useful for routine purposes.

In an extensive study of Illinois soils, Thompson and Robnett (*6*) found that the resilient modulus stress dependency could be adequately characterized as two intersecting straight line relationships. The slopes of these relationships did not vary significantly, and the deviator stress at the point of intersection was always around 6 psi. Therefore, the resilient behavior (at least of Illinois soils) can be reasonably determined by testing at a deviator stress of about 6 psi.

Another approach would be to test at the deviator stress expected in the subgrade. Deviator stress will vary with vehicle loading, pavement design, and the resilient modulus itself. The expected range of deviator stress for different pavement designs (structural numbers) under the standard 18 kip single-axle load is given in Figure 7. The deviator stress is generally in the range of 2 to 8 psi.

For routine testing, Figure 7 can be used to select a testing deviator stress based on a preliminary estimate of the design structural number and the expected resilient modulus. If the test produces a resilient modulus much different from that expected, the test might be continued at a second deviator stress consistent with the first test result.

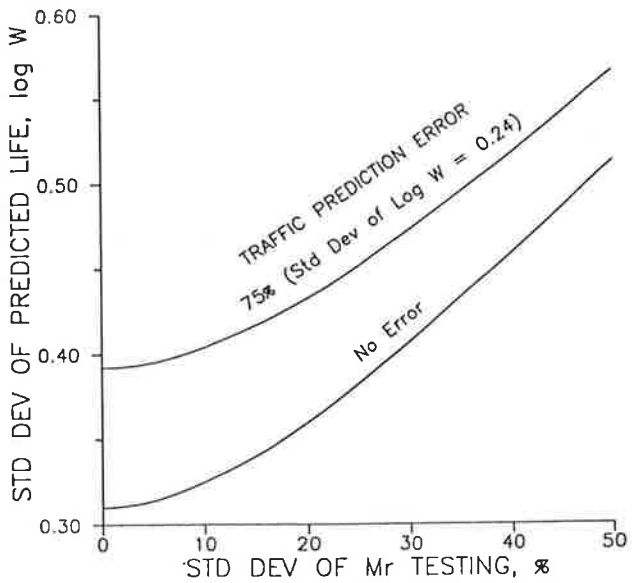

FIGURE 5 Effect of testing accuracy on the standard deviation of predicted pavement life.

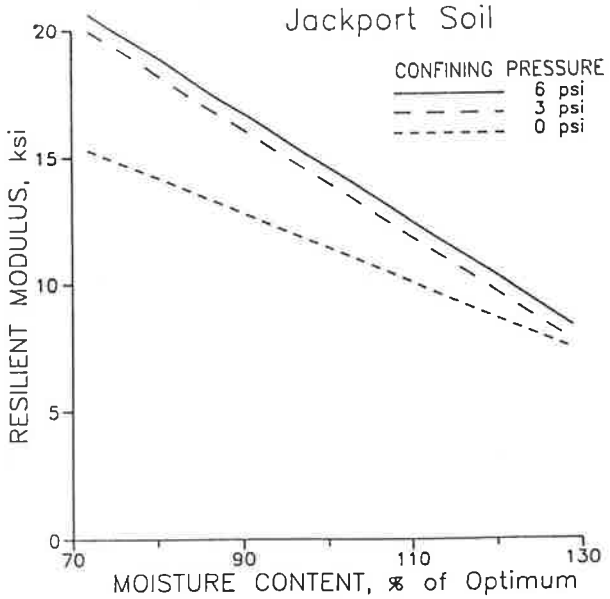

FIGURE 6 Typical influence of confining pressure on M_R.

TABLE 2 COMPACTION METHOD REQUIREMENTS BY AASHTO T274

Degree of Saturation (%)		
As Compacted	In-Service	Compaction Method[a]
< 80	< 80	Gyratory, kneading, or static
< 80	> 80	Static
> 80	> 80	Kneading

[a] At in-service moisture content.

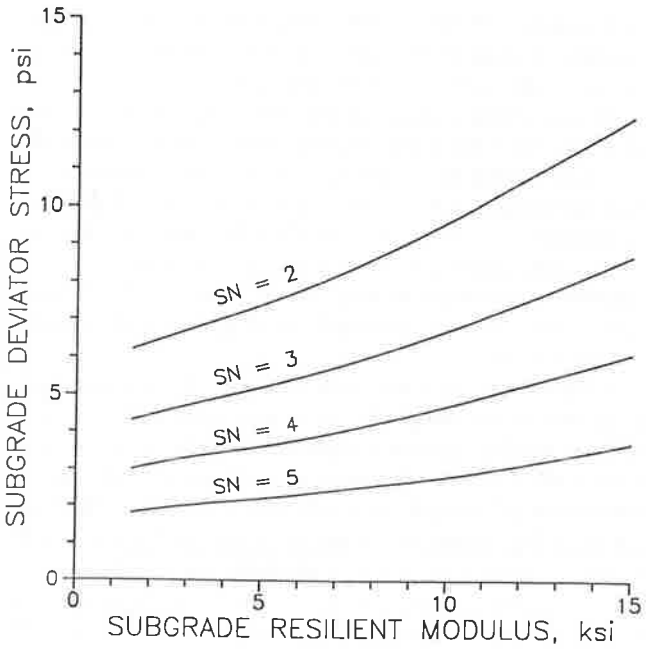

FIGURE 7 Subgrade deviator stress versus M_R for various design structural numbers.

Alternatively, all testing might be conducted at a single, standard deviator stress. Testing at 8 psi would be at the high end of the range of expected deviator stress. Since the resilient modulus decreases with increasing deviator stress, an 8 psi test would produce a resilient modulus that would be slightly conservative for most pavements.

Number of Stress Cycles

To determine the number of stress cycles needed before reading the resilient deformation, deformation readings were taken at 50, 100, and 200 cycles. The 50- and 100-cycle readings were subsequently compared to the 200-cycle readings to determine whether there were any significant differences.

The number of variations between the 50- or 100-cycle and the 200-cycle reading increased as the deviator stress increased. The 50-cycle reading varied from the 200-cycle reading 17 of 324 times (5 percent of the time) at 8 psi and 53 of 324 times (16 percent of the time) at 10 psi. However, the maximum variation amounted to less than 6 percent of the 200-cycle deformation. Therefore, for routine testing the number of stress cycles can be reduced from 200 to 50 with no significant effect on the test results.

Compaction Methods

Field data were obtained from several Arkansas projects to determine the magnitude and variability of density and moisture content during construction. The data were used to estimate the variability in degree of saturation following compaction. Seventy-five to 80 percent of the soils were compacted at moisture contents that resulted in greater than 80 percent saturation after compaction. According to AASHTO T274 (Table 2), kneading compaction should be used for specimen preparation.

To determine the significance of type of compaction, specimens were prepared using both kneading and static methods. Of the three soils tested initially, two (Gallion and Jackport) were found to be significantly affected by the compaction method (Figures 8 and 9). To further investigate the significance of the method of compaction, two additional soils (Leadvale and Clarksville, [Table 1]) were prepared using both compaction methods and tested. Neither of these was significantly affected by the type of

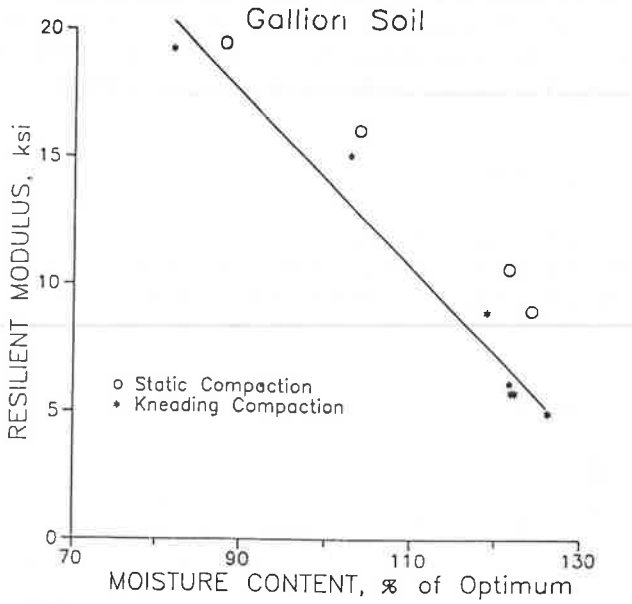

FIGURE 8 Effect of compaction method on M_R of Gallion soil.

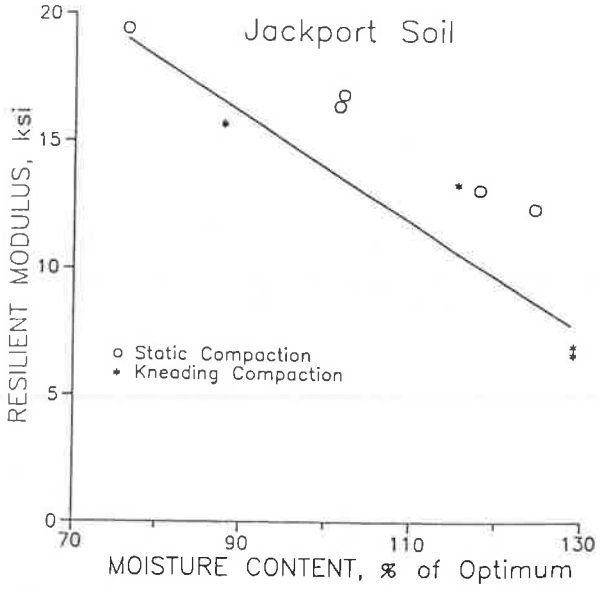

FIGURE 9 Effect of compaction method on M_R of Jackport soil.

compaction. The results for Clarksville soil is shown in Figure 10. Additional soils are being tested to examine the significance of the method of compaction.

CONCLUSIONS

The sophistication required by AASHTO T274 is not necessary for routine soil testing. Testing sophistication should be a function of the required test accuracy and the consequences of inaccurate test results. The prediction error associated with the AASHTO Guide is equivalent to a resilient modulus testing error of about 30 percent. Moreover, there is similar (but currently unsubstantiated) uncertainty associated with the estimation of moisture conditions, freeze-thaw cycling, and future traffic.

A testing error of less than about 15 percent is not significant based on analysis of the overall standard deviation of pavement life prediction (S_o).

Of five soils tested, only two were significantly affected by the method of compaction.

RECOMMENDATIONS

For routine design, the resilient modulus testing of cohesive soils can be simplified by the following measures:

(1) Test at a single confining pressure. A 3 psi confining pressure is realistic and compatible with the AASHTO reliability concept. However, unconfined testing (0 psi) might be considered since it is easier and requires less equipment. The unconfined test would produce conservative results.

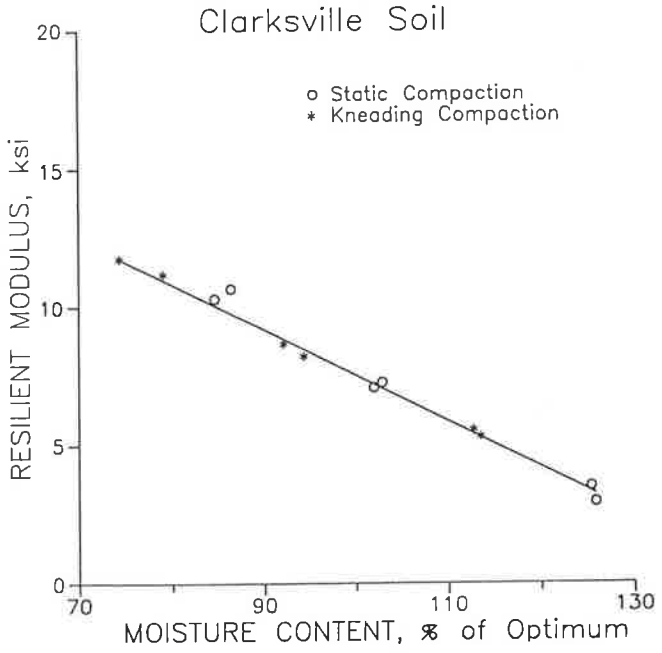

FIGURE 10 Effect of compaction method on M_R of Clarksville soil.

(2) Test at a single deviator stress. A deviator stress of 8 psi can be used for all tests, providing a slightly conservative M_R value for most situations. Alternatively, the stress level can be selected from Figure 7, based on expected modulus and design; in this case, a second deviator stress might be necessary if the modulus differs significantly from that expected.

(3) Reduce the deviator stress cycles from 200 to 50.

By adopting these measures, the time required for resilient modulus testing (assuming a 2-second interval between stress applications) will be reduced from 100 minutes to less than 2 minutes.

Although no examination was made of the effect of conditioning, more time might be saved by making similar modifications in conditioning. In particular, conditioning at the three levels of confining pressure and five levels of deviator stress appears to be unwarranted. Two hundred cycles of the testing stress should suffice for both conditioning and testing.

ACKNOWLEDGMENTS

This paper is based on "Resilient Properties of Arkansas Subgrades," which is being conducted by the Arkansas Highway and Transportation Research Center, University of Arkansas.

The project is sponsored by the Arkansas State Highway and Transportation Department and the U.S. Department of Transportation, Federal Highway Administration.

REFERENCES

1. *Resilient Properties of Arkansas Subgrades.* Research project TRC-94. Arkansas State Highway and Transportation Department and the U.S. Department of Transportation, Federal Highway Administration.
2. Part II, Methods of Sampling and Testing. *Standard Specifications for Transportation Materials and Methods of Sampling and Testing.* American Association of State Highway and Transportation Officials, 1986.
3. R.P. Elliott and S.I. Thornton. *Resilient Properties of Arkansas Subgrades.* Report No. UAF-AHTRC-86–002. University of Arkansas at Fayetteville, 1986.
4. *The AASHO Road Test, Report 5, Pavement Research.* Special Report 61E, Highway Research Board, 1962.
5. ILLI-PAVE. Transportation Facilities Group, Department of Civil Engineering, University of Illinois at Urbana-Champaign.
6. M.R. Thompson and Q.R. Robnett. *Final Report: Resilient Properties of Subgrade Soils.* Transportation Engineering Series No. 14, University of Illinois at Urbana-Champaign, 1976.

Publication of this paper sponsored by Committee on Soil and Rock Properties.

Repeated Static Loading Triaxial Tests for Determination of Resilient Properties of Sands

G. T. H. SWEERE AND P. J. GALJAARD

The possibility of determining the resilient modulus of sand through repeated static loading triaxial test was investigated. Six different sands, with gradings ranging from very coarse to extremely fine, were tested. For each sand investigated, one triaxial specimen was prepared. Repeated static loading triaxial tests and cyclic loading triaxial tests were then carried out on the same specimen. Comparison of the resilient moduli obtained from both types of tests clearly showed the possibility of determining resilient moduli in relatively simple-to-perform, repeated static loading triaxial tests.

Mechanistic design procedures for asphalt pavements often use the resilient modulus M_R to characterize the elastic stiffness of the subgrade soil and materials in the unbound layers of the pavement. Some empirically based design procedures like the recently published AASHTO method (*1*) also use M_R to characterize elastic stiffness of unbound materials.

The test method most widely used for determination of the resilient modulus M_R is the cyclic loading triaxial test. In this test, cylindrical specimens of the material to be investigated are subjected to stresses that closely simulate in-situ stresses in the pavement, and the resulting deformations are measured. The tests are usually carried out at frequencies of 1 to 10 Hz. As complicated servo-hydraulic equipment is needed to apply the loading required at these frequencies, the cyclic loading triaxial test is not suited for routine application. This factor strongly inhibits the implementation of design procedures using the resilient modulus M_R as input.

A strong need therefore exists for development of simpler tests that still allow accurate determination of resilient moduli of unbound materials. This paper describes an investigation into the possibility of determining resilient moduli of sands through repeated static loading triaxial tests. If this possibility exists, simple pneumatic or even dead-load testing equipment can be used to determine M_R.

The research described in this paper is part of a major research project dealing with the structural contribution of unbound material layers to asphalt pavements (*2*). Full details of the research described here can be found in a recently published report (*3*).

Road and Railroad Research Laboratory, Delft University of Technology, P.O. Box 5048, 2600 GA Delft, The Netherlands.

SANDS INVESTIGATED

The six sands investigated in this study represent the sands most widely used for road construction in the Netherlands. The names of the place of origin of the sands will be used in this paper to denote the sands.

The particle size distribution of the sands was determined by washing a sample through a 75 μm sieve. After the material retained was oven dried, a dry analysis was performed. The material passing the 75 μm sieve was subjected to a hydrometer analysis. The results of both the dry sieving and the hydrometer analyses were then combined to yield the particle size distribution of the sands (Figure 1). Using the data obtained in the particle size analysis, the sands were classified using the Extended Unified Soil Classification System (Table 1).

To obtain reference values for the moisture content and the dry density of the triaxial specimens, Proctor compaction tests were carried out on the sands, according to AASHTO T 180, method B (modified compaction level) (*4*). Table 1 shows the resulting values of the optimum moisture content w_{opt} and the maximum dry density $\rho_{d,max}$.

TRIAXIAL TEST PROCEDURES

Triaxial Test Apparatus

Figure 2 shows the schematics of the triaxial test apparatus used for this study. The specimen tested measures 100 mm in diameter and 200 mm in height. The constant confining stress is applied through air pressure in the plexiglass cell, while the deviator stress is applied by a servo-hydraulic actuator through the loading piston. A load cell is incorporated inside the triaxial cell, thereby eliminating load measuring errors caused by the friction between the loading piston and the top of the triaxial cell. Axial deformation of the triaxial specimen is measured by

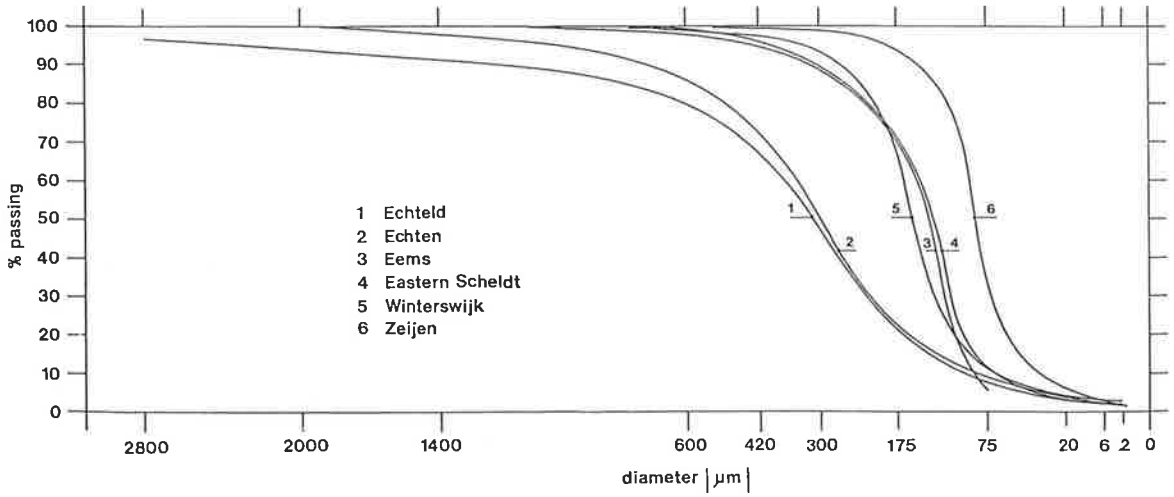

FIGURE 1 Particle size distribution of the sands investigated.

TABLE 1 CLASSIFICATION, PROCTOR, TRIAXIAL SPECIMEN, AND RESILIENT MODULI DATA FOR THE SIX SANDS INVESTIGATED

	Classification Extended USCS		Proctor		Triaxial Specimen		Resilient Modulus		
Sand	Type	Code	w_{opt} (%)	$\rho_{d,max}$ (kg/m^3)	w (%)	ρ_d (kg/m^3)	K_1 (MPa)	K_2 (–)	R^2 (–)
Echteld	Poorly graded sand	SP/SF	12.7	1,745	12.7	1,745	8.09	.56	.92
Echten	Poorly graded sand	SP/SF	13.7	1,712	13.8	1,711	7.64	.57	.96
Eems	Poorly graded sand	SP/SF	13.0	1,665	12.9	1,666	8.85	.56	.96
Eastern Scheldt	Poorly graded sand	SP/SF	15.7	1,668	15.8	1,667	9.80	.54	.92
Winterswijk	Poorly graded sand	SP/SF	10.5	1,697	10.5	1,698	10.53	.53	.96
Zeijen	Silty sand	SMF	15.0	1,593	15.1	1,592	9.74	.52	.96

an LVDT connected to the loading piston outside the triaxial cell. Radial deformation of the triaxial specimen can be measured by three noncontacting sensors, which are mounted through the plexiglass cell on a horizontal plane at half the specimen height.

Cyclic Loading Testing Procedure

Figure 3 shows the stresses applied to the triaxial specimen in the cyclic loading tests. The constant, all-around confining stress σ_3 simulates the constant overburden stress in road construction. The cyclic deviator stress σ_d simulates the in-situ vertical stress due to traffic loading. As shown in Figure 3, σ_d is cyclic, varying between zero and a preset value at a frequency of 1 Hz. The major principal stress σ_1 is then equal to $\sigma_1 = \sigma_d + \sigma_3$, and the intermediate principal stress is equal to the minor principal stress σ_3. The sum of principal stresses θ is equal to $\theta = \sigma_1 + \sigma_2 + \sigma_3 = \sigma_d + 3\ \sigma_3$.

Cyclic loading triaxial tests were carried out at several different combinations of the confining stress σ_3 and the deviator stress σ_d. Each triaxial specimen was tested at 29 different combinations of stresses: σ_3 ranging from 10 to 300 kPa and the stress ratio σ_1/σ_3 ranging from 2 to 6.

Static Loading Testing Procedure

In the static loading triaxial tests to determine the resilient modulus M_R, the procedure suggested by Kalcheff and Hicks (*5*) was followed. The procedure calls for a series of alternate load-on/load-off periods of 5 minutes, followed by a load-on period of 30 minutes (Figure 4). After this period, the axial load is removed and the resilient deformation $\varepsilon_{a,r}$ is measured. The resilient modulus M_R is then calculated as the ratio of the applied deviator stress over the axial resilient strain.

The repeated static loading testing procedure described above requires about one hour to perform for each selected combination of σ_3 and σ_d. As M_R has to be determined for a number of stress ratios, owing to the stress-dependent nature of M_R, this procedure is far too time-consuming for routine application. Therefore, the resilient deformation of the triaxial specimen was also measured after the first load-on period of 5 minutes (Figure 4), to check the possibility of using this strain value for accurate determination of M_R.

Because of the time-consuming nature of the repeate static loading tests, only 10 different combinations of σ_3 and σ_d were used in these tests; σ_3 ranged from 10 to 200 kPa and σ_1/σ_3 ranged from 2 to 4.

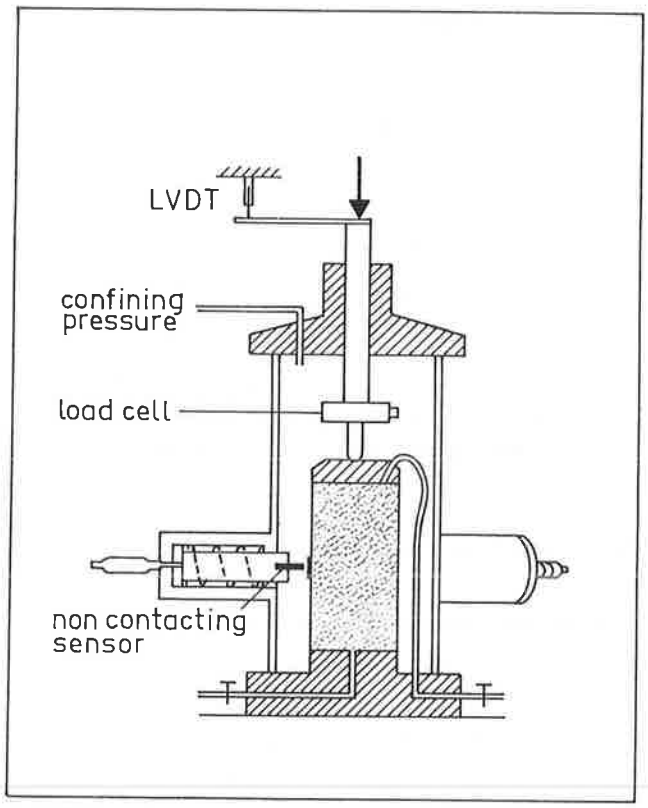

FIGURE 2 Schematics of triaxial test apparatus.

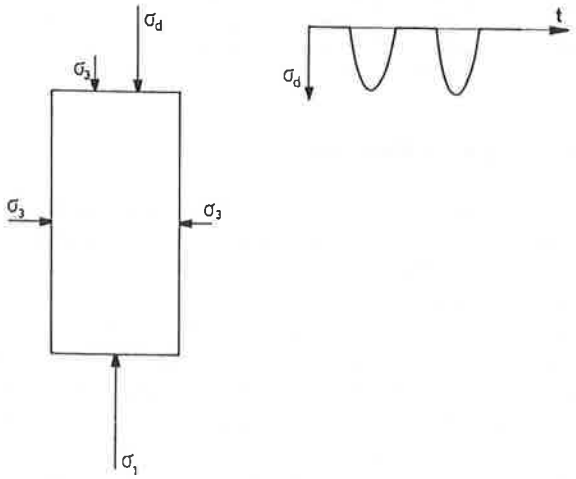

FIGURE 3 Stresses applied to triaxial specimen in cyclic loading tests.

Test Sequence

The cyclic loading and repeated static loading tests for determining M_R were carried out on the same specimen. One triaxial specimen was prepared for each of the sands investigated. At each confining stress level, the repeated static loading tests were carried out first, followed by the cyclic loading tests at the confining stress level. Before actual testing, the triaxial specimen was subjected to several hundred load applications at a small stress ratio to assure a proper seating between the specimen and the loading caps.

Specimen Preparation

The triaxial specimens were prepared in six layers, using a split-mold and a tamping device. The optimum moisture content and the maximum dry density from the modified Proctor compaction tests served as target values for the triaxial specimens. The values obtained for moisture content and dry density of the triaxial specimens are shown in Table 1. Comparison of the target values and the actual specimen values for moisture content and dry density reveals very little deviation.

CYCLIC LOADING TEST RESULTS

The cyclic loading triaxial tests for determining the resilient modulus M_R were carried out at 29 different combinations of stresses. For each stress combination, the axial resilient strain of the specimen was determined, and the resilient modulus M_R was calculated according to

$$M_R = \frac{\sigma_d}{\varepsilon_{a,r}} \tag{1}$$

where

M_R = resilient modulus (MPa),
σ_d = deviator stress (MPa), and
$\varepsilon_{a,r}$ = axial resilient strain (–).

Figure 5 shows the results of the cyclic loading tests for the Echteld sand. The obtained 29 values of the resilient modulus M_R have been plotted in Figure 5 against the sum of principal stresses θ. The relationship between M_R and θ as shown in Figure 5 can be described by the well-known equation:

$$M_R = K_1\left(\frac{\theta}{\theta_0}\right)^{K_2} \tag{2}$$

where

M_R = resilient modulus (MPa),
θ = sum of principal stresses (MPa),
θ_0 = reference stress 1 MPa (MPa),
K_1 = material parameter (MPA), and
K_2 = material parameter (–).

The division of θ by the reference stress θ_0 is done for purely mathematical reasons, i.e., rendering the stress parameter in equation 2 dimensionless.

The values of the material parameters K_1 and K_2 for the Echteld sand are shown in Figure 5, together with the

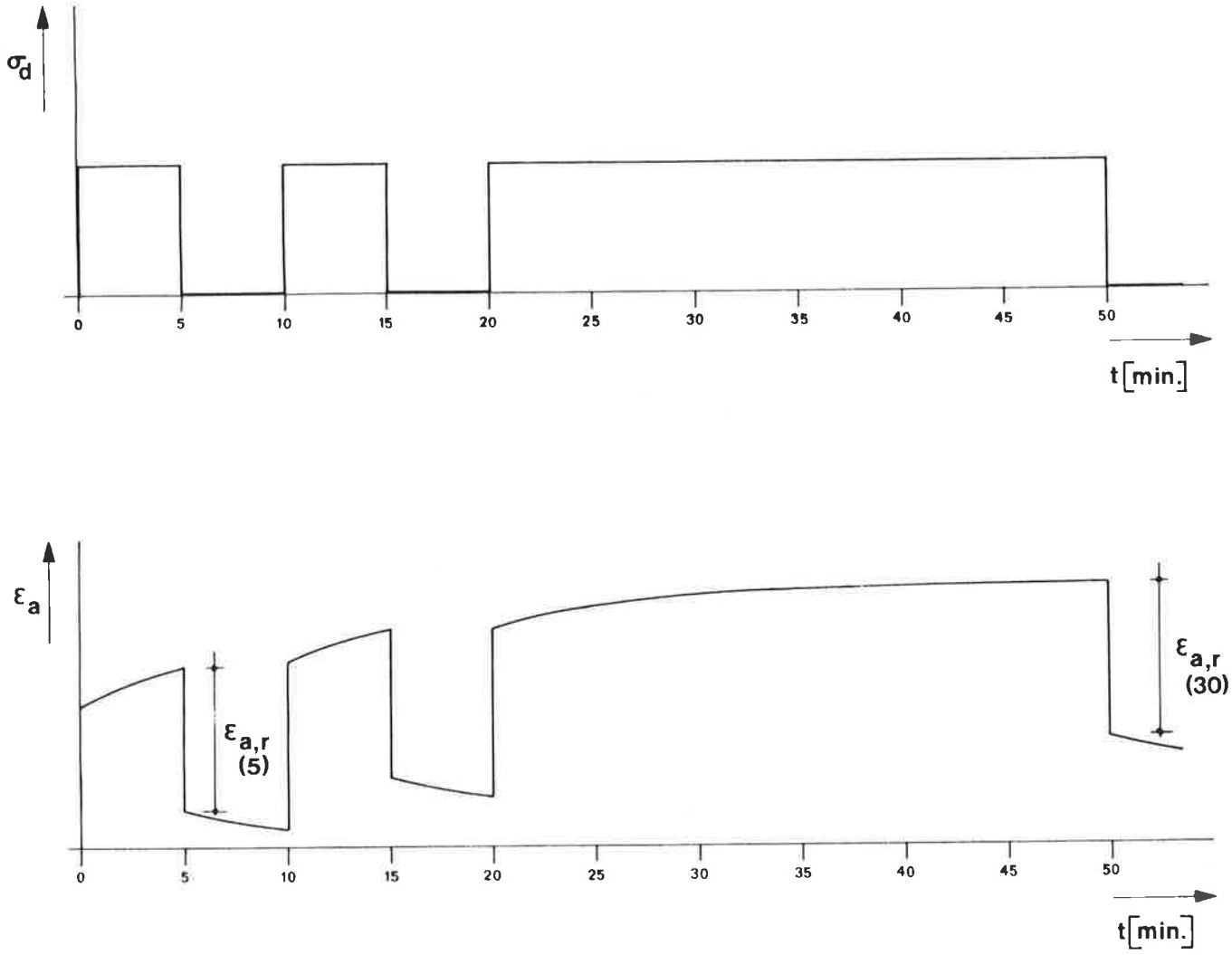

FIGURE 4 Deviator stress σ_d and axial strain E_a versus time for repeated static loading triaxial tests.

value of the multiple correlation coefficient squared R^2. The M_R-θ relationships for the other sands investigated are similar to the one depicted in Figure 5; to limit the length of this paper the individual graphs are not shown here. The resulting values of the material parameters K_1 and K_2 and the R^2 value for the six sands investigated are shown in Table 1.

REPEATED STATIC LOADING TEST RESULTS

The repeated static loading triaxial tests for determination of the resilient modulus were carried out at 10 different combinations of stresses. The axial resilient strain on unloading after the first 5-minute load-on period and the 30-minute load-on period (Figure 4) were determined, and the resilient modulus was then calculated according to

$$M_{R,s} = \frac{\sigma_d}{\varepsilon_{a,r}} \tag{3}$$

where

$M_{R,s}$ = resilient modulus from repeated static loading test (MPa),
σ_d = deviator stress (MPa), and
$\varepsilon_{a,r}$ = axial resilient strain (–).

The individual data points shown in Figure 6 represent the results of the 10 repeated static loading tests for the Echteld sand, calculated from the axial resilient strain on unloading after the 30-minute load-on period. The straight line shown in Figure 6 is the regression line through the cyclic loading test results. To indicate the influence of the stress ratio σ_1/σ_3, different symbols have been used in Figure 6 for the three values of σ_1/σ_3 applied.

As can be seen from Figure 6, the data points from the repeated static loading tests plot closely to the regression line from the cyclic loading tests. The data points from the repeated static loading tests at stress ratio $\sigma_1/\sigma_3 = 4$

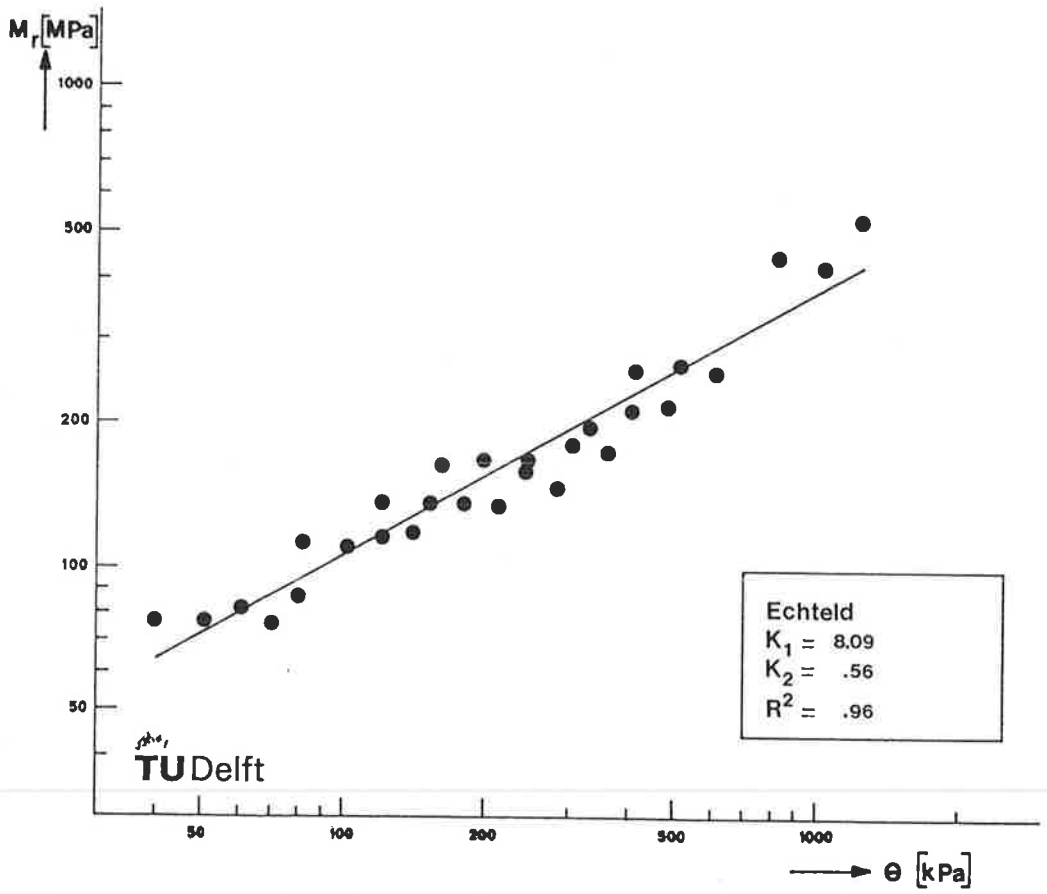

FIGURE 5 Results of cyclic loading tests: resilient modulus M_R versus sum of principal stresses θ, for Echteld sand.

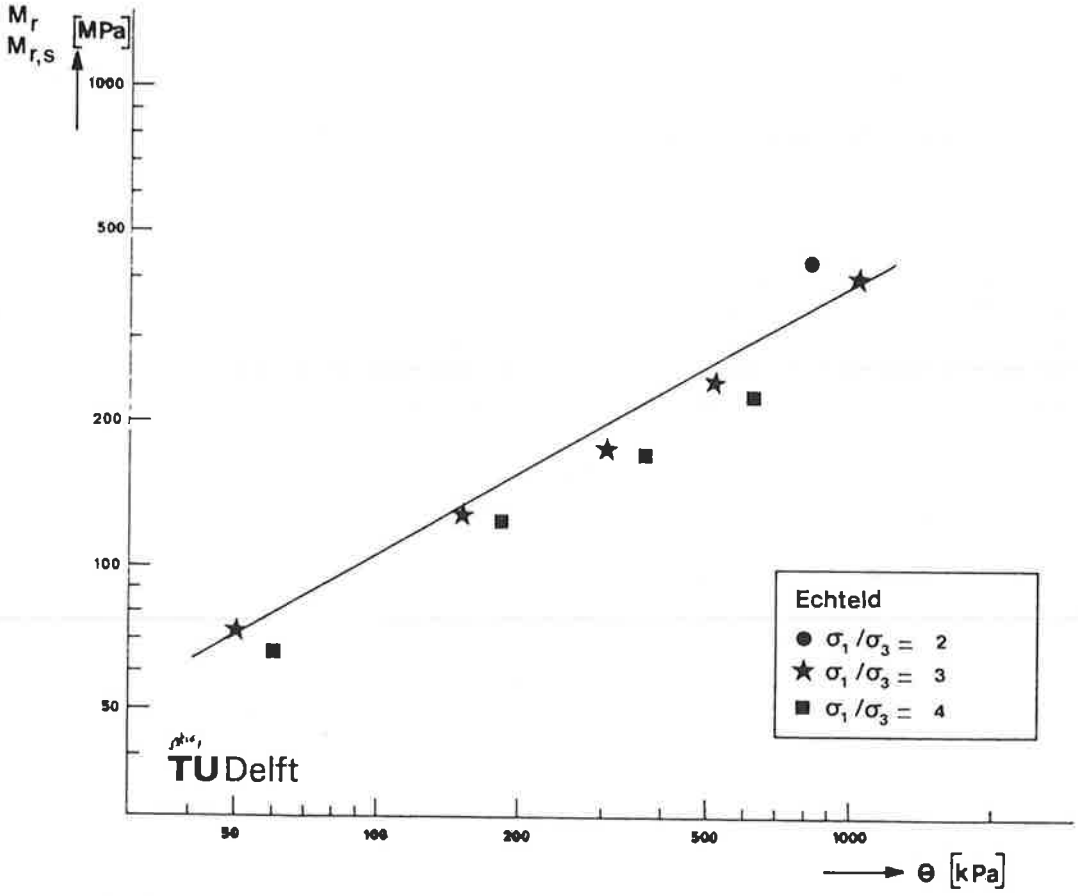

FIGURE 6 Comparison of cyclic loading (straight line) and repeated (static loading) test results.

plot somewhat below the regression line. For $\sigma_1/\sigma_3 = 3$, the data points almost plot on the regression line, and the single data point obtained for $\sigma_1/\sigma_3 = 2$ plots above the regression line. This influence of stress ratio is consistent with that found in the cyclic loading tests. Since the regression line from these tests represents all the stress ratios applied, it passes through the cyclic loading data points for the average stress ratio $\sigma_1/\sigma_3 = 3$. Therefore, the static loading data points for $\sigma_1/\sigma_3 = 3$ plot closest to the cyclic loading regression line.

For the other five sands investigated, results similar to those depicted in Figure 6 for the Echteld sand were found, with a similar influence of the stress ratio σ_1/σ_3. Space limitations prevent showing individual results for these sands here. In the next section of this paper, the data from the repeated static loading tests for all the sands investigated will be grouped together and compared to the results from the cyclic loading tests.

COMPARISON OF 5-MINUTE AND 30-MINUTE LOADING RESULTS

The repeated static loading procedure suggested by Kalcheff and Hicks (*5*) calls for a loading procedure as depicted in Figure 4, and calculation of the resilient modulus using the resilient deformation on unloading after the 30-minute load-on period. The $M_{R,s}$ results thus obtained are plotted in Figure 7 against the resilient moduli M_R from the cyclic loading tests. In Figure 7, the data from all the tests on the six sands have been used.

The straight line depicted in Figure 7 can be described by the following formula:

$$M_{R,s}\,(30) = -3.54 + 0.965\,M_R \qquad (4)$$
$$R^2 = 0.988$$

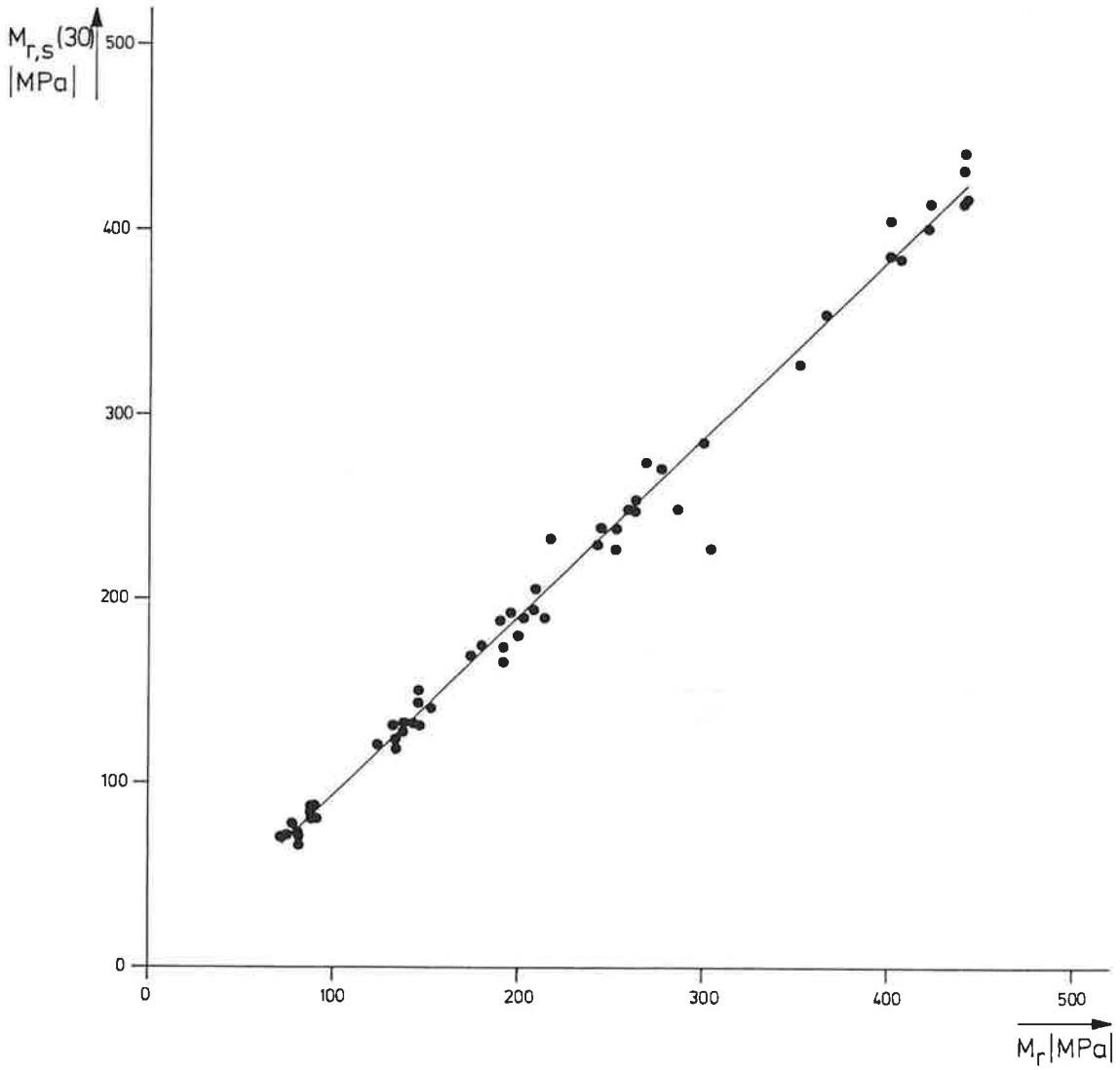

FIGURE 7 Comparison of resilient moduli from static 30-minute loading ($M_{R,s}$) and cyclic loading (M_R) test results.

where

$M_{R,s}$ (30) = resilient modulus from 30-minute static loading test,
M_R = resilient modulus from cyclic loading test, and
R^2 = multiple correlation coefficient squared.

As can be seen from Figure 7 and from the high R^2 value of equation 4, the correlation between the resilient moduli from the repeated static and the cyclic tests is very good. From equation 4, it can also be seen that the data plot almost on a 45-degree line of equality.

The loading procedure depicted in Figure 4 has one main disadvantage: for each determination of M_R, almost 1 hour is required. Since M_R has to be determined for several different combinations of stresses, this procedure is quite cumbersome. Therefore, the possibility of determining the resilient modulus using the resilient strain on unloading after the first 5-minute load-on period (Figure 4) was also investigated. The $M_{R,s}$ results calculated from those strain values are plotted in Figure 8 against the M_R values from the cyclic loading tests. Again, all the data from the six sands were used.

The straight line depicted in Figure 8 can be described by the following formula:

$$M_{R,s}\,(5) = -6.64 + 0.969\,M_R \qquad (5)$$
$$R^2 = 0.990$$

where

$M_{R,s}$ (5) = resilient modulus from 5 minute static loading test,
M_R = resilient modulus from cyclic loading test, and
R^2 = multiple correlation coefficient squared.

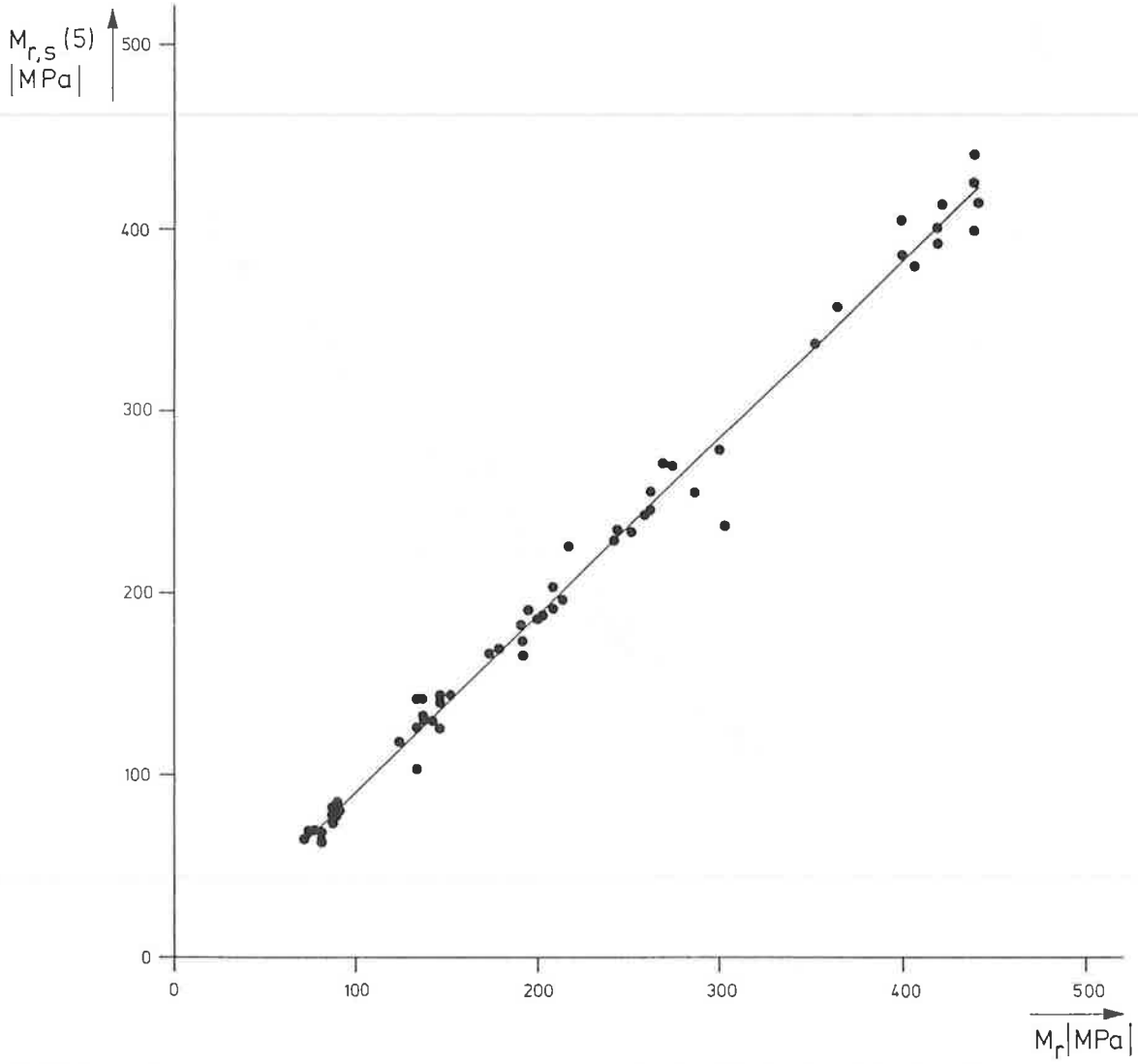

FIGURE 8 Comparison of resilient moduli from static 5-minute loading ($M_{R,s}$) and cyclic loading (M_R) test results.

Once more, a very good correlation between the repeated static loading and the cyclic loading test results is found, the data points again plotting almost on a line of equality.

Comparison of equations 4 and 5 shows that the 30-minute and the 5-minute loading procedure yield almost the same regression equations between $M_{R,s}$ and M_R, with almost the same R^2 value.

CONCLUSIONS

The research described in this paper has shown that, for a wide range of sands, the resilient modulus can be determined using relatively simple repeated static loading triaxial tests. Per stress combination to be investigated, one short load-on period of 5 minutes can be used to determine the resilient modulus. It is suggested, however, that 10 1-minute load-on periods at high confining stress and low stress ratio be executed before starting the actual measurements. Such a procedure assures proper seating between the loading caps and the triaxial specimen. Experience has shown that proper seating is achieved within a few load applications.

The possibility of determining the resilient modulus of coarse, graded crushed stone materials using the same repeated static loading procedure is currently being investigated by the authors.

ACKNOWLEDGMENT

These investigations were supported in part by the Netherlands Technology Foundation (STW).

REFERENCES

1. *AASHTO Guide for Design of Pavement Structures.* American Association of State Highway and Transportation Officials, Washington, D.C., 1986.
2. G. T. H. Sweere, A. Penning, and E. Vos. Development of a Structural Design Procedure for Asphalt Pavements with Crushed Rubble Base Courses. *Proceedings, Sixth International Conference on the Structural Design of Asphalt Pavements*, Ann Arbor, Mich., Vol. 1, 1987, pp. 34–49.
3. G. T. H. Sweere and P. J. Galjaard. *Determination of the Resilient Modulus of Sands by Means of Static Loading Triaxial Tests.* Report 7–86–201–10. Road and Railroad Research Laboratory, Delft University of Technology, 1986.
4. *Standard Specification for Transportation Materials and Methods of Sampling and Testing. Part II. Methods of Sampling and Testing.* American Association of State Highway and Transportation Officials, Washington, D.C., 1978 (twelfth edition).
5. I. V. Kalcheff and R. G. Hicks. A Test Procedure for Determining the Resilient Properties of Granular Materials. *Journal of Testing and Evaluation*, Vol. 1, No. 6, 1973, pp. 472–479.

Publication of this paper sponsored by Committee on Soil and Rock Properties.

Comparison of Alternative Methods of Measuring the Residual Strength of a Clay

J. T. ANAYI, J. R. BOYCE, AND C. D. ROGERS

This paper describes a series of drained tests on Lias clay at various normal stresses in both a reversible shear box and a modified Bromhead ring shear apparatus. The residual failure envelopes were found to be curved at normal stresses below 150 kN/m² (22 lb/in.²). At normal stresses above this value, the modified Bromhead ring shear tests produced lower values of residual shear strength than reversal shear box tests. The results indicate that residual failure surfaces are not developed at normal stresses below 30 kN/m² (4.4 lb/in.²).

When a soil is subjected to shear strain, the shear resistance steadily increases. For any applied effective normal pressure, the limit to the resistance that the soil can offer is known as the peak shear strength. In some cases an experimental test is stopped just after this point and the strength measured is referred to as the shear strength of the soil. If shearing is continued beyond the maximum value of shear strength, the resistance of a clay decreases until a constant value is reached, which is known as the residual strength.

Residual strength is defined by Skempton (*1*) as the minimum constant shear strength attained in a soil (for a slow rate of shearing) at large displacement. He demonstrated that the displacements necessary to cause such a strength are usually far greater than those corresponding to the peak strength and the fully softened state (critical state in overconsolidated clay) as shown in Figure 1. In such a soil the postpeak drop in drained shear strength may be considered as taking place in two stages: first, at a relatively small displacement, the strength decreases to the fully softened or critical state owing to an increase in water content (dilatancy); and second, after large displacements, the strength falls to the residual value owing to the orientation of platey clay minerals parallel to the direction of shearing. The postpeak drop in strength of normally consolidated clay is due only to particle reorientation.

The drained residual strength of cohesive soil has been studied extensively by many investigators. The first major understanding of residual strength was presented by Skempton (*2*) who showed that the strength along any discontinuity in a clay mass is governed by the residual-strength of the clay. Lupini et al. (*3*) have presented an extensive review of previous work on residual strength. They concluded that three modes of shearing are associated with residual strength:

Loughborough University of Technology, Loughborough, Leicestershire LE11 3TU, England.

- Turbulent mode, which usually occurs when soils have a high proportion of rotund particles or have platey particles in which particle orientation does not occur.
- Sliding mode, which corresponds to the case in which a low strength shear surface of strongly orientated, low-friction platey particles forms.
- Transitional mode, which involves both turbulent and sliding modes.

The transition from one mode to another is related to the packing and porosity of the rotund particles present.

It is generally accepted (*2–4*) that the residual shear strength of a soil is independent of stress history effects and specimen size. Rate of displacement has only a small effect. Essentially the decrease in strength to its residual value is related to the orientation of clay particles in the shear zone. This orientation process is largely independent of the speed of shearing.

If this is the case, the application of a large deformation at a high rate of shearing followed by a reduction in the rate of shearing should reduce the time required to mobilize the residual strength in laboratory tests. However, the question of developing pore pressure will arise at a high rate of shearing. This problem will be discussed later in relation to the results of this work.

MEASUREMENT OF THE RESIDUAL STRENGTH OF CLAY

Two types of apparatus can be used to measure residual shear strength: the shear box and the ring shear apparatus. Each of these is discussed in turn. The triaxial test is not used to any great extent in measuring residual strength, because of the complex stress distribution across the failure plane that is produced if the test is continued beyond the peak.

Shear Box

The shear box apparatus is the oldest form of shear test. Generally the soil is held in a box that is split at midheight. A vertical pressure is applied, followed by a horizontal shear force so as to cause relative displacement between the two parts of the box. The magnitude of the shear force

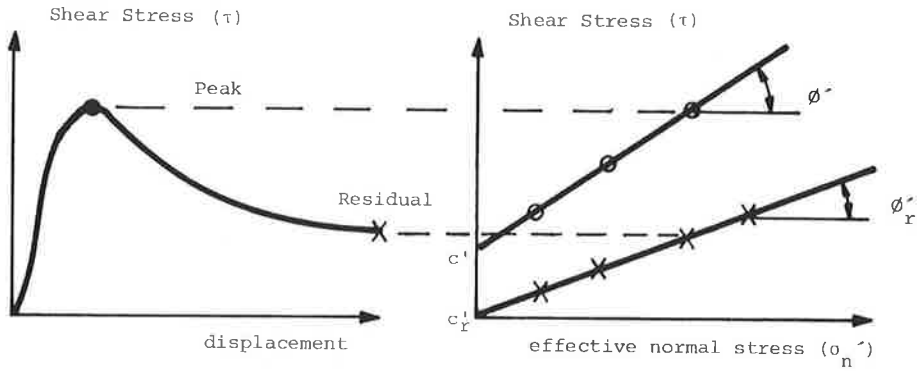

a) definition of peak and residual stress envelopes

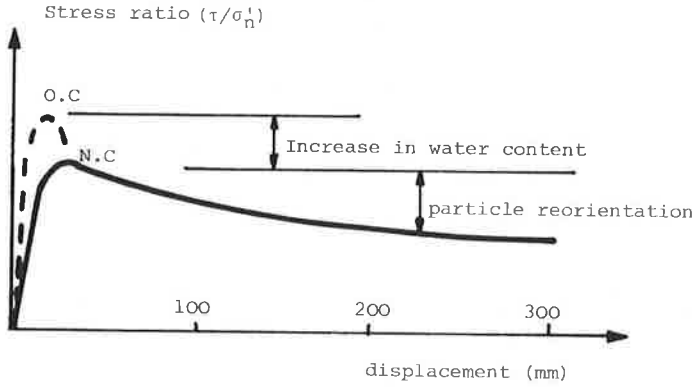

b) difference between normally consolidated (N.C.) and overconsolidated (O.C.) clay

FIGURE 1 Shear stress versus displacement for a typical clay.

is recorded as a function of the shear displacement. The vertical load is usually applied by dead weights, whereas the shear force is often applied by a motor acting through gears so that the test is strain controlled.

At Loughborough the standard shear box has been modified to enable the direction of travel to be reversed automatically. When this equipment is used, the strength along the shear plane formed in the specimen is made to approach a lower limiting value, or residual value, by repeated reversals of the direction of travel of the shear box.

In many ways, the most satisfactory method of measuring residual strength is to obtain undisturbed samples that contain a natural slip surface and to test them in the shear box such that failure occurs by sliding along the existing slip plane. Skempton (*1*) has shown that when tests are satisfactorily carried out on undisturbed samples containing a fully developed slip or shear surface, the residual strength is reached at a relatively small displacement since all water content changes and particle orientation effects have already been brought about by the shearing movements in nature. The strength on such surfaces is defined as the field residual value. In principle, it should be the same as the strength calculated from back analysis of a landslide in which movement has been reactivated along a pre-existing slip surface. Skempton and Petley (*5*) have shown from their investigation of slip surface samples that, in the second run of a test (after reversing the travel of the box), the strength returns closely to the first-run value.

Drained tests were performed in a shear box by Calabresi and Manfredini (*6*) at the University of Rome on intact samples from Santa Barbara. The samples were sheared along different types of structural discontinuities of jointed overconsolidated clay. Calabresi and Manfredini concluded that along joints and bedding planes the same peak value of friction angle as that of an intact clay occurs, but that cohesion is very low, if not negligible. The residual strength is the same in both cases, but along these discontinuities, is usually reached after a smaller displacement. Along the faults, the shear strength is already at its residual value. The intact clay seems more brittle when sheared along planes parallel to the bedding planes, and this may have some influence on the development of progressive failure.

The magnitude of shear displacement available in the shear box is usually small, so more than one travel is needed to obtain the residual strength of any soil. This is achieved by returning the split box to its starting position after completing the extent of its travel and shearing again. This process can be repeated a number of times until a steady (residual) value of shear strength is observed. However, this procedure has the obvious disadvantage that the

particle orientation developed during travel in one direction may be partly destroyed when the direction of travel is reversed.

The development of residual shear strength can be facilitated by the use of a precut shear plane. However, care must be taken to consolidate the specimen under the selected normal load for an appropriate period after the shear plane has been formed. This method has the advantage that the shear surface is a plane, whereas in other shear box tests the shear surface may undulate giving greater values of recorded strength.

Ring Shear Apparatus

All previous work on residual strength of soil has found the ring or torsion shear test to be very useful because there is no change in area of cross section as the test proceeds and the sample can be sheared through an uninterrupted displacement of any magnitude.

Bishop et al. (*7*) stated that any measurement of the residual strength of a soil should satisfy the requirements that the normal and shear stresses at failure should be as uniform as possible in the apparatus used, which must be capable of transmitting the desired combination of normal and shear stresses to the sample. The Bishop ring shear apparatus was built by the Norwegian Geotechnical Institute and Imperial College (*7*). The sample in the ring shear has the following dimensions:

Outside diameter	152.4 mm (6 in.)
Inside diameter	101.6 mm (4 in.)
Initial thickness	19.0 mm (0.75 in.)

It can be subjected to a maximum normal stress of 1,000 kN/m^2 (145 lb/in.^{2}) and a maximum shear stress of 500 kN/m^2 (72 lb/in.^{2}). The annular sample is laterally confined between two pairs of rings and is loaded normally through annular platens. Drainage is by means of a porous ceramic annulus screwed into each platen. Fins are provided on the exposed face of each ceramic annulus to minimize the risk of slip occurring at the soil-ceramic interfaces. The lower confining rings and the loading platen are screwed to the base plate. The upper and lower confining rings are held together by locking screws, which are removed before shear commences. A perspex water bath serves to prevent the sample from drying out during testing. The sample is sheared by steadily rotating the lower half while the upper half reacts against a torque arm. The shear torque is determined from the readings on two opposed tangential proving rings mounted on rigid columns. This machine is the most sophisticated device for measuring the residual strength of soil. However, it is complicated and expensive and is therefore used mainly for academic work at Imperial College (University of London).

The Harvard Ring Shear apparatus is described by La Gatta (*8*). The machine is designed to test disc-shaped specimens with a diameter of 71.1 mm (2.8 in.) or annular specimens of outside diameter 71.1 mm and inside diameter 50.8 mm (2.0 in.). The specimen thickness may vary from 1 to 25 mm (0.04 to 1.00 in.). Specimens can be undisturbed or remolded. In general, the shearing unit consists of a turntable, two loading platens containing porous stainless steel discs to allow drainage, a vertical spacer, a moment transfer plate, and a top plate. The vertical stress is applied by means of a loading yoke and counterbalanced lever system. Three miniature extensometers can be attached to the top plate to measure any tilting during consolidation or shear. Shear stresses are computed from the geometry of the test specimen and the moment acting on the sample.

The expensive and time-consuming nature of ring shear tests to determine the residual strength of soils has prevented the test from becoming a routine procedure in commercial laboratories. However, in 1979 a new simple, robust, and inexpensive apparatus was developed at Kingston Polytechnic, and it is now commercially available. A general view of this apparatus, which is described by Bromhead (*9*), is shown in Figure 2. An annular soil sample 5 mm (0.2 in.) thick with inner and outer diameters of 70 mm (2.76 in.) and 100 mm (3.94 in.) respectively is confined radially between concentric rings. It is compressed vertically between porous bronze loading platens by means of a lever loading system and dead weights. Rotation is imparted to the base plate and lower platen by means of a variable speed motor and gearbox driving through a worm drive. This causes the sample to shear, the shear surface forming close to the upper platen, which is artificially roughened to prevent slip at the platen-soil interface. The settlement of the upper platen during consolidation or shear can be monitored by means of a sensitive dial gauge bearing onto the top of the load hanger. Torque transmitted through the sample is measured by a pair of matched proving rings or load cells bearing on a cross arm. A remolded sample is kneaded into the annular cavity, and the sample is consolidated to the desired normal effective stress. When settlement of the upper platen has stopped, the sample is considered to be fully consolidated and it is then sheared at the appropriate rate.

FIGURE 2 Bromhead ring shear apparatus.

CURRENT WORK AT LOUGHBOROUGH

Aims and Research Philosophy

The aims of the research program at Loughborough are

- To compare the conventional methods of measuring residual strength of clay using the reversible shear box and the ring shear apparatus.
- To find the best method of measuring residual strength of clay and to investigate the laboratory factors that affect the measured value of residual strength.
- To define the actual shape of the residual failure envelope using the recommended method for particular clays.

Most of the work to date has been carried out on samples of clay taken from a site near Rugby, England. The soil is generally a blue, fissured, highly overconsolidated clay known as Lias clay, with layers of limestone occurring in the clay strata. The average water content of these samples was found to be 16 percent. This type of clay has the following index properties: liquid limit, 52 percent; plastic limit, 25 percent; plasticity index, 27 percent. Chandler (*10*) has mentioned that Lias clay is of Jurassic age and is heavily overconsolidated, having been subjected in the past to a maximum overburden in excess of 1,000 m (3,300 ft). Consequently, in its unweathered state, it has a natural water content well below its plastic limit. As a result of weathering, its water content near the surface typically rises to around the plastic limit. The material used in this work was taken from a recently exposed quarry face about 12 m (40 ft) below the surface. The material is therefore hard, but highly fissured as a result of stress relief, and has a natural moisture content somewhat below the plastic limit. Figure 3 shows a photograph of the material in an air-dried condition.

A conventional shear box and a Bromhead ring shear are being used in this work, each being connected to a data acquisition system. In each case, modifications have been made to improve the standard equipment.

The shear box (Figure 4) was modified by introducing a reversing switch, which changes the direction of shearing when the limit in either direction is reached. At the same time, a message is relayed to the data acquisition system.

The main modification to the Bromhead ring shear apparatus was to include small vanes on the top and bottom platens (Figure 5) so that shearing would occur at the midheight of the sample instead of near the top platen. To allow for this, the initial sample thickness was increased from 5 to 10 mm (0.2 to 0.4 in.).

Laboratory Testing

Reversal Shear Box

Lias clay samples were prepared by breaking the air-dried material with a pestle and mortar to form a powder passing

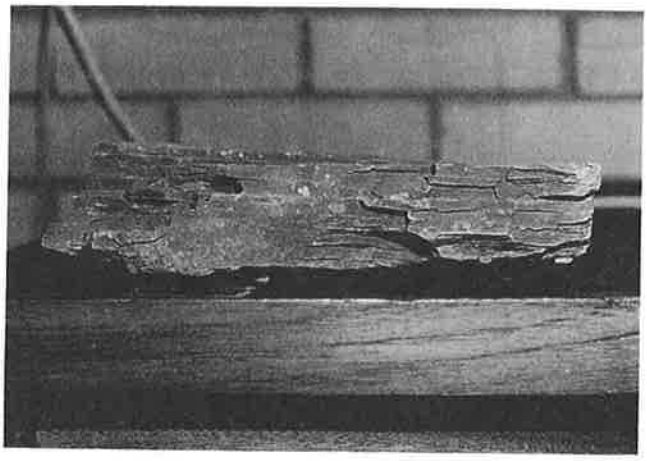

FIGURE 3 Lias clay.

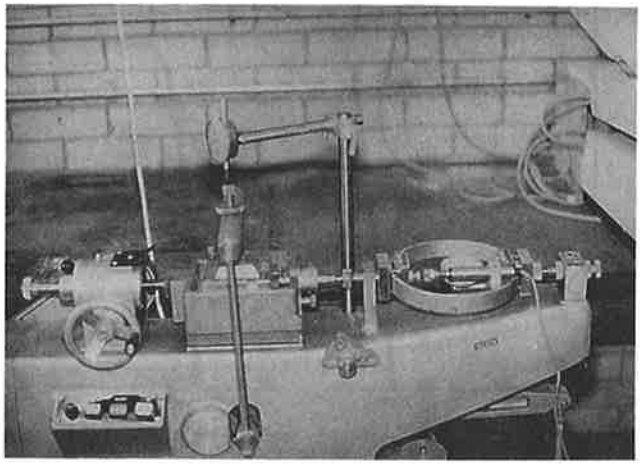

FIGURE 4 Shear box.

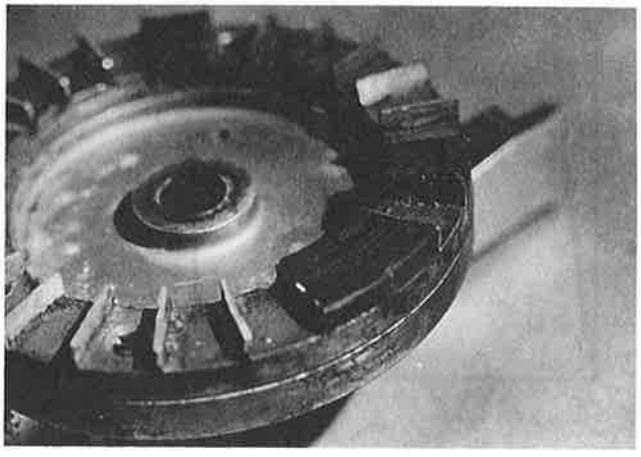

FIGURE 5 Top platen of modified Bromhead ring shear showing vanes.

a 425 m (No. 36) sieve. Distilled water was then added, and the clay thoroughly mixed at a water content near its liquid limit. The clay was then allowed to dry out to a moisture content near the plastic limit. A sample was kneaded into the mold of the shear box after boiling the porous plates for 30 min in distilled water to remove air bubbles.

A series of tests was conducted using various possible techniques to determine which method gave the quickest reliable measurement of the residual strength of the clay. The techniques employed were as follows:

- Formation of shear plane
  - Intact sample subject to slow shearing
  - Precut sample subject to slow shearing
  - Intact sample subject to fast shearing for several reversals followed by slow shearing.
- Rate of shearing
  - 0.24 mm/min (9.4×10^{-3} in./min)
  - 0.024 mm/min (9.4×10^{-4} in./min)
  - 0.0096 mm/min (3.8×10^{-4} in./min)
- Sample size
  - 60 mm (2.36 in.) square
  - 100 mm (3.94 in.) square
- Sequence of normal loads on each sample
  - Single stage
  - Multi-stage

The results of these tests gave rise to certain general conclusions:

1. An intact sample subject to slow shearing with forward and backward reversals forms an undulating shear surface that may lead to high measured values of residual

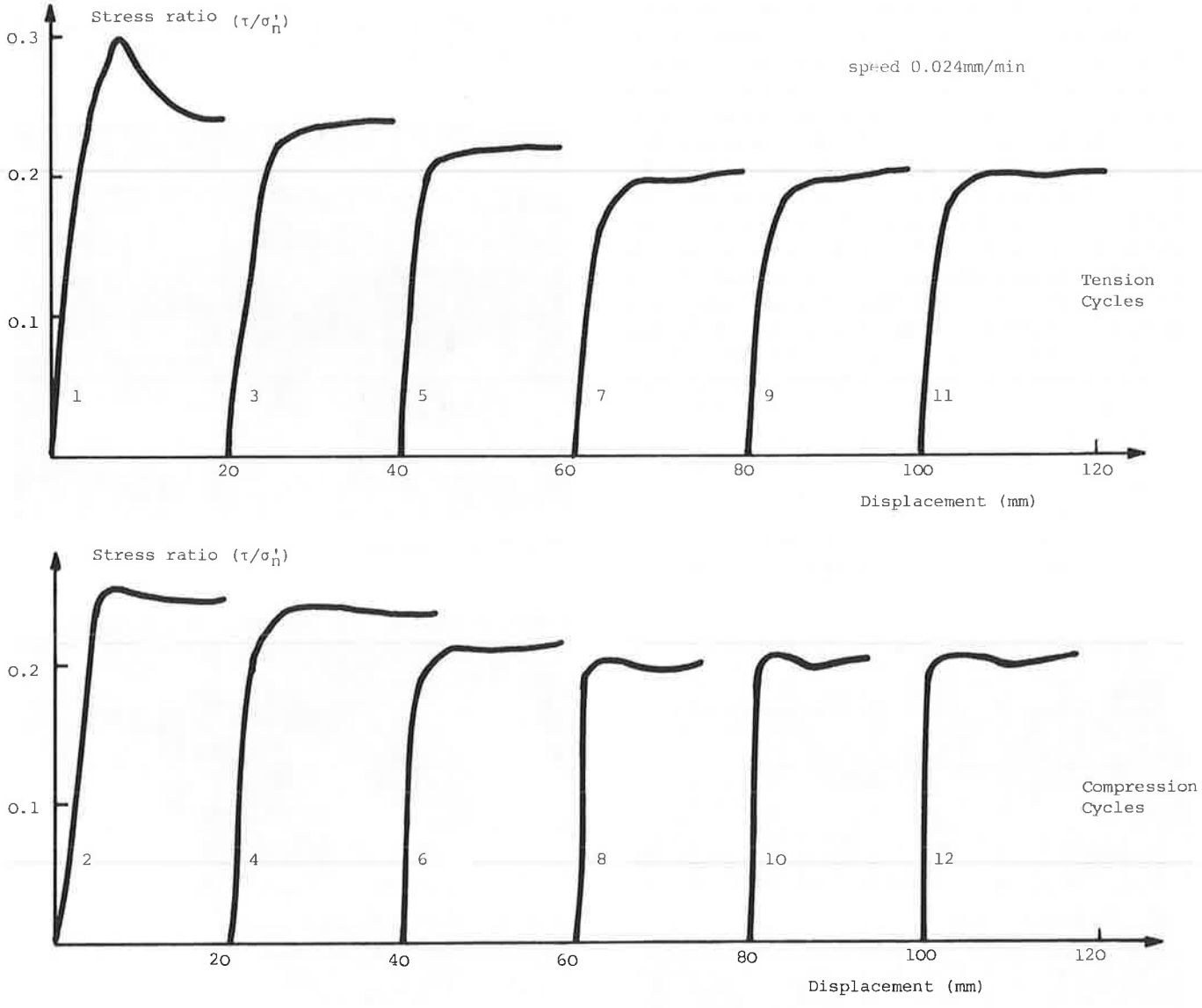

FIGURE 6 Stress-strain curves for reversal shear box test on Lias clay (continuous slow shearing).

strength. The topography of the shear surface can be seen when the sample is examined after the test has been finished. Carrying out the test also takes longer than the other methods do, and there is a problem of excessive soil being extruded at the end of the box. Typical results are shown in Figure 6.

The samples with a precut plane were prepared in two separated half thicknesses (10 mm each) and then put together in the shear box. Experience has shown this method to be easier than cutting the sample with a wire saw.

Fast shearing followed by slow shearing involved first subjecting the sample to several reversals under undrained conditions (300 mm or 11.8 in. displacement at 1.2 mm or 0.047 in./min). Then the rate of shearing was reduced to 0.024 mm/min, and several more reversals were carried out. The readings of the first slow traverse were not taken into consideration to ensure that all the pore water pressure had dissipated. The next traverse was considered to be sheared under drained shearing displacement. This method gave a steady shearing strength in the following cycles and was considered the best method because it gave the lowest value of residual shear strength, was less time consuming, and did not require operator skill in preparing precut samples. Typical results are shown in Figure 7.

2. Rate of shearing was found to have no effect, but a rate of 0.024 mm (9.4×10^{-4} in.) per min is recommended to ensure drained conditions.

3. Figure 8 shows the results of two multi-stage tests using the 60 mm (2.36 in.) square shear box and the 100 mm (3.94 in.) square shear box. The results for the larger sample are slightly lower; the reason for this difference is not known.

4. Multi-stage testing involves the establishment of the residual strength condition at one normal stress, followed by the measurement of residual strength at other normal stresses on the same sample. This technique saves time because the displacement required at each new value of normal stress is only about 20 mm (0.78 in.). There is also less soil extrusion, especially if the normal stress is reduced.

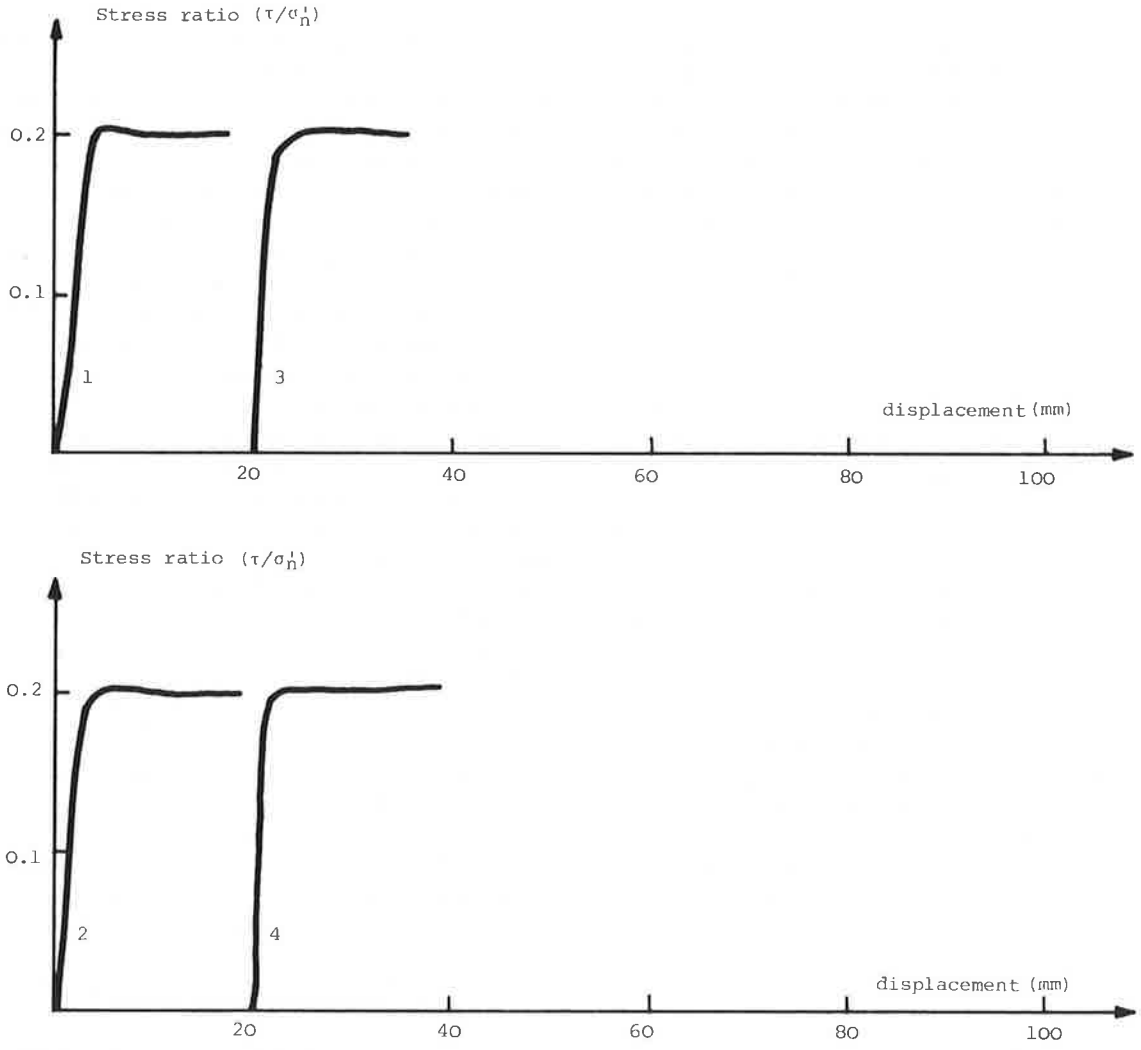

FIGURE 7 Stress-strain curves for reversal shear box test on Lias clay (fast shearing followed by slow shearing).

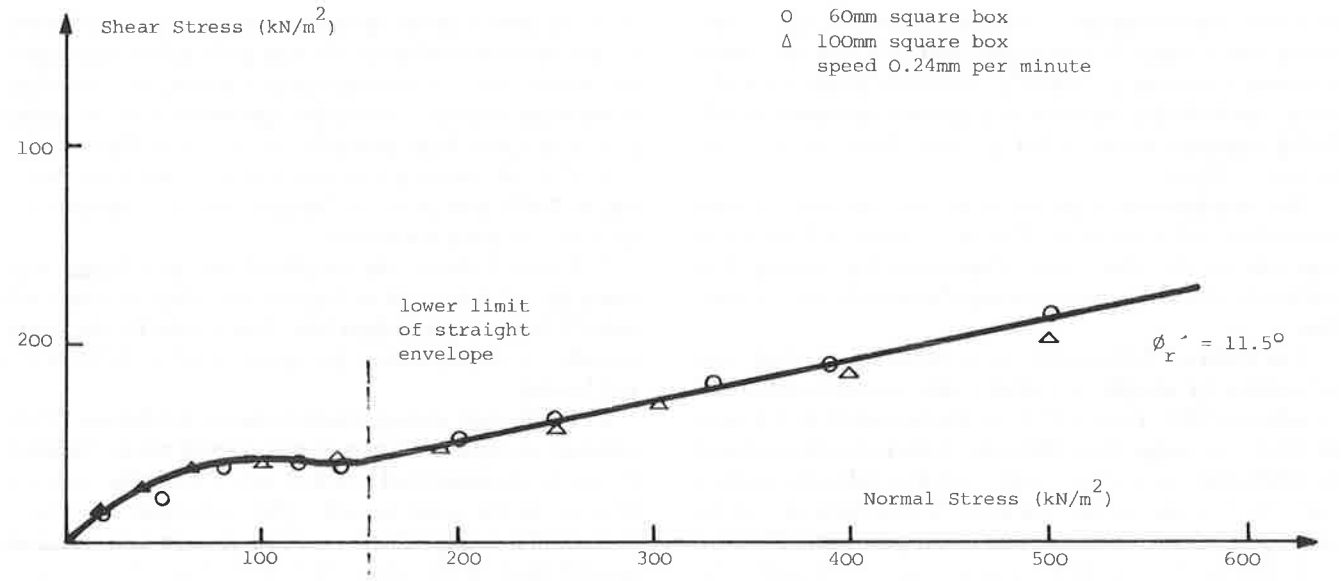

FIGURE 8 Residual strength envelope for Lias clay (reversal shear box tests).

As a result of this series of tests, the recommended technique for reversal shear box tests is to use a 100 mm (3.94 in.) square sample, with the residual shear plane formed by fast shearing, followed by residual strength measurement at a rate of about 0.024 mm (9.4×10^{-4} in.) per min. Multi-stage testing can be used if the sample appears to be in good condition after the previous measurement.

Ring Shear

Lias clay was again used in these tests. The samples were prepared in the same way and kneaded into the lower platen of the Bromhead apparatus at a moisture content near the plastic limit.

Many trial tests were carried out using the original apparatus designed by Bromhead (*9*) and performed in the manner recommended by Bromhead. The sample was left overnight under normal load for full consolidation, and then four or five revolutions were applied to the sample, which produced a failure surface just below the top platen. The sample was left again for the moisture content to equalize before slow shearing. As soon as shearing commenced, the readings of the two proving rings started to become unbalanced, and in some cases, one ring reached zero. Attempts were made to overcome this imbalance in shear forces by carefully equalizing the two proving rings before shearing. Also, small pieces of rubber were introduced between the tip of each proving ring and the torque arm to reduce the stiffness of the proving ring system. It was hoped that this would reduce the effect of any small eccentricity of rotation. In all these trials, no satisfactory measurement of residual strength was achieved.

Continuous monitoring of the tests suggested that there was some remolding taking place at the top of soil sample. This remolding might have happened because of the small clearance between the top platen and the lower platen (sample container), which is necessary for correct functioning of the apparatus. From these observations, ideas for modifications were developed. The concept adopted was to hold the top and bottom surfaces of the sample adjacent to the platens by means of vanes distributed uniformly on the top and bottom platens (Figure 5). Each platen was modified by the addition of 24 vanes, 3.0 mm (0.12 in.) high. Tests using this modified apparatus gave similar readings on each proving ring with a maximum difference of 3–4 percent, which can be attributed to the difference in stiffness of the two proving rings.

Two series of tests were carried out using the modified ring shear. In the first series, tests were performed on Lias clay using one normal stress and two different rates of shearing, 0.17 mm (0.0067 in.) per min and 0.017 mm per min. No significant differences were observed in the results for the two rates of shearing. In the second series, two sets of multi-stage tests were conducted to find the residual failure envelope at a rate of 0.017 mm per min.

The results showed the following features:

- Testing a sample under any given normal stress requires about 300–350 mm (12–14 in.) displacement to reach the residual state. When the sample is sheared again under a higher or lower normal stress, the displacement required to reach the residual stress is only 20–30 mm (0.8–1.2 in.). The multi-stage method is therefore much quicker.
- Only a little soil was extruded from the edge of the sample, so the problems of nonuniform stress distribution and decrease in sample thickness were not encountered.
- Each sample could be tested successfully under four different normal stresses using the multi-stage method.

- It was found that at low normal stresses, 30 kN/m^2 (4.4 lb/in.^{2}) or less, no residual state developed and no minimum shearing resistance was reached.

The total time required to establish the complete residual strength envelope using the recommended multi-stage method is not more than 15 days. With the modified apparatus there is the possibility of some side friction between the soil and the sample container. This friction is not believed to introduce significant errors, but it is hoped the apparatus will be modified again soon to eliminate this possibility.

Results

Reversal Shear Box

Figure 6 shows typical load displacement curves for the Lias clay using a 100 mm (3.94 in.) shear box at a shearing rate of 0.024 mm (9.4×10^{-4} in.) per minute. Each of the numbered shear stages represents a change of shear direction. The curves have a brittle peak characteristic at the early stages of testing (cycles 1 and 2), followed by the usual continuous drop in shear strength after the peak. The curves then show a tendency for the strength to drop a little at each reversal until after about six reversals a constant strength, defined as the residual state, is reached. This is defined as the residual state.

It seems that it is not sufficient to stop the test when a constant load value is obtained over a small displacement. The test should be stopped only when two consecutive compression or tension runs produce the same strength, within about 3 percent. It should be noted that the tension and compression loads seldom correspond exactly. This is thought to be due to the shape of the shear surface, and observations from these curves and others show that this variation between tension and compression runs can be as high as 5 percent. It seems that after a constant value of shear strength is attained in the fifth or sixth cycle, the curves sometimes show a saddle shape (curve 10 in Figure 6). Definition of the strength that represents the residual state is then difficult. The saddle shape indicates that after a minimum value is obtained, some increase in shear load may occur, and this increase may reach as much as 10 percent of the minimum value of shear strength. It is thought that this increase is due to the undulating shear surface.

The saddle shape does not appear in the sequence of curves in Figure 7, which represents the series of slow compression and tension cycles for a sample that has first been subject to fast forward and backward shearing as described earlier. The other obvious features of the curves in the latter case are that the number of reversals required to define the minimum shear strength of the clay is much reduced and that the peak strength observed in the first cycle is much smaller. A shortcoming of this method is that the peak strength cannot be determined, because it occurs during the fast shearing stage when the extent of pore pressure dissipation is uncertain.

Ring Shear

Typical load-displacement curves for Lias clay are shown in Figures 9 and 10. In continuous slow shearing (Figure 9), a displacement of more than 200 mm (8 in.) is necessary to reach the residual state, which takes more than 8 days at a speed of 0.017 mm/min. The test time can be reduced by using a variable rate of shearing as shown in Figure 10. As soon as the peak is reached, the rate of shearing is increased by 25 times for about 250 mm (10 in.). The rate of shearing is then reduced to the slower rate. No readings taken during the fast shearing are considered in determining the residual strength. Readings in the second slow stage were started after 8 hours to allow sufficient time for pore pressures to dissipate. In multi-stage tests, fast shearing is required only for the first normal stress.

Figure 11 shows a typical residual strength envelope for Lias clay, using the modified Bromhead ring shear at two different rates of shearing 0.017 mm/min and 0.17 mm/min (0.0067 in./min). The multi-stage method of testing was used for both rates of shearing.

DISCUSSION

The majority of investigators have shown that the shape of the residual failure envelope is curved for most clays. Skempton (*1*) states that for most clays, the relationship between residual strength and normal effective pressure is nonlinear. Thus when comparing the residual strength of one clay with another on the basis of other soil properties (clay fraction, liquid limit, plastic limit, etc.), it is best to fix a standard pressure that corresponds to the point on the envelope that shows a transition from a curved to a straight line.

Many investigators have tried to define this pressure. Skemption and Petley (*5*) stated it was 200 kN/m^2 (29 lb/in.^{2}), and the same finding was recorded by Hawkins and Privett (*11*). Townsend and Gilbert (*12*) gave an alternative figure of 150 kN/m^2 (22 lb/in.^{2}). Clay particles have a tendency to orientate themselves in a direction perpendicular to the direction of the major principal stress. Thus the shear strength of the clay in this direction is a minimum in comparison with shear strength in other directions. The mechanisms of shearing in both the ring shear and the shear box involve shearing on such a plane, consequently the shearing resistance along these planes should be at a minimum. The curved shape of the residual strength envelopes may be explained by the lesser degree of orientation of the clay at low normal stresses.

The results presented here for Lias clay show that residual shear strength is not developed at low normal pressure, notably at a pressure of 25 kN/m^2 (3.6 lb/in.^{2}), even if it is sheared over a displacement of more than 500 mm (20

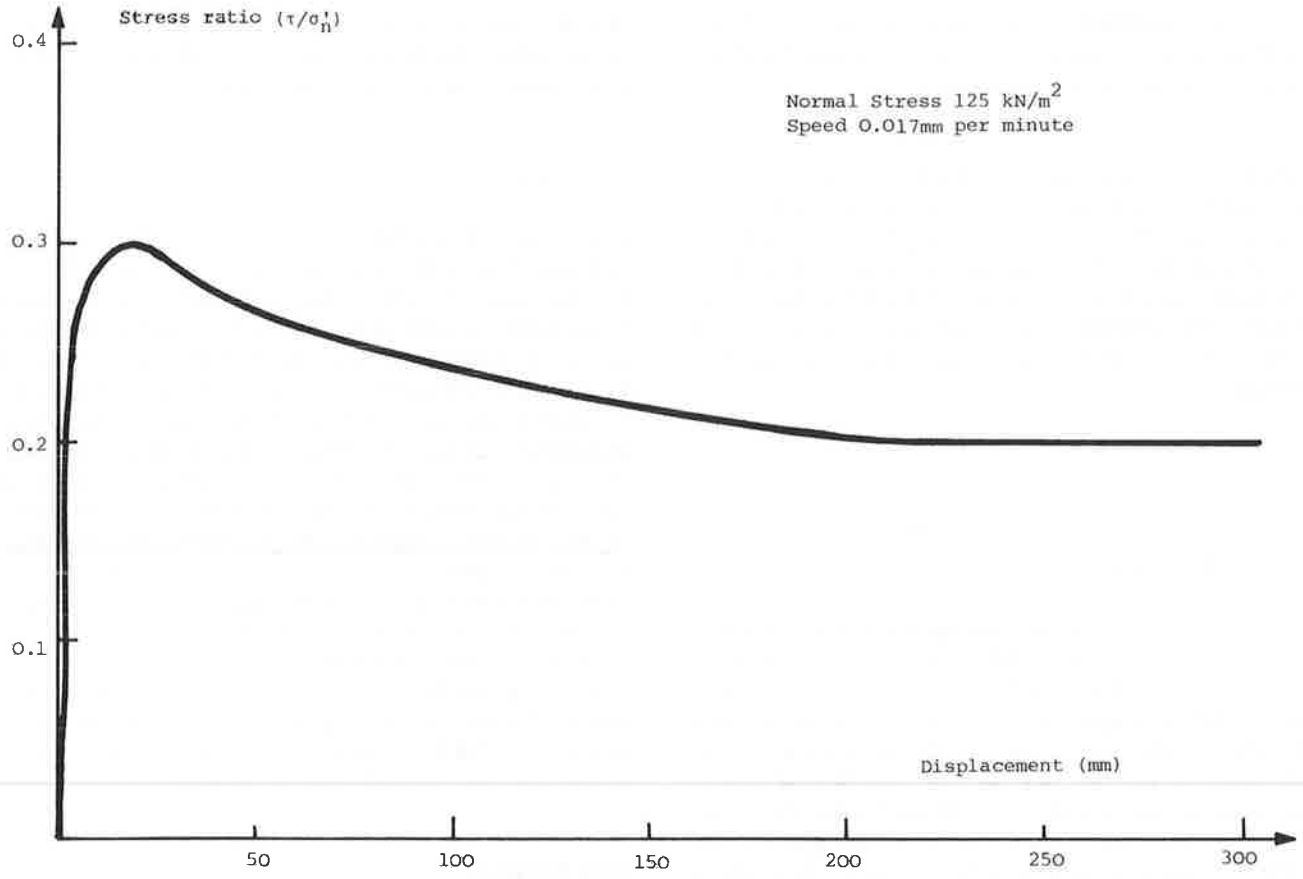

FIGURE 9 Stress-strain curve for Lias clay in ring shear apparatus at constant rate of shearing.

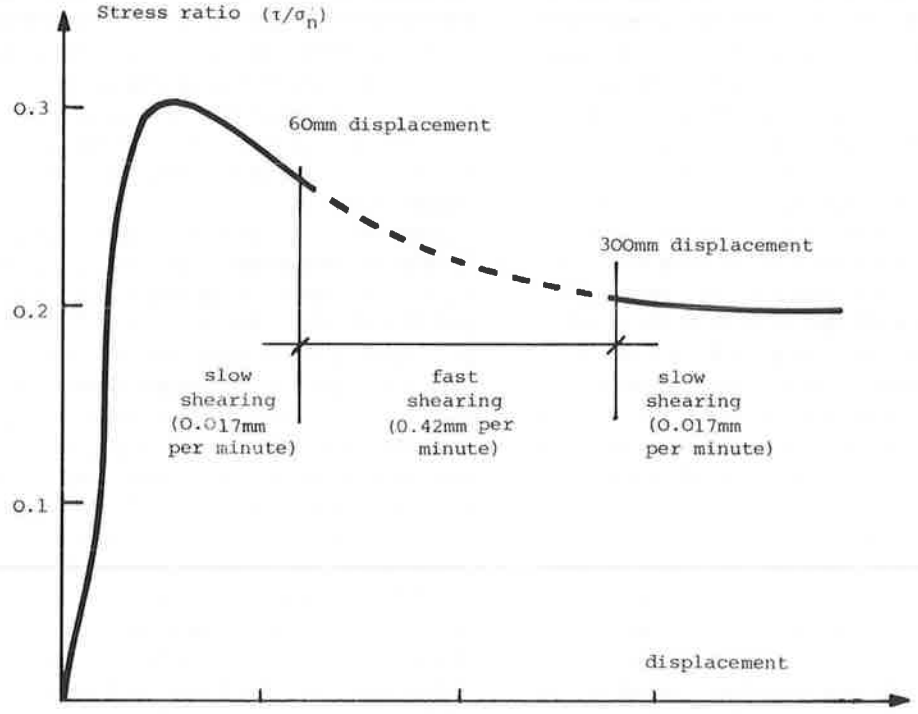

FIGURE 10 Stress-strain curve for Lias clay in ring shear apparatus at variable rate of shearing.

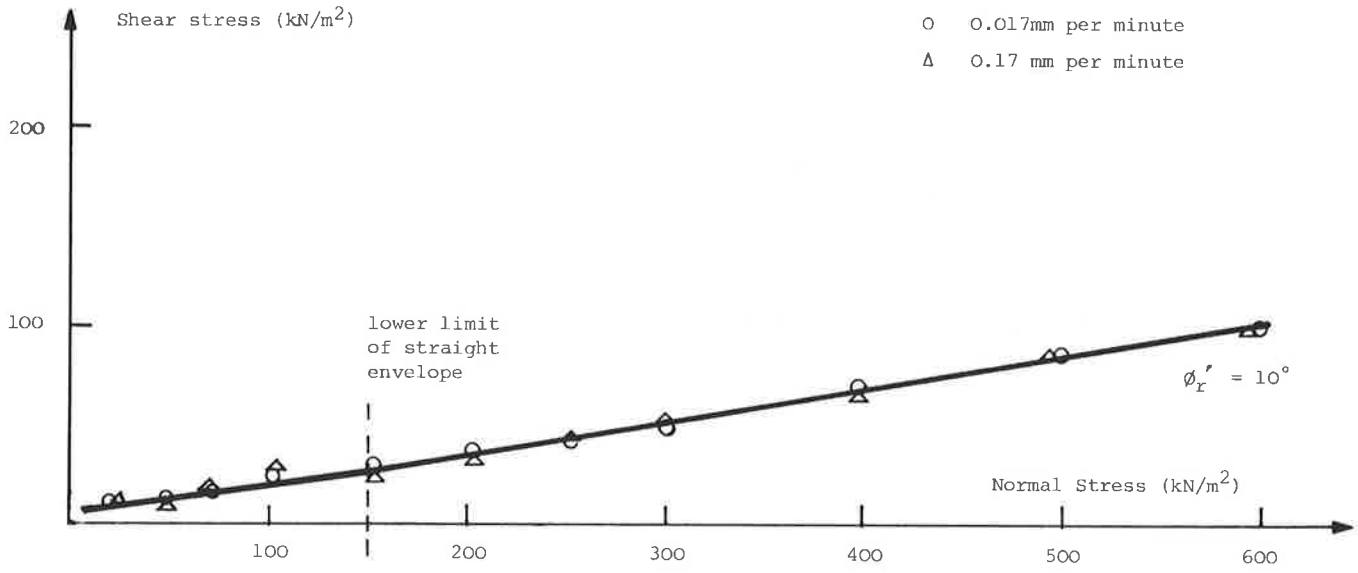

FIGURE 11 Residual strength envelope for Lias clay in ring shear apparatus.

in.). This finding is supported by results of Skempton (*1*) for London clay. These results shown that there is a considerable percentage difference between back analysis and test results at an average normal pressure of 30 kN/m^2 (4.4 lb/in.^{2}).

CONCLUSIONS

From the tests described above on remolded Lias clay, the following conclusions are drawn:

- The shape of the residual failure envelope is curved. This curvature is most pronounced at an effective normal stress below about 150 kN/m^2 (22 lb/in.^{2}). Such an effective stress seems enough to produce full clay particle orientation. Any increase of normal stress beyond this point will not result in any increase in the measured residual strength coefficient (τ_r/σ_n'). Small normal pressures of 25 kN/m^2 (3.6 lb/in.^{2}) were found to be inadequate to develop the residual failure surface for either test method.
- The use of fast shearing, to generate a failure surface, followed by slow shearing, for strength measurement, is the best technique for determining residual strength in both the shear box and the ring shear. This technique is preferred because it saves time and reduces the possibility of producing an undulating shear surface, which may lead to a greater shear resistance being measured.
- The shear box and ring shear both produce similar failure envelopes. However the measured value of residual strength angle, ϕ_r' seems smaller in the ring shear than the shear box. This difference is due to mechanical problems associated with the shear box, although larger samples may reduce this problem to some extent.
- Rates of shearing in the range of 0.01–0.2 mm/min were found to have no significant effect on the measured residual strength.
- In both of the devices, the initial moisture content and initial consolidation pressure were found to have no appreciable effect on the measured residual strength of the clay.
- In the ring shear apparatus, a displacement of over 200 mm (8 in.) is required to attain the residual state under the first normal stress. Under subsequent normal stresses, in the multi-stage method, the residual state can be attained at a displacement of only 20–30 mm (0.8–1.2 in.).

ACKNOWLEDGMENTS

The senior author is grateful to Boyce and Rogers for their helpful supervision and support throughout the work. Acknowledgments are extended to the staff of the Civil Engineering Laboratories at Loughborough University for their help and assistance in building the computer readout system and making modifications to the equipment.

REFERENCES

1. A.W. Skempton. Residual Strength of Clay in Landslides, Folded Strata and the Laboratory. *Géotechnique*, Vol. 35, No. 1, 1985, pp. 1–18.
2. A.W. Skempton. Long-Term Stability of Clay Slopes. Fourth Rankine Lecture. *Géotechnique*, Vol. 14, No. 2, 1964, pp. 75–102.
3. J.F. Lupini, A.E. Skinner, and P.R. Vaughan. The Drained Residual Strength of Cohesive Soils. *Géotechnique*, Vol. 31, No. 2, 1981, pp. 181–213.
4. A.W. Skempton and J.N. Hutchinson. Stability of Natural Slopes. *Proc., 7th International Conference Soil Mechanics*

and Foundational Engineers, Mexico City, State of the Art Volume, 1969, pp. 291–340.
5. A.W. Skempton and D.J. Petley. The Strength Along Structural Discontinuities in Stiff Clay. *Proc., Geotechnical Conference*, Oslo, Vol. 2, 1967, pp. 29–46.
6. G. Calabresi and G. Manfredini. Shear Strength-Characteristics of the Jointed Clay of Santa Barbara. *Géotechnique*, Vol. 23, No. 2, 1973, pp. 233–244.
7. A.W. Bishop, G.E. Green, V. K. Garga, A. Andresen, and J. D. Brown. A New Ring Shear Apparatus and Its Application to the Measurement of Residual Strength. *Géotechnique*, Vol. 21, No. 4, 1971, pp. 273–328.
8. D.P. LaGatta. Residual Strength of Clay and Clay Shales by Rotation Shear Tests. *Harvard Soil Mechanics Series*, Harvard University, Cambridge, Mass., No. 86, 1970.
9. E.N. Bromhead. A Simple Ring Shear Apparatus. *Ground Engineering*, Vol. 12, No. 5, 1979, pp. 40–44.
10. R.J. Chandler. Lias Clay: The Long Term Stability of Cutting Slopes. *Géotechnique*, Vol. 24, No. 1, March 1974, pp. 21–38.
11. A.B. Hawkins and K.D. Privett. Measurement and Use of Residual Shear Strength of Cohesive Soils. *Ground Engineering*, Vol. 18, No. 8, 1985, pp. 22–29.
12. F.C. Townsend and P.A. Gilbert. *Effects of Specimen Type on the Residual Strength of Clays and Clay Shales.* STP 599. American Society for Testing and Materials, Philadelphia, Pa., 1976, pp. 43–65.

Publication of this paper sponsored by Committee on Soil and Rock Properties.

Dynamic Analysis Using the Portable Pavement Dynamic Cone Penetrometer

KOON MENG CHUA AND ROBERT L. LYTTON

The Pavement Dynamic Cone Penetrometer [PDCP] considered in this study is similar to the one used in South Africa. In this study, the PDCP was used in conjunction with an accelerometer mounted at the extreme top of the device. Acceleration, velocity, and displacement histories were obtained. The force history was obtained by matching the measured acceleration peaks with that calculated using a numerical model of PDCP. The Fast Fourier Transform (FFT) technique was used to transform the information recorded in real time to the frequency domain. Spectral analyses were performed, and soil-damping characteristics were obtained for two pavement sections. The study shows that it is possible to determine the hysteretic and the viscous damping ratios in situ using the method of dynamic analysis described here.

The Pavement Dynamic Cone Penetrometer [PDCP] considered in this study is similar to the one used in South Africa and studied by Kleyn et al. (*1*). Traditionally, methods were developed for using the PDCP to predict the California bearing ratio (CBR) value of soils (*1–3*) and, more recently, the elastic modulus as well (*4*).

In this study, the PDCP was used in conjunction with an accelerometer mounted at the extreme top position. The accelerometer was used to record the dynamic characteristics of the PDCP. Velocity and displacement histories were obtained from the accelerations measured. Dynamic analyses were then performed in the frequency domain, and soil-damping characteristics were obtained for two pavement sections.

PAVEMENT DYNAMIC CONE PENETROMETER

Testing using the PDCP basically involved dropping a sliding hammer of about 17.6 lbs over a height of 22.6 in. to drive a steel rod of about 6.8 lbs into the ground. The depth penetrated by the 60-degree cone of tempered steel located at the lower end of the steel rod as a result of a single blow from the hammer is an indication of the material properties of the medium. Figure 1 shows the configuration of the PDCP. The PDCP measurements are reported in terms of the penetration index which is the penetration depth resulting from one blow of the hammer.

The PDCP is commonly used to determine the CBR values of soil. The relationships of the penetration index to the CBR values were obtained by driving the PDCP into a medium with a known CBR value in the field or into a medium contained in a CBR mold or a container with controlled confining pressure when done in the laboratory (*1–3*). This author (*4*) recently developed a relationship of the penetration index to the elastic modulus. The model assumes the soil medium penetrated in one blow to be a horizontal disc; and upon penetration, the cone tip displaces the soil, a radial plastic shock wave propagates in the disc, and plastic deformation takes place. The approach was motivated by the penetration theory presented by Yankelevsky and Adin (*5*).

DYNAMIC ANALYSIS: BACKGROUND

In performing dynamic analyses, it is common for practicing engineers to model a structural system as consisting of masses connected by springs and dashpots. Soil-structure interfaces are also modeled in a similar fashion. Under an excitation force, the springs will respond according to the magnitude of that force instantaneously while the dashpots respond according to the rate with which that force is applied. This is especially evident in soils, in which the response usually lags the excitation input. This behavior is accounted for by damping. The various types of damping will be discussed in subsequent sections.

Waves excited in the soil are a complex form of oscillatory movement propagating through a medium. By complex, it is meant that two components can best describe the phenomenon: the real component and the imaginary component, which is usually associated with the time lag of the response. It is also well known that transient compound oscillations can be represented as sums of harmonic oscillations by means of Fourier series or integrals.

Fast Fourier Transform

Data recorded in real time can be transformed to the frequency domain using the Fourier transform. The

Texas Transportation Institute, Texas A&M University, 501 CE/TTI Building, College Station, Tex. 77843.

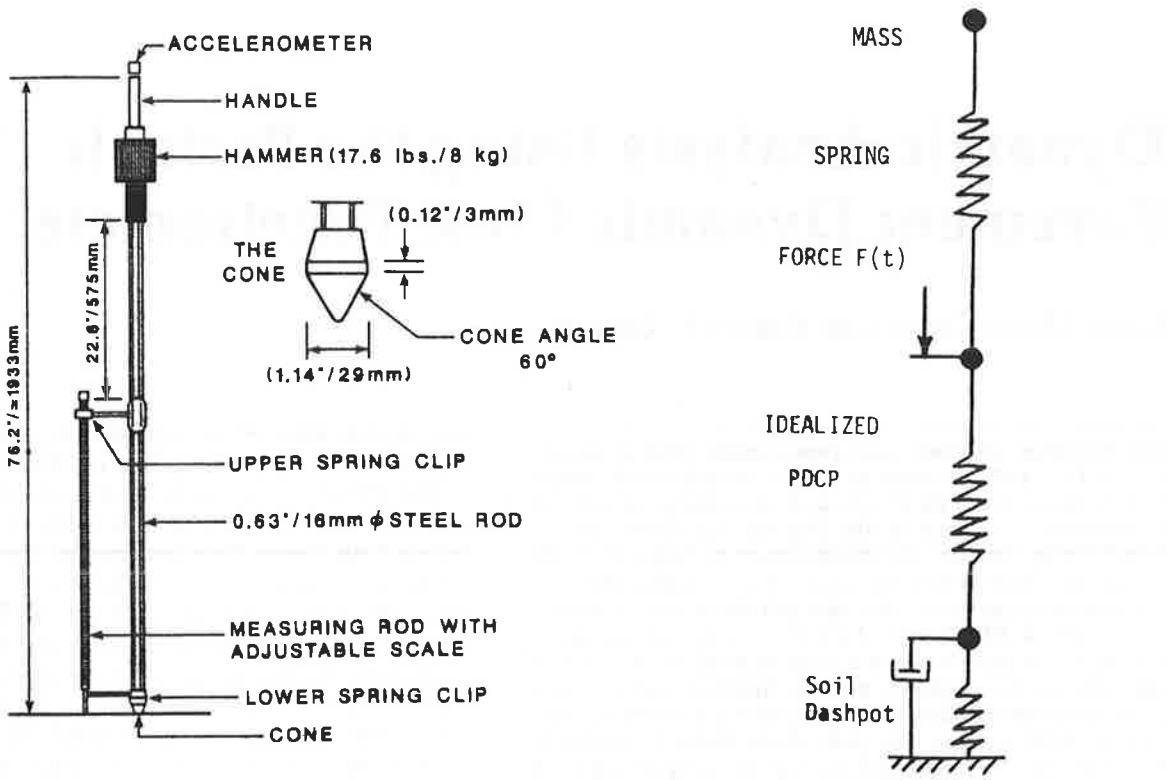

FIGURE 1 Pavement dynamic cone penetrometer.

Fourier transform of the function $x(t)$ is defined as

$$S_x(f) = \int_{-\infty}^{\infty} x(t) \exp(-2\pi i f t)\, dt \qquad (1)$$

where $S_x(f)$ = frequency domain representation of the function $x(t)$, and

$$i = \sqrt{(-1)}$$

If the function $x(t)$ is digitized, the above will be represented as a Discrete Fourier Transform [DFT] and is given by

$$S_x(m\Delta f) \doteq \Delta t \sum_{n=0}^{N-1} x(n\Delta t) \exp[-2i\pi(m\Delta f)(n\Delta t)] \qquad (2)$$

where

$S_x(m\Delta t)$ = digitized representation of the Fourier transform,
N = number of digitized points,
$t = 0, +/-1, +/-2 \ldots$, and
Δf = frequency interval between digitized points.

The time and frequency intervals are related by

$$\Delta f = 1/(N\Delta t) \qquad (3)$$

The Fast Fourier Transform [FFT] (*6*) technique is simply an algorithm that can compute the DFT much more rapidly than other available algorithms.

Damping

A dynamic system undergoing free vibration will eventually come to a halt. The system is said to have undergone damping, in which energy is being dissipated from the system. Damping is usually expressed as a damping ratio, which is the proportion of damping constant to the critical damping constant. A system with a damping ratio greater than 1.0 does not oscillate and is said to be overdamped. Conversely, an underdamped system will oscillate.

Damping is typically classified as structural or internal damping, viscous damping, dry damping, and negative damping. Structural damping is due to internal friction within the material or at connections between the elements of a dynamic system. This is usually explained by the hereditary theory, which attributes the loss of energy to the elastic delay by which the deformation lags behind the applied force. The latter is more commonly referred to as hysteretic damping and is thought to be independent of frequency. Viscous damping occurs, for example, in lubricated sliding surfaces, dashpots, and shock absorbers and is velocity- and frequency-dependent. Dry damping or Coulomb damping results from the motion of a body on a dry surface. The last and probably the least known is negative damping, which results when the nature of damp-

ing is such that instead of dissipating energy from the system, energy is added to it (*7*, pp. 123–125). However, linear viscous damping still occupies the major place in dynamic analysis, and as such, it is common to use equivalent viscous damping ratios (*8*, *9*) to represent the effects of hysteretic damping.

Complex Formulation of Damping

Consider the equations of motion of a structural system expressed in the matrix form. In the time domain, the equations of motion can be expressed as

$$[K]\{r\} + [C]\{\dot{r}\} + [M]\{\ddot{r}\} = \{R\} \tag{4}$$

where

$[K]$ = stiffness matrix,
$[M]$ = mass matrix,
$[C]$ = damping matrix,
$\{R\}$ = load matrix, and
$\{r\}$, $\{\dot{r}\}$ and $\{\ddot{r}\}$ = the displacement, the velocity, and the acceleration matrix, respectively.

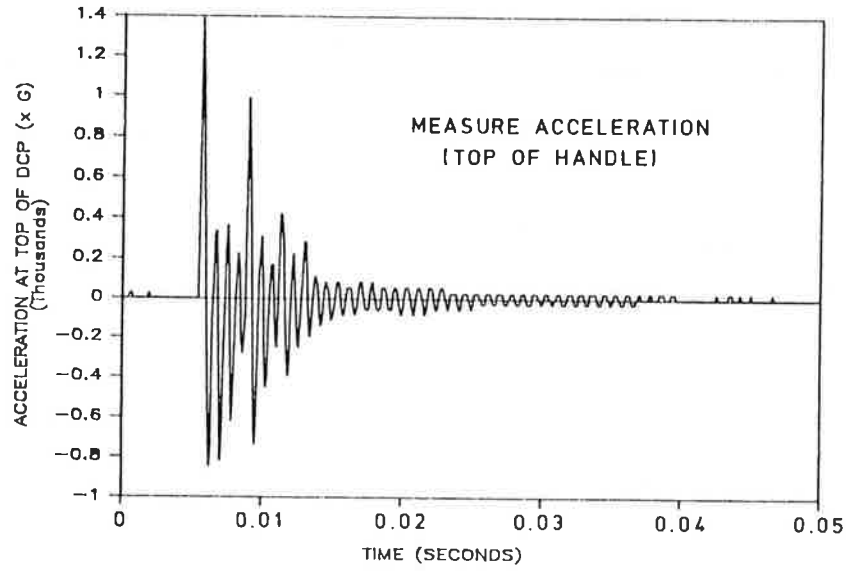

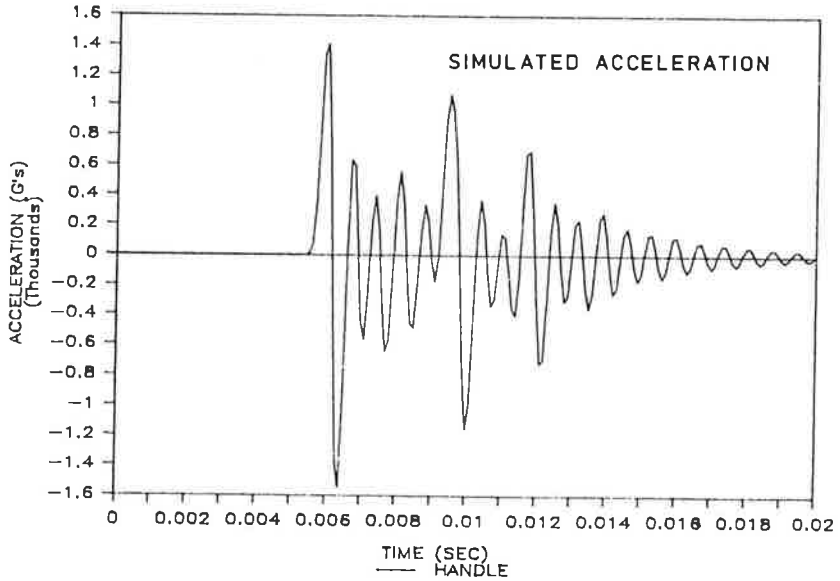

FIGURE 2 Comparing measured and simulated acceleration of the PDCP.

Transforming the above sets of equations into the frequency domain gives

$$([K] + i\omega[C] - \omega^2[M])\{U(\omega)\} = \{S(\omega)\} \quad (5)$$

where

ω = angular velocity (radians/sec),
$\{U(\omega)\}$, $\{S(\omega)\}$ = the Fourier transforms of the $\{r(t)\}$ and $\{R\}$, respectively.

The complex stiffness matrix $[K^*]$ is related to the stiffness and the damping by

$$[K^*] = [K] + i\omega[C_V] \quad (6)$$

where the subscript V refers to viscous damping.

In a single-degree-of-freedom system with both hysteretic and viscous damping, it has been shown (*10*) that the complex stiffness can be expressed by

$$k^* = k(1 + 2i\beta_H + 2i\beta_V) \quad (7)$$

and, if only hysteretic damping is present,

$$k^* = k(1 + 2i\beta_H) \quad (8)$$

where

β_H = the hysteretic damping ratio, and
β_V = the viscous damping ratio.

The above are two of the many models that have been proposed to describe damping. These will be compared

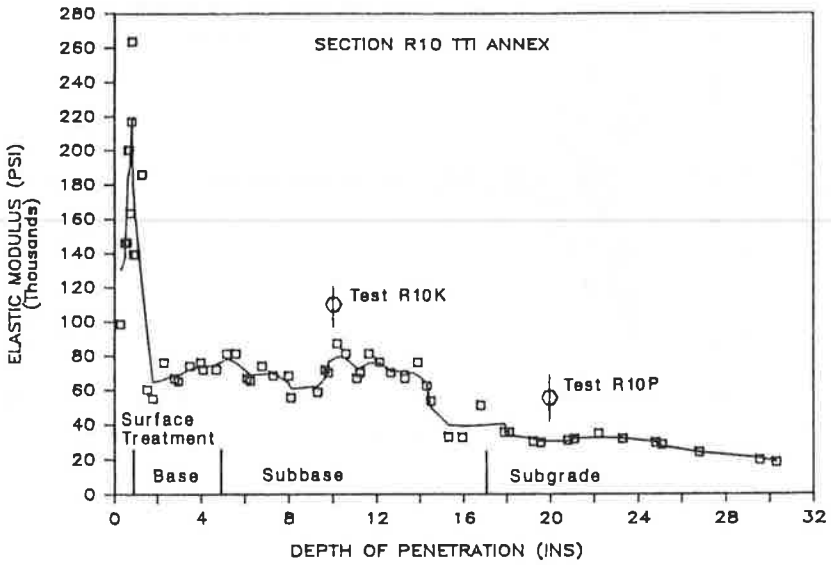

FIGURE 3 Layer characteristics and elastic modulus of section R10.

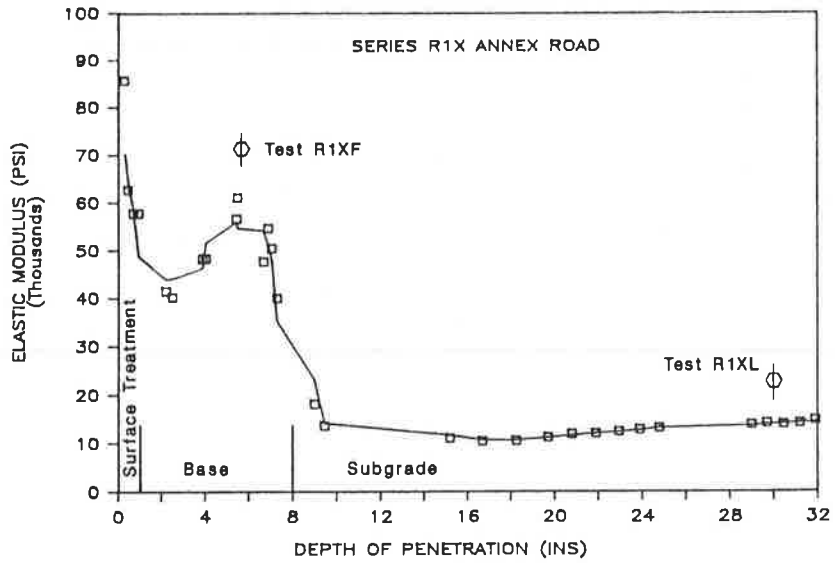

FIGURE 4 Layer characteristics and elastic modulus of section R1X.

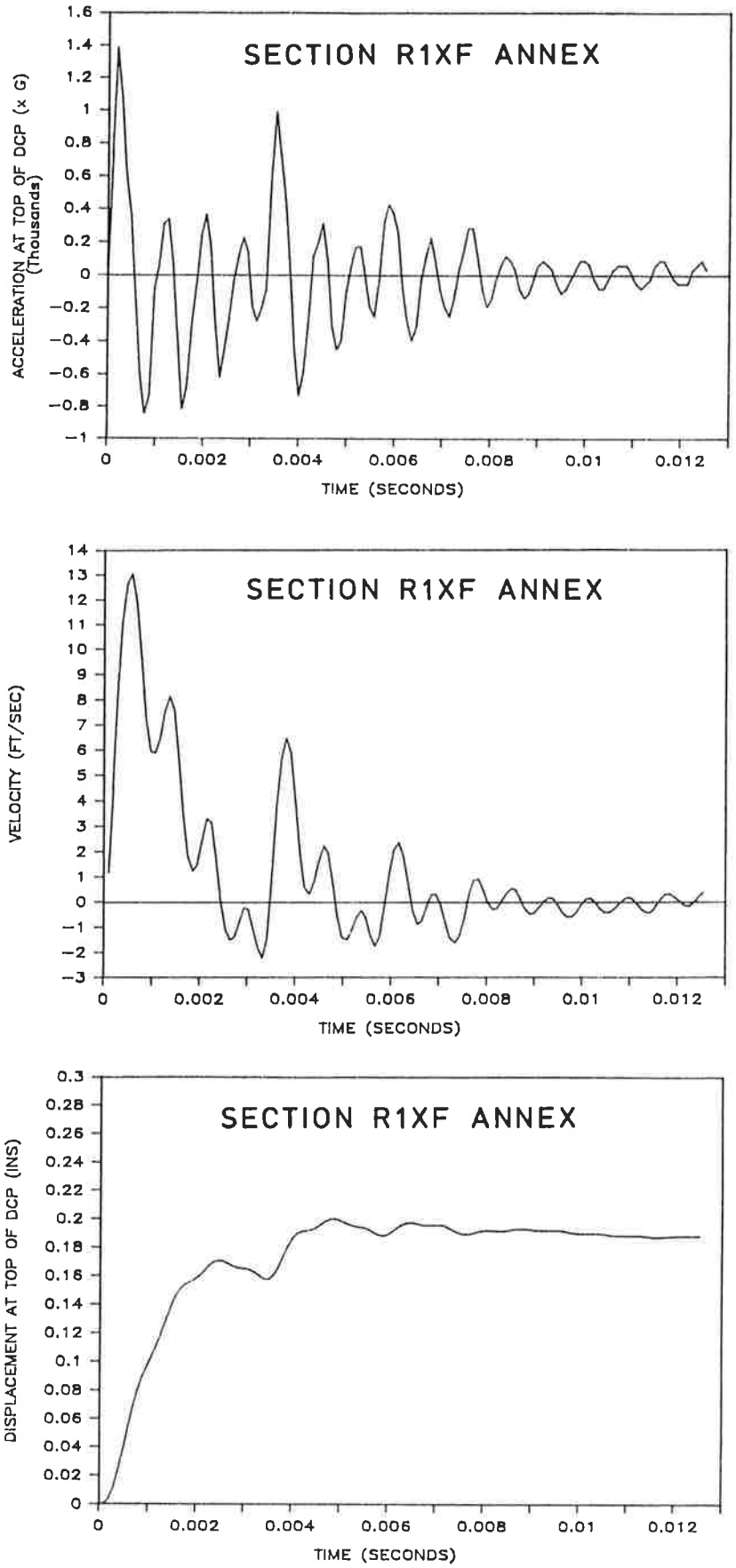

FIGURE 5 Typical acceleration, velocity and displacement histories of the PDCP in medium stiff granular base course material.

with field-measured ratios that will be presented in subsequent sections.

METHOD OF DYNAMIC TESTING USING THE PDCP

An accelerometer was screw-mounted onto the top of the handle of the PDCP (Figure 1). The accelerometer was rated for a shock of up to 100,000 G (where G is the gravitational acceleration) and up to 180 kHz. A 0.05-sec history containing 512 digitized points was recorded for each drop of the PDCP. The recording is triggered by the impact, and a certain amount of pre-impact history is also recorded.

The response considered here, which is the displacement history was obtained by double-integrating the acceleration history. The amplitudes of these impulses were obtained by matching the calculated acceleration peaks with the measured acceleration peaks for all the test cases considered. The calculated acceleration peaks were obtained using a computer program that models the dynamic response of the PDCP under impact load. The program is described below.

Numerical Modeling

To anticipate the dynamic response of the PDCP, a simple computer program was written to model the PDCP as a three-degree-of-freedom structure supported at the cone

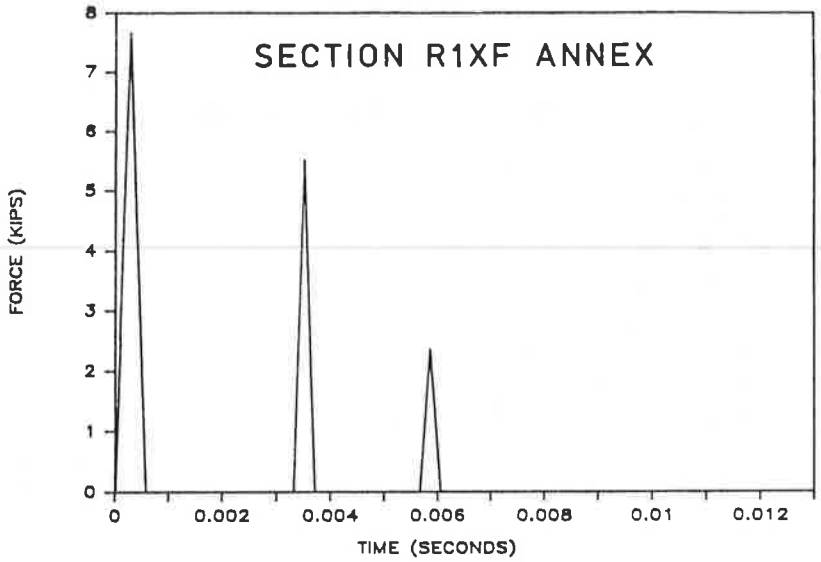

FIGURE 6 Typical calculated force history of the PDCP in granular base course material.

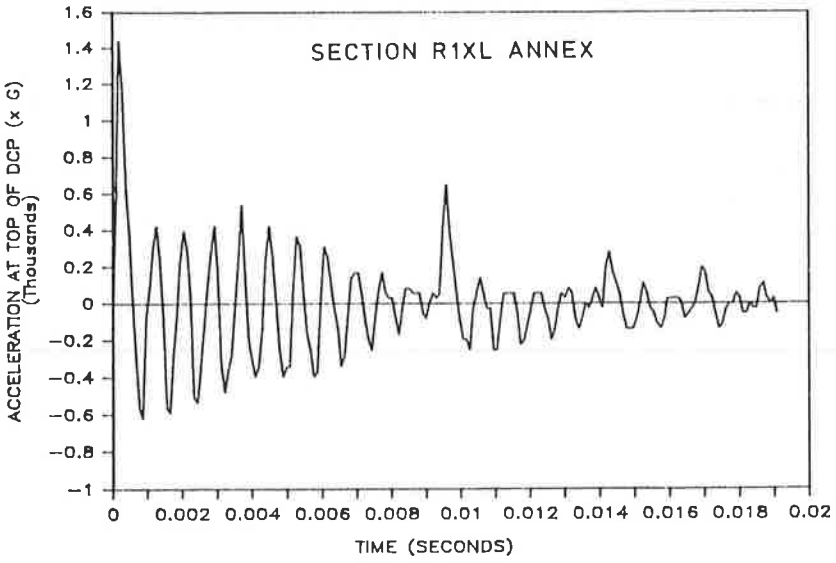

FIGURE 7 Typical acceleration history of the PDCP in silty clay subgrade.

tip by an external spring and a dashpot (Figure 1). It is assumed that the damping within the PDCP is negligible and that the system is damped mainly through the cone tip, which is the only part of the PDCP in contact with the soil.

The force history of the sliding hammer onto the middle of the PDCP consisted of impulses simulated as triangularly shaped force input over a short period of time. The several time periods during which the sliding hammer was in contact with the rod were obtained from the accelerometer reading. The amplitudes of the impulses were obtained by matching the calculated initial acceleration of the point in which the accelerometer was mounted (at the top of the handle) with that measured. The algorithm (*11*, pp. 387–402) performs the step-by-step integration of the equations of motion represented by equation 4 for a multidegree-of-freedom system using the linear acceleration method with the Wilson-θ modification. The latter serves to assure the numerical stability of the solution process regardless of the magnitude selected for the time step.

Figure 2 compares the calculated and the measured acceleration history of one of the tests. The period of the impulse (in this case, the first impulse peaked at 7.75 kips and occurred over 0.0006 sec) was obtained from the first measured acceleration peak. The positive acceleration refers to the downward direction.

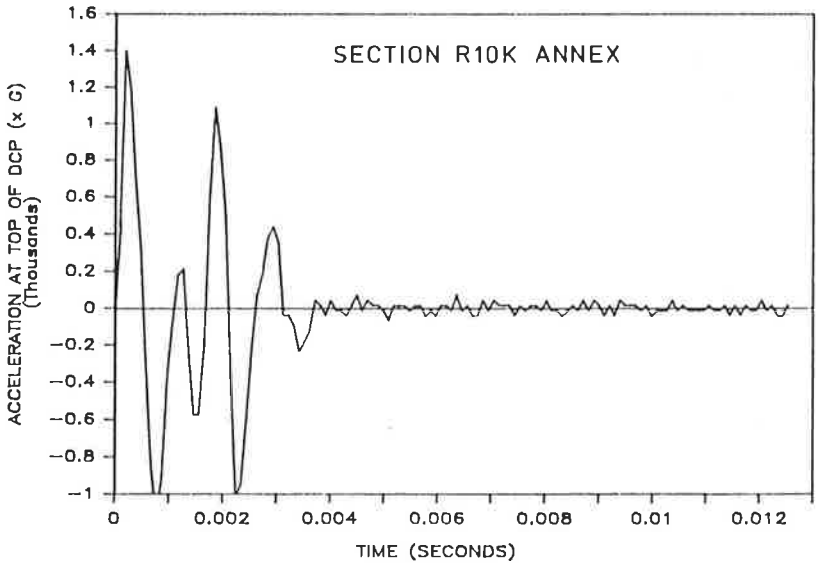

FIGURE 8 Typical acceleration history of the PDCP in stiff granular base course material.

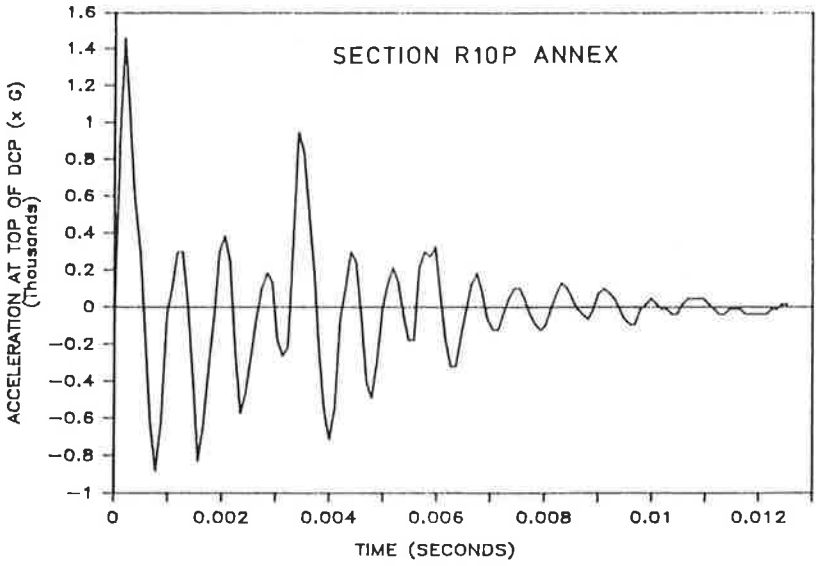

FIGURE 9 Typical acceleration history of the PDCP in sand-gravel subgrade.

Field Testing

Two pavement sections were used in this study. The section configurations and the interpreted elastic modulus profiles obtained using the method described in Chua (*4*) are shown in Figures 3 and 4. Both sections were located at the Texas Transportation Institute Test Annex. The first section, marked R10 (Figure 3), consisted of a 1-in.-thick surface treatment course, over a 4-in. base course and a 12-in. second layer of base of the same crushed stone materials. The subgrade is sand-gravel. Section R1X (Figure 4) is in an access road (near the test section facility) and is a surface-treated pavement with a 7-in. base course and a silty clay subgrade.

Figure 5 shows the acceleration, velocity, and displacement history of a test performed in a granular base course material (test R1XF) in Section R1X. The force history obtained using the numerical model described earlier is shown in Figure 6. Three other typical acceleration histories obtained are shown in Figures 7 through 9. The materials represented by these four tests are a stiff base consisting of crushed stones (test R10K), a loosely

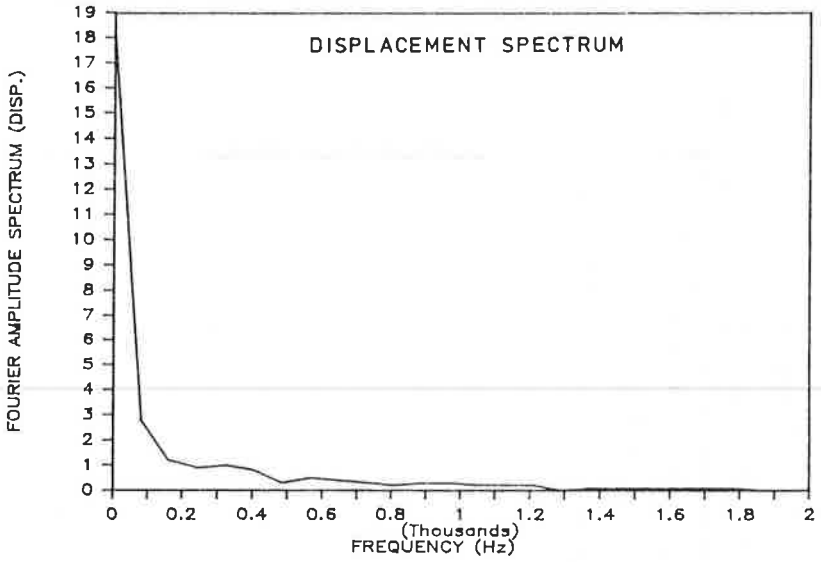

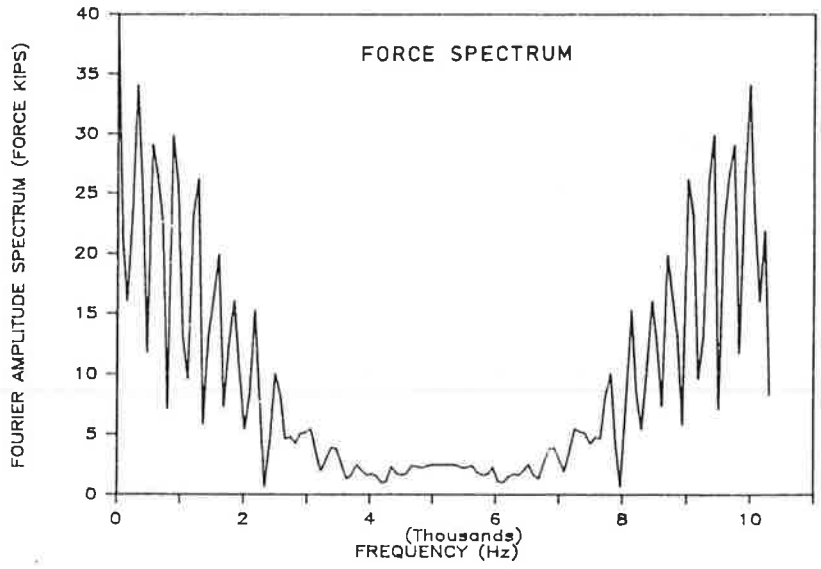

FIGURE 10 Typical PDCP displacement and force spectra.

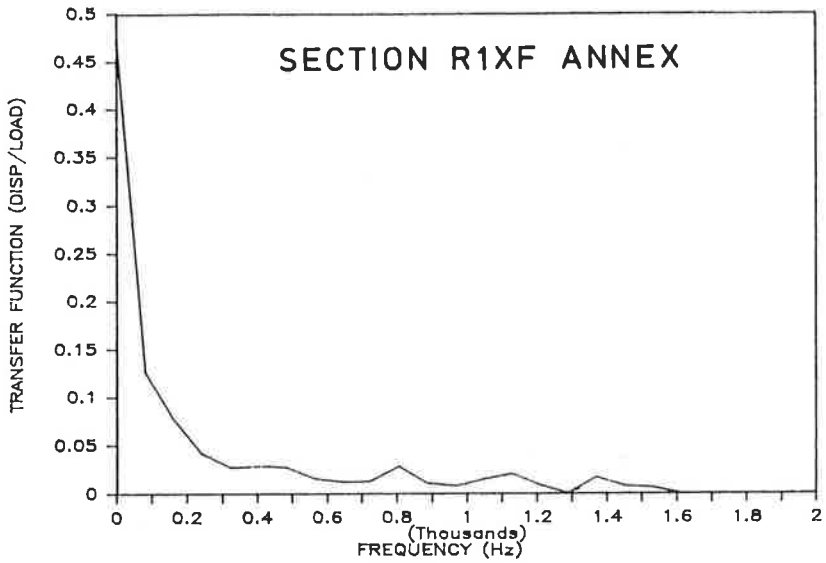

FIGURE 11 Typical transfer function in the frequency domain.

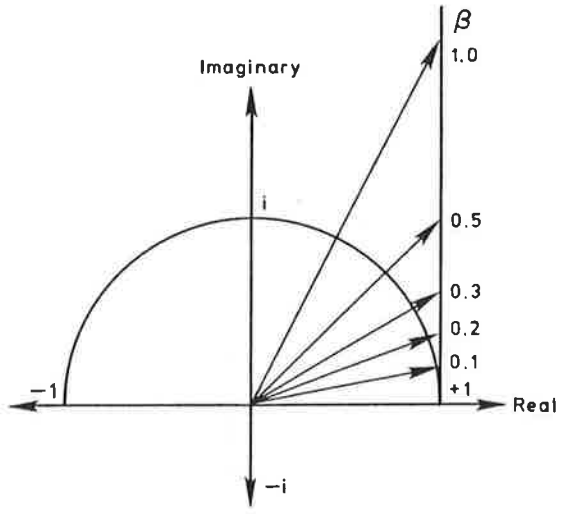

FIGURE 12 Complex damping ratio.

bounded base (test R1XF), sand-gravel subgrade material (test R10P), and a silty clay subgrade (test S1XL). The test identifications are given in parentheses and the respective depths at which the soil was tested are also shown in Figures 3 and 4.

Digital Signal Analysis

Continuing to use test R1XF as an example, the displacement history and the force history that were obtained were transformed into the frequency domain using FFT, and the resulting spectra are shown in Figure 10. In this example, only a period of 0.0124 sec (composed of 128 digitized points), which includes most of the predominant signals, was used because signals recorded before the impact and some times beyond this time period consist mainly of noise, and including them will introduce errors into the spectral analysis. The transfer function, which consists of each component of the displacement spectrum divided by the force spectrum at the corresponding frequency, is shown in Figure 11.

The damping ratio β, in accordance with equation 8 can be obtained from the two components of the complex transfer function by halving the tangent of the lag angle between the real and the imaginary component as shown in Figure 12. The damping ratios for the frequency spectrum obtained for the pavement materials in the two sections are shown in Figures 13 and 14.

DISCUSSION OF RESULTS

Dynamic Behavior of the PDCP

From the acceleration histories shown earlier, it can be seen that the sliding hammer struck the rod several times. In the case of the loose base course (test R1XF, elastic modulus of 60,000 psi), three blows were recorded. The time interval between impact can be seen to vary for different soil types. It can also be seen that the peak is at about 1,400 G for all cases, which implies that the first and most critical force impulse is very similar for all cases. This similarity can be expected because the impact, between steel and steel, occurs over such a short period of time that the whole system is not set in motion yet. This makes the determination of the force history (from the numerical model) a much easier one.

The velocity (referring to Figure 5), as expected, approaches zero with time. The measured displacement for all cases approaches a nonzero asymptote. This will differ from the prediction made using the simple numerical model because the latter assumed a linear elastic spring, whereas in the real case, plastic deformation occurs. For

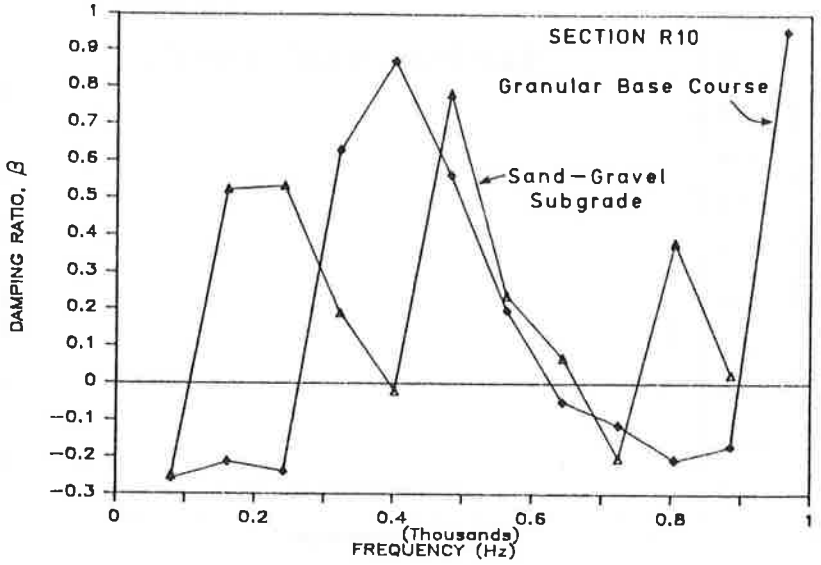

FIGURE 13 Damping ratios determined from spectral analysis for Section R1X.

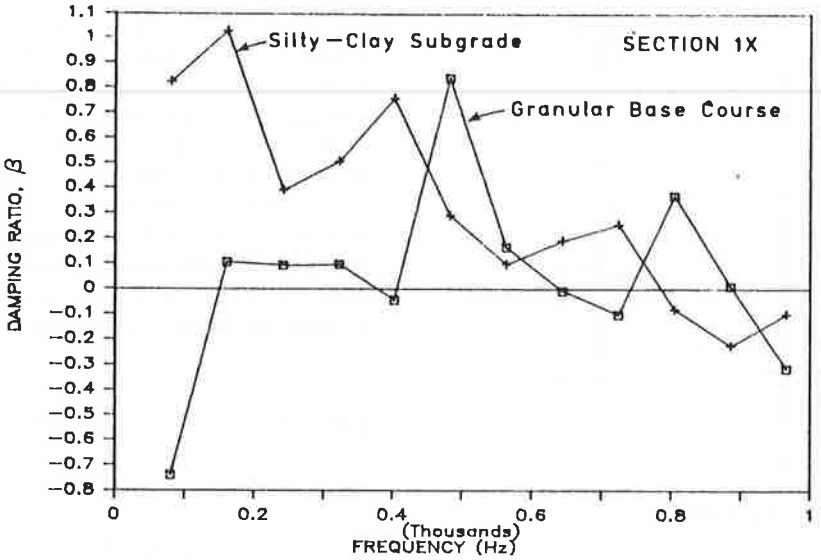

FIGURE 14 Hysteretic and viscous damping ratios.

the same reason, the numerical simulation will show the displacement approaching zero with time.

Damping Ratios

The predominant frequency band, identified from the transfer function spectrum for all the tests performed, was found to be from 0 to 1 kHz (Figure 11). This means that data manipulation performed within this range will be fairly accurate.

Referring to Figures 13 and 15 and assuming that all the damping in the system is due to the hysteretic damping from the soil, the damping ratios obtained suggest that negative damping does exist. While it is not possible at this time to account for this phenomenon (negative damping), it appears that the mean of the damping ratios over the 1 kHz range is still in the positive range. The mean damping ratios for the two base course materials tested were found to be 0.04 and 0.16. The damping ratio for the sand-gravel and the silty clay subgrade was found to be 0.33 and 0.21 respectively. These damping ratios were averaged over the 1 kHz range and assumed to be independent of frequency, as is described by equation 8. These averaged damping ratios are in the range expected of materials such as these (*12*). However, their obvious dependence on frequency suggests further inquiry.

If equation 7 is used, that is, the viscous damping ratio is linearly dependent on the angular velocity or the frequency, then by fitting a line through the data shown in

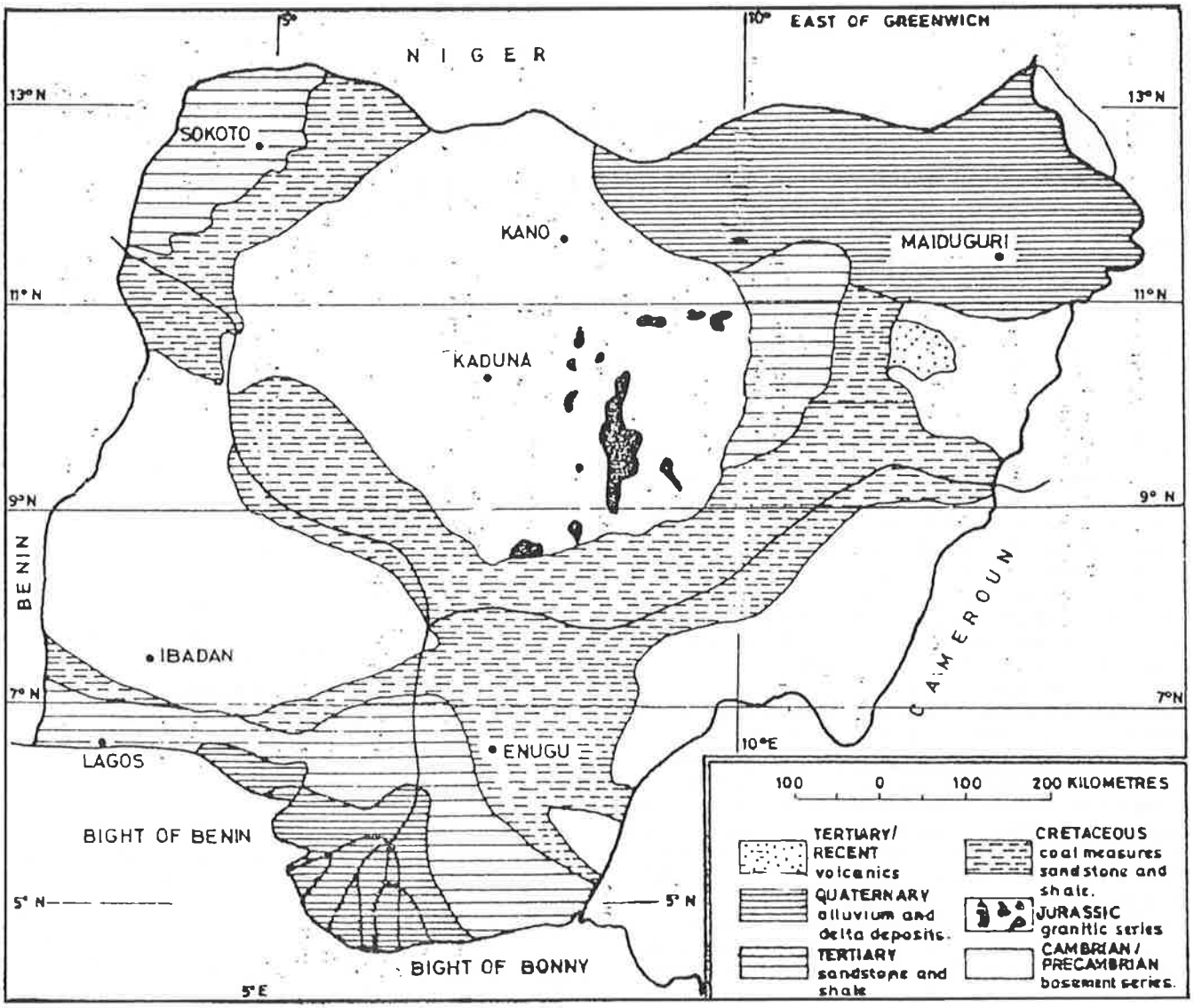

FIGURE 1 Geological map of Nigeria.

tically pitted or vesicular appearance of massive laterites, although termites have also been credited with causing the pitting.

The leaching in solution of colloidal silica and alkalis leaves a residue, which is relatively rich in hydrated oxides of aluminum, iron, and titanium. This iron enrichment produces the red color typically associated with laterite soils. There are, of course, some soils that do not owe their coloration to laterization. Also, the bonding effect of the iron oxides often produces a soil matrix with low compressibility, high permeability, and high angle of shearing resistance for these residual soils (*11*, *12*).

In situ laterites often have a cap rock of cuirasse or iron stone below the softer products of weathering, due to the increasing degree of saturation of the percolating water and the consequent reduction in the rate of solution as it travels downward. This process of weathering takes place everywhere in the country except in the low lands of the extreme southern part where the average annual rainfall is more than 200 cm (80 in.), where mangrove swamp vegetation occurs, and along the flood plains of the many rivers running north-south from the highlands.

In the far northern areas above latitude 11 degrees north, where annual rainfall is generally less than 75 cm and savannah vegetation predominates, the existence of basalts and other tertiary volcanic rocks has led to the formation of high activity clays (vertisols) characterized by extreme shrinkage and swelling characteristics. These are the local black cotton soils and clay shales of northern Nigeria, as found in parts of Bauchi, Borno, Gongola, Kano, and Sokoto states. These soils have been discussed in the literature (*8*, *10*, *13–16*).

CLASSIFICATION

Residual soils are ill defined and of variable origin, which makes their classification difficult. Soil samples may in-

Engineering Characteristics of Some Nigerian Residual Soils for Highway Construction

JOSEPH B. ADEYERI

The engineering characteristics of residual soils from the three major geological zones of Nigeria are analyzed and discussed. The characteristics of the parent rocks seemed to have some influence on the observed textural differences among the three groups of soils. There was also a fair degree of correlation between weathering, as indicated by grain size, and their consistency and swelling characteristics. The group A soils, which are nonplastic and granitic in origin, compact well at relatively low optimum moisture contents. Their CBR values at natural moisture contents, which are lower than optimum, are much higher than those at their optimum moisture contents. The soils are considered suitable as base and subbase materials because they compact well and have high CBR values. The group B soils are sedimentary in origin and have a high plasticity and relatively low CBR values. Unlike the group A soils, their natural moisture contents are higher than their optimums. There appears to be some correlation between the natural moisture content and the maximum dry density. Their high plasticity may make it uneconomical to stabilize them with chemical additives. The group C soils are lacustrine in origin, have very low CBR values, and exhibit a high degree of swelling. Therefore they are not considered suitable as base and subgrade materials. However, appreciable improvements in the compaction characteristics and increases in CBR values were recorded when the soils in this group were blended with local sand.

Nigeria is bounded by the Atlantic Ocean on the south and by semidesert conditions along its northern fringe. The vegetation varies from dense equatorial forests in the south to desert scrubland in the north. The mean annual rainfall varies from more than 3,000 mm (120 in.) in the south to as little as 600 mm (24 in.) in the north.

Climatically the country can be divided into four regions: the subequatorial south, the tropical hinterland, the tropical continental north, and the high plateaus. The highest point is the Chappal Wade of the Gotel Mountains, which are close to the Cameroon border in the eastern part of the country, with an elevation of about 2,419 m (800 ft) above mean sea level. Generally the seasons group into a wet period from about mid-April to mid-October and a relatively dry period for the rest of the year.

The geographical spread of soils follows to a considerable degree the geology of the country, as can be seen on the simplified geological map of Nigeria (*1*) shown in Figure 1 and on the soil map shown in Figure 2. Residual soils constitute the largest proportion of engineering soils in the country. These soils derive from the intense weathering of the crystalline rocks of the basement complex, which underlies most of the country. The soils are predominantly laterites and/or lateritic soils.

FORMATION

Laterites and lateritic soils are fully described in the literature (*2–6*), as are the residual soils of Nigeria (*7–10*). Although there is not complete agreement on many details, it is generally agreed that laterites or lateritic soils are residual soils produced by in situ weathering and chemical decomposition of the parent rock under humid tropical conditions. Weathering starts with the physical breakdown of the parent rocks from differential expansion and contraction of the rock-forming minerals due to temperature variations. Rainwater, which contains dissolved gases from the atmosphere and organic acids from plant decay, penetrates the rock, causing chemical reactions between itself and the constituent minerals of the rock. Colloidal and soluble products of these reactions are leached to lower horizons or are removed altogether. Different parent rocks produce different residual soils, which have many common features and some important differences.

The less stable soluble rock minerals (e.g., biotite, felspars, and micas) are attacked in the weathering process, whereas the more stable minerals (e.g., quartz) are generally unaltered. The result is that the quartz content of some laterites may increase from about 35 percent by weight in the parent rock to more than 50 percent in some residual soils. As much as one-third of the original rock volume could disappear from the rock matrix by leaching accompanied by a corresponding reduction in density. This process is often cited as the cause of the characteris-

Ondo State Polytechnic, Owo, Nigeria. Current affiliation: Department of Civil Engineering, Howard University, Washington, D.C.

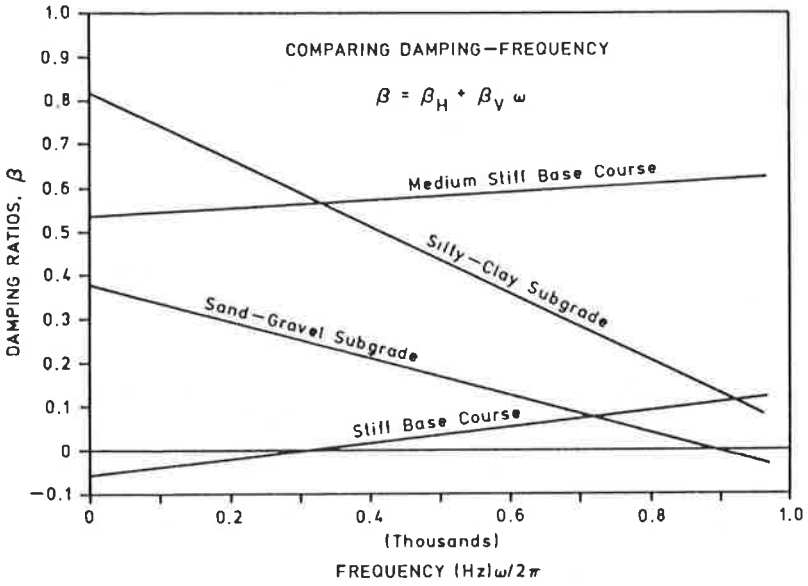

FIGURE 15 Damping ratios determined from spectral analysis for Section R10.

Figures 13 and 14, β_V and β_H can be found. Figure 15 shows the best-fit lines of the damping ratios for the four materials tested. Assuming that this model of viscous damping is correct, it appears that the hysteretic damping is proportional to the stiffness of the materials tested. The overall damping for the granular base course materials seems to increase with the frequency whereas the converse happens for the sand-gravel and the silty clay subgrade. The values of the hysteretic and the viscous damping ratios predicted for the various materials are shown in Table 1.

More likely than either of the foregoing simplified models of damping behavior in the base course and subgrade materials is the idea that the damping depends on the magnitude of the amplitude of movement at a given frequency as well as on the frequency itself. All of this suggests that the traditional methods of representing the damping properties of soils may need to be revised, and other implications of nonlinear vibrations need to be investigated. This makes the response of these materials nonlinear which can, in itself, explain the negative damping ratios that are known to occur with materials with softening stress-strain characteristics (*13*, pp. 439–452; *14*, pp. 130–154).

TABLE 1 DAMPING RATIOS OBTAINED FROM PAVEMENT DYNAMIC CONE PENETROMETER

Material Type	Damping Ratio β_H	Damping Ratio β_V	Remarks
Equation 9: $k^* = k(1 + 2i\beta_H)$			
Granular base	0.04	—	Test R1XF
	0.16	—	Test R10K
Sand–gravel	0.21	—	Test R10P
Silty clay	0.33	—	Test R1XL
Equation 8: $k^* = k(1 + 2i\beta_H + 2i\beta_V \omega)$			
Granular base	−0.06	0.000029	Test R1XF
	0.53	0.000014	Test R10K
Sand–gravel	0.38	−0.00006	Test R10P
Silty clay	0.82	−0.00012	Test R1XL

CONCLUSION

This paper showed typical acceleration, velocity, displacement, and force histories of the PDCP in operation. The data were recorded using an accelerometer mounted on the extreme top of the PDCP. FFT techniques were used to transform the information recorded in real time to the frequency domain. Spectral analyses were performed and damping values were obtained for the base course and the subgrade material in two pavement sections. It was shown that it is possible to determine the hysteretic and the viscous damping ratios using the method of dynamic analysis described here. The averaged damping ratios were in accord with published values.

The study also shows that it is possible to determine damping properties of pavement materials in each layer in a relatively nondestructive manner in situ. The study also shows that it is possible to measure damping values of coarse granular materials. Results indicate that the frequency response is not a single value entity as is often assumed.

As a further refinement of the method presented here, it is suggested that a second accelerometer be mounted on the sliding hammer to record the force history. Also, a more efficient data acquisition unit could be used to improve the sampling rate and thus improve the resolution, in order to reduce the frequency interval between digitized points.

REFERENCES

1. E. Kleyn, J.H. Maree, and P.F. Savage. The Application of the Pavement DCP to Determine the In Situ Bearing Properties of Road Pavement Layers and Subgrades in South Africa. *Proc., 2nd European Symposium on Penetrometer Testing*, Amsterdam, May 1982.
2. J.A. Harison. *Correlation of CBR and Dynamic Cone Penetrometer Strength Measurement of Soils*. Technical Note 2, Australian Road Research Board, Vol. 4, 1986.
3. M. Livneh and I. Ishai. Pavement and Material Evaluation by a Dynamic Cone Penetrometer. *Proc., 6th International Conference on Structural Design of Asphalt Pavements*, University of Michigan, Ann Arbor, July 1987.
4. K.M. Chua. *Determination of CBR and Elastic Modulus of Soils Using a Portable Dynamic Cone Penetrometer*. Paper No. 065. First International Symposium on Penetration Testing, Orlando, Fla., March 20–24, 1988.
5. D.Z. Yankelevsky and M.A. Adin. A Simplified Analytical Method of Soil Penetration Analysis. *International Journal for Numerical and Analytical Methods in Geomechanics*, Vol. 4, 1980, pp. 233–254.
6. J.W. Cooley, and J.W. Tukey. An Algorithm for the Machine Calculation of Complex Fourier Series. *Mathematics of Computation*, Vol. 19, No. 90, 1965, pp. 298–301.
7. T.H. Wu. *Soil Dynamics*. Allyn and Bacon, Inc., Boston, 1971.
8. W.C. Hurty and M.F. Rubinstein. *Dynamics of Structures*. Prentice-Hall, Inc., Englewood Cliffs, N.J., 1964.
9. J.M. Roesset, R.V. Whitman, and R. Dobry. Modal Analysis for Structures with Foundation Interaction. *Journal of the Structural Division*, ASCE, Vol. 99, No. ST3, March 1973.
10. J.T. Christian, J.M. Roesset, and C.S. Desai. Two- and Three-Dimensional Dynamic Analyses. In *Numerical Methods in Geotechnical Engineering* (C.S. Desai and J.T. Christian, eds.), McGraw-Hill Book Co., New York, 1977.
11. P. Mario. *Structural Dynamics: Theory and Computation*. 2nd ed., Van Nostrand Reinhold Co., New York, 1985.
12. H.B. Seed and I.M. Idris. *Soil Moduli and Damping Factors for Dynamic Response Analysis*. Report No. EERC 70–10. Earthquake Engineering Research Center, University of California, Berkeley, 1970.
13. E. Volterra and E.C. Zachmanoglou. *Dynamics of Vibrations*. Charles E. Merrill Books, Inc., Columbus, Ohio, 1965.
14. W.T. Thomson. *Vibration Theory and Applications*. Prentice-Hall Inc., Englewood Cliffs, N.J.

Publication of this paper sponsored by Committee on Soil and Rock Properties.

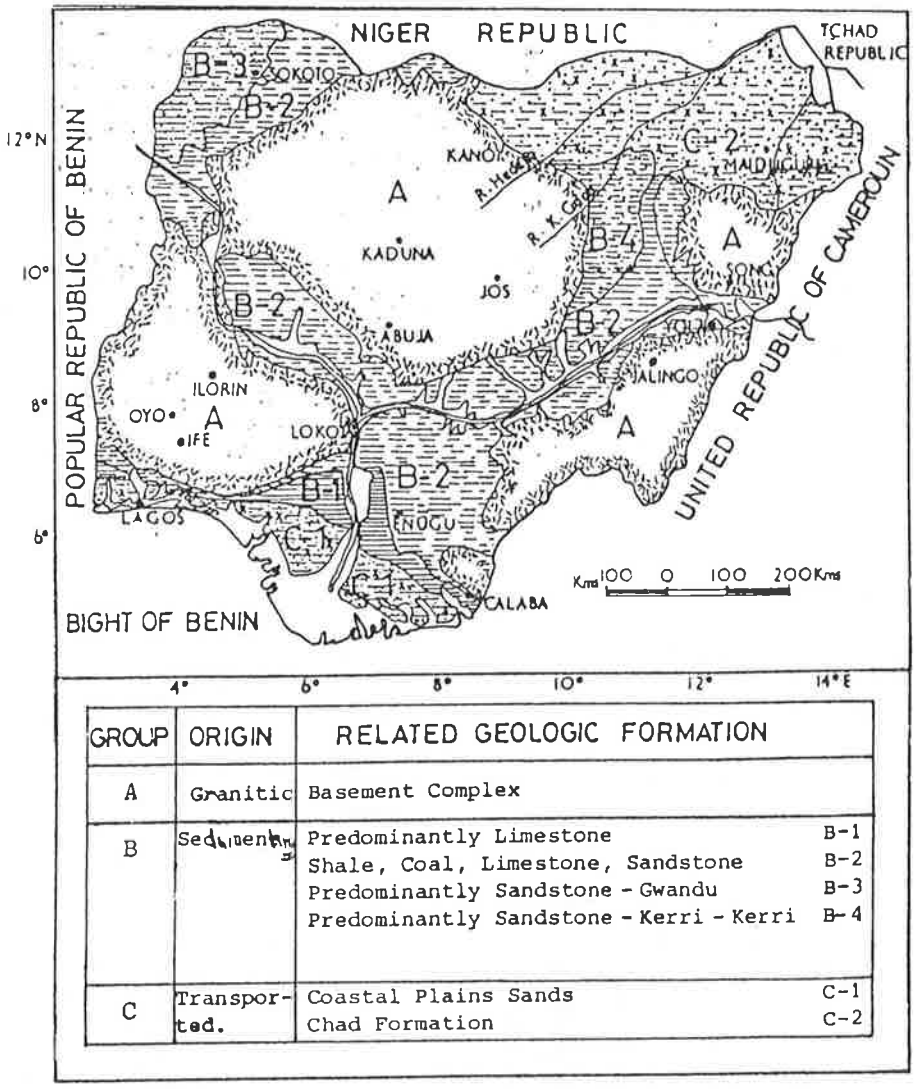

GROUP	ORIGIN	RELATED GEOLOGIC FORMATION	
A	Granitic	Basement Complex	
B	Sedimentary	Predominantly Limestone	B-1
		Shale, Coal, Limestone, Sandstone	B-2
		Predominantly Sandstone - Gwandu	B-3
		Predominantly Sandstone - Kerri - Kerri	B-4
C	Transported.	Coastal Plains Sands	C-1
		Chad Formation	C-2

FIGURE 2 Distribution of residual soils, based on geological formation.

clude materials reflecting different stages in the process of decomposition. Soil handling causes further breakdown, which can also affect the engineering properties of the soil. Many writers have discussed the difficulty of testing these types of soil without changing their in situ properties. Rao and Ouoleye (*17*) have presented data showing the effect of different treatments on the Atterberg limits of a Nigerian residual silty clay of sedimentary origin. Their study showed an irreversible reduction of plasticity on air-drying or oven-drying the soil, which they attributed to aggregation of the particles (Table 1). The liquid limit of the soil was found to vary from 32 to 94 percent, while there was a corresponding change in the plastic limit from 18 to 38 percent, depending on the type of treatment. These results confirm a similar earlier observation by Terzaghi (*18*) on the tests by R.H.S. Robertson of a Hong Kong laterite. Winterkorn and Chandrasekharan (*19*) similarly reported that the liquid limit of Matanzas clay from Cuba increased from 46 to 56 percent by remolding, although the plastic limit was unaffected.

TABLE 1 EFFECT OF HANDLING ON ATTERBERG LIMITS AND STRENGTH OF A NIGERIAN RESIDUAL SILTY CLAY

Sample Treatment	Atterberg Limits		Linear Shrinkage	Strength	
	LL	PL		Cu/P	0'
Natural state	75.0	38.0			
Air dried	94.0	31.0	20.6	0.41	22.5
Oven dried	81.0	34.0	17.5	0.45	28.0
With NaCl[a]	82.0	23.0	15.0	0.49	25.5
With $Na(PO_6)_3$[b]	32.0	18.0	5.0	0.56	34.5

[a]NaCl: Sodium chloride solution.
[b]$Na(PO_6)_3$: Sodium hexametaphosphate solution.

For the Nigerian residual silty clay, it was also found (Table 1) that handling has a pronounced effect on the strength parameters (c, 0). The usual classification tests for evaluating the textural and plasticity characteristics of temperate-zone soils may not be adequate, particularly for lateritic residual soils. Grading analyses are often used for

classifying normal residual soils from the same parent materials. The tests are very useful once their limitations are well understood and should be interpreted taking into consideration the origin (parent rock), mode of formation, and degree of weathering.

The grading analyses of residual soils (decomposed granite and rhyolite) from Hong Kong (*20*) and from some South American countries (*2*) confirm the wide range and variability of residual soils, showing that they can vary from red clay to cemented gravel. On the basis of field and laboratory experience with these soils, many investigators (*2, 12*) have texturally classified them into three main groups:

- Laterite rocks and boulders, which are cemented laterite rock and rock pieces that are used extensively in many African countries as concrete and road surfacing aggregates.
- Laterite and laterite-quartz gravels, which form the most important naturally occurring gravels and are extensively used as base and subbase materials in road construction.
- Laterite fine-grained soils, which have been given little attention in the past, but recent highway subgrade and shallow foundation failures have emphasized the importance of studying and understanding them. The magnitude of the clay fraction affects such properties as consistency, colloidal activity, compaction, specific gravity, and linear shrinkage.

The above textural groups reflect definite stages in the process of laterization.

CURRENT METHODS OF PAVEMENT DESIGN

Pavement design methods in Nigeria have been derived largely from the United Kingdom. The 1973 Nigerian Federal Highway Manual and the pavement design curves (*21*) have been adopted from the Transport and Road Research Laboratory, England (*22*). The design procedure requires estimating the daily traffic in terms of vehicles heavier than 29.8 kN (3 tons) loaded weight and determining the base and subgrade CBR. The base and subgrade materials must also meet required specifications regarding gradation and consistency.

The selection of the pavement structure is then made from CBR-versus-pavement-thickness charts (Figure 3), taking into consideration the expected loading of the pavement. The recommended minimum asphalt pavement thicknesses for roads in the country are as follows (vehicles

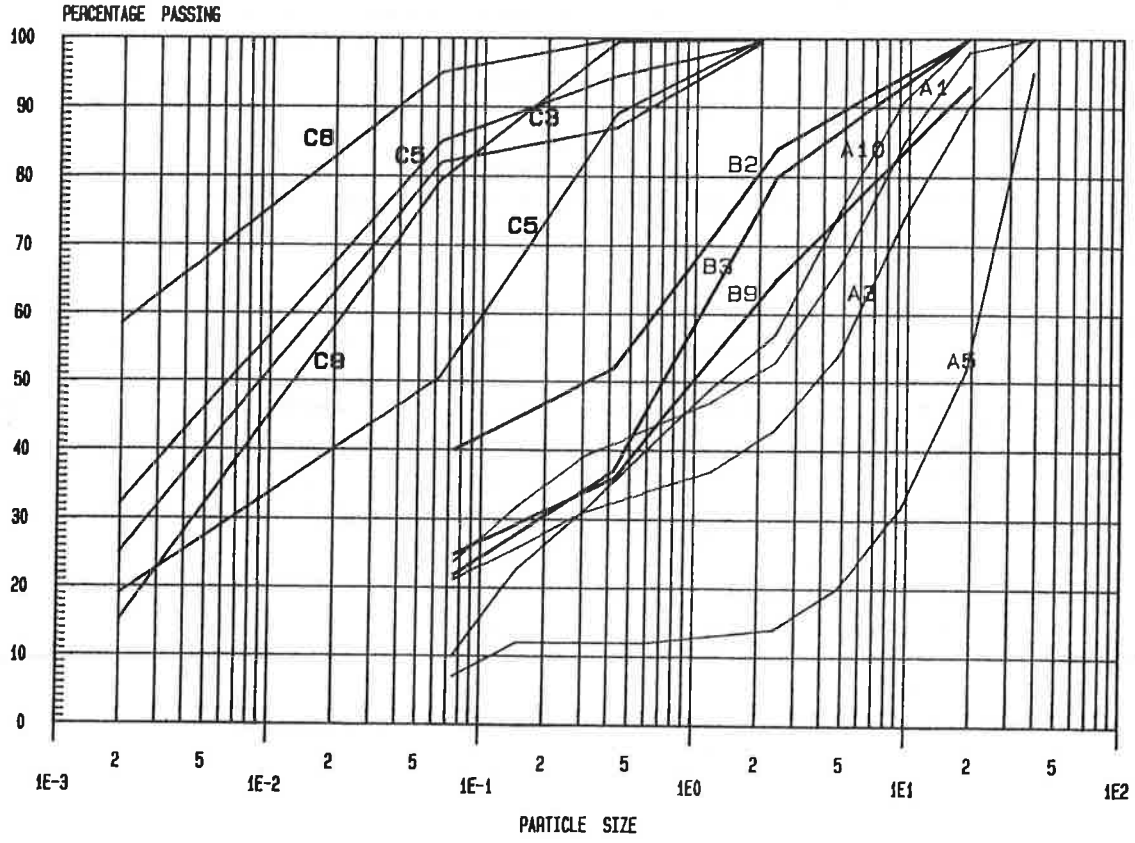

FIGURE 3 Grain size distribution.

are those exceeding 3,000 kg or 1,400 lb laden weight):

Traffic	*Vehicles per Day*	*Thickness (mm)*
Light	0–45	50
Medium	45–450	75
Heavy	450–4500	100

ENGINEERING PROPERTIES

For road construction purposes, the soil properties of primary interest are strength, consistency, gradation, permeability, compressibility, and swelling, from which secondary properties can be derived, e.g., bearing capacity and consolidation characteristics. Some of these properties will be considered for three soil types taken from three locations in Nigeria.

The three locations and the associated soil types (A, B, and C) reflect the three major geologic formations of Nigeria. Group A soils, from Kano State in northern Nigeria, are the weathering products of the basement complex and are granitic in origin. Group B soils, from Cross River State along the Ikom-Obudw road, are sedimentary in origin and are the products of weathering of limestone, shale, and sandstone rock, the decomposition products of which are finer than those of granite and the basement rock complex. Group C soils, from Borno state, lacustrine (quarternary lacustrine sediments consisting mostly of shales, clays, and sandy sediments) products of the Lake Chad formation. The soils from groups A and B are sometimes referred to as laterites and/or lateritic soils, while the group C soils are the local black cotton soils of northern Nigeria.

The data on soils A and B were obtained from the laboratory test results of borrow pits used in road construction in the two parts of the country. Some of these data have been considered by Aggarual and Jafri (*23*) and Sadiku (*24*). Some of the data on soils from group C were taken from published data by Madedor and Lal (*10*) in their work on the classification of Nigerian black cotton soils.

GRADING

The grading curves of representative residual soils from the three different parts of the country are shown in Figure 4. The median diameters (Md) range from 1 mm to 20 mm for the group A soils and from 0.3 mm to 1 mm for the group B soils, and the Md is less than 6 microns for the black cotton soils from Borno State (group C soils). It is not surprising that the black cotton soils are appreciably finer than the other soils. These are fine-grained and high-activity soils of the Lake Chad formation. The difference between the median sizes of the groups A and B soils can

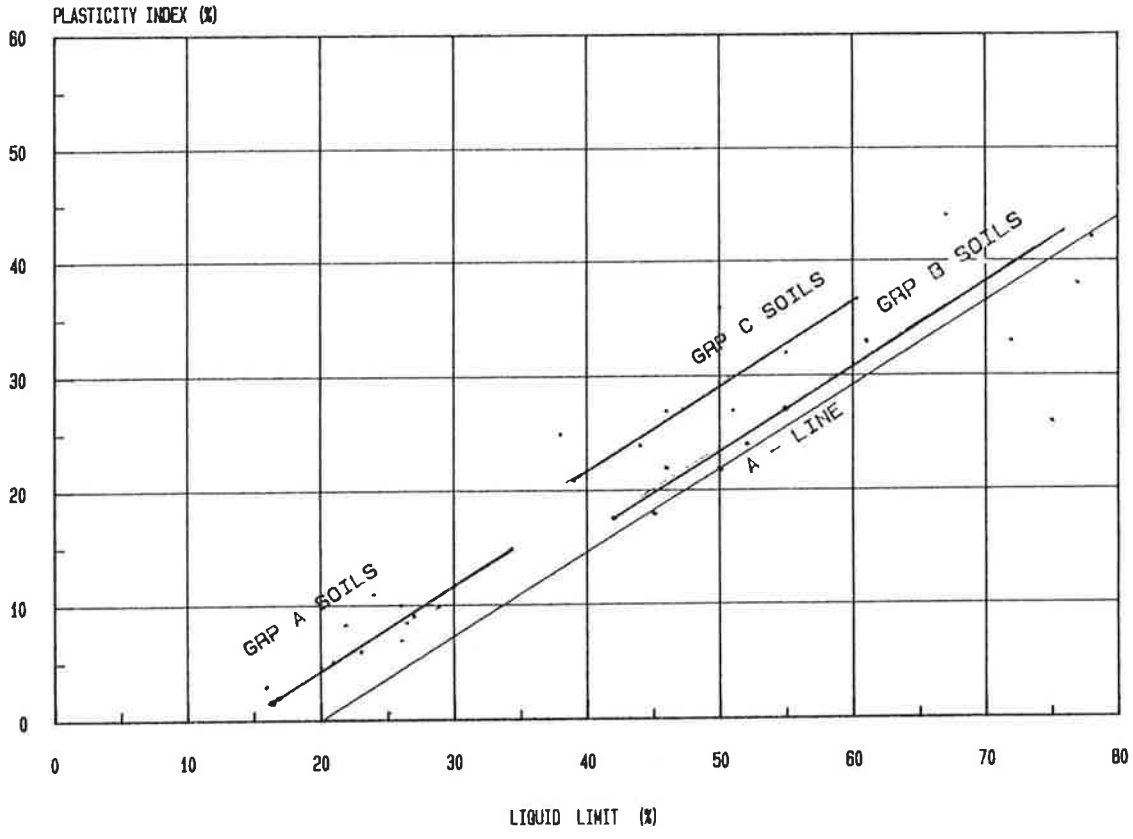

FIGURE 4 Casagrande plasticity chart.

be attributed to the parent materials. The group B soils were found to be predominantly of the A-7 group with a few in the A-2–7 group using the Public Roads Classification system, while group A soils fall under A-2. Although the texture of these three groups of soils is influenced to some extent by the degree of weathering, the petrographic characteristics of parent rocks seem to account more for the textual differences in the soils.

PLASTICITY AND ACTIVITY

The results of investigations into the plasticity characteristics of these soils are shown in Figure 5. The index properties of the soils were obtained on air-dried samples. The tests were performed in accordance with BS 1377, 1975 *(25)*. Also free swell tests were performed on group C soils in accordance with the USBR classification method. All the soils in groups A and C fall above the A-line on the Casagrande Plasticity Chart. They are all inorganic soils of low-to-high plasticity. The group A soils are generally of low plasticity. Most of the soils in group B are above the A-line, although a substantial number fall below the A-line, possibly due to the presence of mica in the soils *(26)*. The Atterberg limits of group B soils are often relatively high, with liquid limits ranging from 45 to 77 and plastic limits from 18 to 38. The percentage passing BS sieve No. 200 is relatively high for the soils of this group, but their relatively low swell in the CBR mold indicates that the clay fraction is apparently not active.

The black cotton soils are very plastic and are expected to present problems if used in road construction. Madedor and Lal *(10)* indicate that residual soils of the black cotton type show a fair correlation between weathering, as indicated by grain size, and other properties of the soil (i.e., free swell and plasticity index). This finding is in line with the findings earlier by Lumb *(20)* for Hong Kong residual soils. On the basis of the analyses of several tests, Madedor and Lal *(10)* derived the following empirical relations for free swell of the soils studied in terms of their index properties:

- Relation between swelling potential and liquid limit (*LL*)

$$FS = 1.93LL - 17.12 \quad (1)$$

- Relation between swelling potential and plasticity index (*PI*)

$$FS = 2.38PI + 13.44 \quad (2)$$

- Relation between swelling potential and clay fraction (*CF*)

$$FS = 1.92CF + 30.43 \quad (3)$$

It should be mentioned that the above equations are based on regression analysis and that there is a degree of subjectivity involved in drawing an "average" line for a mass of scattered data points which form the basis of these

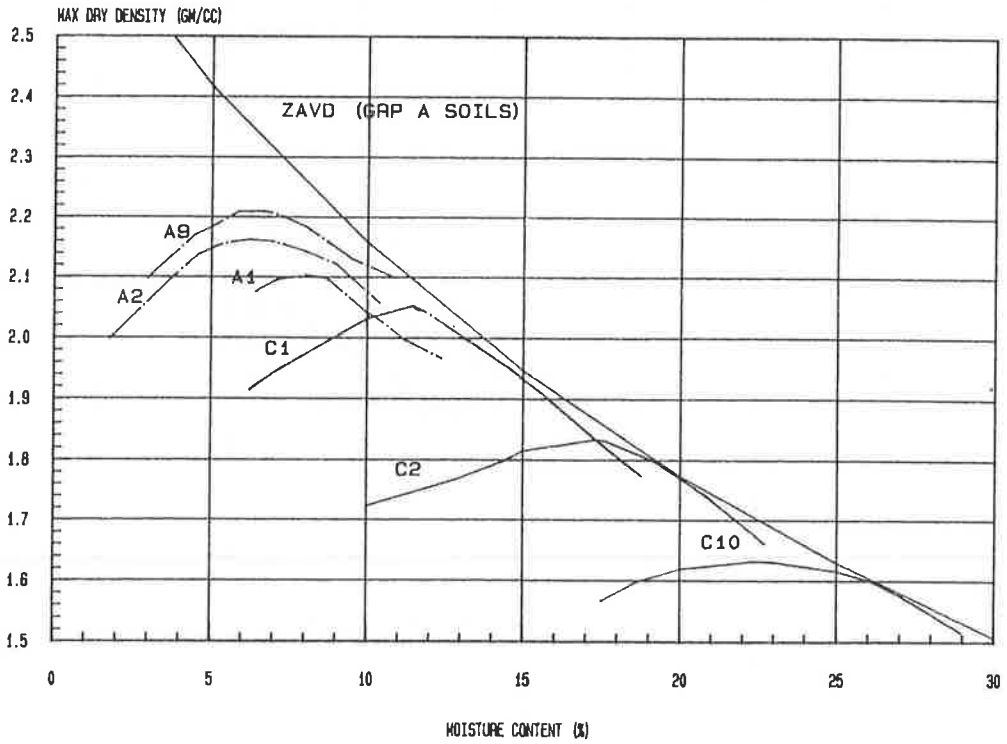

FIGURE 5 Moisture content versus density curves, Group A and C soils.

equations. However, of more importance is the summary of their conclusions:

- Low swell (i.e., ≤ 40%) when $LL < 30$; $PI < 15$ and $CF < 20\%$
- Medium swell occurs if $30 < LL < 50$; $CF > 20\%$
- High swell will take place for $LL > 50$, $CF > 20\%$, expected swell > 80%

In other words, free swell of the soils under consideration (i.e., group C) increases with liquid limit, plasticity index, or clay fraction.

STRENGTH CHARACTERISTICS

At present, very little data exist on the strength characteristics of Nigerian soils, although a number of investigations are being conducted. However, Ola (*16*) has presented some results on the residual strengths of some compacted lateritic soils, showing little or no difference in peak and residual angles of shearing resistance, which range from 30 to 39 degrees for the Nigerian residual soils and which are about 10 degrees for the black cotton soils from Maiduguri. Like all the other geotechnical properties, the strength of the residual soils is a function of the degree of laterization/weathering as well as a function of the parent material. Rao and Ouoleye (*17*) have further shown that the strength of these soils is affected by the type of treatment (Table 1).

Many studies have been made on the compaction characteristics of Nigerian residual soils as a result of the specification requirements for base and subgrade materials in road construction in the country. For the soils under study, the compaction and CBR tests were conducted in line with the general specifications (Roads and Bridges), Federal Republic of Nigeria Highways (*27*), which prescribe West African standard compaction or modified AASHO compaction for the design of highway pavements in Nigeria. The West African standard compaction employs the standard CBR mold, 25 blows per layer for 5 layers using a 4.5 kg rammer falling 45.7 cm. This standard was developed in the early sixties when it was found that the standard proctor specification was not adequate for highway construction in West Africa. Because of the heavy rains and consequent flooding of the roads during the rainy season, design CBR values are usually those of soaked samples. Soaking of compacted samples from 24 to 98 hr is usually specified depending on the part of the country. The compaction characteristics of the soils and the CBR test results are contained in Table 2. The compaction curves for the group A and group C soils are shown in Figure 6, while Figure 7 shows the variation of CBR values with moisture content for the group A soils.

The maximum dry densities for the group A soils are all above 2.0 gm/cc except for A-4. The soils compact well and have relatively low optimum moisture contents. The results of linear shrinkage tests on five of the samples varied from 1.5 to 6 percent, and the optimum moisture contents were within the range of 6 to 12.5 percent. It is noteworthy that the natural moisture contents are 2–3 percent below the optimum moisture contents for the soils in this group. The CBR values (after a 48-hr soaking period) are relatively high (55–94). From the CBR curves (Figure 7), it can be seen that as the moisture content decreases below the optimum, the CBR value increases sharply; some increases are more than 100 percent when the moisture content is only 1–2 percent below the optimum moisture content. This observation points to the possibility of more economical pavement design on the basis of compacting the soils at moisture contents below the optimum if the pavement is well drained, especially in northern Nigeria with an average annual rainfall of about 750 m or less.

The good-to-excellent condition of the road pavements, based on visual inspection and surface deformation measurements after more than 5 yr of use (Table 2), is an additional indication that group A materials are good for road construction even when the CBR values at the optimum moisture content are less than 80 percent, the minimum specification of the Federal Ministry of Works. The inspection consisted of observing each section of the pavement for cracking, rutting, pot holes, and ridability. The surface deformation of the sections of the roads inspected met the Federal Ministry of Works General Specification (*27*), clause 6314, on "Final Surface of Carriage," which states that the accuracy of finish in the transverse profile shall not vary at any point by more than 0.63 mm. It should be mentioned, however, that the light-to-medium traffic in the zone A area must have affected the good ratings the roads (Table 2) received.

The maximum dry densities of the group B soils are low, varying from 1.33 to 2.0 gm/cc, while the CBR values ranged between 7 and 19 percent. The swell after a 48-hr soaking is generally low. The optimum moisture contents are relatively high, up to a maximum of 42.6 percent for soil B–5. However, unlike the natural moisture contents for group A soils, the natural moisture contents for the group B soils range from 8.1 to 58.2 percent and are generally higher than the corresponding optimum moisture contents. For this group of soils, the natural moisture would appear to be more critical than the optimum, justifying the present practice of basing design on soaked CBR values.

A plot of the dry density when compacted at optimum moisture content versus natural moisture content is shown in Figure 8. There seems to be a fairly good correlation between the dry density at optimum moisture content and at the natural moisture content. An approximate value of the dry density at optimum moisture content can be predicted from the natural moisture content, using Figure 8 for the group B soils or soils exhibiting similar compaction characteristics.

The dry density at optimum moisture content of the group C soils ranged from 1.53 gm/cc to 2.07 gm/cc. The soaked CBR values (4-day soaking) are very low (2–5 percent). This confirms the expectation that the soils in

TABLE 2 CONSISTENCY LIMIT AND COMPACTION TEST RESULTS

			Gradation % Passing		Consistency Limits					Compaction							
NO.	Type	Group Classification	75μ	2μ	LL	PL	PI	GI	LS	OMC	MDD	CBR at OMC	MAX Swell	Free Swell	Organic Content	Condition of Pavement
1	A1	A-2-6	24		24	13	11	0	6	8.6	2.10	94				Good
2	A2	A-2-4	21.3		26.5	18	8.5	0	4.4	6.6	2.17	64				Good
3	A3	A-2-4	38		21.9	13.5	8.4	0	3.5	8.3	2.08	61				Good
4	A4	A-2-4	35		26	19	7	0	5.1	12.1	1.99	55				Good
5	A5	A-2-4	7		16	13	3	0		7.1	2.15	75				Good
6	A6	A-2-4	11		27	18	9	0	3.5	8.2	2.18	60				Good
7	A7	A-2-4	19		28.9	18.9	9.9	0		8.8	2.19	88				Good
8	A8	A-2-4	14		20	15.3	4.7	0		6.2	2.20	104				Exc.
9	A9	A-2-4	24		22.5	16.4	6.1	0		7.8	2.21	87				Exc.
10	A10	A-2-4	10		20.9	15.7	5.2	0		8.0	2.17	60				Exc.
11	B1	A-7-5	95		77	39	38	20		35.5	1.33	11	1.0		0.33	NMC (B) 40
12	B2	A-7-6	40		61	28	33	7		14.9	1.74	9	3.8		0.00	18.5
13	B3	A-2-7	22		46	24	22	1		10.7	2.00	18	0.9		0.83	8.1
14	B4	A-7-5	98		72	39	33	20		34.3	1.32	10	2.5		0.61	42
15	B5	A-7-5	98		75	49	26	19		42.6	1.23	7	0.9		0.81	37.2
16	B6	A-7-5	94		72	39	33	20		37.6	1.29	13	1.0		0.78	40.4
17	B7	A-7-6	43		50	28	22	5		16.7	1.78	11	0.00		0.00	15.3
18	B8	A-7-6	37		45	27	18	2		12.4	1.85	12	2.8		0.00	16.2
19	B9	A-2-7	25		52	28	24	1		10.6	1.91	19	2.4		0.00	11.4
20	B10	A-2-7	28		55	28	27	2		11.7	1.88	15	2.2		0.85	11.7
21	C1	A-7-6			46	19	27	16		17	1.82	3.0	3.2	80		Activity Ratio (C) 1.0
22	C2	A-7-6			67	23	44	20		24	1.63	2.0	8.3	110		1.54
23	C3	A-2-4		19	23	17	6	3		7	2.07			30		0.32
24	C4	A-7-6		20	44	20	24	14		17	1.76			70		1.20
25	C5	A-7-6		32	51	24	27	17		18	1.82			80		0.84
26	C6	A-7-5		58.5	78	36	42	20		25	1.53			140		0.72
27	C7	A-7-6		25	55	23	32	19		25	1.59			100		1.28
28	C8	A-7-6		26	50	14	36	18		17	1.58			90		1.38
29	C9	A-7-6		15	38	13	25	16		15	1.87			40		1.67
30	C10	A-2-4		20	26	16	10	0		11	2.65	5	2.5	30		0.50

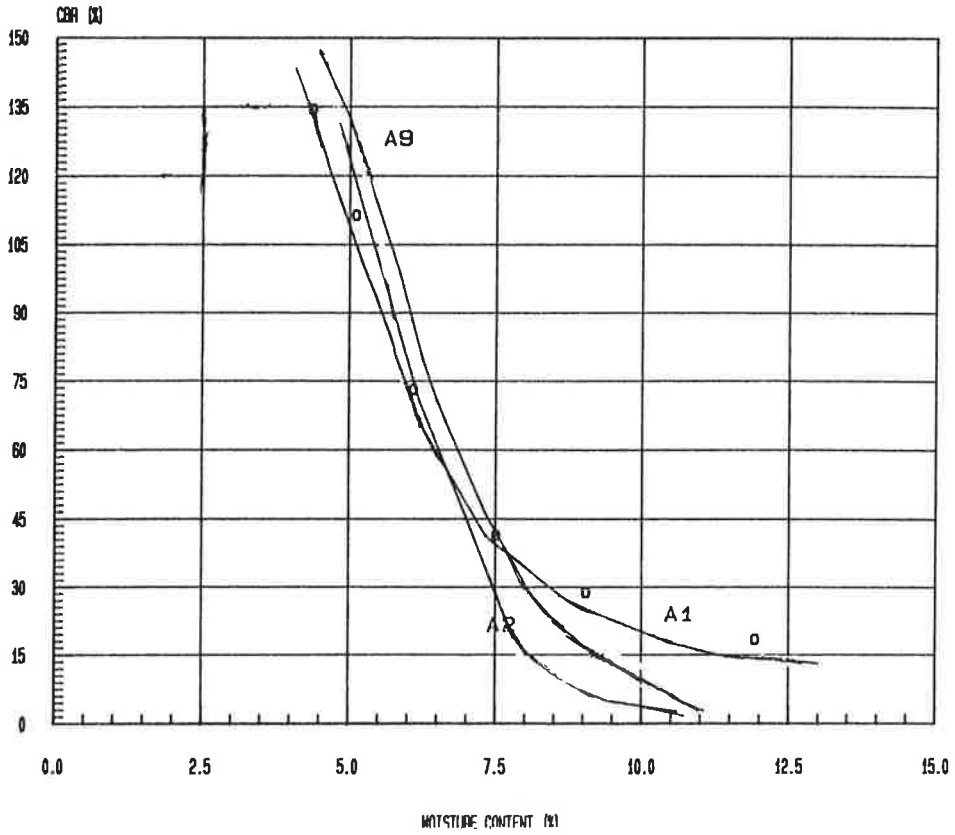

FIGURE 6 Effect of moisture content on CBR, Group A soils.

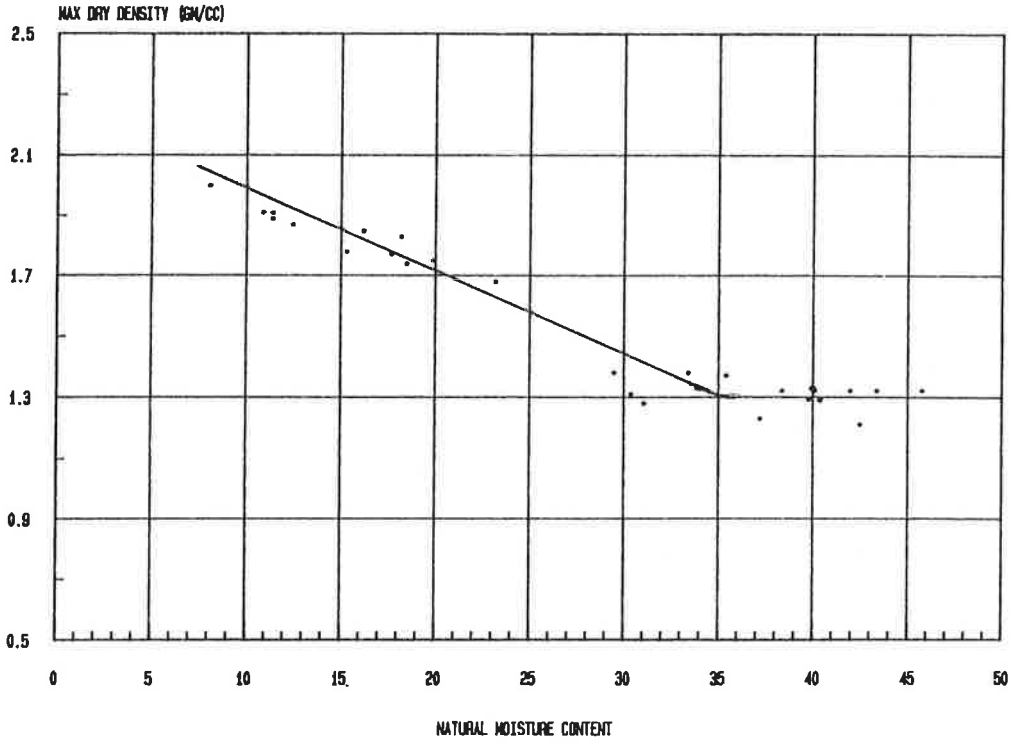

FIGURE 7 Density versus natural moisture content, Group B soils.

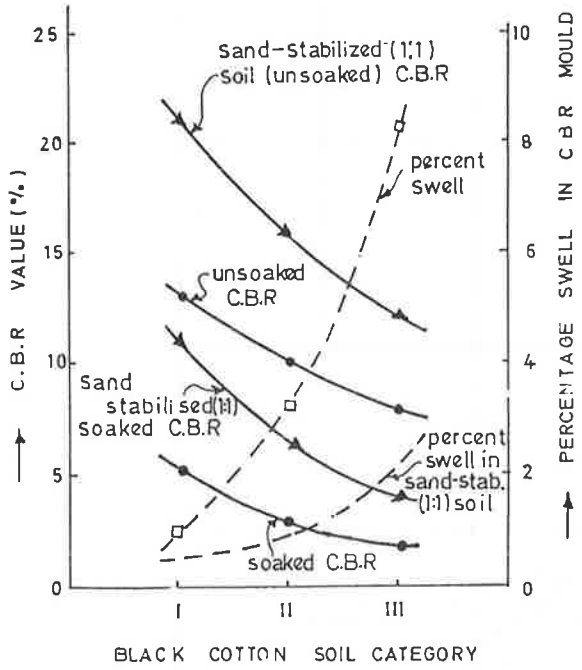

FIGURE 8 CBR values versus percent swell, Category C soils.

this group are not suitable for road construction. The conclusion can also be inferred from the study of the swelling characteristics of the soils. The soils are very expansive, with free swell varying from 30 to 140 percent, and swelling during soaking in the CBR mold was as much as 8.3 percent (sample C-10). The variation of CBR and percent swell for three categories of the black cotton soils are shown in Figure 9 (*10*).

USES

Residual soils are very important and useful as construction materials for a variety of engineering projects. They form the foundation for most engineering structures including buildings, airfields, and earth and rockfill dams and are often used as base and subgrade material for roads. The most notable drawback of these soils when used for unpaved rural roads is their tendency to corrugate in fine weather and to erode in the rain. This tendency can be overcome by providing a satisfactory watertight topping, which is usually achieved through bituminous stabilization of the soils.

Stabilization for the coarser materials (group A soils) is best achieved by the addition of cement. When the proportion of fines is high (≥ ?), plasticity may be reduced by the addition of lime. For example, Ola (*28*) found that a 2 percent addition of lime substantially reduced the plasticity index of laterite, but further addition caused no change.

For group B soils, stabilization with cement, lime, and lime pozzalan or bitumen may not be practical, as experience has shown that soils with a liquid limit greater than 45 percent and a plasticity index over 20 percent cannot normally be economically utilized in soil-cement or soil-lime construction. For bitumen construction, the above limits are 30 and 18 percent respectively. The foregoing is true also of the group C soils. However, laboratory tests show that stabilizing the group C soils with local sand can have beneficial effects. As reported by Madedor and Lal (*10*), there were appreciable increases in the CBR values for the soils (C-1, C-2, C-10) when stabilized with sand in the ratio of 1:1, and there was a corresponding decrease in the swelling potential of the sand-stabilized soils (Figure 9). For the three groups, the soaked CBR values were, as expected, less than the unsoaked CBR values. It is conjectured that the group B soils might benefit from blending with local materials; however, no definitive experimental data exist to prove this possibility.

Another use of residual soils is as slopes for roads, railways, and other embankments. But roads and other cuttings in residual tropical soils can present some problems if they are not well protected. Embankments are usually made as steep as possible to minimize the problem of erosion on flat slopes. In some cases, slopes are as high as 60 degrees, indicating a high angle of shearing resistance for these soils. Gidigasu (*12*) reported studies on Ghana soils that suggest that slope angles of 60–80 degrees may be stable for cuts up to 15 ft high in fairly indurated gravelly laterite soils; for cuts between 15 and 25 ft, the stable angles drop to 50 and 60 degrees. Slopes in loam and clay laterite soils range between 50–60 degrees for cuts less than 15 ft, and 35–50 degrees for higher cuts. However, it is necessary to protect the exposed slope surfaces from erosion. Ways to protect the slopes include spraying them with bitumen, covering them with cement plaster, or grassing them to reduce erosion and penetration of water into the soil. Berms are often used in high embarkments to limit the risk of deep-seated slope failure.

Slopes in coarse-grained soils are usually 50–60 degrees; and in fine-grained soils, slopes are limited to 40–50 degrees.

CONCLUSION

The group A soils are generally good base and subgrade materials for road construction. However, under the influence of wetting, the structure of residual soils often changes, leading to loss of strength. Loss of strength can lead to the failure of road base, subgrade, and road embankments made of these soils, particularly during the rainy season. The strength can be improved and preserved by both mechanical and chemical stabilization.

Group B soils have expansive tendencies and high plasticity indices. Their high plasticity and low CBR values do not recommend their use as road materials. The black cotton soils are very compressible soils and are not considered suitable for road construction because of their low strength and swelling characteristics.

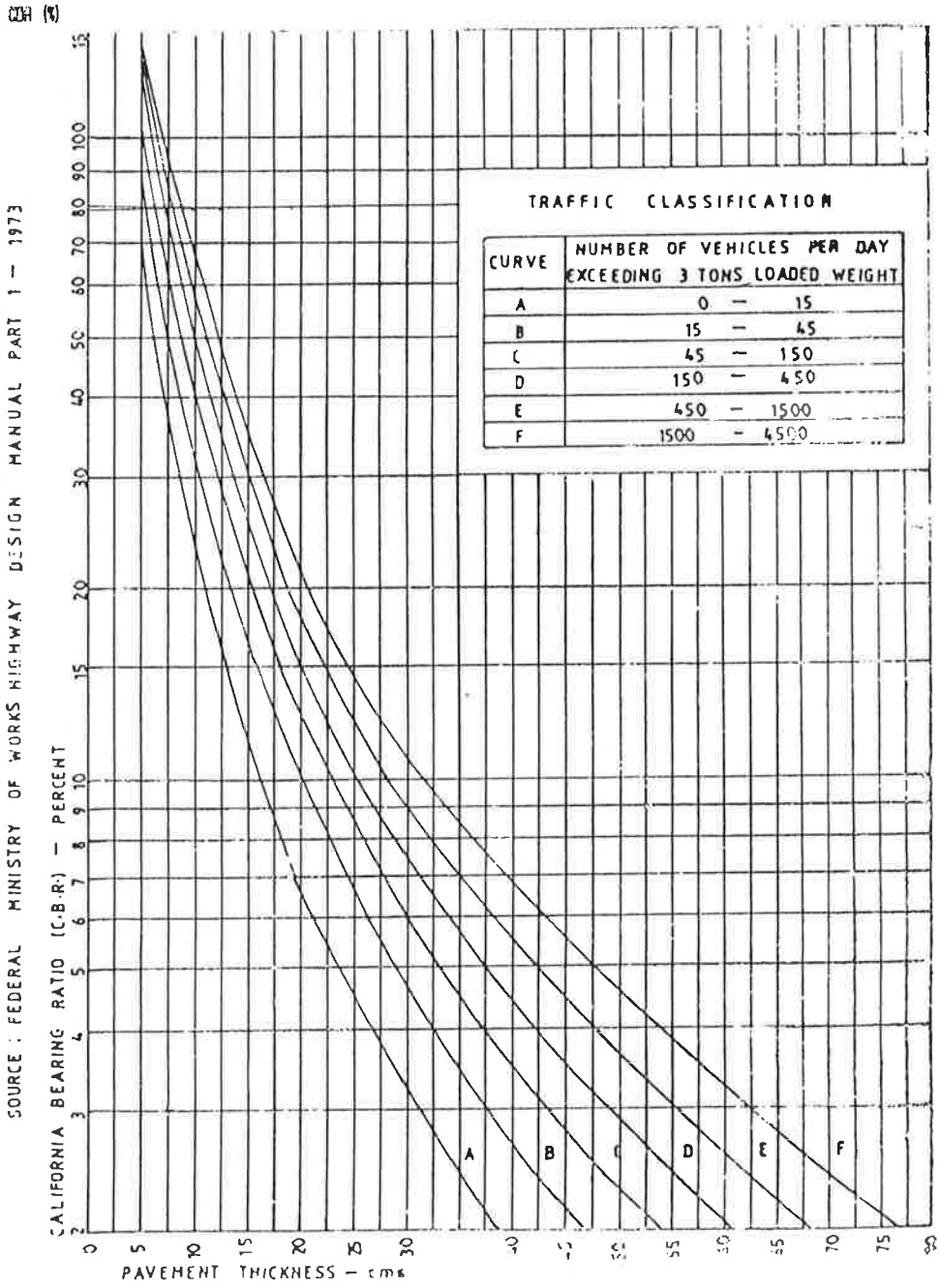

FIGURE 9 Flexible pavement design curves.

REFERENCES

1. B. Durotoye. Geomorphology and Quarternary Deposits of Nigeria. In *Tropical Soils of Nigeria in Engineering Practice* (S. A. Ola, ed.), Balkema/Rotterdam, 1983.
2. A.L. Little. Laterites. *Proc., Third Asian Regional Conference, SM&FE*, Haifa, Vol. 11, 1967, pp. 61–71.
3. A.L. Little. The Engineering Classification of Residual Tropical Soils. Specialty Session on Engineering Properties of Lateritic Soils. *Proc., 7th International Conference of SM&FE*, Mexico City, Vol. 1, 1969, pp. 1–10.
4. L.L. Fermor. What is Laterite? *Geological Magazine*, Vol. 5, No. 8, 1911.
5. J.W.S. De Graft-Johnson, H.S. Bhatia, and M.D. Gidigasu. The Engineering Characteristics of Lateritic Residual Clay of Ghana for Earth Dam Construction. *Proc., Symposium on Rock and Earth Fill Dams*, New Delhi, Vol. 1, 1968, pp. 94–107.
6. M.D. Gidigasu. Parameters for Classification of Fine-Grained Laterite Soils of Ghana. *Proc., 50th Meeting of the Committee on Exploration and Classification of Earth Materials*, ISSMFE, 1971, pp. 57–79.
7. L.W. Akroyd. Formation and Properties of Concretionary and Non-Concretionary Soils in Western Nigeria. *Proc., Fourth Regional Conference for Africa of SM&FE*, Cape Town, 1967, pp. 47–52.

8. J.O. Jackson. Geotechnical Properties of Biu Black Cotton Soil. *Proc., International Conference of SM&FE*, Vol. 1, Stockholm, 1981.
9. L.A. Ajayi. The Laterites and Lateritic Soils of Nigeria. *Geotechnical Practice in Nigeria: ISSMFE Golden Jubilee Commemorative Publication*, August 1985, pp. 7–15.
10. A.O. Madedor and N.B. Lal. Engineering Classification of Nigerian Black Cotton Soils for Pavement Design and Construction. *Geotechnical Practice in Nigeria: ISSMFE Golden Jubilee Commemorative Publication*, August 1985, pp. 49–67.
11. K.E. Clare. *Road Making Gravels and Soils of Central Africa.* Overseas Bulletin 12. British Road Research Laboratory, 1966, 43 pp.
12. M.D. Gidigasu. *Development in Geotechnical Engineering: Laterite Engineering.* Elsevier Scientific Publishing Company, Amsterdam, 1976.
13. H. Pern and K.S. Baua. Expansive Soils. *Proc., Conference on Materials Testing, Control and Research on Roads and Formation Problems*, FMW, Lagos, 1984.
14. R.D. Denman. Some Notes on Expansive Soils with Particular Reference to Northern Nigeria. *Proc., Conference on Materials Testing and Control*, FMW, Kaduua, 1966.
15. A. Ibrahim. Road Design and Construction. Research on Expansive Black Cotton Clay Areas of Maiduguri-Gamborw-Walgo Road in Borno State of Nigeria. *Proc., Conference on Materials and Testing*, Federal Ministry of Works, Kano, 1979.
16. S.A. Ola. Peak and Residual Strengths of Compacted Lateritic Soils. *Geotechnical Practice in Nigeria: ISSMFE Golden Jubilee Commemorative Publication*, August 1985, pp. 79–92.
17. R.R. Rao and O.A. Ouoleye. A Study of the Variation of Consistency Limits in Relation to Strength Properties. *Geotechnical Practice in Nigeria: ISSMFE Golden Jubilee Commemorative Publication*, August 1985, pp. 65–77.
18. K. Terzaghi. Design and Performance of the Sasumua Dam. *Journal, Institution of Civil Engineers*, London, Vol. 9, 1958, pp. 369–394.
19. H.F. Winterkorn and E.C. Chandrasekharan. Laterite Soils and Their Stabilization. *Highway Research Board Bulletin No. 44*, 1951, pp. 10–28.
20. P. Lumb. The Residual Soils of Hong Kong. *Géotechnique*, Vol. 15, No. 2, 1965, p. 180.
21. *Highway Manual*, Part 1. Nigeria, Federal Ministry of Works and Housing, 1973.
22. Transport and Road Research Laboratory. *A Guide to the Structural Design of Bitumen-Surfaced Roads in Tropical and Sub-tropical Countries.* Road Note 31, Department of Transport, United Kingdom, 1977.
23. H.R. Aggarual and R.H. Jafri. A Preliminary Study to Modify Material Specifications for Base Laterites for Secondary Roads. In *Geotechnical Practice in Nigeria: ISSMFE Golden Jubilee Commemorative Publication*, August 1985, pp. 109–131.
24. M.J.A. Sadiku. The Use of Sub-standard Soil Materials in Road Construction. *Geotechnical Practice in Nigeria: ISSMFE Golden Jubilee Commemorative Publication*, August 1985, pp. 133–137.
25. British Standard Institution. *Methods of Testing Soils for Civil Engineering Purposes.* British Standard 1377, London, 1975.
26. A. Casagrande. Classification and Identification of Soils. *Proc., ASCE*, Vol. 113, pp. 783–816, 1948.
27. *General Specifications for Roads and Bridges*, Vol. 11. Nigeria, Federal Ministry of Works, 1970.
28. S.A. Ola. *Soil Stabilized Compressed Blocks.* Geotechnical Report No. 1, University of Benin, 1983.

Publication of this paper sponsored by Committee on Soil and Rock Properties.

Design and Construction of Highway Embankments over Amorphous Peat or Muck

TIMOTHY CROWL AND C. W. LOVELL

Construction of highway embankments over deposits of amorphous peat and muck is made difficult by the low shear strengths, high compressibilities, and excessive amounts of creep typically associated with soils of this type. The objective of this research was to develop a procedure for the design and construction of low embankments over such materials for use by the Indiana Department of Highways. This paper begins with a review of the compression behavior of these soils, including a method for predicting embankment settlements from the results of laboratory tests. A soil testing program is then developed for determining parameters required for embankment design and construction. Field vane shear tests are recommended for the measurement of the undrained shear strength, and creep tests are recommended for calculating parameters to predict settlement. The paper concludes by presenting a procedure for the design and construction of embankments over amorphous peats and mucks. The procedure relies on stage loading, preloading, and in some instances geotextiles, to overcome the problems ordinarily encountered during construction over such soft soils.

Numerous deposits of amorphous peat and muck are located within the State of Indiana, and elsewhere. Many difficulties are encountered when highway embankments are constructed over these soft soils. In the past, highway engineers have relocated roadways to avoid construction over peat or muck. In other instances, the organic material was excavated and replaced with a more suitable material. However, as neither of these methods is economical by modern standards, highway departments have been forced to develop more sophisticated methods which allow construction directly across deposits of such materials.

Two characteristics of amorphous peats and mucks make them undesirable as materials for embankment foundations. Materials of this kind compress excessively when subjected to an applied load. Most of the compression results from the relatively high amounts of secondary compression associated with organic soils. These deformations occur over a long time, which compounds the problem. Deposits of these materials possess low preconsolidation pressures, so a large compression response is likely even at low stress levels. Amorphous peats and mucks are also characterized by very low shear strengths. Shear failures, which are both expensive and time-consuming to renovate, can occur very easily either during or after construction. Deposits of amorphous peat and muck vary greatly, so that representative values of compressibility and shear strength are difficult to define. Details of peat and muck behavior are covered in previous reports, Gruen and Lovell (*1*) and Joseph (*2*).

As a result of these typical characteristics, efforts to construct highway embankments over these materials have often resulted in poor performance in the form of excessive total settlements, large differential settlements, and shear failures. Moreover, attempts to predict embankment settlements from the results of laboratory tests are often unsuccessful.

It is the aim of this paper to present a procedure for designing and building embankments over amorphous peat and muck, as developed by Crowl and Lovell (*3*). This procedure will include use of a soil testing program to determine parameters needed during embankment construction. In addition, by using the method for settlement prediction presented here, it is hoped that more reliable settlement predictions may be achieved.

PROCEDURE FOR DESIGN AND CONSTRUCTION

Site Exploration

An important step in determining the behavior of embankments over amorphous peat or muck is obtaining reasonable soil parameters for analysis. However, before these parameters can be established, representative soil characteristics of the deposits must be determined. This is not an easy task when dealing with materials of this type.

Finding representative characteristics of the deposits is difficult because amorphous peats and mucks typically vary so much. To find the range of existing soil conditions at the site, a preliminary soil survey should be conducted. Disturbed samples may be taken at various depths using a hand auger or a power auger, and used to determine water

T. Crowl, Haley and Aldrich, Rochester, N.Y. C. W. Lovell, School of Civil Engineering, Purdue University, West Lafayette, Ind. 47907.

content, organic content, and specific gravity. As the compressibility and preconsolidation pressure of the soil throughout the deposit are also needed, creep tests should be performed on undisturbed samples. Field vane shear tests should be conducted throughout the site at various depths to determine the undrained shear strength.

The most critical value to be measured during the site investigation is the undrained shear strength. The designer must select a conservative value because of the low factors of safety used in design. For projects such as earth dams Terzaghi and Peck (*4*) recommend spacing borings at a maximum of 100 feet. The variability of deposits of amorphous peat and muck requires more extensive testing. For the purposes described in this paper, a spacing of not greater than 25 feet along the embankment centerline is recommended. Tests should be performed near the surface, at mid-depth, and near the bottom of the deposit to obtain sufficient information regarding the strength profile.

The values of undrained shear strength obtained from field vane shear testing depend on the rate of loading, soil anisotropy, and progressive failure according to Bjerrum (*5*). These limitations should be considered when interpreting field vane shear tests for use in design analyses. It should also be noted that the behavior of amorphous peats and mucks is assumed to be similar to that of soft clays, and that the use of field vane shear testing in the manner described above applies to these materials as well.

During site investigation, the depth of the amorphous peat or muck in the region of the proposed embankment must be determined. A procedure for estimating the thickness of peat deposits, provided in ASTM Standard Specification D4544-86, uses graduated steel rods of 9.5 ± 1.0 mm diameter and 1.0 or 1.2 m length. The rods can be threaded together for use in deposits of any reasonable thickness. Testing involves pushing or driving the rod into the deposit until resistance to penetration is observed to increase sharply. The depth at which resistance increases should be recorded as the deposit thickness. If sampling is desired, a piston-type sampling device as described in MacFarlane (*6*) can be attached to the rod assembly. This method has a number of limitations, and the Standard Specification should be consulted.

The soft clays and marls which often underlie amorphous peats and mucks can influence the behavior of the constructed embankment, and should be sampled as well to determine their effects on embankment behavior. It is advisable to continue sampling with depth until a layer of adequate strength is reached.

Embankment Design

Embankments constructed over soils of this nature can be designed with or without geotextiles, depending on the initial shear strength of the deposit. In some instances, geotextiles are necessary to allow construction to begin. Geotextiles have been found not only to reduce the horizontal deformations of embankments, but to increase stability, bridge weak areas of the subsoil, and provide a barrier between embankment and foundation soils. This paper will cover the design of embankments with or without geotextiles.

Embankments without Geotextile Reinforcement

After the site investigation, the results of field vane shear tests provide a range of values of the undrained shear strength in the deposit. Rather than using an average value of the shear strength, a conservative value (in some cases the lowest measured value) should be used during design analyses. The variability typical of these soils can cause considerable variation in shear strength, and the average value could be significantly greater than the measured lower values.

The factor of safety used in this paper for overall bearing capacity, rotational failure, and lateral squeeze is 1.3. Attewell and Taylor (*7*) state that for embankments constructed on a compressible foundation, a factor of safety on the order of 1.5 is ordinarily used during stability analysis. Values as low as 1.2 have been used when soil data and site conditions were well established. When analyzing the stability of a preloaded embankment, Stamatopoulos and Kotzias (*8*) state that a factor of safety ranging from 1.1 to 1.3 can be used, assuming that the correct input values have been used during analyses. Thus, although a value of 1.3 is used herein, when selecting a factor of safety, considerable judgment based on previous experience should be exercised.

Overall Bearing Capacity: The overall bearing capacity calculation is a simple one. This step is used to find an approximate value of the allowable height. For a strip loading on soils of this type, the bearing capacity equation reduces to

$$q = cN_c \tag{1}$$

where

q = ultimate pressure (psf),
c = undrained shear strength (psf), and
N_c = bearing capacity factor determined from Vesic (*9*).

The maximum allowable load providing a safety factor of 1.3 should be calculated. Once the allowable load is known, the height of this load is found as

$$H = \frac{q_{all}}{\gamma} \tag{2}$$

where q_{all} = allowable pressure (psf) and γ = unit weight of embankment soil (pcf).

Lateral Squeeze: The weight of an embankment will tend to squeeze the foundation soil laterally. Jurgenson (*10*) states that the force required to cause lateral squeeze

of a soil between two rigid plates is equal to

$$P = \frac{1}{a} cBL^2 \tag{3}$$

where

P = total applied load (lb),
a = one half of deposit thickness (ft),
c = undrained shear strength (psf),
B = length of embankment (= 1 ft for unit length), and
L = one half of embankment base width (ft).

A diagram illustrating these variables is provided in Figure 1. The total load, P, for the height of the embankment found in the previous step is then calculated for a unit length of embankment. From this, the required value of the undrained shear strength is

$$c_{req} = \frac{Pa}{BL^2} \tag{4}$$

The resulting factor of safety (C_{avail}/c_{req}) must be greater than 1.3. If this is not the case, the height of the first load may be decreased, or the geometry of the embankment can be adjusted to provide a longer base length.

In addition, lateral squeeze has been evident in instances where the applied stress produced by the embankment is greater than three times the undrained shear strength of the foundation soil. Therefore, the value of c_{req} calculated in Equation 4 must also be at least one-third of the applied stress. If this is not the case, the required shear strength (c_{req}) should be increased to satisfy this criterion. The resulting factor of safety (c_{avail}) must be greater than 1.3.

Embankment Spreading: The lateral earth pressure developed within the embankment, as shown in Figure 2, must be resisted by shearing stresses at the base. If sufficient resistance is not provided by the foundation, the embankment may become unstable. The lateral earth pressure force, P_a, developed within a noncohesive embankment is

$$P_a = 0.5\gamma H^2 \tan^2\left(45 - \frac{\phi}{2}\right) \tag{5}$$

where

γ = unit weight of embankment soil (pcf),
H = height of embankment (ft), and
ϕ = angle of friction of embankment soil.

The resistance, P_r, provided by the foundation soil is

$$P_r = cl \tag{6}$$

where c = undrained shear strength (psf) and l = lateral distance from crest to toe of embankment (ft).

A safety factor of 2 against embankment spreading is suggested for geotextile reinforced embankments (*11*) and has been adopted for unreinforced embankments as well. A calculated factor of safety less than this value will require the use of a lesser height of load.

Rotational Failure: To investigate the stability of the embankment with respect to rotational failure, STABL4 (*12*) or STABL5 (*13*) should be used. The stability analysis should be performed for the allowable embankment height

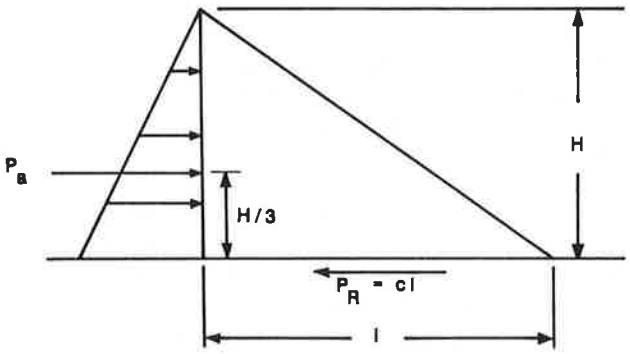

FIGURE 2 Embankment spreading.

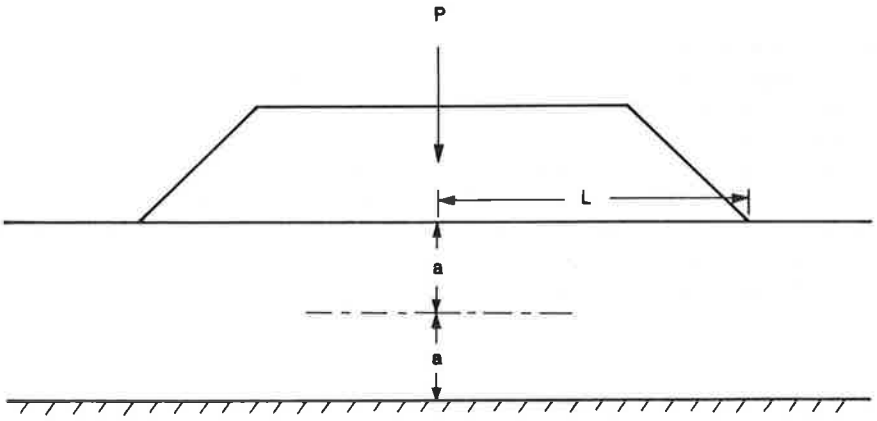

FIGURE 1 Description of variables in Equation 3.

found after the preceding analyses. If the stability analysis yields a factor of safety less than 1.3, another iteration should be performed using a lesser height of load.

Resistance provided by the embankment material in unreinforced embankments may be included in the stability analysis only if an overconsolidated or desiccated layer exists at the surface of the deposit. Otherwise, any lateral movements in the embankment can create tension cracks, sharply reducing the resistance within the embankment.

Geotextile Reinforced Embankments

If geotextiles are used during embankment construction, the allowable safe height of construction is increased as a result of the stabilizing action of the reinforcement. This section will discuss the design of geotextile reinforced embankments, and is based on a design manual by Christopher and Holtz (*14*). The manual provides a more in-depth coverage of the topic, and is recommended reading when designing with geotextiles.

Overall Bearing Capacity: The overall bearing capacity is calculated in the same manner as for the unreinforced embankments. Once again, the recommended factor of safety is 1.3. Once the allowable pressure is calculated, the safe height can be calculated. For geotextile reinforced embankments, the average applied pressure can be estimated as $P/2L$, where P and L are as illustrated in Figure 1.

Lateral Squeeze: Geotextiles have no influence on the extent of lateral squeeze. The required value of the undrained shear strength is therefore found in the same manner as unreinforced embankments. Embankments constructed with geotextiles require a factor of safety of 1.3 against lateral squeeze.

Rotational Failure: Using STABL6 (*15*), a stability analysis should be performed for the calculated height of load. The value of the fabric strength required should be adjusted until the minimum factor of safety is 1.3.

Embankment Spreading: When constructing embankments with geotextiles, the lateral earth pressures exerted by the fill are resisted by the reinforcement. If sufficient friction is not developed between the embankment and the reinforcement, or the foundation and the reinforcement, the embankment may become unstable. Instability may also occur if the foundation soils beneath the embankment cannot resist the applied shear stress.

These two failure modes dictate that the reinforcement must provide enough frictional resistance to prevent sliding along the interface. In addition, the tensile strength of the geotextile must be adequate to prevent rupture or tearing. The lateral earth pressure developed within a noncohesive embankment is given in Equation 5. The resisting force, P_r, provided by the geotextile is found as

$$P_r = 0.5\gamma l H \tan \phi_{sf} \tag{7}$$

where ϕ_{sf} = soil-fabric friction angle and l = lateral distance from crest to toe of embankment (ft).

The value of ϕ_{sf} is equal to

$$\phi_{sf} = \tan^{-1}(4P_a/\gamma l H) \tag{8}$$

The specified value of ϕ_{sf} should be at least 2/3 (ϕ_{soil}).

A factor of safety against embankment spreading is found by dividing the resisting force by the actuating forces. A minimum factor of safety of 2 is recommended by Fowler (*11*).

The lateral earth pressures must be resisted by tension forces in the reinforcement. To prevent splitting or tearing, Fowler recommends a minimum factor of safety of 1.5. The resulting required fabric strength is given by

$$T_f = 1.5P_a \tag{9}$$

where T_f equals fabric tension force.

Limit Fabric Deformation: The stresses required to resist lateral spreading are developed through strain in the geotextile. The modulus of the geotextile controls the amount of strain. The resulting distribution from lateral spreading is assumed to vary linearly from zero at the toe to its maximum value beneath the crest of the embankment.

This assumption is not conservative considering that most geotextiles possess stress-strain curves that develop concave-upward, not linearly. A factor of safety equal to 1.5 should be used to determine the geotextile tensile modulus, E_f. If the required modulus is calculated from the tensile strength force, T_f, the factor of safety is included. The minimum geotextile tensile modulus, E_f, required is found as

$$E_f = \frac{T_f}{\varepsilon_{max}} \tag{10}$$

where ε_{max} is the maximum strain in percent expected in the geotextile along the embankment centerline.

Using the assumed linear strain distribution, the maximum strain is two times the average strain beneath the embankment. A value of 5 percent average strain is recommended for design. The maximum strain would then be 10 percent, and the required fabric tensile modulus may be found as

$$E_f = 10T_f \tag{11}$$

The embankment will also deform until the required fabric strain develops to prevent a rotational stability failure. The actual behavior of the embankment in this condition is unknown, and assumptions outlined in Christopher and Holtz (*14*) have been used. The resulting minimum required modulus to control a rotational failure is found as

$$E_{fr} = \frac{T_{fr}}{0.10} \tag{12}$$

where T_{fr} = required tensile strength of fabric and E_{fr} = minimum fabric modulus.

For additional information on geotextile selection and evaluation, the reader should refer to a modern comprehensive reference, i.e., Christopher and Holtz (*14*); Mitchell and Villet (*16*).

Stage Loading

The softness of amorphous peats and mucks often makes construction to the full height in one stage impossible, particularly if a surcharge is to be placed. Construction will therefore have to be performed in stages. Once the maximum first load, as calculated in the preceding analyses, has been applied, the foundation will begin to consolidate. The consolidation will result in a strength gain, allowing further loads to be placed without inducing failure in the embankment foundation.

To determine the duration of each stage load required for consolidation to occur, pore pressure transducers should be placed in the foundation. After excess pore pressures induced by the previous loading have dissipated, no further strength gain will develop. Field vane shear tests should then be performed in the foundation beneath the embankment, and in areas next to the embankment to determine the extent of the strength gain. Using the increased values of undrained shear strength, the aforementioned analyses should be performed to calculate the allowable height of the second stage load. The procedure of applying the load, allowing pore pressures to dissipate, measuring the increased shear strength, and placing subsequent loads should continue until the final embankment or surcharge height is reached.

Preloading

One of the problems of building highway embankments over amorphous peat and muck is the large amount of secondary compression taking place over an extended period. To reduce the amount of settlement that occurs during the service life of an embankment, a surcharge in excess of the final design embankment height should be placed. The necessary height of surcharge is found by first using the Gibson-Lo model (*17*) to predict settlements produced by the design height of the embankment.

The Gibson-Lo model provides a prediction of the one-dimensional compression of soils. This model is stated in the following equation from Edil and Simon-Gilles (*18*):

$$\varepsilon(t) = \Delta\sigma[a + b(1 - e^{-(\lambda/b)t})] \tag{13}$$

where

$\varepsilon(t)$ = strain at time t,
$\Delta\sigma$ = applied stress increment,
a = primary compressibility,
b = secondary compressibility, and
λ/b = rate factor for secondary compressibility.

The input parameters required for this model are obtained from the results of creep tests. To obtain the most accurate results, the creep tests should be performed at stress levels simulating actual field loading, rather than using a conventional load increment ratio.

Creep testing begins by reconsolidating the samples at their preconsolidation pressure in the loading frame. Edil and Simon-Gilles (*18*) recommend sustaining the load until deformation is reduced to 0.001 to 0.003 mm/day. At this point, the next load is applied, corresponding to the stress level induced by the design embankment height. The load should be sustained until enough data are collected to accurately calculate the values required for the Gibson-Lo model. For the materials tested during this project, a load duration of 10,000 minutes was found to be sufficient.

After creep tests are completed, the parameters required for the Gibson-Lo model are found using a method presented by Lo, Bozozuk, and Law (*19*). In this method, the logarithm of strain rate is plotted versus time, as shown in Figure 3. The straight line portion of this curve corresponds to the time range of secondary compression. If the straight line is extended back to the y-axis, the parameters can be found by solving simultaneously the following equations:

$$\text{line slope} = 0.434(\lambda/b) \tag{14}$$

$$y\text{-intercept} = \log(\Delta\ \sigma\ \lambda) \tag{15}$$

$$a = \frac{\varepsilon_f}{\Delta\sigma} - b + be^{-(\lambda/b)t_f} \tag{16}$$

where ε_f = last strain reading and t_f = time of last strain reading.

The three parameters a, b, and λ/b obtained from laboratory tests depend somewhat on the value of stress increment, final stress level, and the average strain rate. Stress increments less than approximately two times the stress level tested in the laboratory will cause little variation in the value of the parameters. However, this is true only for laboratory conditions. The parameters obtained from the analysis of field and laboratory performances are different as a result of the discrepancies between these conditions.

During research conducted by Edil and Mochtar (*20*), both the laboratory and field behaviors of organic soils under loading were observed. The results were compared to determine any relationships between the two conditions. From this comparison correlations could be developed between the model parameters for laboratory and field performance. Figure 4 provides a curve of consolidation stress versus primary compressibility, and distinguishes between data points from laboratory tests and from field observations. The figure indicates that the primary compressibilities in the field and the laboratory are comparable for the same stress level. Therefore, the laboratory value of the parameter a will compare with the field value when

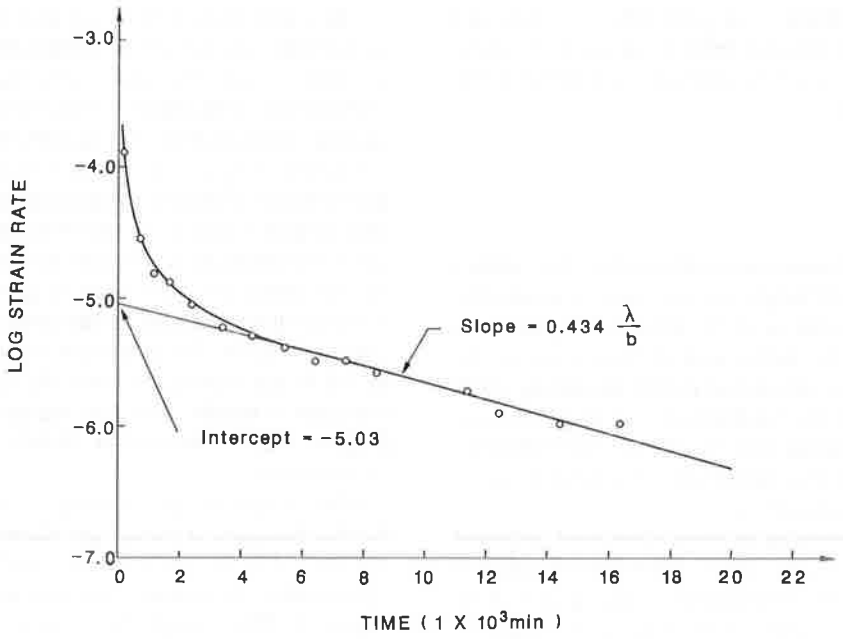

FIGURE 3 Plot of log strain rate with time from laboratory tests (*19*).

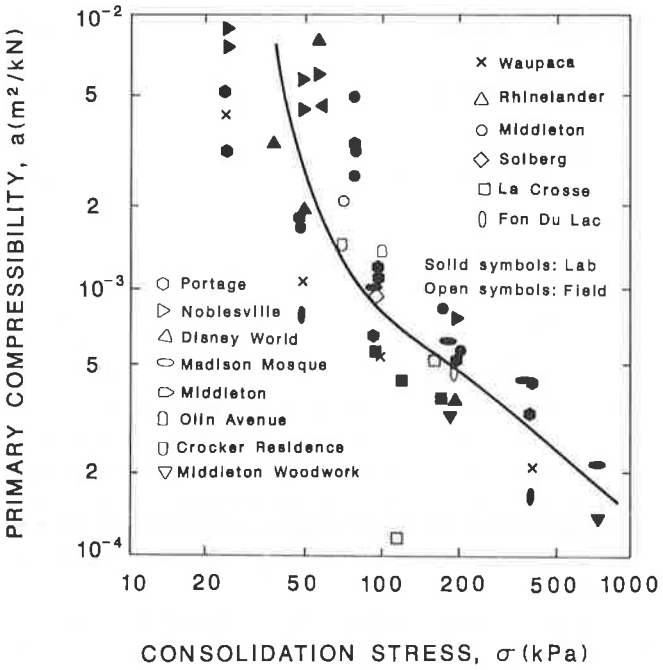

FIGURE 4 Primary compressibility versus stress level (*20*).

the variation of soil properties is considered. In addition, the curve fitted through the plotted points can be used to correct the value of the parameter a when a prediction is desired at a different stress level.

Figure 5 provides a curve of the secondary compressibility factor, b, versus stress level. The points plotted are for peat data only. As this figure illustrates, the field value of b is higher than the laboratory value at equivalent stress levels. Using Figure 5, a plot of b_{field}/b_{lab} versus consolidation stress was constructed as illustrated in Figure 6. Once again, it should be noted that Figure 6 represents data from observations made on peat only.

A plot of strain rate versus λ/b is provided in Figure 7. This figure indicates that no correlation exists between $(\lambda/b)_{lab}$ and $(\lambda/b)_{field}$.

As previously mentioned, the value of a_{lab} is approximately equal to a_{field}, and therefore no correction will be required. Figure 6 can be used to calculate b_{field} from the results of laboratory tests. Using Figure 7, the value of $(\lambda/b)_{field}$ can be determined. If the field strain rate is not known from previous experience, Edil and Mochtar (*20*) recommend using a value two to three orders of magnitude smaller than that observed in the laboratory.

It should be recognized that the recommended correlations in Figures 4 through 7 are best-fit lines through data with a considerable amount of scatter, and that these correlations therefore provide only an approximate relationship between laboratory and field performances. Using them can help improve predictions; however, they still may not provide sufficient reliability, and should therefore be used with caution. As a result, the use of laboratory test results for settlement prediction is still a matter for question. The most reliable settlement predictions can be obtained by observing field performance for calculating the Gibson-Lo model parameters.

Using the corrected parameters, settlement prediction can be conducted using the Gibson-Lo model. The amount of settlement expected within the service life of the embankment can be deduced from the results of settlement

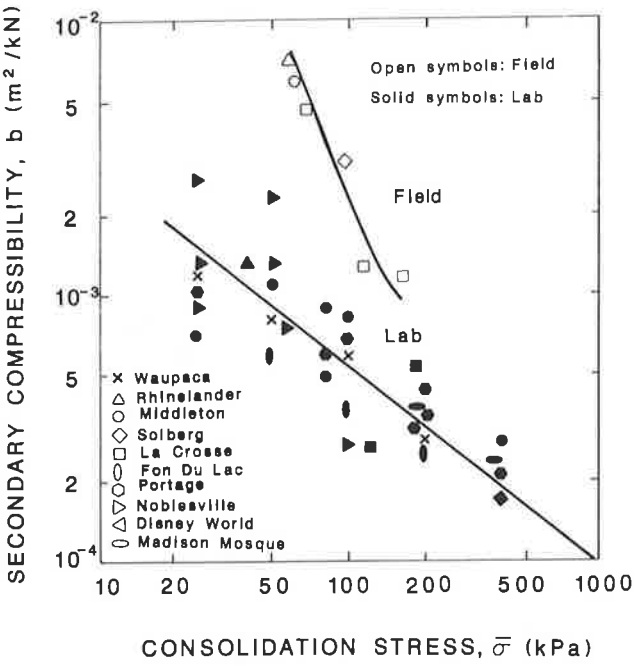

FIGURE 5 Secondary compressibility versus stress level (*20*).

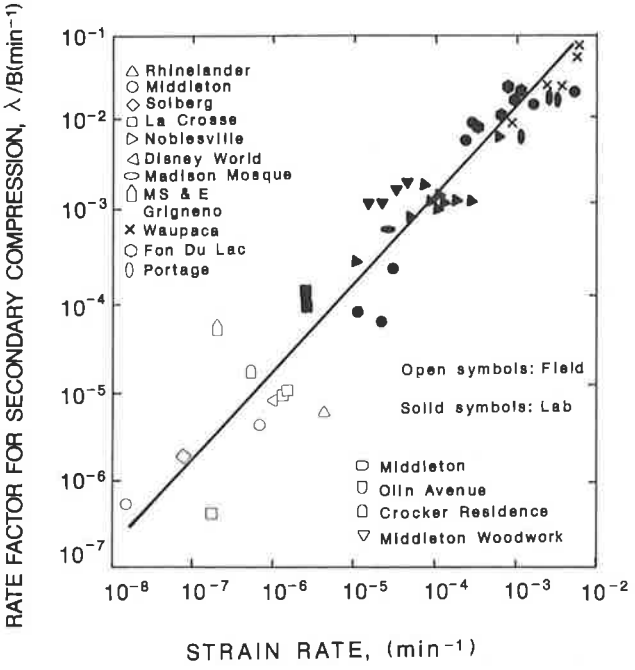

FIGURE 7 Dependency of rate factor for secondary compression on average strain rate (*20*).

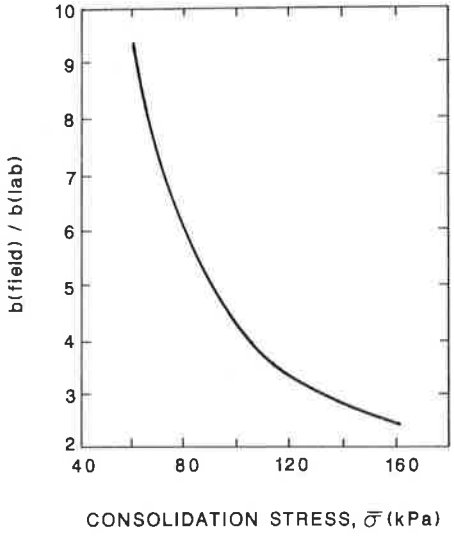

FIGURE 6 Correction curve for laboratory values of secondary compressibility (*20*).

prediction. The objective of the surcharge is to induce that amount of settlement during the time required for primary consolidation. To calculate the height of surcharge required to accomplish this, the Gibson-Lo model should be used to predict the settlement produced by various heights of surcharge, until the appropriate value is obtained. The results of creep tests simulating loading by the design embankment height may be used, so long as the stress increase of the surcharge plus the embankment is less than twice that used during these tests, as concluded by Gruen (*17*). After the height of surcharge is determined, the analyses presented for embankment design must be performed, to ensure that the surcharge does not create any instabilities.

Field Observations

To help monitor the behavior of the deposit of amorphous peat or muck when loaded, several field observations should be made. The most obvious of these is a record of settlements along the embankment centerline. These measurements can be compared with the predicted settlements to check their accuracy; they can also be used to calculate the field strain rate of the deposit so that the rate factor for settlement prediction can be corrected if necessary. Settlement measurements will also be used to determine when the required amount of settlement has occurred, allowing the surcharge to be removed.

Inclinometers should also be placed in the embankment site to measure any lateral movements of the embankment. Data obtained from inclinometers should be interpreted carefully, as these soft materials can flow around the inclinometer. As mentioned previously, pore pressure transducers should be installed to observe the dissipation of excess pore pressures. All types of field instrumentation should be installed to provide redundancy. This will allow for any equipment that becomes inoperable or is disturbed during construction.

Embankment Materials

Deposits of amorphous peat or muck occur in low-lying areas and are very wet. Therefore, portions of the embankment will become saturated, particularly as settlement occurs. Because of this, a well-graded material possessing a limited amount of fines should be chosen for construction above the water table. This will allow embankment drainage and will reduce the effects of wetting/drying or freezing/thawing.

Construction Sequence

Barsvary et al. (*21*) present a sequence of construction for embankments over soft subsoils. A diagram of their procedure is illustrated in Figure 8. Before actual construction begins, they recommend placing a working platform on the foundation soil for construction mobility and easier placement of the geotextile. If geotextiles are to be used, they should be placed on the working platform, transverse to the alignment of the embankment. After placing the embankment to a height of one foot, the geotextile should be folded back on top of this material as shown in the figure. The geotextile should then be anchored by compacting earth above the folded region as in Step 4. The core of the embankment is then placed and compacted. Subsequent lifts should then be constructed by placing and compacting the edges as shown in Step 6, followed by placement and compaction of the embankment core. Compaction lifts should be kept at about the same level, to aid compaction by lateral constraint.

CONCLUSIONS

This paper has investigated the problems associated with the construction of highway embankments over amorphous peats and mucks, and a number of conclusions have been reached.

1. The use of relationships developed by Edil and Mochtar (*20*) correlating the results of laboratory tests with field behavior will improve the results of settlement predictions made with the Gibson-Lo model. However, these correlations are approximations and should be used with caution.
2. Field vane shear testing may be a useful method for measuring the undrained shear strength of amorphous peats and mucks. However, the limitations of vane shear testing, as discussed in Bjerrum (*5*), should be considered when interpreting test results. It should also be restated that a conservative value of the undrained shear strength should be used during design analyses because of the variability normally encountered with these soils.
3. In order to construct embankments over deposits of amorphous peat or muck, stage loading will be required in most instances, especially when a surcharge is to be applied. The strength gain from consolidation will allow placement of subsequent loads without inducing failure in the foundation.
4. To reduce the amount of settlement during the service life of the embankment, a surcharge should be placed to speed up compression of the foundation.
5. For deposits of extremely soft materials, geotextiles may be required for successful construction. To supplement the information provided in this report, the reference by Christopher and Holtz (*14*) should be consulted.

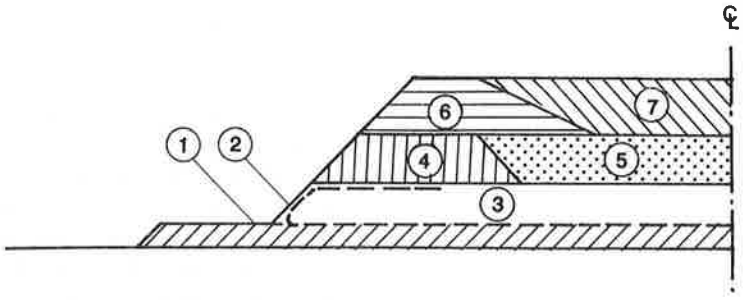

STAGE I

1. Place working platform
2. Place geotextile transverse to alignment
3. Place 0.3 m granular and fold back geotextile
4. Place and compact earth to anchor geotextile
5. Place and compact embankment core

STAGE II

6. Place and compact earth to profile grade at edges
7. Place and compact earth to profile grade at core

FIGURE 8 Construction sequence (*21*).

6. The procedure presented in this paper has recently been submitted to the Indiana Department of Highways, which provided financial support for this research project. At this time, the design and construction procedure is still in the experimental stage and has not been implemented. Therefore, several test embankments should be constructed using this method to evaluate its validity and usefulness.

REFERENCES

1. H.A. Gruen, Jr. and C.W. Lovell. Compression of Peat Under Embankment Loading. In *Transportation Research Record 978*, TRB, Washington, D.C., 1984, pp. 56–59.
2. P.G. Joseph. *Behavior of Mucks and Peats as Embankment Foundations.* MSCE Thesis and Joint Highway Research Project Report No. 85–16, School of Civil Engineering, Purdue University, West Lafayette, Indiana, 1985.
3. T. Crowl and C.W. Lovell. *Behavior of Mucks and Amorphous Peats as Embankment Foundations.* Joint Highway Research Project Report No. 87–2, School of Civil Engineering, Purdue University, West Lafayette, Indiana, 1987.
4. K. Terzaghi and R.B. Peck. *Soil Mechanics in Engineering Practice.* Second ed., John Wiley and Sons, Inc., New York, 1967.
5. L. Bjerrum. Embankments on Soft Ground. *Proceedings of ASCE Specialty Conference on Performance of Earth and Earth Supported Structures*, Purdue University, Vol. 2, 1972, pp. 1–54.
6. I.C. MacFarlane. *Muskeg Engineering Handbook.* Muskeg Subcommittee of NRC Associate Committee on Geotechnical Research, University of Toronto Press, 1969.
7. P.B. Attewell and R.K. Taylor. *Ground Movements and Their Effects on Structures.* Surrey University Press, London, 1984.
8. A.C. Stamatopoulos and P.C. Kotzias. *Soil Improvements by Preloading.* John Wiley and Sons, Inc., New York, 1985.
9. A.A. Vesic. Analysis of Ultimate Loads of Shallow Foundations. *Journal of the Soil Mechanics and Foundation Division*, Vol. 99, No. SMI, 1973, pp. 45–73.
10. L. Jurgenson. *The Shearing Resistance of Soils.* Contributions to Soil Mechanics 1925–1940, Boston Society of Civil Engineers, 1937, pp. 184–217.
11. J. Fowler. *Design, Construction, and Analysis of Fabric-Reinforced Embankment Test Section at Pinto-Pass, Mobile, Alabama.* Technical Report EL-81–8. USAE Waterways Experiment Station, Vicksburg, Miss., 1981.
12. C.W. Lovell, S.S. Sharma, and J.R. Carpenter. *Slope Stability Analysis with STABL4.* JHRP-84/19, Joint Highway Research Project, Purdue University, West Lafayette, Indiana, 1984.
13. J.R. Carpenter. *STABL5/PC STABL5 User Manual.* JHRP-86/14, Joint Highway Research Project, Purdue University, West Lafayette, Indiana, 1986.
14. B.R. Christopher and R.D. Holtz. *Geotextile Engineering Manual.* Prepared for Federal Highway Administration, National Highway Institute, Washington, D.C., 1985.
15. D.N. Humphrey. *Design of Reinforced Embankments.* Ph.D. thesis. School of Civil Engineering, Purdue University, West Lafayette, Indiana, 1986.
16. J.D. Mitchell and W.C.B. Villet. *NCHRP Report 290: Reinforcement of Earth Slopes and Embankments.* TRB, Washington, D.C., June 1987, 323 pp.
17. H.A. Gruen, Jr. *Use of Peats as Embankment Foundations.* MSCE thesis. School of Civil Engineering, Purdue University, West Lafayette, Indiana, 1983, 149 pp.
18. T.B. Edil and D.A. Simon-Gilles. Settlement of Embankments on Peat: Two Case Histories. *Advances in Peatlands Engineering*, National Research Council of Canada, Ottawa, Canada, 1986, pp. 1–8.
19. K.Y. Lo, M. Bozozuk, and K.T. Law. Settlement Analysis of the Gloucester Test Fill. *Canadian Geotechnical Journal*, Vol. 13, No. 4, 1976, pp. 339–354.
20. T.B. Edil and N.E. Mochtar. Prediction of Peat Settlement. *Proceedings, Sedimentation/Consolidation Models*, American Society of Civil Engineers, San Francisco, Calif., 1984, pp. 411–424.
21. A.K. Barsvary, M.D. MacLean, and C.B.H. Cragg. Instrumented Case Histories of Fabric Reinforced Embankments over Peat Deposits. *Proceedings*, Vol. 3, *Second International Conference on Geotextiles*, Las Vegas, Nev., 1982, pp. 647–652.

Publication of this paper sponsored by Committee on Soil and Rock Properties.

Investigation of the Failure of a Hydraulically Placed Embankment

ARA ARMAN AND PAUL M. GRIFFIN

A study was performed to determine the causes of differential subsidence of a hydraulically constructed sand embankment in a fresh water swamp. Among other test methods, an electric cone penetration test (ECPT) was used to determine the cause(s) for embankment, and thus pavement, distress. Because very little historical design and construction information was available to the authors for analysis, the approach used was of a forensic nature rather than that of a well-defined research study. The electronic cone penetrometer, in combination with other tests, proved to be an invaluable tool in determining the condition of the sand embankment. Consolidation test results and embankment and subgrade profiles obtained by ECPT and borings eliminated the possibility of continuing settlement of subgrade soils. The problem is within the hydraulically placed sand fill. It was determined that the sand embankment when hydraulically placed was not sufficiently densified and that in later years the top 6 ft of the embankment, which is above the water table, experienced various degrees of densification under traffic loadings. Remedial options were studied and recommendations were made for field evaluations of these methods.

A 4.3-mile section of route I-10 between Baton Rouge and New Orleans, Louisiana, has been experiencing continuing, excessive pavement distress in the form of differential subsidences of 2–8 in. along its length.

This section of I-10 crosses a fresh water swamp. It was constructed during the period September 1967–July 1970 by removing approximately 15–20 ft of soft, alluvial organic clays overlying competent Pleistocene deposits and by replacing the soft organic clays with hydraulically placed sands pumped from sand bars of the Mississippi River. The sand for the fill was pumped about 15 mi from a dredge located on the river. The specifications for the sand required that it contain no more than 3 percent organic material, with 75–100 percent passing the No. 40 screen and 0–10 percent passing the No. 200 screen. The solid-to-water ratio of the pumped slurry was reported to be 14–18 percent by volume (*1*).

Following the pumping of the sand, a sand surcharge of approximately 200 psf was applied for a period of 3 yr to eliminate primary consolidation of any remaining soft layers and to minimize secondary settlement. A sand embankment about 15–25 ft thick was thus formed to provide the foundation for this section of the highway.

The highway profile consists of two roadways (Figure 1), each having a two-lane pavement 24 ft wide, with paved shoulders on the outside and inside, 10 ft and 6 ft wide respectively. The highway has a 52-ft depressed median between the roadways (64 ft between travel lanes).

The pavement, constructed in accordance with the AASHTO rigid pavement design method, consists of 12 in. of compacted shell placed over the sand embankment as subbase, with a 4-in.-thick black base and an 8-in.-thick continuously reinforced concrete pavement (CRCP). During recent years, the CRCP surface has exhibited signs of excessive vertical displacement.

In April 1985 the Louisiana Department of Transportation and Development (LDOTD) and Louisiana State University (LSU) initiated a study to investigate the causes and possible remedies and rehabilitation schemes to save the embankment.

This paper presents the method of investigation used to determine the causes for differential subsidence and the conclusions derived from the study.

LITERATURE

In spite of the fact that hydraulic fills have been used for construction of dams, roadways, and structural foundations, there is little useful information on design, construction, or postconstruction procedures availablein the archival journals (*2*).

Cases cited in the literature indicate that when clean sand is used for hydraulic fill, relative densities obtained without mechanical compaction vary from 40 to 80 percent (*2–4*, *5*,p.402). However, relative densities obtained without compaction in excess of 70 percent are rare, which may result in the subsidence of the embankment (*2–4*, *6–7*). This is particularly true when ponding is used (i.e., the pumped sand is deposited under water without allowing the water to drain).

Practitioners disagree concerning the critical nature of the presence of fines in pumped sand (*2*, *4*). There is also disagreement on the use of relative densities for controlling hydraulic fills (*3*). The lack of sensitivity and scatter in the numerical values of relative density measurements render such measurements less desirable for quality control (*8*).

Louisiana Transportation Research Center, P. O. Box 94245, Baton Rouge, La. 70808.

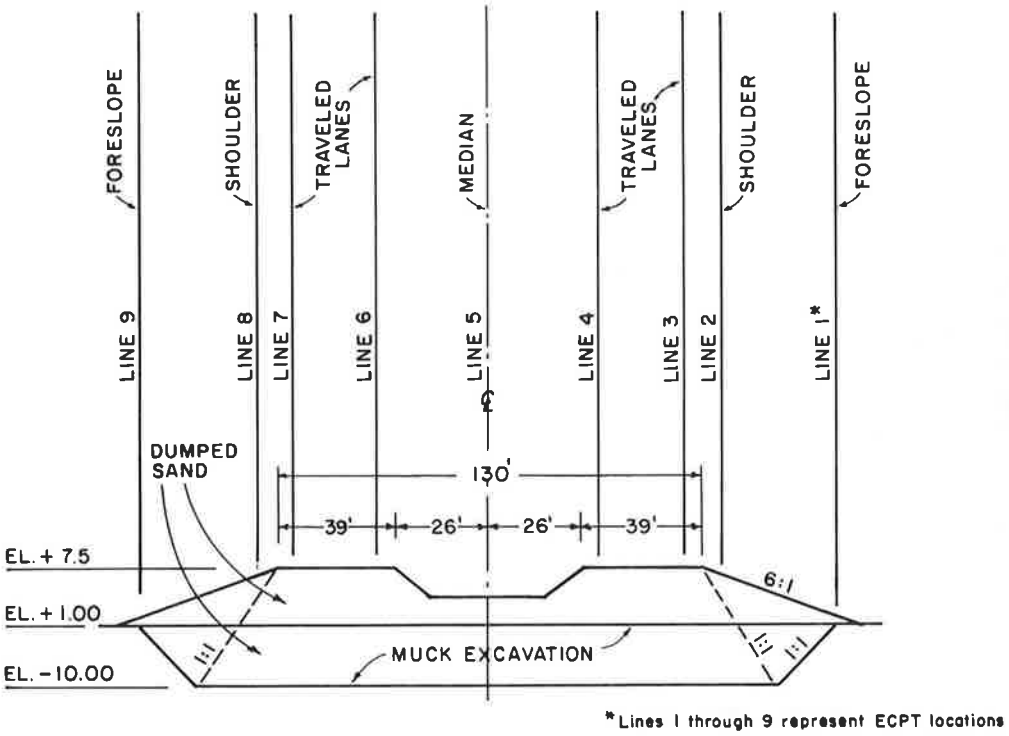

FIGURE 1 Embankment profile and ECPT locations.

Reitz et al. (*3*) state that "numerical data reported for this (hydraulic sand fill) should not be based on correlations from Standard Penetration Testing N values. . . . The writers strongly urge that where fill quality can be tested as fill is being placed, the more reliable determinations of relative densities by physical testing be used."

METHODOLOGY

Upon review of historical testing and construction data on the section of roadway under study, it was determined that the baseline information on subsidence vs. time and original pavement (or natural ground) elevations was either very scant or totally unavailable, as were other data from monitoring instruments that would be essential for such an investigation. The available information was fragmented and incomplete. Virtually no design information was available on the embankment or on the pavement, except as indicated in general terms in this paper. The LDOTD Research Division files were made available to the authors so the historical data could be analyzed. The project engineers of this investigation and the LDOTD Rehabilitation Advisory Group also provided much valuable data and information.

Nevertheless, because of missing links in the data and because of the lack of baseline information, the nature of the methodology used in this investigation was more that of forensic engineering than that of a research project.

The following sets of data were made available and studied in connection with this investigation:

- Subgrade soil borings that were performed by LDOTD in 1985 (Figure 2)
- Standard penetration tests (SPT) (Figure 3)
- Dutch cone penetrometer tests
- Embankment material classification and gradation tests
- Electric cone penetration tests (ECPT)
- Inclinometer observations
- Aerial photographs
- Water table data
- Consolidation tests performed on clay representing soils underneath the embankment

Additionally, interviews concerning construction procedures, maintenance problems, field observations, etc., were conducted with the LDOTD and FHWA representatives.

The authors requested the LDOTD to contract Fugro International, Inc., to perform electric cone penetrometer tests (*9*) at three different sites selected by LDOTD and the investigators. Two of the selected sites were in the distressed portion of the subject project. A third, reference site was selected in a section of I-10 about 1 mi east of the subject embankment. This latter section of the embankment was constructed immediately following the completion of the subject section, also using excavation of the organic clays and hydraulically pumped sand from the Mississippi River. In spite of the fact that the third site investigated has been subjected to the same traffic and static loads, it has experienced relatively insignificant pavement or embankment distress.

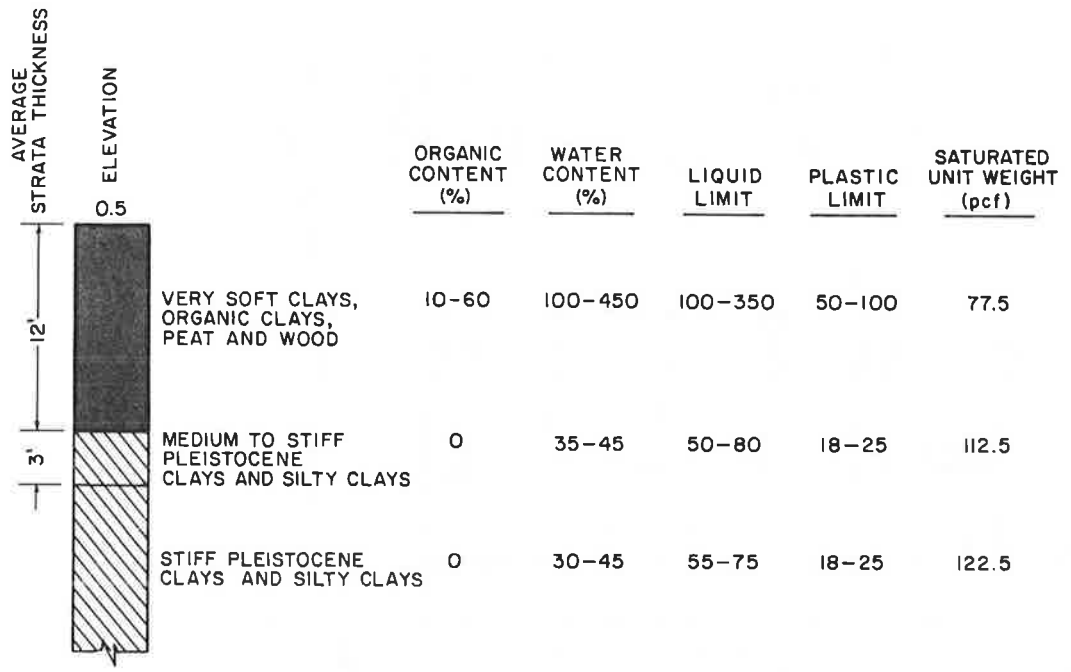

FIGURE 2 Typical subgrade soil profile.

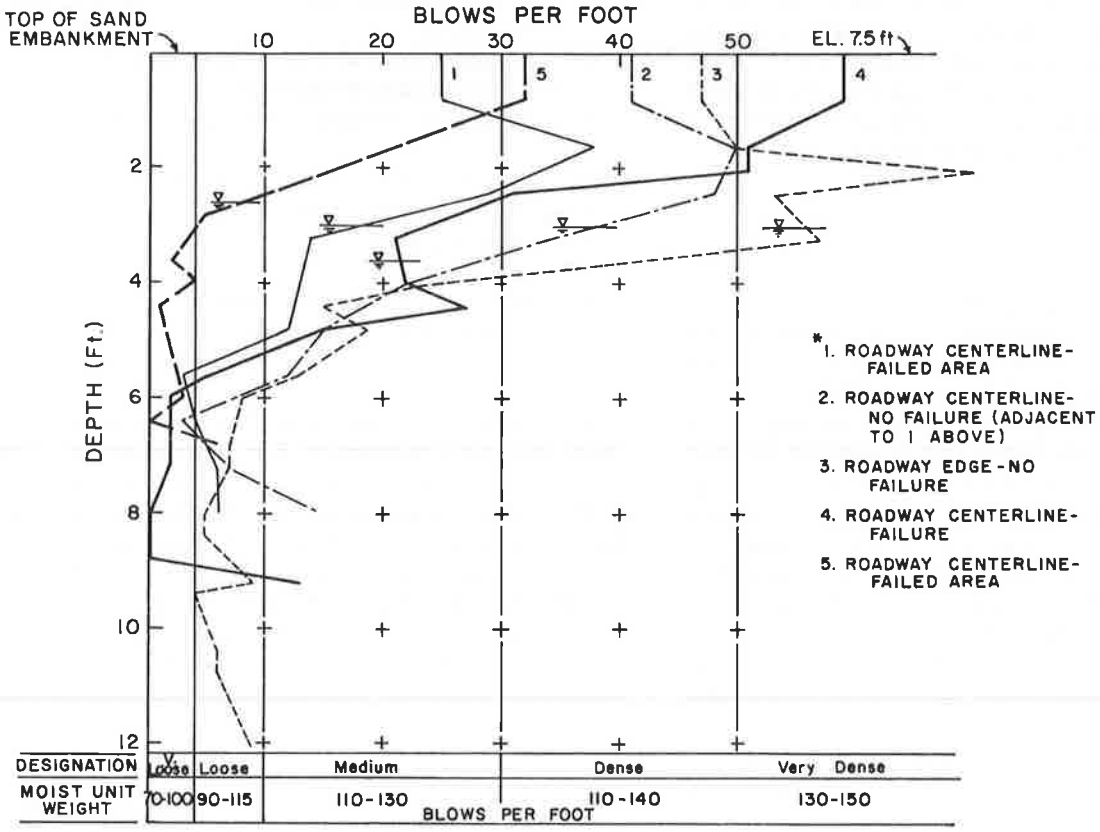

FIGURE 3 Standard penetration tests.

Approximately 180 electric cone penetrometer soundings were performed, concentrated about equally on the three selected sites.

The results of all observations, discussions, and tests were correlated and analyzed, along with additional statistical and numerical analysis performed to determine stress distribution, consolidation, and densification patterns. Scanning micrographs of sand samples were also taken to determine anomalies, if any, in the sand particles (Figures 4 and 5). Embankment rehabilitation methods were reviewed and further field evaluations were recommended.

TEST RESULTS

Soil borings and SPTs performed by LDOTD show that, in general, the profile of the embankment and the underlying material is relatively uniform. The embankment consists of fine silty sand of medium density from 0 ft (datum: the bottom of the pavement structure or the top of the embankment) to a depth of 6 ft, underlain by a loose, fine silty sand to a depth of 9 ft. From 9 to about 18 ft, the embankment was composed of the same silty sand; however, its density was low. The underlying material from 18 to 21 ft is composed of a very-soft-to-stiff silty clay with scattered pockets of soft clays.

The number of blows obtained from SPT tests varies from an average of about 35 in the top 6 ft of sand embankment to 6 blows in the 6- to 9-ft depth and 2–0 blows below 9 ft (Figure 3). Typical sand gradations show that the sand is uniform in size with about 95 percent retained on No. 200 screen and with negligible percentages of clays and colloids. Field exploration identified the location of the water table at about 6 ft below the top of the embankment.

Inclinometers installed through the shoulders and anchored in the stiff Pleistocene clay layer did not show any lateral displacement throughout the approximate 1-yr observation period. During the same time, however, pavement distress continued and extended to new areas.

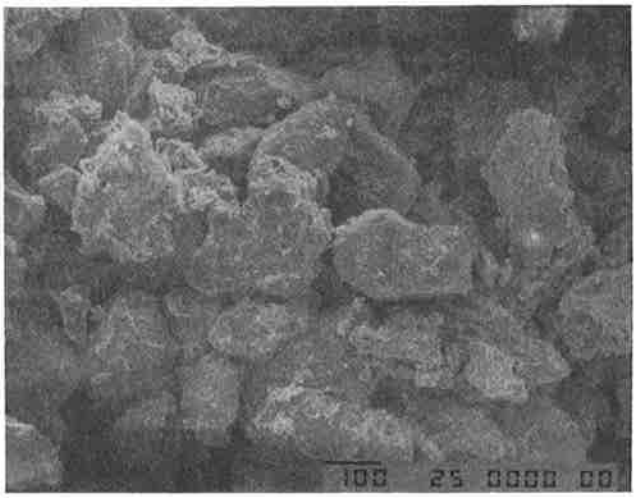

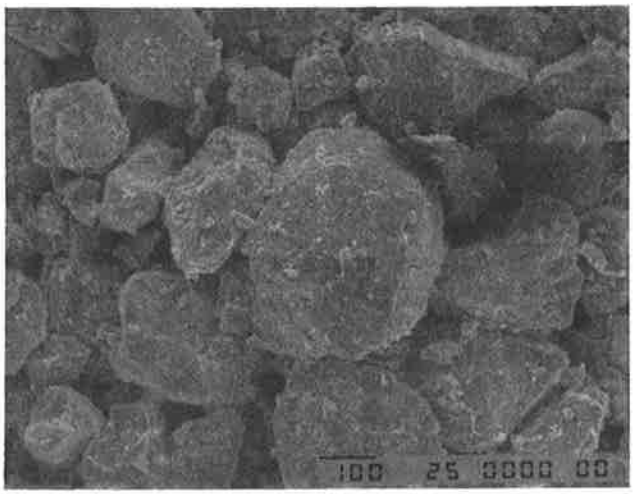

FIGURE 4 Scanning micrographs of sand (100 magnification; scale shown represents 100 microns).

DENSITY TESTS

Density tests performed in the median showed that the dry unit weight of the sand embankment above the water table is in the vicinity of 100 lbs per cubic ft, or about 84 percent of standard proctor density for this sand (Table 1). The water level at the median is shown to be 4.2 ft below the surface, which in turn is about 2 ft below the top of the embankment section under the roadway pavement. These data place the water table in the embankment at about 8 ft below the pavement surface, or 6 ft below the top of the embankment. The moisture content of the sand in the top 3 ft of the median indicates the presence of capillary moisture; consequently, pseudo-cohesion induced by these capillary forces exhibited itself in the form of relatively higher strengths at the surface layers (Figure 5).

The relative densities, based on *N*-values, vary from 80 to 50 percent within the top 6 ft, to from 30 percent to less than 20 percent from 6 ft below the top of the embankment to the bottom of the sand fill. Experience in the area has shown that these polished and relatively rounded sands are unstable at low relative densities because they do not possess interlocking capabilities. Additionally, the micrographs indicate that the size of sand particles used in this embankment vary from one site to another.

SCANNING MICROSCOPY

Scanning electron micrographs of sand specimens obtained from a representative site (Figure 4) show the rounded and/or polished nature of the sand typical of the

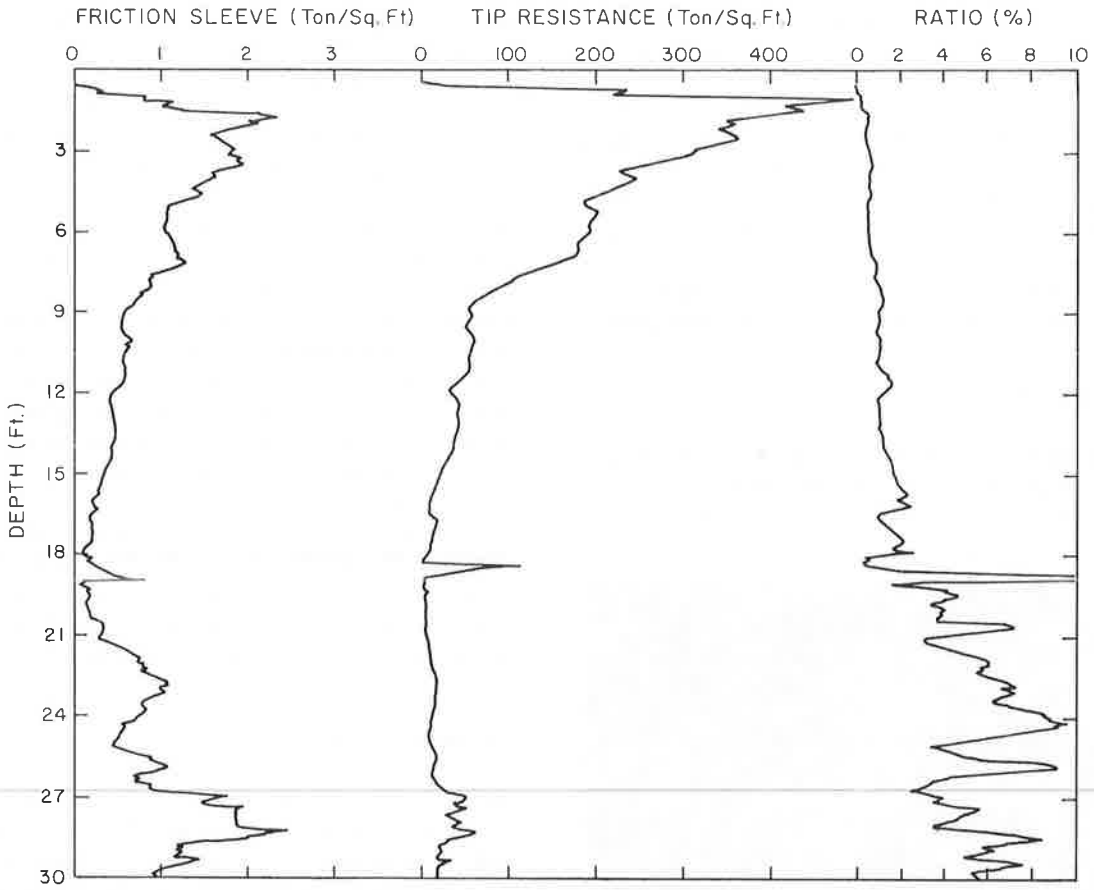

FIGURE 5 Typical ECPT results for the median.

TABLE 1 DENSITY OF IN SITU SAND IN MEDIAN

	Depth 0–1.3′	Wet Density Clay Material	Dry Density Removed	Moisture
	1.3′–2′	105.6 lb/ft^3		
S-1	2′–2.7′	111.4	98.9 lb/ft^3	6.8%
S-2	2.7′–3′	116.1	100.9	10.4%
S-3	3′–3.3′	121.6	104.0	11.6%
S-4	3.3′–4′	128.6	101.8	19.5%
S-5	4.2′	Water Level; No Test	105.4	22.0%

NOTE: Standard (ASTM D698) density of this sand 118 #/cu.ft.

Mississippi River sands of this area. A note of caution should be incorporated into this latter discussion: Specimens used to perform scanning electron microanalysis are not necessarily representative specimens, because the area or the sample size viewed is very minute. These images should be considered indicators rather than definitely representative specimens.

ELECTRONIC CONE PENETROMETER (ECPT) TESTS

Electronic cone penetrometer tests were performed on three roadway sections as discussed earlier. Each section covered both roadways from foreslope to foreslope (200 ft) for a length of 400 ft. Approximately 60 soundings, each 30 ft deep, were performed in each of three test sections. Fugro International, Inc., provided the plots of each sounding for analysis (Figures 5 and 6).

The summary of ECPT results fitted with third-order polynomial curves (Figures 7, 8, and 9) shows that in sites 1 and 2, the density of the sand in the embankment, and thus the dimensional stability, varies substantially based on the location across the roadway. Test results also show that the sand in the embankment under the shoulders (identified as lines 2 and 8, Figure 1) is of medium density in the 0- to 3-ft depth, is loose from 3 to 6 ft, and is very loose from 6 to 15 ft.

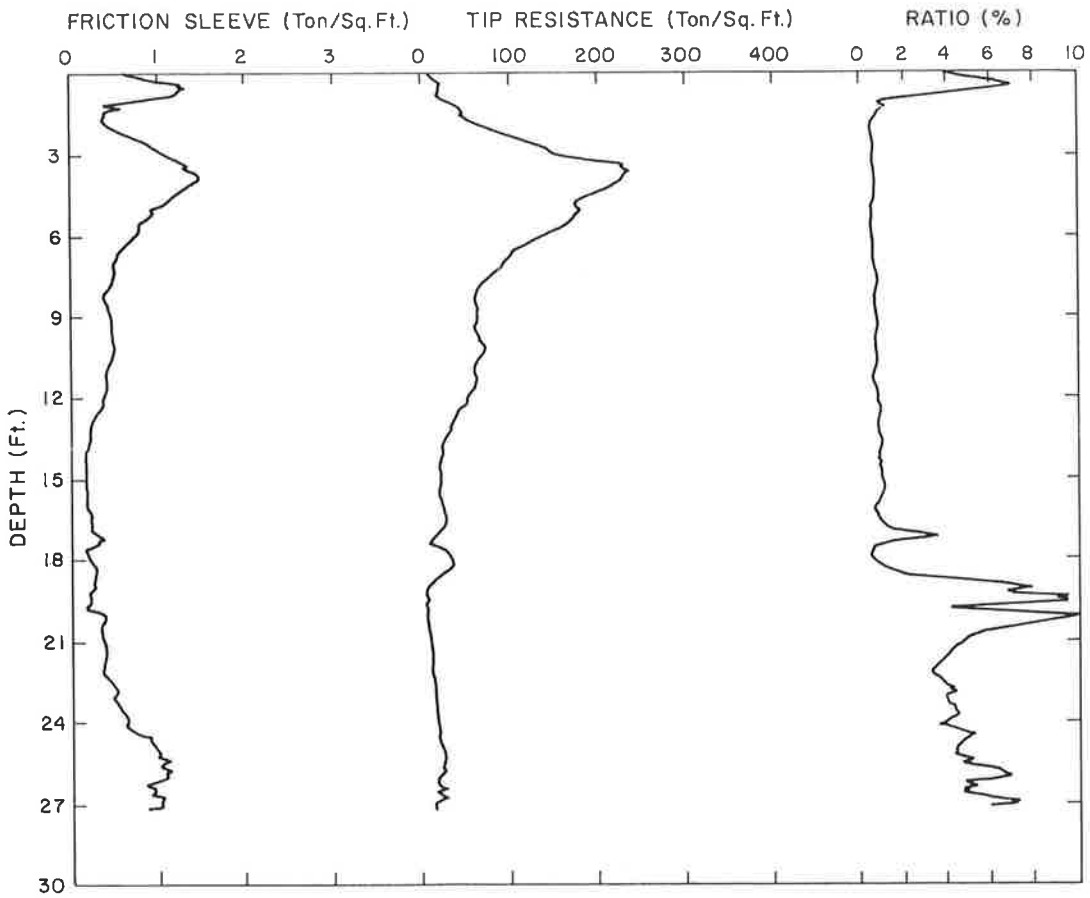

FIGURE 6 Typical ECPT results for traveled lanes.

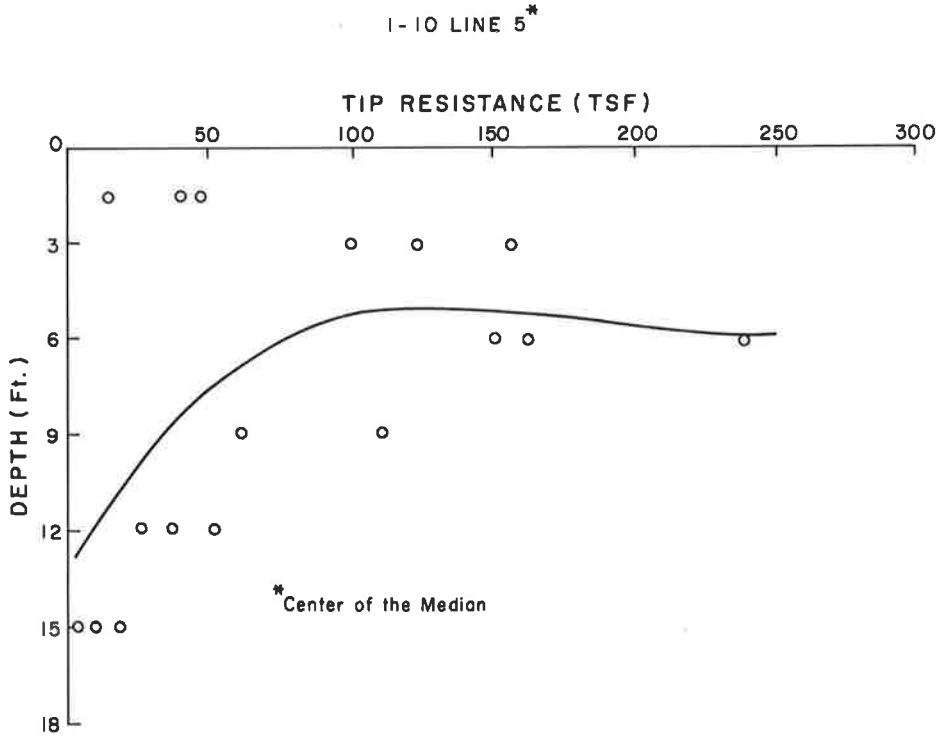

FIGURE 7 Summary of ECPT results for the median.

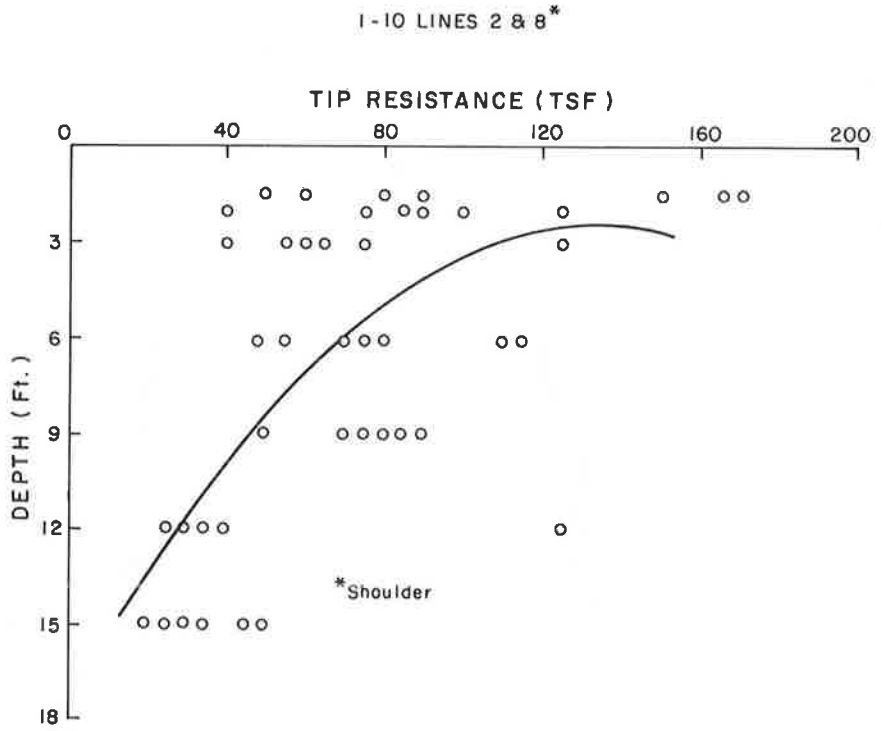

FIGURE 8 Summary of ECPT results for the shoulder.

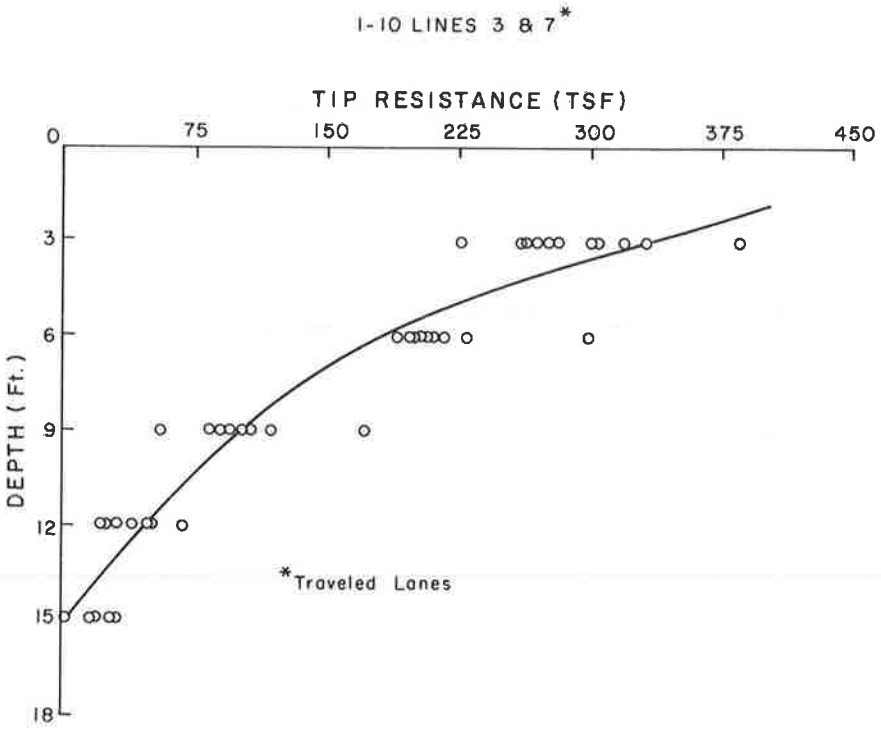

FIGURE 9 Summary of ECPT results for traveled lanes.

In contrast to the above, the sand under traveled lanes (lines 3, 4, 6, and 7, Figure 1) appears to be very dense to dense from 0 to 6 ft, after which the density appears to drop drastically to medium to loose. Typical ECPT tip resistance in the top 3 ft of the embankment at the shoulder is about 140 TSF, while under the traveled lanes (lines 3, 4, 6, and 7) it is about 450 TSF or higher.

The tip resistances under traveled lanes are about 320 percent of those at shoulders.

The ECPT results of line 5 (Figure 7), located at the center of the median, indicate the presence of loose-to-medium to dense sands at depths of 0–6 ft.

Typical tip resistances in the top 6 ft of the median vary from 50 TSF to about 150 TSF, similar to those at shoulders (Figure 8). The top 3 ft of the shoulder material appear to be slightly denser than the comparable layers at the centerline of the median.

Third-order polynomial curves developed high coefficients of correlations (95 to 98 percent) for data under the traveled lanes. However, under the centerline of the median and shoulders, because of the scatter of the data, the correlation coefficients were in the order of 50 percent.

The ECPT results of site 3 (section showing no distress) indicated that the sand was densified to a greater depth and more uniformly across the roadway sections. Sand in the embankment at site 3 appeared to be very dense to dense to a depth of about 9 ft, with a medium density to a depth of about 12 ft, and decreasing to a loose sand below that elevation.

Typical tip resistance at the centerline of the median was measured to be about 175 TSF at 0–6 ft. At similar depths under the traveled lanes (line 3) of site 3, typical tip resistance was about 400 TSF, or about 230 percent of that at the median.

In general, the ECPT results show the presence of pockets of soft clay under the sand embankment varying in thickness from 4 to 9 ft at sites 1 and 2, and from 1 to 5 ft at site 3.

CONSOLIDATION TESTS

Samples of the soft clay representing the layer under the sand embankment were obtained from nonloaded locations near the embankment. These samples were assumed to be representative of original soft clay layers existing under the embankment, since soil classification and elevation of the soils were similar to those under the embankment. The LDOTD Research Division tested the samples.

An analysis of the test results was performed by these investigators. Results showed that under the worst case (assuming a 10-ft-thick layer of soft clay, single drainage, and 0 TSF original overburden), the settlement of the soft clay should have been completed in approximately 5 yr, with no substantial secondary consolidation expected after 9 yr. The embankment has been in place for about 15 yr (3 yr of which were under surcharge), and the pavement is still experiencing subsidence.

ANALYSIS OF TEST RESULTS

The following analysis is presented based on results of investigations of the data and observations.

Test results show that there are pockets of soft clay under the embankment, the thicknesses of which vary from 4 to 9 ft at sites 1 and 2 and from 1 to 5 ft at site 3. A plot of the thickness contours of the soft clay layers at sites 1 and 2 shows that, in general, pockets of the soft clays are only 1–3 ft thick under the roadway sections and deeper only at very isolated locations, generally away from traveled lanes. Yet an investigation of the site 1 eastbound roadway showed signs of extensive maintenance patching of subsidence areas and of new and continuing subsidence throughout the entire test site (including areas containing no soft clay pockets).

Tests at site 3 also showed the presence of 1–3 ft of soft material under the roadway, with a few isolated pockets of deeper soft clay layers. It is significant to emphasize and recognize that site 3 has not, thus far, experienced damaging subsidence.

Considering the above evidence and the results of consolidation tests and analysis, along with the fact that the original embankment was surcharged following its placement, it was concluded that the soft clay was not the cause of continuing subsidence.

Liquefaction as a possible cause for the failure was suggested. A review of test results shows that saturated loose sands are at an elevation of about 8 ft below the surface of pavement, under an overburden pressure of about 1,000 lbs/sq ft. It is highly unlikely that shock waves from traffic loading could develop significant enough stresses in the pore water to overcome such an overburden pressure and develop a quick condition. Thus, liquefaction has been ruled out as a cause of continuing failures.

A review of the density, SPT, and ECPT tests at the median shows that the density of the sand varies from one test site to the other, indicating that deposition or placement rather than controlled compaction at these locations has affected the density and that the sand was not densified originally in a uniform manner. Construction information available to these authors shows that compaction or densification of the fill was not required by the specifications. While a review of the centerline of the median shows the densification is in a narrower and controlled band, the scatter of the ECPT data from test line 5 (and lines 2 and 8) indicates lack of controlled densification. The similarity of tip resistance values at sites 1, 2, and 3 leads one to conclude that the median is representative of as-placed density of the sand embankment. It is also concluded that the presence of moisture at the median has contributed to the tip resistances near the surface by developing capillarity-induced pseudo-cohesion.

A review of the ECPT results of sites 1 and 2 shows that the sand embankment under traveled lanes is denser up to a depth of about 5 ft than at other locations across the roadways. It also shows that all densities at sites 1 and 2 drop substantially at about 6 ft below the top of the embankment, at an elevation coinciding with that of the

water table. The sand at site 3 appears to have been densified originally to a greater depth and to a higher degree. However, densities under traveled lanes at site 3 are also higher.

Interviews of LDOTD personnel indicate that the embankment represented by sites 1 and 2 was constructed by pumping sand into an excavated ditch filled with ground water, while the construction of the section of the road represented by site 3 was achieved by placing the pumped sand inside a construction levee system that was kept partially pumped. The placement of the fine sand slurry under water in the case of sites 1 and 2 did not allow the dissipation of pore pressures, which would have allowed the sand to settle to a denser state, nor did it allow the capillary forces resulting from the seepage of water out of the pores to assist in further densification.

Data which would clearly identify detailed construction procedures used on sites 1, 2 and 3 were not available to these investigators. Therefore, the reasons for differences in the quality of the embankments among sites 1 and 2 and site 3 are based on the interpretations of test and interview results only. It is clear, however, that the embankment represented by site 3 was densified during the construction to a more uniform, higher density and to a greater depth than that at sites 1 and 2.

CONCLUSIONS

The variations of densities under the traveled lanes and at locations away from the traveled lanes in the top layers of the embankment represented by sites 1 and 2 lead to the conclusion that the sand, as placed in this embankment, initially had a relatively low density throughout the layer above the water table, and additional densification has taken place under the wheel loadings.

Considering the polished and rounded shape of Mississippi River sand particles and the evidence that adequate densification was not obtained during placement, it is concluded that sand under travel lanes densified gradually under heavy traffic loads and impacts, causing serious pavement distress.

Because of the higher degree and greater depth of original densification of the sand, the section of the road (site 3) on the east has not experienced similar subsidence and distress. However, lower layers of the sand in that embankment are also loose.

The electronic cone penetrometer proved to be an excellent, indispensable, and economic tool to identify the condition of the embankment and to reconstruct the physical events leading to the distress of this embankment.

Evidence shows that originally the hydraulic fill was placed partially under water. This procedure did not allow the submerged portion of the sand embankment to densify (below 6 ft) into a stable mass. The relatively loose sand under travel lanes above the water table densified under traffic loading, causing displacement of sand particles and thus a reduction of volume associated with densification. The sand embankment has subsided differentially due to loading by traffic and is continuing to subside.

RECOMMENDATIONS

The original plans and specifications for the placement of the embankment should have required at least partial dewatering of the excavation prior to and during the placement of the hydraulic embankment. With the polished and fine sands of the lower Mississippi River, it is particularly necessary that water be allowed to escape from the pores following placement so that pore pressures can dissipate, thus allowing relatively uniform densification to take place aided by seepage-induced capillary forces. The dewatering should have been followed with a controlled compaction procedure, preferably using vibrators.

Considering the quality of the sand deposits available in most parts of the lower Mississippi River Basin and other alluvial areas, it is recommended that such sands not be used for hydraulic embankment construction without a thorough analysis of their fundamental properties. Properties such as particle shape, surface characteristics, and gradation must be considered carefully.

Placement procedures and quality control requirements for hydraulic embankments should be considered and specified prior to design and construction. Routine quality control procedures, for example, do not apply to this type of construction.

Construction procedures should specify a means of dewatering the sand after it is placed, particularly where the water table is high.

An electric cone penetrometer should be used for quality control of this type of construction.

REMEDIAL RECOMMENDATIONS

A number of soil improvement methods have been considered for possible remedial procedures for this project. Such methods as dynamic compaction, vibroflotation, vibroreplacement, and blasting are among the methods considered.

When dynamic compaction is applied to a strip of sand located adjacent to very soft material, the sand, under dynamic loading, may migrate out of its boundaries, infringing into the soft soils. Furthermore, densification by dynamic compaction results in change in the volume of the embankment, which requires the addition of a considerable amount of new fill material over the existing embankment. Vibroflotation and vibroreplacement will also result in reduction of volume, presenting problems similar to that caused by dynamic compaction.

Densification by blasting is a chancy process practiced by very few specialty contractors. The results are not readily predictable. If blasting works, it requires the addition of new embankment material, and it is expected that in this case it would be uneconomical.

None of the above, in situ improvement methods were considered practical for the solution of this problem.

The nature of the problem does not lend itself to a ready-made, simple recommendation. The following solutions have been considered:

- Abandon the existing roadway and build an elevated highway at an approximate cost of $56 million. This alternative is the most drastic and expensive solution; it does not appear to be necessary or feasible at this time.
- Remove the pavement and the embankment and reconstruct both for about $52 million. This alternative presents serious problems in terms of traffic safety and economic impact upon Baton Rouge and New Orleans, resulting from the partial removal from service of the main artery between these two cities.
- Rehabilitate the embankment and replace the CRCP pavement at a cost of about $14 million. This alternative appears to be the most reasonable. If it can be accomplished, disruption to traffic can be minimized, existing materials can be reused, and the cost to the state can be drastically reduced. An embankment densification or stabilization scheme such as densification by grout (lime-fly ash or portland cement) injection, installation of lime columns, or vibroflotation may be used. It is the opinion of these investigators that the rehabilitation of this embankment using densification by injection grouting can be achieved with minimum disruption to traffic and in a relatively short period of time.

At the time of the preparation of this paper, plans were underway to perform field studies on the effects of densification and/or stabilization of the sand embankment by grouting. A section of the embankment will also be tested to determine the effects of dewatering of the embankment materials.

ACKNOWLEDGMENT

This project was conducted in cooperation with the Federal Highway Administration and the U.S. Department of Transportation.

REFERENCES

1. J. W. Starring. Sand Fill Pumped 15 Miles for Interstate Construction. *Civil Engineering*, ASCE, Vol. 41, No. 2, 1972.
2. R. V. Whitman. Hydraulic Fills to Support Structural Loads. *Journal of the Soil Mechanics and Foundations Division*, ASCE, Vol. 96, No. SM1, 1970 pp. 23–47.
3. H. M. Reitz and A. H. Hunter, Jr. Compaction of Hydraulically Placed Fills. *Journal of the Geotechnical Engineering Division*, ASCE, Vol. 100, No. GT10, 1974, pp. 1165–1167.
4. W. J. Turnbull and C. I. Mansur. Compaction of Hydraulically Placed Fills. *Journal of the Geotechnical Division*, ASCE, Vol. 101, No. GT5, 1975, pp. 493–495.
5. S. J. Paulos and A. Hed. *Density Measurements in a Hydraulic Fill*. STP 523, ASTM, 1973.
6. Construction of Embankments. *NCHRP Synthesis of Highway Practice 8*. Highway Research Board, 1971, pp. 21–22.
7. Treatment of Soft Foundations for Highway Embankments. NCHRP Synthesis of Highway Practice 8, 1975, pp. 9–10.
8. A. Arman and K. L. McManis. *The Effects of Conventional Soil Sampling Methods on the Engineering Properties of Cohesive Soils in Louisiana*. Louisiana State University Engineering Research Bulletin No. 7, 1977, pp. 1–294.
9. M. T. Tumay, Y. Acar, and R. Boggess. Subsurface Investigation with Piezo-Cone Penetrometer. *ASCE Special Publication on Cone Penetration Testing and Experience*, American Society of Civil Engineers, New York, 1981, pp. 325–342.

Publication of this paper sponsored by Committee on Transportation Earthworks.

Considerations for Stabilizing Drained Failures of Slopes

WILLIAM M. ISENHOWER

Three drained slope failures bordering I-37 in San Antonio, Texas, occurred during the fall and early winter of 1986. One failure resulted from adverse natural seepage conditions, whereas the other two failures resulted from a broken water main and a disrupted surface drainage system. The latter two failures were stabilized by eliminating the water entering the slopes. Several procedures were considered for stabilization of the first failure. Use of horizontal drains was judged to be the most effective in raising the long-term factor of safety for the slope. The design of horizontal drainage systems is reviewed and sample calculations are provided to illustrate that many combinations of drain length and spacing can result in approximately equal gains in factor of safety with time and that longer drains that can achieve higher long-term factors of safety can be only marginally more expensive than systems with shorter drains. A second finding is that there is a limit on the benefit of increasing drain length to increase long-term factors of safety.

The Texas State Department of Highways and Public Transportation has experienced many slope stability failures in San Antonio over the last 20 yr. These failures have been repaired using several methods that have met with varying degrees of success. This paper discusses three recent failures of cut slopes, the factors causing them, and the methods considered to stabilize the slopes. In each case, the failure was the result of unfavorable seepage conditions, but the source of the seepage causing failure differed for each case. The latter part of this paper discusses the design of horizontal drainage systems for stabilizing slopes with adverse seepage conditions.

HISTORY

The slope stability failures discussed in this paper border I-37 in San Antonio, Texas (Figure 1). An 8,000-ft section of I-37 from south of Fair Avenue to south of Hot Wells Boulevard was placed in a depressed (i.e., a cut) section so crosstown streets could remain at grade. This section of I-37 was initially constructed without frontage roads. In 1986, plans were being prepared for the construction of frontage roads in this section. Because of the history of slope stability failures, the author began working with personnel of the San Antonio District in September 1986 to assess potential slope stability problems that might be associated with construction of the frontage roads.

The soil in this area is poor; it is a highly fissured, expansive clay with vertically oriented seams of coarser grained materials. The plasticity indices for the clay are in the 60–70 range. Problems with the expansiveness of the clay have plagued this highway since it was built. Expansion of the clay after the cut was opened affected ride quality to such a degree that leveling-up of the highway was required before it was first opened to traffic. The severity of the problem is evidenced by the damage many houses in the surrounding neighborhoods have suffered from the highly expansive clays. In addition to the vertical movements found under the pavement, significant horizontal swelling movements have been observed at overpass abutments and embankments. The swelling of soil at the abutments has been aggravated whenever the joint between the abutment and the concrete riprap below the overpass has opened. This opening allows any water entering the expansion joint at the abutment to enter the soil below the abutment.

In 1986, rainfall in San Antonio was greater than average. The long-term yearly average rainfall for San Antonio is about 27.5 in. per year. The rainfall in 1986 was approximately 44 in., with most of the rain occurring in the fall and winter months. Three slope failures occurred during the fall of 1986. The first failure occurred just north of Southcross Boulevard during September and October. The depth of the cut in this area is about 38 ft. The progress of this failure was slow. The second and third failures occurred on the same night in December 1986 after a period of intense rainfall; the former, north of New Braunfels Avenue where the cut is about 45 ft deep; and the latter, just south of Southcross Boulevard where the cut is about 35 ft deep. Investigation revealed that although each failure occurred because of unfavorable seepage conditions, the origins of the unfavorable conditions differed.

Several slope stability failures had taken place in cut slopes in this section before the three failures discussed in this paper, and more failures occurred in the spring. The earlier failures were usually shallow sloughs, no more than a few feet deep, and were repaired by stabilizing the clay

Texas State Department of Highways and Public Transportation, Highway Design Division, D-8PD, 11th and Brazos, Austin, Tex. 78701-2463.

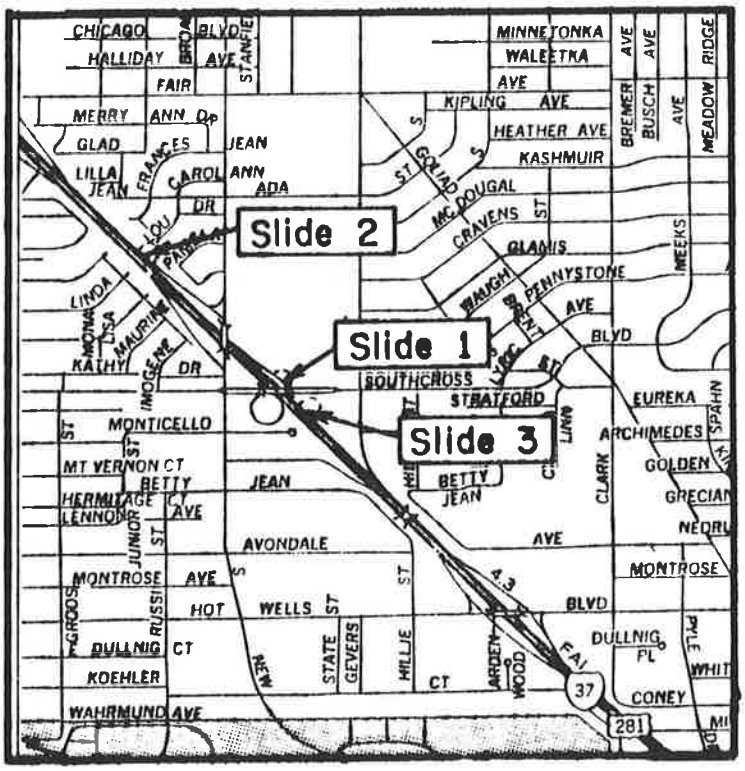

FIGURE 1 Location map.

with lime and constructing slide suppresser walls at one-third and two-thirds of the slope height. The lower slide suppresser wall was constructed of 24-in.-diameter drilled shafts with a spacing of 5 ft, with a 4-ft-wide panel supported by the shafts. The first slide suppresser wall failed structurally at the joint at the base of the panel. The shafts were repaired by reinforcing them with H-pile sections, and a second slide suppresser wall was constructed higher on the slope. The second slide suppresser wall was constructed of H-pile sections with surplus guardrail spanning between H-piles. The repair to this section has performed well and has required no further maintenance.

OBSERVATIONS

Observations were started in September 1986. At first, observations were concentrated on the area repaired with slide suppresser walls located about 100 yd north of the location of the first slope failure. Three slope indicator tubes and three groundwater observation wells were installed on a line parallel to the crest of the slope. Early photographs show that the surface of a shopping mall parking lot near the crest of the slope about 100 yd south of the repaired section had cracked, but that no large vertical movements at the top of the slide had taken place. The large crack in the concrete riprap had occurred several years previously and was believed to be symptomatic of erosion of the ground surface beneath the riprap and not of a slope failure. A program to take slope indicator measurements every 3 to 4 weeks at the three locations in the area to the north was started in October.

By middle to late fall, it had became apparent that the first slide (slide 1) was in the area south of the section being monitored. It is interesting to note that the progression of this failure was slow, occurring over several months. In early December, a 30-ft slope indicator casing was installed at the downhill edge of the entrance ramp, roughly in the middle of the slide mass. Slope indicator measurements were taken with time, and the measurements are summarized in Figure 2. The slope indicator measurements found a slip surface at a depth of 20.5 ft.

The direction of natural seepage in the area of the failures is from east to west. During dry summer months, the seepage can be detected by the the color of the grass: green on the eastern side of the highway cut and brown on the western side. The first failure is adjacent to a shopping mall parking lot. The asphalt parking surface forms a relatively impermeable barrier against evaporation and transpiration of groundwater in this area. The depth to the water table was measured to be steady at about 5.8 ft below the surface of the parking lot near the slope failure. The natural structure of the soil was revealed when the soil was excavated for lime treatment. The natural soil was found to contain two vertically oriented sets of joints: one set was brown due to iron stains, and the other was the grayish color of the parent material. The brown joints point off to the east toward an observation well that was

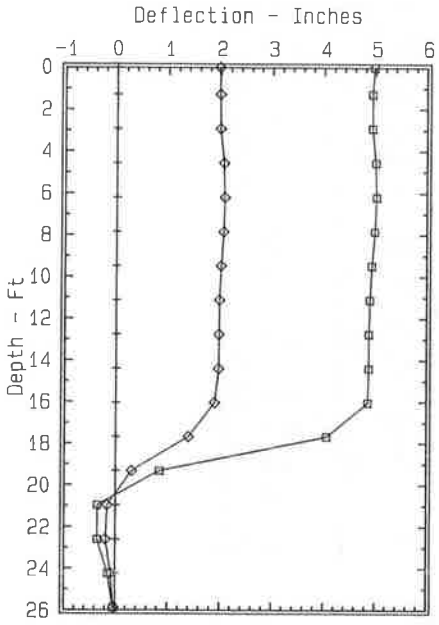

FIGURE 2 Slope indicator.

usually dry. The gray joints are oriented along a north-south alignment and line up with an observation well where the water levels are high. The orientation of the joints leads one to believe that the direction of natural seepage is not perpendicular to the alignment of the highway, but intersects the cut at an angle.

The second slope failure is adjacent to a residential area located north of slide 1 on the eastern side of the highway. Here, grass lawns and large trees consume some ground water. In September 1986, the houses along the alignment of the northbound frontage roads were destroyed or removed. When the second failure was inspected, a large flow of groundwater was observed to be saturating the slope. It was suspected that the groundwater source was a broken water main because of the steady, consistent flow. To confirm this suspicion, water samples were taken and tested for presence of chlorine. The water samples tested positive, and after a search was conducted, the broken main was found in the yard of one of the removed houses and repaired. The slope dried out quickly after the water main was repaired. The elapsed time between the removal of the house, when the water main was probably broken, and the second failure was about 4½ months.

The third failure occurred between Southcross Boulevard and a large structure that was constructed to drain the area above the cut. Inspections made after the failure found that construction of buildings adjacent to the cut had left a low depression outside of the right-of-way that could pond surface water and that it was possible that the newer buildings had not been connected to the sanitary sewer system. Inspection of the buildings also revealed architectural damage due to swelling soils. Later when the slide mass was being lime-stabilized, the soil was found to be saturated, suggesting that the combined effects of the ponded water and septic field had saturated the slope.

STABILITY ANALYSES

Analyses of slope stability are necessary for the evaluation and planning of any repair measures. The two primary reasons for performing stability analyses are to evaluate the conditions causing the first stability failure and to evaluate the effectiveness of the various options available for repair of the slope.

One can perform stability analyses using two different approaches. The preferred approach is to analyze the stability of the slide in question using a suitable technique, usually a computer program. This approach has the advantage that the specific slope geometry and seepage conditions can be considered. A second approach is to use stability charts for simple slopes. These charts are developed for slopes with specified seepage conditions. This second approach is less flexible than the first approach.

Both approaches require information on the shearing properties of the soil and the position of the water table. To evaluate an existing failure, the stability analysis is used to check the data for shearing properties that will be used in later analyses. Ideally, one should obtain a factor of safety of 1.0 and good agreement between the predicted and observed failure surfaces.

Stability analyses of slide 1 were made using UTEXAS2 (*1*). This program, an updated version of UTEXAS that has been modified to analyze reinforced slopes, uses Spencer's method (*2*) and can search for critical surfaces that are circular or noncircular. Spencer's method is similar to the method of Morgenstern and Price (*3*) in that all equations of equilibrium are satisfied. In Spencer's method, the problem is simplified by assuming that the angles of thrust between all slices are equal. The factor of safety calculated using this method is slightly higher and more accurate than the widely used simplified Bishop procedure (*4*). The reader is referred to Spencer (*2*) for further details.

Because the soil profile at slide 1 was relatively homogenous, the shearing properties were back-calculated for the observed failure surface by using the following procedure:

1. Values of effective stress shearing parameters (c' and ϕ') were assumed, and the factor of safety for the observed failure surface was evaluated. Holding cohesion constant, values of ϕ' were varied until the factor of safety equal to 1.0 was bracketed. The value of ϕ' corresponding to a factor of safety of 1.0 was calculated using linear interpolation. This procedure was repeated for several assumed values of cohesion. Values of ϕ' versus c' for the single surface analyses are plotted in Figure 3.
2. The procedure used in step 1 was repeated, using the search mode for critical failure surface of the program to find the combinations of c' and ϕ' for a factor of safety of 1.0. These combinations of ϕ' versus c' were plotted together with the values found in step 1. The back-

calculated shear strength parameters are the combination of c' and ϕ' where the two lines touch. Typically one will find that the c'–ϕ' line from the single surface analyses is straight and the c'–ϕ' line from the search analyses is curved and is tangent to the single surface line.

The above procedure finds the shearing strength parameters that allow a stability analysis to match the observed failure surface using the automatic search mode, given the assumed groundwater condition in the slope. The water table used in this procedure was based on field observations. The position of the water table at the top of the slope was fixed by long-term measurements at an observation well at the top of the slope. The position of the water table on the slope face was determined by the wet condition of the face and standing water found in post holes when the guardrail bordering the entrance ramp was removed.

The results of the analyses made for the two steps discussed above are shown in Figures 3 to 5. The water table was assumed to be that shown in Figure 6, where the line of seepage was near the slope profile. The comparison of the single-surface and search modes of analysis found $c' = 100$ psf and $\phi' = 18.8$ deg. The value for ϕ' is reasonable compared with published correlations of angle of friction with plasticity index.

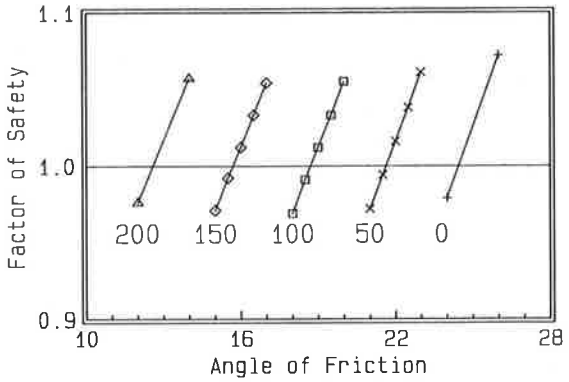

FIGURE 3 Single surface analyses.

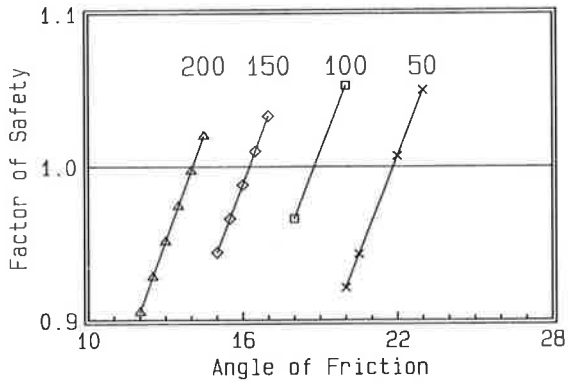

FIGURE 4 Search analyses.

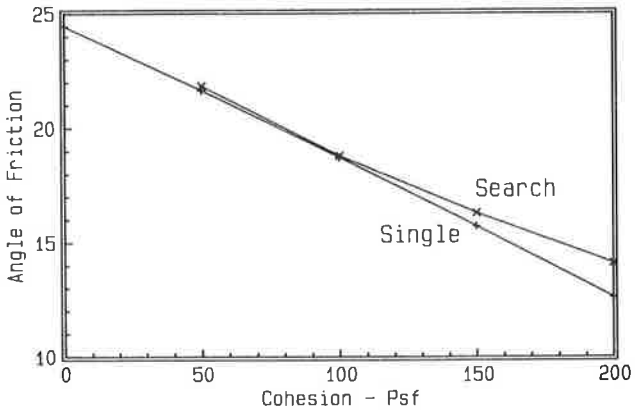

FIGURE 5 Back-calculated shearing parameters.

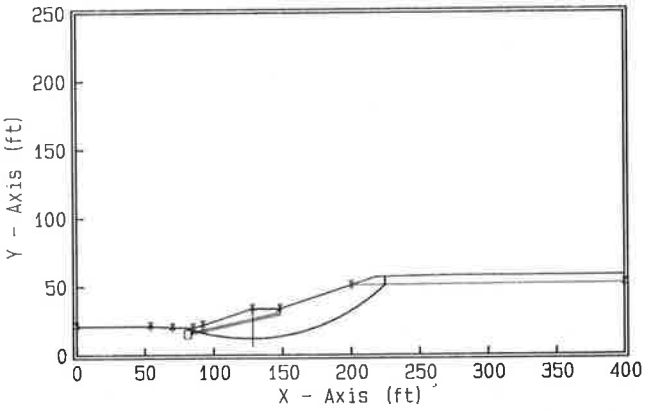

FIGURE 6 Existing conditions.

EVALUATION OF REPAIR MEASURES USING HORIZONTAL DRAINS

The obvious solution to stabilizing these slope failures is to lower the position of the groundwater in the slopes. For slide 2, this task is easily accomplished by repairing the broken water main and letting the slope drain naturally. For slide 3, the position of the water table was lowered by repairing the surface drainage facilities to eliminate ponding and by connecting the newer buildings above the failure to the sanitary sewer system. Controlling the natural seepage that caused the first failure will require the installation of subsurface drains.

A review of the relevant literature found that bored horizontal drains should work best for this application. Unfortunately, guidelines for design of horizontal drainage systems are not widely available, and the designer is faced with several questions concerning design:

- To what degree can horizontal drains raise the factor of safety against failure?

- What is the best scheme for installation of drains? Specifically, what combination of rows and lengths are most effective for draining the slope?
- How long will the drains take to become effective and raise the factor of safety to an acceptable level?

Because the conditions for each site are different, the best scheme is different for each site. However, some general comments can be made that are true for many sites. These questions are addressed in the following sections.

Change in Factor of Safety

Several approaches are available for estimation of the increase in factor of safety by the lowering of the water table by drains. Two simple methods are to use the stability charts developed by Hoek and Bray (*5*) or the charts developed by Bishop and Morgenstern (*6*). A third alternative is to make site-specific slope stability analyses using an appropriate computer program. These alternatives will be discussed in turn.

Hoek and Bray Charts

Hoek and Bray (*5*) have developed a set of five charts to estimate the factor of safety for simple slopes with assumed seepage profiles ranging from dry conditions to fully saturated conditions. One may enter Hoek and Bray's charts for the existing conditions and check the predicted factor of safety. Then one may refer to one of the charts for conditions of lowered groundwater to estimate the change in the factor of safety for lowered groundwater conditions. The user may have difficulty in using these charts for shallow slopes because the lines defining the angle of slope are not defined on some charts and the contours on the charts become quite dense in the region for shallow slopes.

Bishop and Morgenstern Charts

A second approach is to use the pore-pressure ratio, r_u. This factor is equal to the ratio of average pore pressure over vertical total stress along the shear surface. The pore-pressure ratio is defined as

$$r_u = \frac{u}{\gamma h}$$

where u is the average pore pressure, h is the depth of the point in the soil mass below the soil surface, and γ is the total unit weight of the soil. Bishop and Morgenstern (*6*) have developed design charts to estimate the factor of safety as a function of the pore-pressure ratio r_u, ϕ', and $c'/\gamma H$ for the case of a simple slope without a toe berm or bench. Bishop and Morgenstern have evaluated the factor of safety for various combinations of slope angle and shearing properties and fit regression lines through the results so that the factor of safety could be estimated using stability coefficients, m and n. The factor of safety is estimated from

$$F = m - nr_u \tag{1}$$

Assuming a factor of safety of 1.0 for a failed slope, one may estimate the value of r_u for the slope from

$$r_u = \frac{m - 1.0}{n} \tag{2}$$

The stability coefficients m and n were developed by Bishop and Morgenstern and presented in design charts as functions of ϕ', $c'/\gamma H$ (H = slope height), and bedrock depth factor D (depth to bedrock = DH). The value of r_u needed to raise the factor of safety to an acceptable level, F_d, is then calculated from

$$r_u = \frac{(m - F_d)}{n} \tag{3}$$

Now one can compare the two values of r_u and estimate how much the water table needs to be lowered to raise the factor of safety to the desired level. If the value of r_u is near zero or negative, it is likely that lowering of the groundwater alone will not be enough to raise the factor of safety to the desired level. In these cases, it will be necessary to flatten the slope in addition to lowering the ground water. In cases where r_u is positive, one may estimate the amount that the water table needs to be lowered from

$$\Delta z_w = \frac{r_u \gamma h}{\gamma_w} \tag{4}$$

where γ_w is the unit weight of water. Calculation of the distance that water should be lowered is useful in estimating how effective different locations for drains will be in raising the factor of safety.

Site-Specific Stability Analyses

In many cases, use of the stability charts is prevented because the unique conditions at a given site require that a site-specific stability analysis be made. The conditions at slide 1 will be used as an example of site-specific stability analyses. At this location, a freeway entrance ramp crossed the slope, forming a bench. The presence of the bench deviates from the slope geometry assumed by the developers of the stability charts. Stability analyses for several alternatives for repair were made so their relative effectiveness could be established. These analyses demonstrate the effectiveness of lowering the groundwater. The alternatives for repair of this slope follow:

- Installation of horizontal drains to lower the water table in the slope.
- Lowering of the ground water table by 10 ft. This case represents using a trench drain at the crest of the slope or several rows of short horizontal drains at several elevations on the slope.
- Reshaping the slope to put a bench near the top of the slope. This alternative was analyzed because it provided additional space to build frontage roads.

Installation of long horizontal drains from the toe of the slope was examined for four cases. The first case was to lower the ground water to an elevation 10 ft below the elevation of the main lanes of the highway as shown in Figure 7. This case is an ideal (and unrealistic) condition in which the water table is lowered below the critical failure surface and raises the factor of safety to the maximum level possible. The factor of safety for this condition is raised to approximately 1.76.

Three more realistic cases representing the effects of horizontal drains are those shown in Figures 8 through 10, which represent long-term conditions with horizontal drains installed at an elevation 4 ft above the toe of the slope. These cases differ in that the drain lengths are 50, 100, and 150 feet. In each of these cases, pore water pressures in the soil were assumed to be equal to zero above the water table. The assumption of zero pore pressures above the water table is conservative because any hydraulic gradient due to downward flowing seepage will increase the vertical effective stress, thereby increasing the soil's shear strength. For the case of the 50-ft drains, the factor of safety was raised to 1.28. For 100- and 150-ft drains, the factor of safety rose to 1.41 for both cases. Both cases have the same factor of safety because the critical surface does not extend into the zone covered by the additional length of the longer 150-ft drains.

In contrast, the second alternative, lowering the groundwater to 10 ft below the slope profile, could raise the factor of safety to only 1.26. This level is significantly lower than for the first alternative in which 100-foot drains were used.

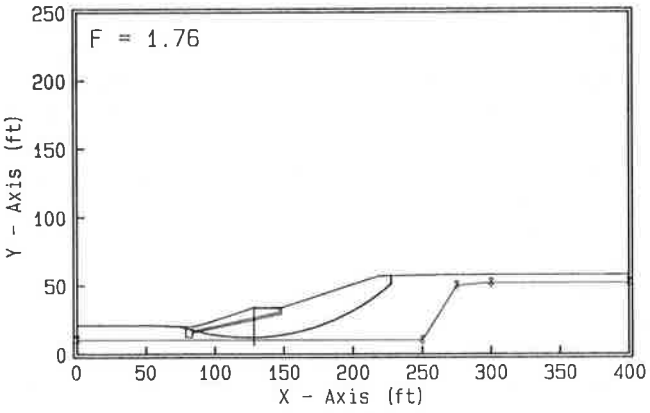

FIGURE 7 Maximum drainage.

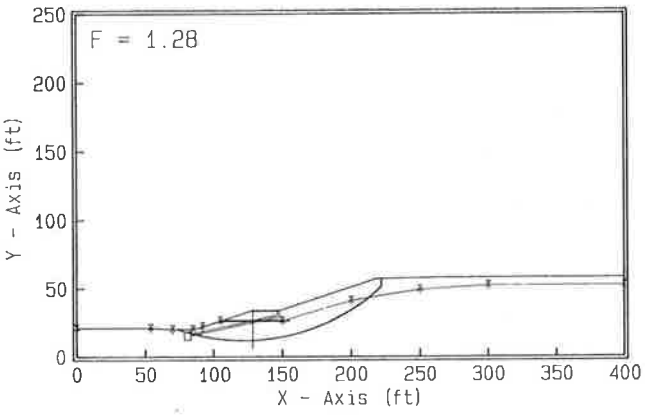

FIGURE 8 Fifty-ft drains.

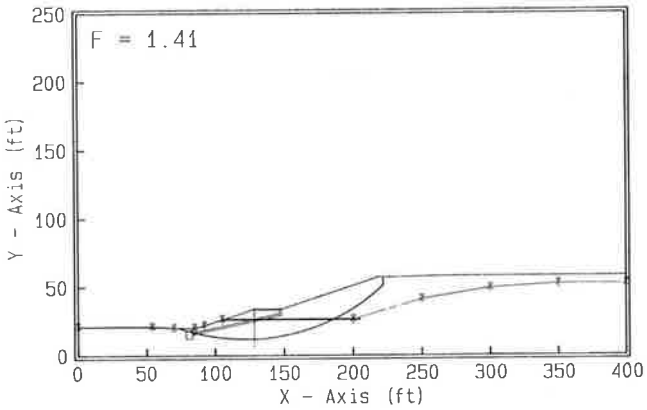

FIGURE 9 One-hundred-ft drains.

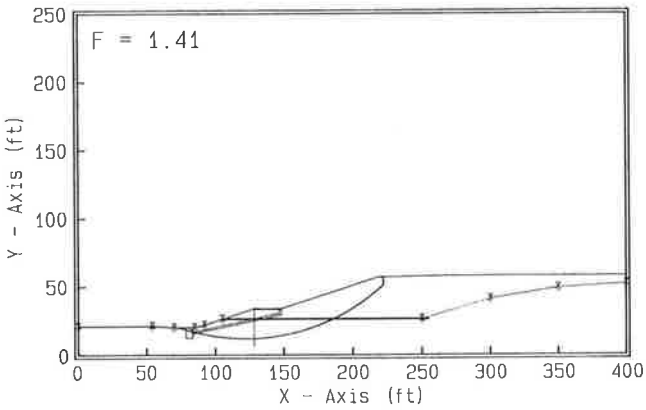

FIGURE 10 One-hundred-fifty-ft drains.

The critical surface and line of seepage assumed for this alternative is shown in Figure 11.

The third alternative, cutting the crest 10 ft, was found to be only marginally effective. This alternative could raise the factor of safety to only 1.04. Reshaping the slope is only marginally effective when the cut removes only a

small section of the slide mass at the crest of the slope. The critical surface for this analysis is shown in Figure 12.

In summary, the most effective scheme for raising the long-term factor of safety is to install horizontal drains from near the toe of the slope. The general effectiveness of the horizontal drains is limited by the lower limit of elevation from which the drains can be drilled.

Installation Schemes for Drains

The second question regarding the use of horizontal drains to stabilize a slope is related to selecting the scheme for installing the drains that results in the best drain performance and lowest cost. Specifically the questions relate selection of the best location, length, and lateral spacing of drains and determination of the relative advantages and disadvantages of these factors related to performance.

Nonveiller (*7*) has investigated the efficiency and time response of horizontal drains using a three-dimensional finite difference seepage analysis coupled with a slope stability analysis that used the pore water pressures calculated in the seepage analysis to calculate effective confining stresses in the slope. Nonveiller considered three schemes of equal total drain lengths: in a single row from the toe of the slope, in two rows at the toe and midpoint of the slope, and on 10 levels up the slope. Nonveiller found that long drains from the toe are more efficient at lowering the pore pressures in the slope than multiple levels of drains and thus were able to raise the factor of safety the greatest amount. In addition, Nonveiller found that smaller horizontal drain spacings are more efficient in lowering average pore pressures and respond faster after installation because each drain covers a smaller volume of soil.

Kenney et al. (*8*) and Nonveiller (*7*) have studied the relative efficiency of spacing of drains and length of drains on raising the factor of safety. Both have found that closely spaced drains work better than widely spaced drains and that longer drains work better than shorter drains. Closely spaced drains are more effective becuase they can lower the average pore water pressure between adjacent drains to a lower value than more widely spaced drains can. Longer drains are more effective because they can lower the pore water pressures farther into the slope than shorter drains can. Obviously, there is a limit to the gain in efficiency from increasing drain length. For example, in the analyses presented in the previous section, both the 100- and 150-ft drains were found to raise the factor of safety to the same value. The increase in the factor of safety depends primarily on the lowering of the water table near the critical failure surface. Changes in the water table beyond the critical failure surface have no effect on the calculated factor of safety.

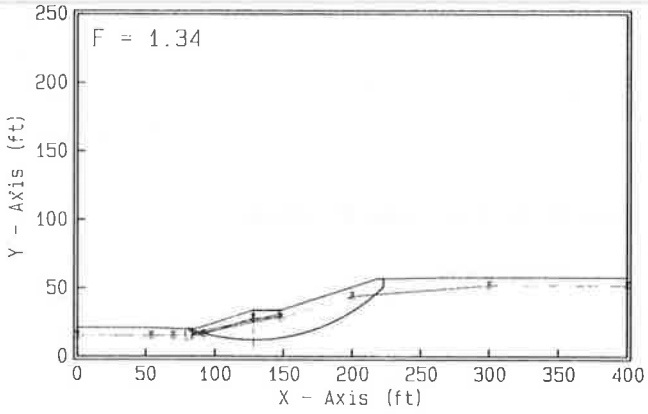

FIGURE 11 Ten-ft drainage.

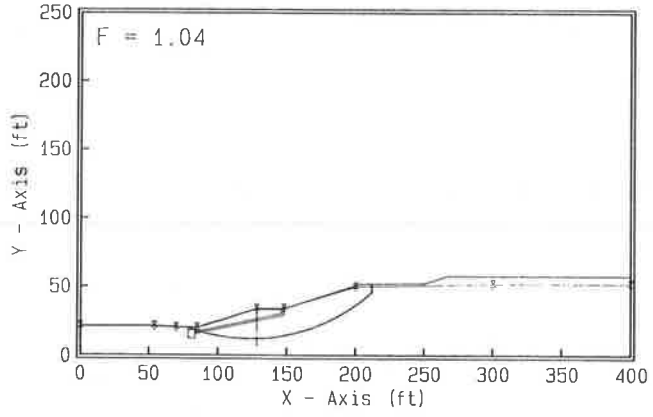

FIGURE 12 Cut-crest slope.

Time Response of Horizontal Drains

In any event, the selection of the spacing and length of drains should be based not only on the long-term factor of safety, but also on the effectiveness of drains in lowering the water table (and thereby raising the factory of safety) in a reasonable period of time. Nonveiller's study found that drainage systems with equal spacing ratios (drain spacings squared over drain length) responded similarly in obtaining a given factor of safety soon after installation. Nonveiller also found that larger differences were obtained at later times, with longer drains obtaining higher factors of safety. Thus, one can design several drainage systems that can obtain a given factor of safety in a fixed time period and that have a variety of different drain spacings and lengths. At this point, one needs to compare the relative cost of different systems of drain spacings and lengths that have approximately equal early time responses, but different long-term factors of safety, to determine whether the gains in long-term factors of safety are worth the additional expense. Ideally, this comparison should be made on a case-by-case basis. However, no readily available computer program is available that allows one to do this. Fortunately, Nonveiller's work allows one

to make some sample calculations to approximate the costs involved.

Nonveiller presented data for the rise in factor of safety with time of horizontal drains installed with various lengths and spacings for the case of 2 horizontal : 1 vertical slopes. The time factor for a rise in the factor of safety with time is expressed by

$$\theta = \frac{tc_v L}{(H_i S)^2} \tag{5}$$

in which t is time, c_v is the coefficient of consolidation, L is the drain length, H_i is the height of the slope, and S is the drain spacing. The units of the time factor are 1/length. The value of θ for a rise in factor of safety from 1.0 to 1.2 is 0.0049/ft (0.016/m). Using drain lengths of 50, 100, and 150 ft, a time period of 180 days, a coefficient of consolidation of 0.093 ft^2/day, and a slope height of 40 ft, the following drain spacings, numbers of drains, total drain lengths, and adjusted drain lengths were calculated (Table 1).

These calculations were based on the conditions existing at slide 1 in San Antonio and on an assumption of a slide width of 200 ft. The spacing for each drainage system was planned so that a factor of safety of 1.2 could be achieved in 180 days. The number of drains is equal to a slide width of 200 ft divided by the drain spacing. The total drain length is simply the length of the individual drains multiplied by the number of drains, and the adjusted drain length is equal to the total drain length plus an arbitrary additional cost of 50 ft of drain per drain that was added to reflect the cost involved in moving and aligning the drilling rig, surveying drain locations, and providing facilities to handle outflow from the drains. The 50-feet-of-drain-per-drain charge is intended for illustration only and may not apply to all situations.

The purpose of these calculations is to illustrate that increases in the long-term factor of safety can be achieved for little additional expense over the cost of systems that have similar short-term effectiveness. A secondary purpose is to illustrate that there is an upper limit to the benefits of increasing drain length. For this example, there is no reason to use 150-ft drains because the long-term factor of safety is no higher than that achievable using 100-ft drains.

SUMMARY AND CONCLUSIONS

Drained failures of cut slopes often occur when unfavorable seepage conditions are present. The three slides discussed in this paper were all in the same soil formation and all failed due to adverse seepage conditions, but the source of ground water was different for each slide. Natural seepage caused one failure, a broken water main caused the second failure, and ponded water on the crest and a possibly unconnected sewer line caused the third.

Repair methods differed for each slide. Long-term stabilization of the first slide required control of the natural seepage in the slope. Installation of a system of horizontal drains was judged to be the most appropriate method for control of seepage. Repair of the other slides was accomplished by eliminating the source of water saturating the slopes.

Drained shearing parameters were back-calculated from the geometry of the failure and stability analyses with critical circle searches. Later analyses found that long horizontal drains installed at the toe of the slope were more effective in raising the factor of safety than either cutting the crest of the slope or using shorter horizontal drains or trench drains.

A review of the literature on horizontal drains revealed that long drains installed at the toe of the slope are more effective in raising the long-term factor of safety than are shorter drains installed at higher elevations. The time response of drains was found to increase with decreasing spacing of drains and increasing length of drains. Examples of calculations for drain spacings needed to raise the factor of safety to 1.2 in 180 days were presented for the conditions representing slide 1. These calculations illustrate that many combinations of drain spacing and length can achieve similar short-term time responses, and that the costs of systems that can achieve higher long-term factors of safety can be installed with minor increases in total cost. A secondary purpose of the illustration is to show that there is a limit to the benefits gained by increasing individual drain length.

TABLE 1 SPACING AND COST FACTORS FOR EXAMPLE HORIZONTAL DRAIN SYSTEM

	Individual Drain Length (ft)		
	50	100	150
Drain spacing (ft)	10.4	14.6	17.9
Number of drains/200 ft	19	14	11
Total drain length (ft)[a]	950	1400	1650
Total cost (drain-ft)[b]	1900	2100	2200
Long-term factor of safety	1.28	1.41	1.41

[a] Assuming a stabilized width of 200 ft.
[b] Assuming an additional cost of 50 drain-ft per drain.

REFERENCES

1. S.G. Wright. *UTEXAS2 (University of Texas Analysis of Slopes—Version 2): A Computer Program for Slope Stability Calculations.* Geotechnical Engineering Software, GS86-1, The University of Texas at Austin, 1986, 109 pp.
2. E. Spencer. A Method of Analysis of the Stability of Embankments Assuming Parallel Inter-Slice Forces. *Géotechnique*, Vol. 17, No. 1, 1967, pp. 11–26.
3. N.R. Morgenstern and V.E. Price. A Numerical Method for Solving the Equations of Stability of General Slip Surfaces. *Computer Journal*, Vol. 9, No. 4, 1967, pp. 388–393.
4. A.W. Bishop. The Use of the Slip Circle in the Stability Analysis of Slopes. *Géotechnique*, Vol. 5, No. 1, 1955, pp. 7–17.
5. E. Hoek and J.W. Bray. *Rock Slope Engineering.* Institution of Mining and Metallurgy, London, 1977, 402 pp.
6. A.W. Bishop and N.R. Morgenstern. Stability Coefficients for Earth Slopes. *Géotechnique*, Vol. 10, No. 4, 1960, pp. 129–150.
7. E. Nonveiller. Efficiency of Horizontal Drains on Slope Stability. *Proc., International Conference on Soil Mechanics and Foundation Engineering*, Stockholm, Vol. 3, 1981, pp. 495–500.
8. T.C. Kenney, M. Pazin, and W.S. Choi. Design of Horizontal Drains for Soil Slopes. *Journal of the Geotechnical Division*, ASCE, Vol. 103, No. GT11, 1977, pp. 1311–1323.

Publication of this paper sponsored by Committee on Subsurface Drainage.

Effect of Slag Type on Tufa Precipitate Formation

JOHN OWEN HURD

Tufa, a precipitated form of calcium carbonate, has been observed occluding underdrain outlets, catch basins, and storm sewers in various counties in east and northeast Ohio. Previous research determined that slag used as a subbase was the only factor directly related to the formation of tufa precipitate. However, no differentiation was made among the various slag types used. This study was initiated to determine whether different types of slag affected the formation of tufa precipitate. A total of 37 projects with different types of slag subbase were inspected. Subbases composed of blast furnace slags or steam boiler slag did not promote formation of tufa precipitate. However, because of the presence of free lime in steel slags and slacker aggregate, subbases composed of these materials did promote the formation of tufa precipitate (open hearth slag to a lesser extent than the other types). Long-term stockpile aging of open hearth slag appeared to reduce the amount of free lime sufficiently to lessen the volume of tufa precipitate to acceptable levels.

Tufa, a precipitated form of calcium carbonate, has been observed occluding underdrain outlets, catch basins, and storm sewers in various counties in eastern and northeastern Ohio, as shown in Figure 1. Examples of this condition are shown in Figures 2 and 3. The blockage of the highway drainage system impedes proper drainage of the highway pavement subbase and subgrade, resulting in accelerated deterioration of pavement such as that observed in Figures 4 and 5. The section of freeway has a low volume of truck traffic, yet severe deterioration has occurred.

Feldman (*1*) found that the use of slag as subbase was the only factor directly related to the formation of tufa deposits observed in Ohio. Although precipitate formations have been linked to the use of recycled portland cement concrete for subbases in other states, Ohio has yet to use this particular material as a subbase. Free lime (calcium oxide) in the slag subbase dissolves as water from the roadway surface percolates through the subbase to the subsurface drainage system. This reaction can be expressed by the following chemical equations:

$$CaO + H_2O \rightleftharpoons Ca(OH)_2 \quad (1)$$

$$Ca(OH)_2 \rightleftharpoons Ca^{++} + 2(OH)^- \quad (2)$$

The resulting calcium hydroxide solution produces drain waters with pH values consistently above 11.0. The high pH of the drain waters creates an environment in which the weak carbonic acid, H_2CO_3, formed by the air and water in the underdrain pipes and storm sewers, disassociates into hydrogen and carbonate ions. This reaction can be expressed by the chemical equations:

$$CO_2 + H_2O \rightleftharpoons H_2CO_3 \quad (3)$$

$$H_2CO_3 \rightleftharpoons H^+ + HCO_3^- \quad (4)$$

$$H\,CO_3^- \rightleftharpoons H^+ + CO_3^= \quad (5)$$

In a high pH environment Equations 4 and 5 will be favored to go from left to right.

The carbonate ions in solution combine with the calcium ions to form calcium carbonate. This reaction is expressed by the chemical equation:

$$Ca^{++} + CO_3^= \rightleftharpoons CaCO_3 \quad (6)$$

In a high pH environment the equation above is favored to go from left to right, resulting in formation of tufa precipitate in the underdrain and sewer systems.

Although Feldman determined that slag used as subbase material was the cause of tufa precipitate formation, no differentiation was made among the various types of slag used in highway construction. Different types of slag have significantly different compositions (*2, 3*). The various types of slag used in highway construction in Ohio are discussed briefly.

Blast furnace slag is produced as a byproduct during production of crude iron. It is formally defined as "the nonmetallic product consisting essentially of silicates and alumino-silicates of lime and other bases, which is developed in molten condition simultaneously with iron in a blast furnace." Iron ore, coke, and fluxstone (lime and other metallic oxides) are "burned" in the blast furnace at approximately 3,000°F. The fluxstone reacts with the impurities in the iron ore to form molten slag and molten crude iron. In this carefully controlled process the entire amount of lime and other fluxstone are used to remove impurities from the iron ore. This results in slag which is composed of complex silicates and alumino-silicates, and is devoid of free lime and other simple metallic oxides. Although blast furnace slag is a basic (pH greater than 7.0) material, it is relatively insoluble in plain water because of the complex nature of its constituents.

Ohio Department of Transportation, Columbus, Ohio 43215.

FIGURE 1 Areas in Ohio where tufa precipitate has been observed.

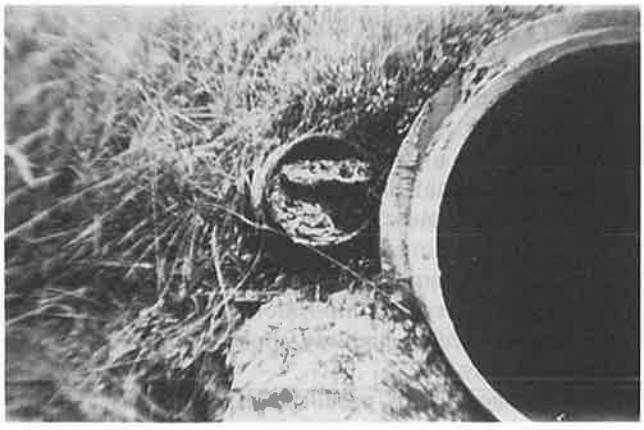

FIGURE 2 Tufa precipitate occluding underdrain outlet.

FIGURE 3 Tufa precipitate flume on fill slope.

There are two types of blast furnace slag used in highway subbases. Air-cooled blast furnace slag is allowed to solidify in mass under atmospheric conditions. After it has solidified, the slag is dug and crushed into the desired grading. Granulated slag is rapidly solidified by immersion in water to form a glossy, granular product sometimes referred to by users as popcorn.

Steel-making slags are nonmetallic byproducts formed during the refining of crude iron into steel. Practically all steel in the United States has been produced by open hearth, basic oxygen, or electric arc furnaces. Current environmental restrictions have eliminated use of the open hearth process. However, stockpiles of open hearth slag are still available.

The steel furnaces are charged with an abundance of flux material so as to remove almost all the impurities in crude iron. The resulting slags are composed of not only the complex silicates and alumino-silicates, as in blast furnace slag, but also free lime and other simple metallic

FIGURE 4 Deteriorated pavement section.

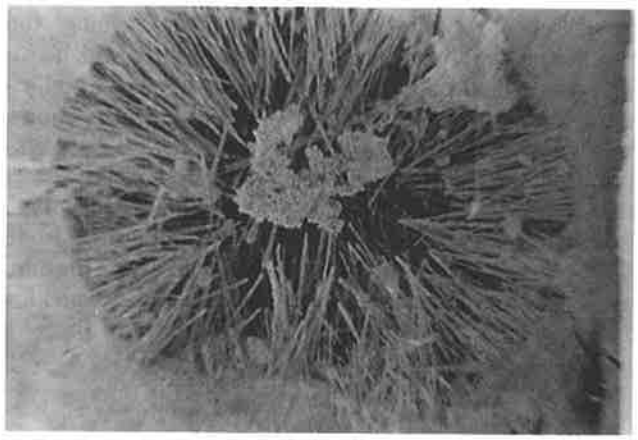

FIGURE 6 Free lime in steel slag vesicule.

FIGURE 5 Tufa precipitate at edge of shoulder.

oxides. Figure 6 shows free lime in vesicules of steel slag. Generally, electric arc slags and basic oxygen slags have much higher concentrations of free lime, approximately 2 percent to 12 percent by weight, than open hearth slags. The specific free lime content of open hearth slags has not been measured. Steel slags are basic materials and the free lime portion is highly soluble in water.

Slacker aggregate is a byproduct of burning limestone to form the lime flux used in iron and steel furnaces. This product has a high concentration of free lime. The specific amount has not been determined, but it is equal to or greater than that of basic oxygen slag. Its use has been discontinued in the latest Ohio Department of Transportation specifications.

Steam boiler slag is actually not slag at all but an acidic bottom ash formed by burning coal to produce electric power. It is devoid of any free lime and other simple metallic oxides.

Because previous research did not distinguish the various types of slag with their different compositions, this study was undertaken to determine whether the type of slag used in subbase affected the formation of tufa precipitate. Comparing the chemistry of tufa precipitate formation to the composition of the different types of slags, it was believed that steel slags and slacker aggregate would produce tufa precipitate while the blast furnace slags and steam boiler slag would not. To confirm this hypothesis, several highway projects in which different types of slag had been used for subbase material were inspected to determine whether tufa precipitate was present.

SITE SELECTION

The computer records of the Ohio Department of Transportation Bureau of Tests were searched to develop a listing of all projects where slag samples had been taken for any use. Unfortunately these records dated back only to projects sold after 1968. Therefore, no specific information was available on most of the projects studied by Feldman. Information on the initial listing was limited to project number and year, slag use for each sample taken, and type of slag for each sample. The projects to be inspected were selected from the initial listing by a process of elimination.

Projects in which slag had not been used as subbase material were eliminated from the list of candidate sites. The remaining projects were looked up in bidding pamphlets listing the amount of various items used on each project. The amount of subbase on the project, the type of project, and whether underdrains had been provided were determined for each project.

Projects in which underdrains either had not been provided or provided only in small amounts were eliminated from the list of candidate sites, as were projects with very small amounts of new subbase, such as small widening and resurfacing projects. It was felt that conclusive results would be obtained only by observing projects with large quantities of slag subbase and numerous underdrain outlets.

It was intended at first to inspect only those projects where the subbase was composed entirely of one particular

type of slag. As this would have severely limited the number of projects observed, some projects in which two types of slag had been used were added after some preliminary conclusions were reached from initial inspections. An attempt was made to limit the two slag-type projects to those with either both blast furnace slags or both steel slags. When this was not possible, additional two-slag type projects were selected which had a predominance of one type of slag. When information was available, slag producers' records were checked to verify the slag types listed for the projects. Types of slags and the number of projects using those slag types are summarized in Table 1.

TABLE 1 SUMMARY OF SLAG TYPE AND NUMBER OF PROJECTS INSPECTED

Slag Type	Number of Projects
Air cooled blast furnace	7
Granulated blast furnace	5
Combined blast furnace	2
Steam boiler	2
Basic oxygen steel	7
Open hearth steel	2
Combined steel	4
Slacker aggregate	1
Combined blast furnace and steel	7
Total	37

INSPECTION

Limits of projects selected for inspection were located on Ohio Department of Transportation highway maps. The general locations of these projects are shown in Figure 7. These sites were clustered about steel-making areas where slag is economically competitive with natural aggregates. It had been planned to inspect approximately 50 projects in all. However, some projects were deleted when certain conclusions became obvious after partial data collection. For example, inspection of projects with basic oxygen slag subbase was discontinued after it became obvious that this type of slag produced large volumes of tufa precipitate. A total of 37 projects, as shown in Table 1, were actually inspected.

On each project, underdrain outlets into catch basins and onto slopes inspected were observed. The presence of tufa was noted and a subjective evaluation made as to the severity of the tufa precipitate formation. Once it was determined that tufa was present on a single slag-type project, approximately one-fourth of the remaining underdrain outlets were observed. In cases where no tufa was seen, each outlet found was observed until the project was complete. On two slag-type projects, each outlet was observed and the limits of the presence or non-presence of the tufa noted.

FIGURE 7 Locations of projects inspected.

OBSERVATIONS

No tufa was observed on any project where the subbase was composed entirely of either air-cooled blast furnace slag, granulated blast furnace slag, or a combination of these. No tufa was observed on any project where subbase was entirely composed of steam boiler "slag."

Large volumes of tufa were observed on all projects where the subbase was composed entirely of basic oxygen steel slag. Within five to ten years after construction, underdrain outlets were almost completely blocked by the precipitate. The same held true for the project in which the subbase was composed entirely of slacker aggregate.

Tufa was observed on projects where the subbase was composed entirely of open hearth steel slag. In general, the amount of precipitate on these projects appeared to be significantly less than that on the basic oxygen projects.

Since 1977 Ohio Department of Transportation specifications have required a six-month stockpile aging of steel slags; however, this requirement was unrelated to tufa precipitate formation. In 1975 and 1976 the requirement was added on most projects by either plan or proposal note. Before 1975 no aging was required. Table 2 summarizes the sale dates of projects in which steel-making slag was used as the subbase.

When subbases were composed entirely or mostly of basic oxygen slags, no significant difference was observed between the volume of tufa on pre-1975 projects and on post-1975 projects. All projects in which subbases were composed entirely of open hearth slag or of a combination of open hearth slags and blast furnace slags were sold after 1975. Therefore the amounts of tufa for six-month-aged versus non-aged open hearth slag could not be compared.

There was one observation of consequence on one of the "open hearth" projects. The subbase on this particular project was composed entirely of open hearth slag which had been stockpiled for approximately 10 years before use. Although some tufa was observed at a few underdrain outlets four years after installation, the volume was not great enough to cause concern.

At the time this report was written plans were being prepared for pavement rehabilitation projects on several of the steel slag projects inspected. The work includes partial pavement replacement as well as complete replacement of plugged underdrain systems. After construction these projects will be monitored to determine whether the steel slag subbases still produce significant tufa precipitate 10 or more years after installation. Based on observation of the one project under construction, it did not appear that the amount of material lost from the subbase during the tufa production process significantly affected subbase strength.

TABLE 2 SUMMARY OF PROJECT DATES FOR PROJECTS WITH STEEL SLAG SUBBASE

Year of Project Sale	Number of Projects
Prior to 1975 (no aging)	10
1975 and 1976 (6 month aging?)	2
After 1976 (6 month aging)	9
Total	21

CONCLUSIONS

1. Blast furnace slags used as subbase materials do not promote formation of tufa precipitate, owing to the insolubility of the complex silicates and alumino-silicates composing blast furnace slags.
2. Steam boiler "slag" used as subbase material does not promote formation of tufa precipitate, because this material is an acidic byproduct of coal burning power production and not a true slag.
3. Steel slags and slacker aggregate used as subbase materials promote formation of tufa precipitate in subsurface drainage systems because of the presence of free lime (calcium oxide) in these materials. Open hearth slag produces smaller volumes of tufa than other types of steel slag.
4. Short term (six-month) stockpile aging as currently required by Ohio Department of Transportation specifications does not reduce the amount of free lime in steel slags sufficiently to reduce the volume of the tufa precipitate.
5. Based on limited data it appears that long-term aging of open hearth slag reduces the amount of free lime sufficiently to keep the volume of tufa precipitate at acceptable levels.

RECOMMENDATIONS

1. Blast furnace slags and steam boiler slag may continue to be used as subbase material without hindrance.
2. Steel slags should not be used as subbase material where subsurface drainage systems are used unless it can be shown that exposed free lime has been removed from the graded material.
3. Further research should be conducted to determine acceptable levels of exposed free lime and the time required in stockpile aging to remove the free lime from various steel slags. Observation of new underdrain systems replacing plugged systems on pavement rehabilitation projects should be included in this research. The effect of washing stockpiles with water or spent pickling liquor to speed up the process should be included in this research.
4. Research should be undertaken to determine the amount and types of reactive calcium compounds present in recycled portland cement concrete and similar materials which have been linked to tufa-like precipitate formations.

ACKNOWLEDGMENTS

Many thanks are extended to John Molnar, Stan Virgilitte, and Robert Jones of the Standard Slag Company for providing valuable information during the course of the study. This research was funded by the Ohio Department of Transportation.

REFERENCES

1. R.M. Feldman. *Tufa Precipitation and Its Effect on Drainage of Highway Pavement.* FHWA/0H-81/010. Kent State University, Kent, Ohio, 1981.
2. H.T. Williams. *The Corrosive Resistance Properties of Iron and Steel Making Slag Under Natural Environments.* The Standard Slag Company, Youngstown, Ohio, 1969.
3. *Slag and Its Relation to the Corrosion Characteristics of Ferrous Metals.* National Slag Association, MSA MF 172-13, Alexandria, Va., 1972.

The findings and opinions expressed are those of the author and do not consitute a standard or specification.

Publication of this paper sponsored by Committee on Subsurface Drainage.

Washington State DOT Meets the Challenge of Hazardous Waste

OSCAR R. GEORGE AND MARK G. UTTING

Geotechnical exploration during design of the $100 million Tacoma Spur Freeway (SR 705) revealed unexpected coal tar contamination. This discovery was traced to a long-abandoned coal gasification plant which operated on the site around the turn of the century. Further discoveries during construction included two large, buried tanks filled with tar waste, and copper contamination from ore spilled in an old train derailment. A three-year cooperative effort by the Washington State Department of Transportation (WSDOT) and the Washington State Department of Ecology (WDOE), assisted by a hazardous waste consultant, ensured that design and construction proceeded with minimal delay. Solutions produced by the joint effort included three specially designed on-site concrete vaults for storing 26,450 tons of problem waste and the removal of 15,900 tons of extremely hazardous waste to a hazardous waste facility in Arlington, Oregon. In addition, 1300 tons of copper-contaminated soil were removed and transported to a smelter in El Paso, Texas, for recovery of the ore. Total project cleanup costs were almost $6 million. Long-term groundwater monitoring has been planned and is expected to show a significant decrease in previous contaminant concentrations reaching the adjacent City Waterway.

During design of the $100 million Tacoma Interstate Freeway Spur (SR 705), geotechnical exploration revealed the presence of black "mystery gunk." The discovery led to extensive investigation and problem solving in the Washington State Department of Transportation's (WSDOT) first encounter with hazardous waste. A coal gasification plant, built on the site about 100 years ago, was identified as the source of the contamination. Coal tar waste containing polycyclic aromatic hydrocarbons (PAH) was identified as the contaminant of most concern, leading to an extensive site cleanup program. Cleanup of the tar and other contaminants found on the site added almost $6 million to the cost of the project. However, knowledge gained during work on this project has been invaluable in developing criteria for addressing any future discoveries of hazardous waste on WSDOT projects.

This paper presents a case history of the remedial investigation and site cleanup on the Spur project. Special emphasis is given to the team approach used for problem solving and technical solutions to the problems.

O. R. George, Washington State Department of Transportation, District 3, 5720 Capitol Blvd., Tumwater, Wash. 98502. M. G. Utting, The Hydrogroup, Inc., 1310 Ward St., Seattle, Wash. 98109.

PROJECT DESCRIPTION

The Spur begins at Interstate SR 5, just west of the Tacoma Dome, and runs north to connections with the Tacoma Central Business District and Schuster Parkway (Figure 1).

The alignment crosses over reclaimed tidelands lying between downtown Tacoma, located on steep rising hills to the west, and City Waterway on the east. City Waterway is a manmade, southerly extension of Commencement Bay in Puget Sound. All except a short stretch of roadway, between 15th Street and 23rd Street, is carried on elevated, reinforced concrete structures. Previous uses of the land below included extensive rail trackage facilities and yards in addition to numerous industrial and commercial activities.

The project has been constructed in six stages, in separate contracts. Stage 1, the Tacoma Dome off-ramp, began in 1982 and was completed in 1983 to coincide with the opening of the Dome. Stages 2 through 5, the remainder of the Spur, were still under construction when this paper was written. The contract phase of Stage 6, which will add an additional southbound lane to Interstate SR 5 and ensure safe access to and from the Spur, began late last year.

DISCOVERY OF THE PROBLEM

In February 1984, during drilling conducted to evaluate the Spur's foundation requirements, concern arose over possible soil contamination. A tar-like substance was encountered in several borings between 21st and 24th Streets, bounded on the west by A Street and on the east by the City Waterway.

At that time, the Spur Stage 2 contract was being advertised for bids. Contract documents for Stages 3, 4, and 5 were being developed on a fast track schedule for advertisement in the summer and fall of 1984.

At WSDOT's request, samples of the suspect material were tested by the Washington Department of Ecology (WDOE). Test results confirmed the presence of toxic chemicals, including 13 polycyclic aromatic hydrocarbons (PAHs).

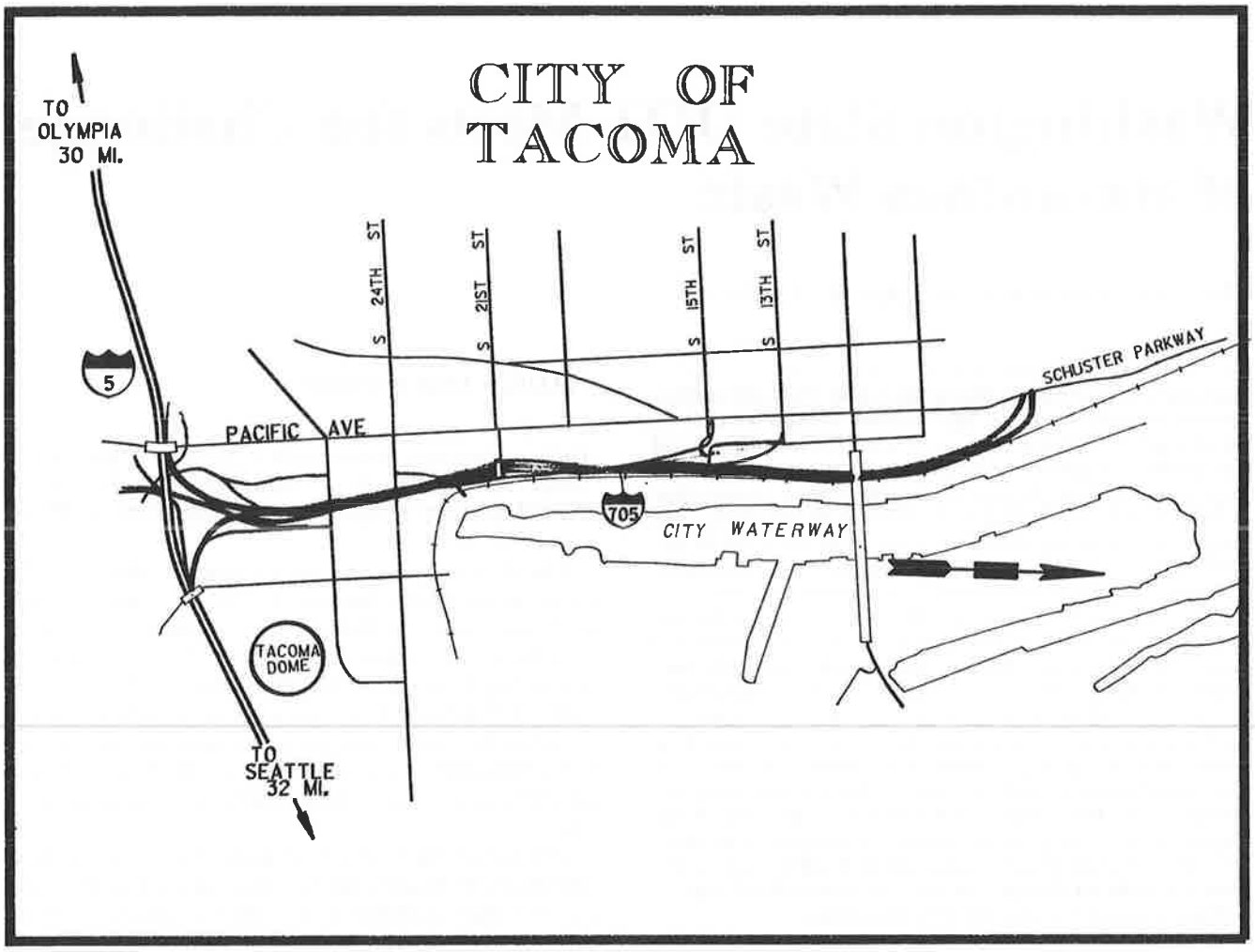

FIGURE 1 Tacoma Spur alignment.

In April 1984 representatives of WSDOT and WDOE met and defined mutual objectives. These were determined to be as follows:

(1) evaluate and address the potential for adverse environmental impacts,
(2) ensure the safety of the public and those involved in constructing the project,
(3) keep construction of the Tacoma Spur on schedule, and
(4) keep the public informed as to the problem.

Solving and managing the hazardous waste problem and fulfilling these objectives was a team process from the outset. Many of the ensuing activities were virtually a pioneering effort. No clear-cut criteria were available for handling this type of situation, as environmental regulations leave much room for interpretation.

Soon after the April meeting, Hart Crowser, Inc., a Seattle firm with considerable experience in hazardous waste matters, was hired by WSDOT to help evaluate the problem.

Hart Crowser was asked to conduct a soil and groundwater quality evaluation of the site. The evaluation was to include a historical review, determination of location, degree of contamination, and a quantitative assessment of the current and future migration of these contaminants into the City Waterway. The evaluation report was completed in November 1984.

History of the Site

Hart Crowser reviewed newspapers, books, reports, maps, and photos to reconstruct the history of the site.

The site was originally tidal land, the subsurface of which contained overconsolidated glacial deposits (till and silts) underlying more recent soft sediments. The area had been used for industrial purposes since the early days of the City of Tacoma, but was extensively filled later. The original tidelands were now covered by 2 to 50 feet of fill material.

In the late 1800s, the site was occupied by a coal gasification plant built to supply water gas for lighting and

heating a growing Tacoma. Water gas (primarily a mixture of hydrogen and carbon monoxide) is a combustible fuel produced by passing pressurized, superheated steam through a bed of mixed coke and coal.

Most of the plant was located between South 21st and South 23rd Streets next to A Street (Figure 2). Review of historical files and SANBORN insurance maps revealed that two gas holding tanks and a tar pump area had been used during plant operations from 1884 through 1924. A third tank was built on the site sometime between 1928 and 1930. Figure 2 shows the tank locations.

The coal gasification plant, including the original two holding tanks, was abandoned after 1924, when a more modern plant was constructed in a different area of Ta-

Base map prepared from USGS 7.5-minute quadrangles of Tacoma North and Tacoma South, Washington.

FIGURE 2 Vicinity map.

coma. The third tank appears to have been used well into the 1940s, perhaps as storage for gas produced elsewhere. At that point, it too disappeared from the scene.

The gasification plant was all but forgotten until preliminary substructure borings for the Tacoma Spur revealed what the newspapers reported as a black "mystery gunk."

Site Contamination

A series of 29 soil borings/monitoring wells was used to define the types and extent of soil and groundwater contamination. Priority pollutant analyses based on both organic vapor readings and on visual classification were made on selected samples. Analyses findings were compared with the list of contaminants likely to result from coal gasification activities.

Discussions with WDOE resulted in narrowing the contaminant focus to polycyclic aromatic hydrocarbons (PAH), trace metals, and selected volatile organics. The analyses showed that polycyclic aromatic hydrocarbons (PAH) were the contaminants of most concern. These compounds have been identified as hazardous constituents in coal tar waste and can constitute up to 12 percent of the tar by weight. Washington State dangerous waste regulations (WAC 173-303) classify waste containing 1 percent or more total PAH (as quantified by WDOE's PAH test) as extremely hazardous waste. Lower concentrations are not officially classified but are generally referred to as problem waste. Problem waste materials fall into a gray area which contains no clear cut regulations to guide disposal: they are not entirely clean, yet at the same time not dirty enough to necessitate the stringent disposal procedures required for extremely hazardous waste.

Metals, volatile organics, and other contaminant concentrations found were judged to fall below federal and state waste and drinking water classification standards.

Soil Contamination

One of the first objectives of the project was to assess the extent of coal tar waste in the soil. The results of the priority pollutant analyses and WDOE's PAH waste classification test led to the identification of the following three categories of contamination in the soil:

- Tar: These were visually identifiable as tar or tar-like material. These materials generally had PAH concentrations in excess of 1 percent and were classified as extremely hazardous waste.
- Oily silt or sand: These materials were generally dark to black in appearance and had a strong creosote-like odor. Because the PAH concentrations were below 1 percent, oily silt or sand were classified as problem waste.
- Odorous materials: These materials had no visual sign of contamination and PAH concentrations were under 5 mg/kg. Because of the low PAH concentration levels, these materials were classified as solid waste.

The extent and distribution of these materials were initially estimated based on the results of the soil borings and lab results (Figure 3). Levels and types of contamination were estimated by interpolation between the borings, resulting in an estimate of 40 to 100 cubic yards of tar and 4,500 to 6,000 cubic yards of oily silt or sand.

Groundwater Contamination

Water samples taken from the boring wells indicated only mildly elevated levels of PAH or metals contamination. There were no measurable impacts on either surface water or groundwater users. These conclusions were based on water levels, soil boring logs, and in-site hydraulic test data used to characterize the groundwater flow conditions. Water quality analyses were performed on selected samples. The hydrology of the site was relatively straightforward (Figure 4). Precipitation infiltrated the areas in or near the project site and then flowed as shallow groundwater in the general direction of the City Waterway, where it discharged. The project site lies in a regional groundwater discharge area. Underlying the project site was low permeability glacial till, preventing contaminated water beneath the site from flowing downward to contaminate water supply wells in the area, and allowing contamination to discharge from the site to City Waterway.

Groundwater flow rates and water quality data were used to calculate the loading rate to the Waterway. This analysis indicated that groundwater contamination concentrations entering the Waterway were below the existing salt water chronic exposure levels for marine organisms. Samples taken from the Waterway indicated no detectable concentrations of these contaminants.

Because of these results, WSDOT and WDOE were satisfied that groundwater discharge from the site presented no immediate danger to City Waterway. Therefore, the team concentrated on the problem of soil contamination.

Legal Responsibilities

The legal responsibility for remedial action on such a site is complex. State and federal law stipulate that potentially responsible parties include past and present waste generators as well as past and present owners of the site. In this case, WSDOT clearly had no role in creating the contamination. However, the need for project excavation within the contamination area would cause WSDOT to become a hazardous waste generator. WSDOT, faced with a pressing construction schedule and the potential for significant cost increases for delays, chose to pursue remedial investigation and cleanup as part of the Spur construction project. The Federal Highway Administration (FHWA) concurred in this decision.

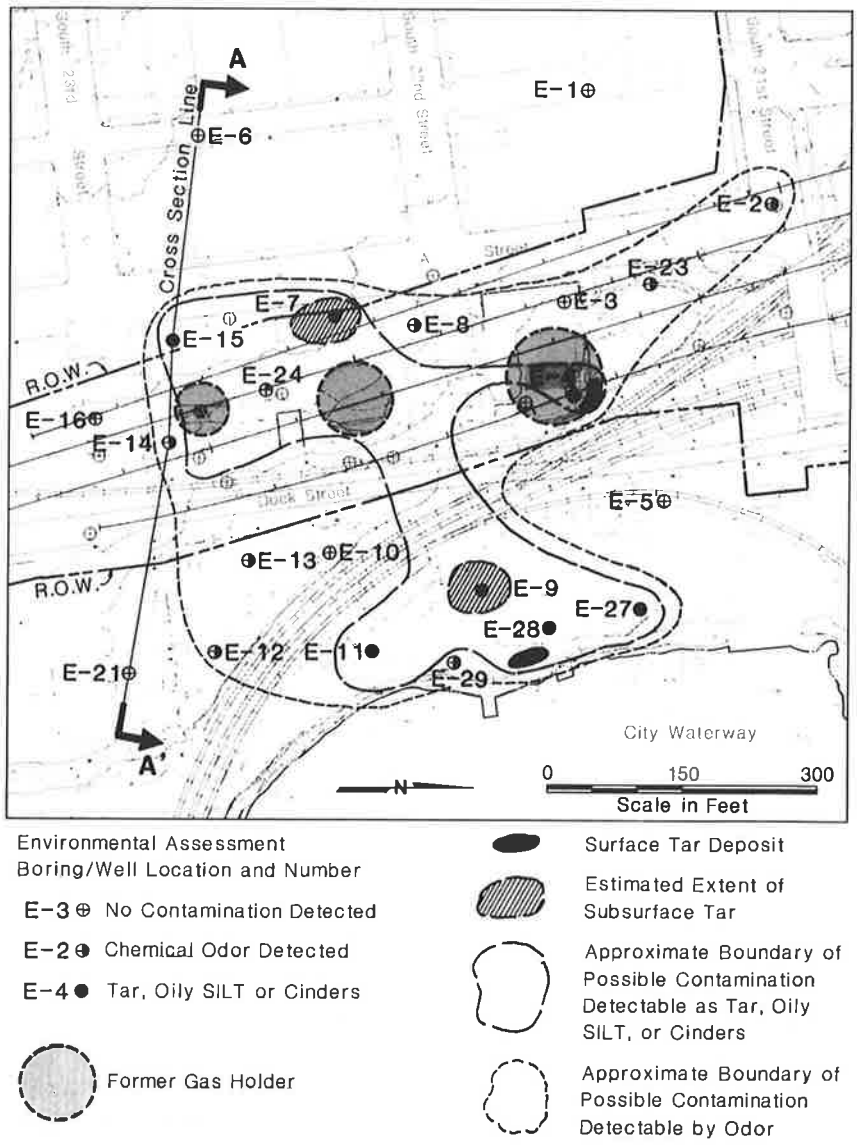

FIGURE 3 Pre-excavation estimate of subsurface contaminants.

Planning for Site Cleanup

The Hart Crowser investigation was followed by months of meetings among the consultant and WSDOT and WDOE staffs. Other participants included the FHWA and the Tacoma-Pierce County Health Department (TPCHD). During this process, the public was kept informed through a series of joint WSDOT-WDOE press releases.

Major decisions resulting from these meetings were as follows:

(1) All tar-like material encountered during construction activities would, as a designated Extremely Hazardous Waste, require disposal at an approved hazardous waste facility.

(2) Less contaminated material, identified as oily silt or sand or odorous material could be contained on site in an approved storage vault. On-site storage would require a solid waste permit from TPCHD.

(3) Visual identification methods would be used during construction to expedite safe handling and disposal of contaminated materials.

(4) Plans and provisions for handling and disposing of contaminated material would be included in the project's Stages 4 and 5 contract documents.

(5) Provision would be made for long-term monitoring of groundwater impacted by the contamination.

As plans were made for dealing with the contaminated material in Stages 4 and 5 in the summer of 1984, work began on the Stage 2 and 3 contracts. Stage 2 and 3 construction was limited to areas north of the suspected contamination.

The project team determined that contract documents for Stages 4 and 5 would include a plan showing the nature

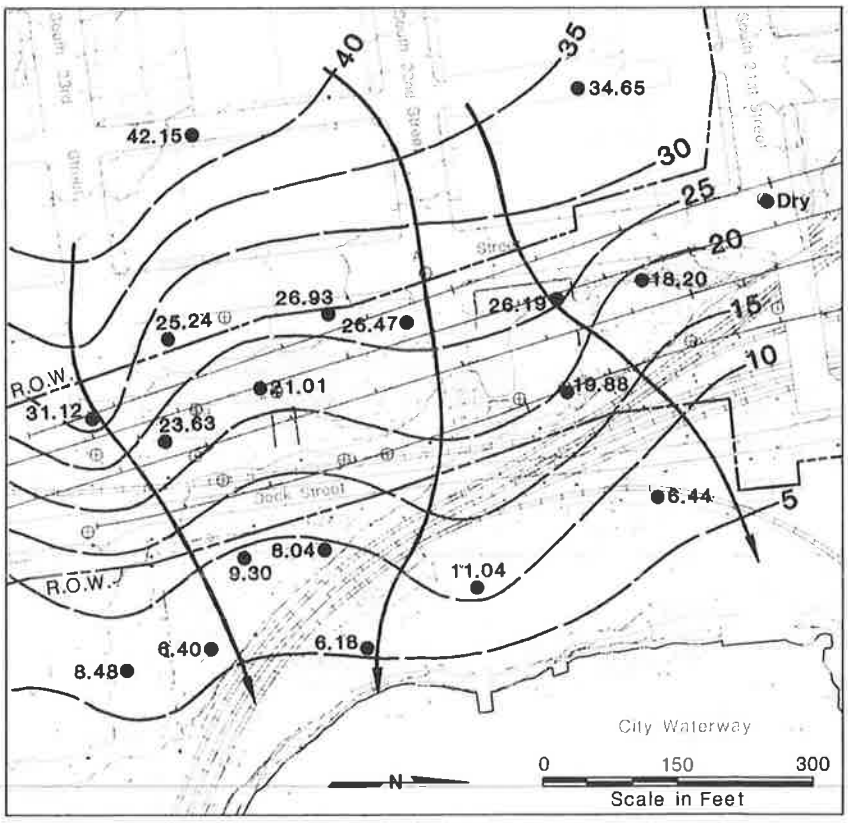

FIGURE 4 Water table elevation contour map.

and the approximate boundaries of the contamination. Provision would be made for monitoring of all excavation operations by WDOE. Contract specifications would be included for handling and disposing of all contaminated material.

The contractor would be required to hire a safety consultant to advise on safety precautions required for personnel and equipment working around the contaminated materials.

The Stage 5 contract was to include construction of a secure decontamination area. Here, personnel and equipment exposed to contaminated material would be cleaned before leaving the construction area. Plans also included construction of a concrete vault in the project area to permanently secure and encapsulate oily silt or sand encountered during excavation activities. Provision was made for a possible second vault.

Holes would be drilled and wells developed for long-term monitoring of groundwater. The wells would be located both east and west of the tar contamination site, in the on-site storage vaults, and around the storage vault area.

Stage 4 and 5 Construction Begins

In December 1984 construction began on the 21st Street Interchange, Stage 4 of the project.

No tar was found in the Stage 4 area. However, 1200 tons of oily silt or sand were uncovered during excavation, and stockpiled in a secure location for disposal in the Stage 5 contract.

In August 1985 WSDOT awarded a contract for Stage 5 of the project. Work on Stage 5, which included the Spur from 21st Street south to SR 5, began in late September 1985.

Early in the contract, an oblong, concrete storage vault (Figure 5) with a capacity of 6,000 cubic yards was constructed within the state right of way, in an open area at the south end of the project. Vault walls were 4 inches thick, reinforced by a 10-gauge, 6-by-6 wire mesh at the center. Once the vault was filled to capacity, a 4-inch reinforced slab, sloped to drain, was to be placed on top. The slab would then be covered with 10-mil polyethylene sheeting and a 2-foot layer of clean soil.

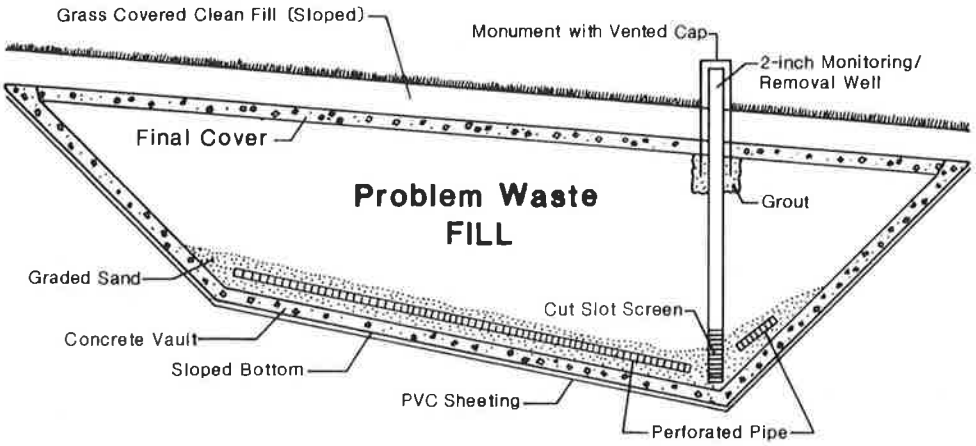

FIGURE 5 Problem waste vault schematic design.

As excavation began in the suspected contamination area, both tar and oily silt or sand were uncovered. Using procedures agreed on earlier by WSDOT and WDOE, WSDOT's inspector visually identified the type of contamination.

Tar was transported to the Chem-Security Systems, Inc., hazardous waste facility in Arlington, Oregon, for permanent storage.

Contract provisions called for transportation to be handled by a company licensed and approved by EPA and USDOT for transporting. Transport vehicles entered the project site at the decontamination area where they were fitted with a polyethylene protective liner. After being loaded with tar at the excavation site, they returned to the decontamination area. There, the exterior of the vehicle was steam-cleaned, the protective liner was sealed, and a tarp overlay was secured.

Before leaving the decontamination area, the vehicle was inspected and the driver was provided with a signed shipping manifest and approval to leave the project site. Upon the vehicle's arrival at the Arlington, Oregon waste storage facility, the load was weighed and its chemical composition was tested for conformance to a waste material profile previously furnished by WSDOT. Tar delivered to the waste facility would be only accepted in a solid state. Liquid tar encountered at the project site had to be solidified by mixing it in cement kiln dust before shipment.

Oily silt, sand, or odorous materials which were uncovered were hauled to the on-site concrete storage vault and deposited there. The procedure was subject to WSDOT's approval of the haul road, the method of placement in the vault, and the precautions taken by the contractor to prevent contamination of the surrounding areas.

Unexpected Discoveries: Storage Tanks

As the contractor pursued bridge footing excavation near 23rd Street on December 20, 1985, he encountered the brick and mortar walls of a large buried storage tank. This tank was 60 feet in diameter, 20 feet deep, and uncovered at the top. It contained 1260 tons of mixed, tar-like material.

On February 6, 1986, the contractor partly unearthed two additional open-topped, brick and mortar structures to the north of the first tank. The first structure, a container measuring 6 feet by 8 feet by 10 feet deep was filled with tar. The second, a tank 87 feet in diameter and 20 feet deep, contained approximately 5500 tons of mixed, tar-like material. Historical data had indicated that large holding tanks for gas had existed at one time in this vicinity. However, the discovery that the lower sections of the tanks were still there, buried in the ground, was a complete surprise.

The tanks had originally been built entirely above ground. The project team speculated that when the old coal gasification plant was closed, instead of removing the manufacturing equipment (tanks, pipes, sumps, etc.), the site was filled to a level 10 to 15 feet above the original surface. The pipes and lower sections of the tanks were left. Since a large amount of coal tar was originally dumped in the area, much of the fill used in the operation contained tar.

The worst material was probably placed in the tanks for containment because much of it was semiliquid and could flow. The material rested there for more than 60 years until uncovered by the Spur contractor.

Based on analyses of representative samples, all of the material in the large tanks and the smaller "tar pit" was classified by WDOE as extremely hazardous waste. In addition, much of the fill surrounding the tanks was also found to have sufficient PAH concentrations to be placed in the same classification. The edge of the area contained considerable material with lower levels of contamination, which was considered problem waste.

The unexpected discoveries caused a dramatic increase in the amount of contaminated material requiring removal during construction. This is quite evident in the comparison shown below.

	Quantities of Contaminated Material Removed (tons):	
	Maximum Expected	Amount Removed
Extremely hazardous waste	120	15,900
Problem waste	7,200	26,450

In the final tally, 731 truckloads of extremely hazardous waste were removed from the project site and hauled to Arlington, Oregon. The increased amounts of problem waste required building two additional on-site concrete storage vaults. (One vault had been called for in the contract.) All three vaults were filled to capacity by the time project excavation was completed.

Unexpected Discoveries: Copper Ore Contamination

As removal of tar-related material continued, the interagency team was busily trying to solve yet another toxic surprise. In August 1985, soon after the award of the Stage 5 contract, WDOE advised WSDOT that it had discovered soil that appeared to contain copper ore in the project area.

The copper-laden material was scattered near 26th Street in an area 300 feet by 150 feet below the bed of a single track rail line. Checking the rail line's records indicated that, over the years, this location had been the scene of a large number of freight train derailments. The cargo involved in at least one of these derailments contained copper ore.

Two bridge pier footings were to be constructed as a part of the Stage 5 contract in the area where the copper was found. In addition, major utility relocation related to the project called for extensive trench excavation through the area. The utility relocation was required to begin early in the Stage 5 contract to maintain the job schedule.

First, metal, fish bioassay and EP toxicity analyses were conducted on the soil samples. A fish mortality rate of 100 percent in the bioassay analysis led to designation of soil with a copper concentration of 9500 ppm and above as dangerous waste. This material required removal and disposal off the site.

Further testing was needed to determine the impacts of soil with lower copper concentrations. Four sampling trenches and a groundwater monitoring well were used to evaluate migration of metals into the soil in areas of high surface contamination.

Tests were conducted on samples of soil at various depths in the trenches and on water samples taken from the well. Water samples indicated no groundwater contamination: in fact, the groundwater met drinking water standards. Soil analysis results confirmed that soil with copper concentrations below 9500 ppm could be left in place with no danger of future contamination of the groundwater. As a precautionary measure, all such material left in place was covered with two feet of fine-grained material.

Several options were considered for disposal of the 1300 tons of soil with copper concentrations of 9500 ppm and above, including a recovery and recycling option suggested by Hart Crowser. This option was selected, which led to reconsideration by WDOE of the material's original designation as dangerous waste. That designation would have eliminated the option of reprocessing by any facility not approved to treat dangerous waste. After some reevaluation the dangerous waste designation was removed, based on the fact that the copper ore had been processed and was not left as waste. Although it had been spilled, it still maintained an economic value in recoverable metals.

The decision resulted in an agreement between the Stage 5 contractor and ASARCO Incorporated of El Paso, Texas. The copper-laden material was hauled by truck to an ASARCO-owned facility in Tacoma, Washington, by the contractor. There, it was loaded into freight trains and taken to the ASARCO El Paso Plant. Treatment in El Paso consisted of conventional copper smelting technology, which reduced the copper-laden soil to a marketable product and an inert slag.

Team Problem Solving

The state's successes in managing these hazardous waste problems can be attributed directly to the team effort by the agencies involved. While WSDOT had full responsibility for managing the construction project, WDOE was the regulatory agency responsible for contamination issues. All actions and responses resulted from team problem solving. Other team agency members included the FHWA and the Tacoma-Pierce County Health Department.

Through frank discussions of the issues and consideration of possible alternate solutions, the agencies were able to establish a mutual trust.

WDOE's position from the outset was one of firmness: however, it maintained a willingness to work towards cooperative solutions. In this spirit of teamwork, WDOE, despite its position as regulatory agency, established no direct requirements. Instead, it asked for proposals on the evaluative or cleanup method and then suggested modifications as necessary.

Much of the contaminated material encountered during the project did not fall specifically under Washington State's dangerous waste regulations (WAC 173-303). However, the material was clearly contaminated and a variety of regulations [i.e., federal Superfund laws (42 USC 9601) or Washington State water quality laws, (RCW 90-48)] could have been applied.

The interagency team approach allowed construction to proceed with minimal delays. Cleanup methods were developed to provide a measured response to the environmental problems at reasonable cost.

Groundwater Monitoring

Programs were developed by the team for long-term monitoring of groundwater in two distinct locations.

Five wells will be installed to monitor groundwater between the former coal gasification plant site and the City Waterway. Monitoring will reveal the effects of removing contaminated tar and soil from that site.

Well installation, sampling, and testing will end as soon as other contractor activities in that area are completed. Water quality indicator parameters (total organic carbon, total organic halogen, pH and temperature) will be measured regularly, while more major analyses (base neutral extractable and volatile organics) will be performed less frequently, using priority pollutant scans. The results are expected to show a steady decline in PAHs and trace metals over the long term, based on the removal of an estimated 95 percent or more of the PAH-bearing waste during the Spur contract.

Thirteen wells were installed to monitor possible contamination from any of the three problem waste storage vaults. Four of the wells were installed within the vaults (two in Vault #1 and one each in Vaults #2 and #3). The other nine wells were placed outside the vaults. Testing of samples from these wells has already begun, and water quality indicator parameters will be measured regularly. Increases in these parameters as they are sampled and measured will trigger additional sampling to verify those results and to examine more specific parameters.

During the initial sampling from wells within the vaults, water was found in two of the vaults. It was attributed to the presence of water in the original material, in addition to rain water entering the vaults before the top slab was constructed. The water was pumped out of the two vaults; water from one of the vaults was treated to remove contaminants before disposal. Tests of water samples from the nine wells outside the vaults have indicated no contamination.

Cost

The total cost for the hazardous waste activities of this project has approached $6 million. Cost to date:

- Handling and disposal of extremely hazardous waste (includes construction and removal of a decontamination-site, demolition and removal of the tar tanks and appurtenances, and monitoring well installation): $4,000,000
- Handling and disposal of problem waste (includes construction of three concrete storage vaults and monitoring well installation): $550,000
- Handling and disposal of copper contaminated soil: $600,000
- Treatment of contaminated water: $350,000
- Consulting services: $350,000
  - TOTAL: $5,850,000

EPILOGUE

At the time this paper was written, construction of the Tacoma Spur was still under way. However, all excavation in the vicinity of both the old coal gasification plant site and the copper contamination site had been completed. It is likely that most, if not all, of the contaminated waste material had been discovered and removed. Total cost of activities related to hazardous waste was slightly less than $6 million. Further responsibilities for monitoring groundwater in the area will continue for at least the next five years.

A team approach by the Washington State Department of Transportation and the Washington State Department of Ecology led to timely and cost effective solutions to the contamination problems. A large hazardous waste site was cleaned up, and a source of considerable potential contamination of Tacoma's City Waterway was essentially eliminated.

Separation of the contaminated material into extremely hazardous waste and problem waste sharply reduced the total cleanup costs. Using on-site concrete vaults to permanently store problem waste effectively isolated that contamination from its surroundings. The cost of building the vaults and depositing the problem waste on site was $6 million lower than the cost of transporting and disposing of the same amount of material at the hazardous waste site in Arlington. Another significant factor of the separation concerned WSDOT's long-term liability for both forms of tar related contamination.

Should future laws require further action for either extremely hazardous or problem waste, the state's separation of those materials will enable proper action to be taken.

From the experience gained on the Spur Project, WSDOT has developed a Hazardous Waste Response Program, which includes WSDOT "Hazardous Waste Guidelines." The guidelines describe general procedures to be used if hazardous waste is discovered on future WSDOT projects, and address both the design and construction phases of a project. Technical support will be available for future projects through an on-call agreement between WSDOT and a hazardous waste consultant.

Publication of this paper sponsored by Committee on Physicochemical Phenomena in Soils

Transportation Agency Liability for Hazardous Materials and Waste: A Practical Approach to Minimizing Legal, Financial, and Environmental Risks

GREGOR I. MCGREGOR

Superfund and similar state statutes on hazardous waste liability affect many transportation agency operations: land acquisition; project design and construction; facility operation and maintenance; leases, sales, and other dispositions of property; and relations with other government agencies, employees, and the public. Concepts of strict liability can make the agency liable even if it acquired land innocently, not realizing it was contaminated with hazardous waste; even if the agency contaminated property by its own activities which were legal at the time; and even if the agency long ago sold contaminated land "as is." This paper describes practical ways to deal with these emerging liabilities. The hazardous waste site assessment is an essential tool to discover and assess contamination prior to acquisition. Clauses in purchase agreements and leases can protect the agency if waste is discovered later. The agency can negotiate rights of indemnification and other means of reimbursement. Cleanup costs can be paid from Superfund or reimbursed by responsible parties using provisions in Superfund itself, rights to seek contribution, or warranties and consumer remedies. There are some limited defenses against agency liability, such as the "third party" and "innocent landowner" defenses. Use of eminent domain helps reduce liability. Following the suggestions in this paper, the agency will find that most waste contamination is manageable using proper techniques to report releases, plan for emergencies, comply with the National Contingency Plan, stay off the Superfund list, comply with state requirements, clean up sites expeditiously, know "how clean is clean," hire qualified consultants and contractors, protect employees, and build defenses or pursue claims.

New concepts of hazardous waste liability, introduced in Superfund, affect many transportation agency operations: land acquisition; project design and construction; facility operation and maintenance; leases, sales and other dispositions of property; and relations with other government agencies, employees, and the public. The transportation agency can be liable even if it bought land innocently, not realizing it was contaminated with hazardous waste; even if the agency long ago contaminated property by its own activities that were legal at the time; and even if the agency sold contaminated land "as is" with full indemnification by the buyer.

Fortunately, there are practical ways to deal with these emerging liabilities. The hazardous waste site assessment is an essential tool to discover and assess contamination prior to acquisition. Clauses in purchase agreements and leases can protect the agency if waste is discovered later. Cleanup costs can be paid from Superfund or be reimbursed by responsible parties. There are some limited defenses against agency liability. Use of eminent domain can reduce liability. Qualified consultants and contractors can assist cleanup to Superfund standards of "how clean is clean." Most waste contamination is manageable using proper techniques.

McGregor, Shea & Doliner, P.C., 27 School Street, Suite 300, Boston, Mass. 02108.

TRANSPORTATION AGENCY LIABILITY

Federal and state statutes on hazardous waste drastically affect how transportation agencies conduct their activities. The issue of legal liability for releases of hazardous material to the environment has made compliance with these laws very important. Failure to do so may be fatal to a project, carefully prepared budgets, agency credibility, and individual careers. These new legal requirements expand the liability and responsibility of both the public and private sectors. The laws affect anyone who has anything to do with use of hazardous materials or with generation, storage, transportation, use, treatment, disposal, or cleanup of hazardous waste.

The focus of this paper is the contamination of real estate, but it is important at the outset to realize that hazardous waste is regulated in the context of hazardous material generally. Hazardous waste management and cleanup is just one aspect of dealing with material having hazardous characteristics.

The thrust of existing federal legislation is to allow and encourage state hazardous material programs that are more strict and more comprehensive than the federal. As a result, most states have enacted their own statutes and created their own hazardous waste agencies. Local govern-

ments are beginning to adopt their own hazardous material and hazardous waste ordinances and bylaws dealing with storage or with transportation through the community.

Superfund Liability

State transportation agencies, because they own and lease property and operate facilities, may find themselves subject to the Comprehensive Environmental Response, Compensation, and Liability Act (CERCLA), commonly known as Superfund. Superfund was enacted in December 1980 and was reauthorized in 1986 with major revisions. It establishes a fund to clean up uncontrolled hazardous waste dumps and to respond to spills. Superfund created a process for identifying liable parties and ordering them to take responsibility for cleanup operations. A transportation agency may face this liability once it becomes either the owner or operator of a site or facility from which there has been a release, or threat of release, of a hazardous substance. Regardless of whether the contamination is the result of the agency's own actions or those of others, the agency may be held responsible for cleaning up any resulting contamination either to its own or to other property. If the agency is not responsible for the contamination, however, it may seek to recover reimbursement for its cleanup costs from either the responsible parties or from the Superfund. The primary liability provision of Superfund is Section 107, which states:

> Notwithstanding any other provision or rule of law, and subject only to the defenses set forth in subsection (b) of this section—
> (1) the owner and operator of a vessel or a facility,
> (2) any person who at the time of disposal of any hazardous substance owned or operated any facility at which such hazardous substances were disposed of,
> (3) any person who by contract, agreement, or otherwise arranged for disposal or treatment, or arranged with a transporter for disposal or treatment, of hazardous substances owned or possessed by such person, by any other party or entity, if any facility or incineration vessel owned or operated by another party or entity and containing such hazardous substances
> * * *
> shall be liable for—
>
> (A) all costs of removal or remedial action incurred by the United States Government or a State or an Indian tribe not inconsistent with the national contingency plan;
> (B) any other necessary costs of response incurred by any other person consistent with the national contingency plan;
> (C) damages for injury to, destruction of, or loss of natural resources, including the reasonable costs of assessing such injury, destructions, or loss resulting from such a release;
> (D) the costs of any health assessment or health effects study carried out under section 104(i).

In the event of a release, EPA is given authority to begin to contain the release by removing the contaminated material in a temporary cleanup effort and to take remedial action to eliminate further threats. EPA determines the priority for sites that require cleanup. EPA initially will attempt to have the responsible parties clean up the site voluntarily. Sometimes EPA will approach these "Potentially Responsible Parties" (PRPs) to see if they will cooperate. For a given site, this may include hundreds of industrial and governmental generators of waste, previous landowners, and transporters. The PRPs must decide quickly whether and on what terms to fund the cleanup. If this is not done, EPA will begin work through its own contractors. EPA can charge the responsible parties for those costs. If a court determines liability after the responsible parties' refusal to pay, they could be required to pay triple damages. In the alternative, the PRPs can conduct the cleanup themselves and then seek recovery of their own response costs directly against any responsible parties.

Liability under Superfund is considered strict, joint and several, and retroactive. Liability is strict in the sense that it does not matter whether a person acted knowingly or reasonably. Liability is created by the requisite connection with a site as on owner, operator, generator, or transporter. Liability is joint and several in that each responsible party may be held liable for the entire amount of response costs. Thus EPA may seek recovery from any or all responsible parties. Liability is retroactive in that it attaches not only to present, but also to prior owners and operators of a site. This feature, coupled with strict liability, changes drastically the old practice of selling property "as is." Although an owner or operator contractually can arrange for indemnification from another party (such as a seller or buyer or lessee), the owner or operator still will be primarily liable for cleanup costs even while being able to get reimbursed. This right to seek reimbursement does not negate the basic liability, which cannot be passed off.

As an owner or operator of a site, or as a generator or transporter of waste taken to a site, a transportation agency may be liable for punitive damages up to treble the costs incurred by EPA if the agency fails to properly provide response action in accordance with a formal EPA administrative order. Such treble damages will be imposed on top of the actual cleanup costs.

Due to the complex nature of remedial actions, which often are coupled with long-term monitoring programs, hazardous waste cleanups usually are extremely expensive. Consequently, cleanup costs easily can exceed the value of the property itself. Under Superfund, however, liability for a single incident is generally limited to all costs of response (such as assessment, containment, and cleanup) plus additional amounts up to $50 million (depending on the type of site) for any damages imposed. There are no limits to liability, though, when there is willful misconduct or willful negligence; where the primary cause of the incident was a violation of safety, construction, or operating standards or regulations; or where the responsible party fails or refuses to provide cooperation and assistance requested by a public official under the National Contingency Plan (NCP).

In 1986 the United States Congress reauthorized Superfund. The amended statute contains stronger cleanup standards for contaminated sites; disclosure requirements for those who use, store, or produce hazardous substances on site; and five times the funding of the original Super-

fund, which expired in September 1985. The new Superfund gives EPA several deadlines and goals, specific settlement procedures, and stronger enforcement powers.

Some states have added features of their own to create state Superfunds. These state statutes, which Congress has invited to go beyond federal Superfund, may regulate more types of waste, impose stricter liability, afford fewer defenses, create private rights of action to sue for damage to real estate or personal property, allow the state to record a lien to secure reimbursement of cleanup costs (known as a Superlien if it takes priority over other recorded interests), and mandate "how clean is clean."

Hazardous Waste Management

The Resource Conservation and Recovery Act (RCRA) protects the environment by managing hazardous waste. It establishes what is called a "cradle-to-grave" approach to regulation of waste. The RCRA regulations promulgated by EPA set up licensing or notification requirements for those who generate or transport this waste or who treat, store, or dispose of it (known as TSD facilities).

The goal of this comprehensive new regulatory program is improved solid waste management and resource recovery programs throughout the nation. EPA has established criteria for identifying hazardous waste, requirements for containers and labels, specifications for recordkeeping, and procedures for the "manifest" system for documents accompanying waste, identifying its nature, origin, routing, and destination. As a generator of hazardous waste, a transportation agency must know what chemicals it uses, what wastes it produces in what quantities, where they go, and whether the wastes are handled correctly. Under Superfund, the hazardous waste generator remains liable for its waste if any release occurs during its transportation, storage off-site, or treatment or disposal. Because a transportation agency regularly uses a variety of chemicals in large quantities, it also may be classified as a storer of hazardous waste.

In 1984, RCRA was amended to cover Small Quantity Generators (SQGs). Thereby, 100,000 to 200,000 generators were added to the previously regulated community of about 15,000. RCRA now reaches much smaller operations, although the paperwork and licensing requirements are somewhat less strict.

Underground Storage Tanks

Underground chemical or petroleum storage tanks are covered by 1984 amendments to RCRA, which created the program for Leaking Underground Storage Tanks (LUST). The amendments govern, for the first time on a nationwide scale, the design, installation, maintenance, monitoring, and failures of underground storage tanks. The focus of this new regulatory thrust is to protect groundwater in the United States by release prevention, detection, and correction.

Basically, owners of underground storage tanks and pipes must register present tanks (and past removals); meet New Tank Performance Standards for new installations; make tanks leak-proof for their entire lives; install leak-detection systems; keep required records; and install no bare steel tanks except in those rare soils that will not cause rust. Otherwise tanks must be corrosion proof or have cathode protection. Owners also must take corrective actions on leaks and save funds available to cover potential damages from leaks. There are some exemptions for farm or residential tanks with less than 1,100 gallons of motor fuel for noncommercial purposes, tanks storing heating oil at the premises where it is consumed, and storage tanks in an underground area such as a basement but above the surface of the floor.

Transportation agencies own and operate thousands of these tanks, which were to be registered or removed by the May 7, 1986, deadline. New tank notifications are due within 90 days of installation. They must meet the New Tank Performance Standards for construction, monitoring, and cleanups.Since the federal program authorizes and encourages states to run their own LUST programs and to seek this delegation from EPA, it is fair to assume that this will happen throughout the nation.

Worker Safety Obligations

Equally important to transportation agencies are the national uniform standards for disclosure of chemical hazards to workers. This disclosure is done by labeling chemicals, distributing Material Safety Data Sheets (MSDSs), and training employees in handling hazardous materials and responding to emergencies. The MSDS is a written document with extensive information on chemical identification, hazards, and protective measures. There must be an MSDS for each hazardous chemical in the workplace.

The employer is required to establish and implement a hazard communication program, which is a written plan listing hazardous chemicals as an index to MSDSs; to provide methods to inform employees of hazards of nonroutine tasks and in unlabeled pipes; and to inform on-site contractors about hazards to which their employees will be exposed. As of May 1986, the most important segment of hazard communication, that of training, took effect. The idea is for employees to understand the information being provided. The training must be be given to all employees exposed to hazardous chemicals before their initial assignment to such work and whenever the hazards change.

Accompanying the Superfund reauthorization in 1986 were amendments requiring OSHA to promulgate regulations to protect the health and safety of workers involved in hazardous waste operations. These regulations will cover the many persons involved in site investigations, feasibility studies, remedial action planning, and cleanup at contaminated sites. At a minimum these regulations are expected to cover site analysis, worker training, medical

surveillance, protective equipment, engineering controls, maximum exposure limits, handling methods, decontamination procedures, and emergency response. The transportation agency that uses its own personnel or outside contractors for these activities on contaminated property should be aware of these special regulations to protect workers engaged in hazardous waste operations.

Common Law Liability

The common law consists of legal principles enunciated by the courts. If Superfunds are legislature-made laws, then common law is court-made. These traditional rights provide access to court for private citizens, businesses, and agencies to seek injunctions and money damages for environmental harm. By and large, RCRA and Superfund statutes do not preempt these remedies. They are important avenues to seek redress in the courts. This court-made law thus is a catchall behind regulatory law regarding clean air, clean water, hazardous substances, and many other subjects. Examples include principles of public and private nuisance, trespass, negligence, strict liability for abnormally dangerous activities, groundwater rights, surface water rights, and riparian rights of owners of property abutting bodies of water.

Presently the common law offers an important remedy for money damages for personal injuries and for property damages not covered by Superfund. Using these doctrines, victims of hazardous substances released into the environment may file suit if they suffer damages. Legal wrongs from releases of chemicals to the environment are called "toxic torts." Liability for these toxic torts will be a cutting edge of law reform during the 1980s.

TECHNIQUES TO MINIMIZE LIABILITY

Amid all the environmental laws and regulations and court decisions dealing with hazardous waste, what is a transportation agency to do? How can hazardous waste considerations be integrated into operations? How can the public interest be protected? How can liabilities be minimized? How can hazardous waste be managed?

Unless ways are found to answer these questions, the alternative is business as usual: unwitting acquisition of contaminated land, selection of project sites where wastes are located, construction delays when wastes are encountered, cost overruns to deal with them, leaking underground tanks at agency facilities, improper storage and releases of chemicals, uncontrolled spills for which the agency is not prepared, unacceptable risks to agency personnel, difficulties in disposing of property even by transfer to other agencies, diversion of resources to deal with EPA and state enforcement orders, and involvement in expensive, time-consuming litigation.

Fortunately, there are several practical techniques for transportation agencies wishing to manage hazardous waste problems in ways that minimize legal, financial, and environmental risks. Using the following suggested techniques, the agency can understand its new legal duties, anticipate potential contamination, understand the level of compliance, and act responsibly when contamination is discovered.

Site Assessments

The risks of Superfund liability can be significantly reduced by an important preventive step taken prior to acquisition of property. The hazardous waste site assessment, when done properly, will present the agency with the information it needs to decide whether to purchase a piece of property and, if so, at what price and with what contingencies regarding discovery of waste.

A transportation agency should conduct site assessments routinely before property is purchased so that project delays and cleanup expenses will be avoided when waste problems are discovered later in project implementation. Without this protection, agencies may face liability far more costly to remedy than the relatively small investment of time and money needed to conduct a thorough survey. Ideally, the site assessment is done before executing a purchase agreement. If not, the purchase agreement itself should provide for this site assessment, much as it may provide for structural and property line surveys (and even termite and asbestos inspections for buildings). The site assessment should be something more than the typical field investigation and brief report for a few dollars. It is a more useful tool if it is accurate and complete. A proper site assessment must include the following:

- An exhaustive physical survey of topography; geologic setting; surface and groundwater flow; building and utility layouts; the condition of all structures above and below the ground, including underground tanks; and suspicious site characteristics such as liquid breakouts, soil discolorations, odors, abnormalities in vegetation, extensive filling and regrading of the land, and buried objects (such as pipes, drums, and tanks) in the ground. It must include drilling test wells to obtain groundwater samples to be tested in a laboratory for a range of contaminants.
- A history of the plant and site, documenting industrial, commercial, and waste disposal activities; past and present owners, using appropriate property maps; subdivision plans and deeds; the products manufactured or materials dumped in the past; and the nature of production or treatment processes.
- A review of the permit and enforcement history of the property to check what past and present activities on the property were properly licensed by federal, state, and local agencies and boards. The review should include a visit to hazardous waste agencies to examine lists of licensed or known contaminated sites. Otherwise the transportation agency, as new owner, may be taking over a facility already in violation of the law. Also, court orders or ongoing litigation could affect future uses of the property or could impose monetary damages and penalties against the agency as new owner.

- An assessment of hazardous substances on the property, including air pollution, water pollution, and other means of land contamination. If hazardous materials are discovered or suspected, the assessment should calculate the impacts on downstream, down-gradient, and downwind receptors of those materials. This information is essential to assess financial exposure in a businesslike manner.
- A review of all applicable federal, state, and local legal requirements, including zoning and other land use controls. Otherwise, the buyer may have an unrealistic set of expectations on developability of the land. The same review is useful to anticipate who needs permits from whom to do what for any new activity.
- A method that meets the criteria imposed by state environmental agencies for the preliminary screening or initial assessments, which usually are done after contamination is discovered. Although data collection by methods required by state agencies may be more expensive initially, it may save time and effort later if waste is discovered. Otherwise, the work of the site assessment may have to be duplicated under government orders.
- An evaluation of potential threats to the environment and to public health, safety and welfare by proximity to population, water supplies, recreation areas, and other sensitive receptors.
- Information about the consultant's prior personal knowledge of the site, the sources and reliability of information gathered, and any constraints on the site assessment.
- The supervision of a professional with the qualifications to render the factual and scientific judgments in the assessment report.
- Estimates by qualified engineers and environmental scientists to give a range of expected impacts on project plans, EPA cleanup requirements, and costs if a site assessment identifies hazardous waste.

Contract Clauses

A transportation agency, as a buyer of property, is vulnerable to liability under Superfund primarily as the purchaser of land on which contamination exists, as the landowner who contaminates the land or environment, or as the landlord who leases property to a person who contaminates it. In all three situations the agency will want to look beyond Superfund cost recovery actions to seek reimbursement. Even if the cleanup funding comes from Superfund itself, the agency will want to seek redress from the seller or lessee.

Clauses are available to insert in purchase contracts and leases to distribute liability properly, recover costs, and manage cleanups. These measures do not enable the agency to escape liability for site cleanup and damages, but rather to secure reimbursement from, or cleanup by, the party in fact responsible for waste. All legally responsible parties under Superfund remain liable regardless of any private indemnifications or other agreements, until the EPA issues a final settlement and release of liability.

The purchase agreement should expressly state that acquisition is contingent upon favorable results of a site assessment. That way the agency has the option of not becoming an owner and thus incurring no liability under Superfund. If the agency opts to acquire the property anyway, an indemnification clause should be included in the original contract for sale. The clause should state that the seller remains liable for all (or specified) hazardous waste cleanup costs. The clause should give the agency the option to require the seller to conduct the cleanup. This type of clause allows the agency to go after the seller directly, using this private contractual agreement. A well-drafted clause can help avoid lengthy settlement negotiations through the Superfund cost-recovery procedures. Indemnification can allocate costs to the seller up front, throughout cleanup operations and until final settlement with EPA.

As an alternative to complete indemnification, the agency may be able to negotiate a cost-sharing agreement where the parties agree to share cleanup costs. This alternative may result in a lower purchase price. Another approach is a buy-back agreement, where the seller agrees to take back the property and reimburse the agency if hazardous waste is discovered.

It is particularly important that a lease of public property indemnify the agency for contamination by the lessee. It should give the agency access to the property to conduct site investigations during the lease. This is important because when a transportation agency leases lands for various purposes, including user services like gasoline stations, it will be liable under Superfund for contamination caused by its lessee. The lease also should require the tenants to obtain private insurance or self-insurance sufficient to cover the potential cost, with documentation provided to the agency to demonstrate this insurance. This provision will help ensure that the agency does not end up bearing the burden of cleanup because the actual costs exceed the resources of the lessee as a responsible party.

Warranties and Consumer Remedies

Once a transportation agency becomes the owner of property discovered to be contaminated, it may seek remedies under real estate law and consumer law. In some states, for example, the theory of warranty of merchantability provides a right to money damages from the seller based on the fact (if it can be proved) that the property is no longer suitable or of the same nature contracted for. In other states, a theory known as "waste" may allow the new owner to bring an action for damage by seller's activities destroying the value of the property. Most states also have consumer protection statutes providing remedies to purchasers of real property where the seller has misrepresented facts or failed to disclose material facts that might have changed the buyer's mind about the purchase.

Still other remedies may lie in actions for fraud and misrepresentation. Although the rule of *caveat emptor* (buyer beware) applies to contracts for the sale of land, this doctrine would not bar a purchaser from relying on the statements and representations of a seller as to material facts that are available to the seller and not available or discoverable by a buyer exercising reasonable diligence. Using this doctrine, a buyer might be able to rescind a contract for sale of property whenever such misrepresentations of the seller relate to the land, its physical condition, and its quality.

Legal Defenses

There are some limited defenses against Superfund liability. First, even though a transportation agency may be a PRP under Superfund, liability will not exist if it can be established that a release or threat of release, and the resulting damages, are solely the result of an act of God, an act of war, or actions of a third party. To invoke this "third party" defense, an agency would have to show that the release was caused exclusively by an act or omission of another party and that the agency exercised due care with respect to the hazardous substance concerned and took precautions against foreseeable acts or omissions of any such third party and the foreseeable consequences. An employee, agent, or contractor (except common carrier by rail) does not qualify as a third party.

Second, Superfund can release a party from liability where an "innocent landowner" defense is established. By virtue of key definitions in Section 101(35)(A), an owner of contaminated property may be shielded if the owner acquired it after the waste disposal and if the owner can establish one of the following: acquisition without any knowledge or reason to know of the disposal; acquisition by inheritance or bequest; or acquisition as a government entity by any involuntary transfer or acquisition or by eminent domain authority using purchase or condemnation.

To use this defense, the owner also must show the exercise of due care with respect to the hazardous substance concerned and precautions against foreseeable acts or omissions of any third party and the consequences. This defense cannot be used by any previous owner otherwise liable under Superfund or by any owner who obtained actual knowledge of the release or threatened release while owning the property, subsequently transferring it to another without disclosing this knowledge. The defense also cannot be used by one who caused or contributed to the release or threatened release.

This defense will be important for transportation agencies that use eminent domain. Note that the exercise of eminent domain authority can cut off liability whether done by purchase or by actual condemnation. Some agencies acquire property by inheritance or bequest, so this defense will help there, too.

If the agency wishes to invoke this defense because it did not know and had no reason to know of the waste disposal, Section 101 makes clear that it "must have undertaken, at the time of acquisition, all appropriate inquiry into the previous ownership and uses of the property consistent with good commercial customary practice in an effort to minimize liability." This means the agency should perform a thorough hazardous waste site assessment.

This site assessment tool also will be useful to the agency invoking the shield of eminent domain or inheritance or bequest, because it can help document that the disposal on the property took place before acquisition, as this innocent landowner defense requires.

Third, by virtue of Section 107, no state or local government is liable under Superfund for costs or damages "as a result of actions taken in response to an emergency created by the release or threatened release of a hazardous substance generated by or from a facility owned by another person," except if there is negligence or intentional misconduct.

Fourth, Section 107 states that no person is liable "as a result of actions taken or omitted in the course of rendering care, assistance, or advice in accordance with the National Contingency Plan ("NCP") or at the direction of an on-scene coordinator appointed under such plan, with respect to an incident creating a danger to public health or welfare" as the result of a release or a threat of release. This does not preclude liability, however, for negligence. Compliance with the NCP is very important.

COPING WITH CONTAMINATED PROPERTY

If a transportation agency has not avoided liability for hazardous materials released to the environment, it can manage the problem in a businesslike manner. Most such problems are manageable. This is not to say they are cheap.

Reporting Releases

Superfund provides that any person in charge of a vessel or facility generating, storing, disposing, or transporting hazardous substances immediately must notify the National Response Center upon receiving knowledge of a hazardous release if the release is above the threshold for "reportable quantities" as defined by EPA regulations. Therefore, discovery of hazardous substances on a property, any sudden or nonsudden accidental release at a facility, or an accidental release by a transporter must be reported if it is of a reportable quantity. A transportation agency itself may be the source of the reportable release or it may detect contamination from a user of its facility or from an abutting property.

Note that state laws impose additional reporting obligations.

Staying Off the Superfund List

A transportation agency should obtain EPA and state lists of priority and potential cleanup sites. It should examine whether its wastes went to these sites or if its properties are on the lists. The agency should be familiar with hazard-scoring methods for potential sites, interview past and present employees, document historical disposal on-site and off-site, check disposal vendor histories to identify potential Superfund liabilities, and review EPA records to see what the agency knows or thinks was done with wastes. These steps can help the agency prioritize its own site cleanups in order to try to avoid being on the Superfund list, or, if it is advisable, to encourage Superfund listing the site to increase the chances of outside funding of the cleanup.

Complying with the National Contingency Plan

The NCP establishes procedures and standards for responding to releases of hazardous substances, pollutants, and contaminants. It outlines criteria, which must be applied in the investigation and evaluation of hazardous waste sites and determination of proper cleanup response. The NCP also designates the roles of federal, state, local, and private parties in effecting a cleanup plan. Transportation agencies involved in cleanup activities on land they own or lease must comply with these procedures and standards. Furthermore, in evaluating cleanup plans for abutting properties, the agency should check compliance with the NCP to help ensure that a safe and effective cleanup is undertaken.

Complying with State Requirements

State requirements for hazardous waste management generally follow a format similar to the federal requirements previously described. Notification may be required; notification will activate state and local contingency plans; response must be coordinated with local authorities including fire, police, and health boards; waste must be characterized using official lists; reportable quantities may be different; and state and local boards and agencies may impose their own administrative orders (or file their own lawsuits) seeking cleanup according to their own procedures and standards.

This is especially important in a home rule state where municipalities are authorized to promulgate their own ordinances and bylaws, which may be more stringent than those of the state. The transportation agency must find out about these local requirements for emergency response planning, release notifications, and cleanups. These likely will differ from one community to another.

Communicating Effectively

The transportation agency should open lines of communication to the environmental agencies (federal, state, and local), disclose contamination, and remedy it. It is important to demonstrate a positive commitment so as to lessen environmental agency concerns: fashion a proposed remedial action plan and implement it after getting agency approvals; set up an internal management structure to coordinate these activities, drawing on health, safety, legal, and financial personnel; and use in-house staff or specialized consultants who are experienced in remedial action. The voluntarily cleanup is a necessary adjunct to EPA programs and is a useful tool for business and government to meet legal obligations while keeping costs under a semblance of control.

Knowing How Clean Is Clean

The recent Superfund amendments establish permanent remediation as the goal of hazardous waste cleanups. These require that preference be given to the choice of a remedial action that will permanently reduce the toxicity, mobility, or volume of hazardous substances and to remedies using alternative treatment technologies. EPA is directed to select remedial actions that will satisfy applicable, relevant, and appropriate requirements (ARARs) set forth under federal or more stringent state standards. Permits usually required under other environmental laws are waived for on-site actions, but these actions must comply with the standards set by regulations pursuant to those laws.

Specifically, remedial actions at least must attain Recommended Maximum Contaminant Levels (RMCLs) as established under the Safe Drinking Water Act and water quality criteria under the federal Water Pollution Control Act. Regulations pursuant to RCRA, TOSCA, the Clean Air Act, and the Marine Protection Resource and Sanctuaries Act apply to disposal and incineration of hazardous waste on land and at sea.

State law varies on how clean is clean because there is little statutory or regulatory language on the matter. It should be expected that states will address remediation standards either by guidelines or regulations over the next few years, probably based on research on health effects and levels of risk, to determine what levels of contaminants are acceptable in site mitigation. Ultimately, the degree to which a site is cleaned will depend on the severity and extent of the contamination, the substances involved, the remedial technologies available, whether a threat exists to public health or the environment, and cost.

Being a Businesslike Responsible Party

When the EPA or state agency names a transportation agency as responsible for a contaminants site, the agency should name a point person immediately; gather information quickly; assemble a team of experts; forge links to the agencies and community involved; and begin to make administrative, technical, and legal decisions in a businesslike way. The goal is to implement a cost-effective solution to environmental problems at the site with a fair

allocation of costs. In practical terms, agency liability will depend on the relative volumes and percentages of materials disposed on the site (or shipped to a site by the agency as a generator), their nature and toxicity, the degree of involvement in site operations, the number of other PRPs, the imminence and degree of hazard, the extent of groundwater or surface contamination, the migration of contamination off-site, present or potential impacts on public health, and whether there were knowing or intentional violations of law. It also makes a difference whether the agency is a "deep pocket," among many small generators, into which EPA may reach for cleanup costs.

Based on these factors, the agency should decide carefully whether to be part of the solution or part of the problem, taking a leadership role on the PRP committee or a "let them sue us" approach. The middle ground is as a "willing participant," acknowledging PRP status but being a "follower" willing to pay a fair share of a PRP settlement. If the agency is the deep pocket generator, it should try to convince the EPA to enlarge the PRP universe by bringing in other PRPs to share liability.

The agency should be aware of the Superfund defenses that may be invoked and should be careful to conduct itself so as to invoke them; prepare claims it can pursue using Superfund provisions, indemnification clauses in real estate contracts, and theories of contribution; and keep track of costs so as to seek reimbursement using these means.

Hiring Qualified Contractors

To ensure that the transportation agency selects a hazardous waste consultant and contractor capable of properly undertaking site assessments or remedial actions, it is important to develop and apply criteria for those under consideration.

The agency should retain only those professionals who have a good general understanding of the legal and regulatory issues involved, including their own and their clients' responsibilities regarding notification and liability. The contractor should have adequate and appropriate staff already available to develop the information needed for site assessments and remedial action plans. It should have a track record in preparing reports of this sort in a manner understandable to nontechnical people as well as to other experts. The reputation for quality work and integrity should be good. The contractor should be willing to consider approaches other than those in which it specializes and to retain the necessary subcontractors for work it cannot perform itself, such as complex hydrogeologic studies.

There should be a contract in writing with the consultant. It should include several provisions to protect the interests of the agency. It must delineate the scope of work and carefully identify specific work tasks, personnel responsible for accomplishing them, timetables, and budgets. It is important to know specifically what services the agency is purchasing and to ensure that cost and time overruns do not occur. Of course the contract should include contingencies, such as unexpected discoveries of additional waste. Incentives should be added to achieve the final work product in a timely manner, with disincentives for delays.

The contract should indicate that the consultant is hired to assist the legal department of the transportation agency in rendering legal advice to the agency. In this way, much information generated by the consultant can be transmitted directly to the agency attorney for evaluation and decision, and may be less available in lawsuits by way of discovery. The contract also should provide indemnification and hold-harmless clauses between the state agency and the contractor covering negligence, gross negligence, and willful misconduct in the contractor's performance. The agency also should be aware that the consulting firm might need to hire subcontractors for certain aspects of the work. The agency should retain control over the hiring of additional subcontractors, which should be after a demonstration of need and due notice from the prime contractor. The same criteria should be applied to these proposed subcontractors.

Protecting Employees

Transportation agencies that contract out for cleanups should be aware of the new worker safety obligations, discussed above, enacted at the same time as the reauthorized Superfund. OSHA has begun to issue regulations specifically designed to protect workers engaged in hazardous waste operations. These training and safety mandates cover employees performing response operations under Superfund; corrective actions at RCRA sites; emergency response actions; actions at sites designated by a state or local government; and operations at facilities regulated pursuant to RCRA.

Note that these provisions will apply to agencies conducting their own work. Note also that these provisions encompass initial investigations at sites before the presence or absence of hazardous substances has been confirmed. They also supply to employees engaged in duties at agency facilities storing, treating, or disposing of hazardous substances. The agency should be prepared to meet (and make sure that contractors meet) these requirements for periodic medical surveillance of employees, air monitoring, handling of hazardous substances, decontamination procedures, and development of emergency plans along with training programs.

CONCLUSION

Proper hazardous waste management is firmly established as a fundamental legal requirement governing transportation agencies along with other sectors of government and business. It is part of a comprehensive regulatory program controlling hazardous materials generally, in many aspects of manufacturing and government activities. The present

emphasis on response to releases of hazardous substances is shifting to prevention by emergency planning.

States will continue to supplement federal programs with stricter state Superfunds, management laws, and right-to-know laws. Communities will use home rule authority, where available, to go beyond the federal and state basic programs.

The concept of strict liability for releases to the environment is here to stay, and the courts are willing to enforce these new forms of legal obligations. EPA and state agencies are gaining new enforcement tools such as administrative penalties and new cleanup authorities to deal with contaminated sites. It makes sense for transportation agencies to anticipate and appreciate their new responsibilities and manage their affairs so as to minimize the legal, financial, and environmental risks.

Publication of this paper sponsored by Committee on Physiochemical Phenomena in Soils.

Ground-Penetrating Radar as a Means of Quality Control for Soil Surveys

J. A. DOOLITTLE AND R. A. REBERTUS

Ground-penetrating radar (GPR) can be used to chart the presence, depth to, and lateral extent of diagnostic subsurface soil horizons. During the past 7 yr, USDA-Soil Conservation Service and participants in the National Cooperative Soil Survey have tested GPR in diverse physiographic regions on a wide variety of soils. The principal use of GPR has been to estimate the taxonomic composition of soil map units and to determine the accuracy of soil mapping completed by conventional sampling procedures. As the users of soil surveys become more diverse, demands are being made for more detailed and quantitative information, and often to depths greater than are presently being attained in most modern surveys. Ground-penetrating radar techniques have been used to supply more detailed and quantitative analysis of soil variability. Compared with conventional surveying methods, GPR provides continuous spatial data of subsurface features, greater depth and lateral coverage per area sampled, and higher levels of confidence in site evaluations. However, the relative success of GPR investigations remains highly site- and interpreter-dependent.

Soil surveys, the production and interpretation of soil maps, were first conducted in the United States in 1899. Since then, the nature and objectives of soil surveys have changed greatly. Prior to the 1950s, soil surveys were oriented largely toward providing technical assistance for soil conservation and agricultural programs. In the 1950s, information and interpretations in soil survey reports were expanded to include forestry, engineering, urban, and other uses not considered in earlier survey reports. Modern soil surveys provide data useful in estimating soil properties and in planning the general location and construction of highways, power transmission lines, sewers, water and drainage systems, dwellings, and waste disposal systems.

In urbanizing areas where land use is most intense, the need for soil information and interpretation continues to evolve at an unprecedented rate (*1*). Users are requesting more detailed and site-specific information with narrower confidence limits, and to depths greater than are presently attained in modern soil surveys (*2*). As users require more accurate and detailed information concerning the characteristics, composition, and variability of soils within map units, the need for more intense sampling and quantitative description of soil variability is being recognized. To fulfill these needs, different approaches to and methods of observing soils may be required.

Even with the development of soil interpretations for different types of land uses, class differentials used in soil classification do not exceed depths of 2 m. Many nonagricultural uses require information from zones deeper than the limits of modern soil survey investigations. The use of soils for sewage lagoons, sanitary landfills (trench), dwellings with basements, excavated ponds, reservoirs, or as sources of sand, gravel, or roadfill, often requires information on soil properties to depths beyond the limits of soil survey investigations or requires additional information where observations made have been insufficient to establish reliable standards. In some areas, conventional methods of observing soils are becoming inadequate for the needs of more exacting users of soil surveys.

While the uses of soil surveys have evolved greatly, surveying tools have changed little since 1899. Though aided by backhoes and mechanical probes, the spade and auger have remained the primary sampling tools of soil surveyors. While effective in most areas, conventional methods of observing soils are slow and tedious and produce incomplete data as a result of the limited number of observation sites and the small area actually observed. It is estimated that more than 99.9 percent of the area delineated on soil maps is not observed below the surface (*2*). The potential for errors is great. In areas where soils are poorly drained, have high densities, or contain large amounts of coarse fragments, surveying costs increase because of time required for field investigations. Errors resulting from insufficient observations and inadequacy of information from deeper soil depths are more conspicuous in these areas.

The depth of observation, efficiency of sampling, and the quality and quantity of data could be increased in many areas if faster and less labor-intensive methods were available to improve or complement existing soil survey techniques. Since the late 1970s, the USDA-Soil Conservation Service (SCS) has been exploring the potential of GPR technology to assist and improve soil survey operations (*3*).

J. A. Doolittle, USDA-Soil Conservation Service, 160 East 7th Street, Chester, Pa. 19013. R. A. Rebertus, Delaware Agricultural Experiment Station, Department of Plant Science, College of Agricultural Sciences, University of Delaware, Newark, Del. 19717–1303.

Ground-penetrating radar is being used to increase the accuracy and precision of soil surveys by providing continuous spatial records of the subsurface, greater depth and areal coverage per unit sampled, and higher levels of confidence in site evaluations. Advantages of GPR systems are speed of operation, capacity to produce large quantities of continuous subsurface data, and high resolution. Compared with conventional methods of observing soils, ground-penetrating radar techniques are faster, more economical, less likely to overlook subsurface features, and nondestructive.

THE GPR SYSTEM

The ground-penetrating radar is an impulse radar system designed for shallow subsurface site investigations. Pulses of electromagnetic energy radiate into the ground from a transmitting antenna. Each pulse consists of a spectrum of frequencies distributed around the center frequency of the antenna. Whenever a pulse contacts an interface separating layers of differing electromagnetic properties, a portion of the energy is reflected back to the receiving antenna. The receiving unit amplifies and samples the reflected energy and converts it into a similarly shaped waveform in a lower frequency range. The processed, reflected waveforms are displayed on a graphic recorder or are recorded on magnetic tape for future playback or processing. The graphic recorder uses a variable gray scale to display data. It produces images by recording strong reflections as black and lesser intensity reflections in shades of gray.

The GPR systems used by USDA-SCS are the Subsurface Interface Radar (SIR) System-8 and System-3 manufactured by Geophysical Survey Systems, Inc. The SIR System-8 consists of a control unit, tape recorder, graphic recorder, and power distribution unit. A microprocessor, which has programs to enhance signals, remove background noise, and amplify weak signals obscured by background noise, is available with this unit.

The SIR System-3 consists of a profiling recorder and a power distribution unit. The profiling recorder houses the radar control electronic and graphic recorder in a single unit. Compared with the SIR System-8, the SIR System-3 unit is easier to use, more portable, and less expensive. Both systems can be powered by a motor vehicle battery or by two 12-v marine batteries.

Five antennas (80, 120, 300, 400, and 500 MHz) have been used to investigate earthen materials. Two higher frequency antennas (900 and 1000 MHz) are available, but their use has been limited to the investigation of reinforcing steel, road pavements, and bridge deckings. The lower frequency antennas (80 and 120 MHz) have longer pulse widths and greater radiation powers and emit signals that are less rapidly attenuated by earthen materials. The higher frequency antennas (300, 400, and 500 MHz) have shorter pulse widths and greater powers of resolution, but are limited to shallower depths. For most field work, the 120 MHz antenna has been found to provide the best balance of probing depth and resolution. The 80 MHz antenna is heavy and cumbersome and is difficult to maneuver in rough or forested terrain.

Each of these antennas has a fairly broad radiation pattern. Theoretically, the radiation pattern is conical with the apex of the cone at the center of the antenna. Reflections from an interface are a composite of returns from within the area of radiation.

A vehicular installation of the GPR has proven to be the most practical approach for soil survey operations in nonforested areas. A four-wheel-drive vehicle provides a mobile, weatherproof base for routine field work and is also used for transporting the equipment. The control and recording units are "shock-mounted" on a shelf within the vehicle. An antenna is towed behind the vehicle in a sled at speeds of 3 to 8 km/h for most field work. The sled protects the antenna and smooths surface irregularities. GPRs have also been mounted on all-terrain vehicles, boats, helicopters, skis, and snowmobiles. In forested or rugged terrain, surveys are often conducted by hand-towing the antennas and the electronics.

HISTORICAL DEVELOPMENT

In the early 1970s, soils were considered to be "essentially radar opaque because of their high electrical conductivity" (*4*). However, in 1979, the feasibility of using GPR for soil survey investigations was successfully demonstrated in a study conducted by the National Aeronautics and Space Administration (NASA), USDA-SCS, and Florida Department of Transportation (*5*). Since then, the use of GPR for soil survey investigations has developed slowly. Use of GPR remains restricted for the following reasons:

- Limited awareness of this geophysical technique,
- Results that are dependent on the skill and experience of the operator,
- Initial high costs of equipment,
- Limited knowledge of its performance in various media and geographical areas, and
- Rapid signal attenuation and severe depth restrictions in some media.

In organic soils, GPR has been used to determine the thickness of organic soil materials(*6–12*), estimate the degrees(s) of humification (*9, 11, 13*), classify Histosols (*7, 14*), and profile the topography at the base of the organic materials (*14–16*).

In recent years there has been a notable increase in the number and types of GPR applications on mineral soils. Applications include characterizing soil map unit composition (*3, 17, 18*), determining water table depths in coarse-textured soils (*19*), summarizing microvariability of depths to soil horizons (*20*), characterizing soil properties (*17*), determining the depth to bedrock (*21*), assessing soil-

landscape relationships (*22, 23*), and improving soil-salinity management (*24*).

FACTORS INFLUENCING AREAS OF APPLICATION

Ground-penetrating radar does not perform equally well in all soils. The maximum probing depth of GPR is, to a large degree, determined by the conductivity of the soil. Soils having high conductivities rapidly dissipate the radar's energy and restrict the probing depth. The principal factors influencing the conductivity of soils to electromagnetic radiation are degree of water saturation, amount and type of salts in solution, and the amount and type of clay.

Moisture content is the primary determinant of soil conductivity. Electromagnetic conductivity is essentially an electrolytic process that takes place through moisture-filled pores. As water-filled porosity increases, the rate of signal attenuation increases and the probing depth of the radar is restricted.

Electrical conductivity is directly related to the concentration of dissolved salts in the soil solution. In unirrigated areas, the concentration of dissolved salts in the soil profile and the probing depth of the GPR are influenced by parent material and climatic parameters. Soils formed in regolith weathered from shale or limestone generally contain more ions in solution than soils developed from felsic crystalline rocks. In general, most soluble salts are leached in humid regions. In semi-arid and arid regions, soluble salts of potassium and sodium and the less soluble carbonates of calcium and magnesium are likely to accumulate in soil profiles, the depth of accumulation being a function of precipitation, soil textures, and bulk densities.

Ions absorbed to clay particles can undergo exchange reactions with ions in the soil solution and thereby contribute to the electrical conductivity of the soil. The concentration of ions in the soil solution is dependent on the clay minerals present, the pH of the soil solution, the degree of water-filled porosity, the nature of the ions in solution, and the relative proportion of ions on exchange sites. Smectitic and vermiculitic clays have higher cation-exchange capacities than kaolinitic and oxidic (e.g., gibbsite and goethite) clays, and, under similar soil-moisture conditions, are more conductive (Table 1). Table 2 illustrates how the maximum probing depth of electromagnetic radiation increases as clay content decreases and the proportion of low-activity clays increases.

Soil texture influences the performance of GPR. Generally probing depths are 5–25 m in coarse-textured materials, 2–5 m in moderately coarse-textured materials, 1–2 m in moderately fine-textured materials, and less than 0.5–1.5 m in fine-textured soils. As discussed earlier, these probing depths become less as the concentration of soluble salts in solution and the exchange activities of clays increase.

Acknowledging these limitations, geographic generalizations can be made as to the areas in the United States in which GPR techniques are likely to produce satisfactory results (17). Figure 1 is a map of the United States summarizing the suitability of different geographic areas for GPR investigations of soils. This map is very generalized and ignores the site-specific nature of the radar.

The potential for utilizing GPR techniques for soil investigations is high in areas of coarse- or moderately coarse-textured soil materials, areas of highly weathered soils having low proportions of 2:1 type clays or concentrations of soluble salts, and uplands underlain by felsic crystalline bedrock.

GPR APPLICATIONS TO SOIL SURVEYS

Increasing the Quantity of Soil Data

Within USDA-SCS, GPR has been used as a reconnaissance, investigatory, and quality control tool. The principal use of GPR has been to estimate the taxonomic com-

TABLE 1 CATION-EXCHANGE CAPACITY OF CLAY MINERALS (*25*)

Clay Mineral	Capacity (meq/100 g)
Vermiculite	100–150
Montmorillonite	80–150
Chlorite	10–40
Illite	10–40
Kaolinite	3–15

TABLE 2 PROBING DEPTH OF GPR IN RELATION TO MINERALOGY CLASS AND CLAY CONTENT

Soil	Mineralogy Class	Percent Clay	Probing Depth
Vaiden	Montmorillonitic	>60	15 cm
Rhinebeck	Illitic	35–60	40 cm
Kirvin	Mixed	35–60	2 m
Sites	Oxidic	35–60	5 m

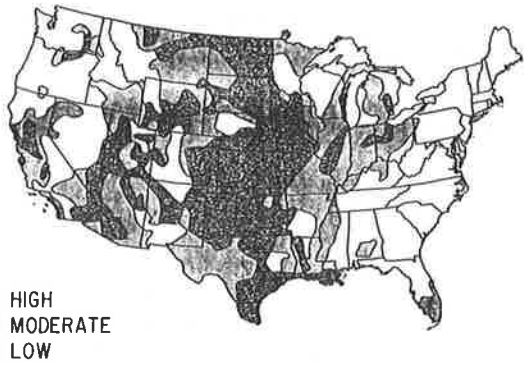

FIGURE 1 Potential for ground-penetrating radar soils interpretations.

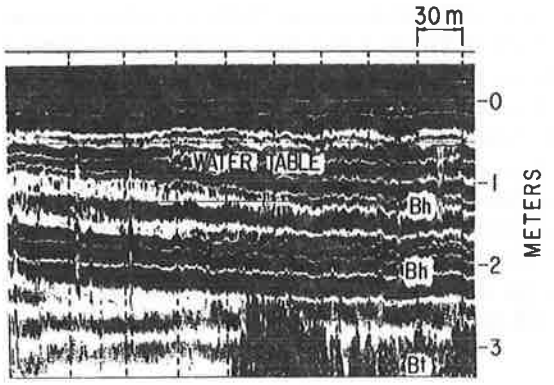

FIGURE 2 A GPR profile charting the water table, and the Bh and Bt horizons.

position and variability of soils within map units obtained with traditional survey procedures. Many of the diagnostic subsurface horizons described in Soil Taxonomy (*26*) can be identified and traced using GPR.

Abrupt changes in texture, density, moisture, or organic carbon content will generally produce strong reflections and distinct GPR imagery. Distinct radar images that are produced by abrupt changes in moisture (water table), organic carbon content (Bh horizons), and texture (Bt horizon) are illustrated in Figure 2. This graphic profile was recorded within an area of sandy, siliceous, hyperthermic Arenic Haplaquods (Immokalee series) in Florida. Dark lines have been drawn to highlight the upper boundary of the water table and the major subsurface diagnostic horizons. The presence and depth to diagnostic soil horizons and soil features are used to classify soils. Knowledge of the lateral extent and depth of these horizons, obtained with GPR, can be used to determine their spatial variability within mapping delineations and thereby document map unit composition.

Ground-truth boring and test data are needed to calibrate radar imagery and to confirm interpretations. To scale the radar data, the dielectric constant of the medium, the propagation velocity of the radar pulse in the medium, or the depth to an interface must be known. Generally, for most soil investigations, one soil boring will suffice to establish a depth scale and to identify soil horizons. In areas of complex soil patterns, more than one boring is often required to properly identify images appearing on the graphic profiles.

The precision of GPR for determining the depth to subsurface features has been well documented. For soil features occurring within depths of 2 m, the difference in measurements between the scaled radar images and the auger boring data is generally within 2.5 to 5.0 cm (*3*).

The precision of data collected using GPR decreases with increasing depth and with soil variability. In an area of loamy, mixed, mesic Arenic Hapludalfs and mixed, mesic Typic Udipsamments (Matea and Plainfield series) in Michigan, the difference in measurements between the scaled radar imagery and the auger boring data were less than 10 cm in 71 percent of the observation sites and less than 5 cm in 43 percent of sites. Differences between the two methods of measurement are attributed to the wide range in water table depths (0.68–4.2 m) and the presence of discontinuous finer-textured strata in these predominantly coarse-textured soils.

In soils having horizons with irregular or broken boundaries, the agreement between the scaled radar imagery and the auger boring measurements will be less. During field investigations of cultivated Histosols within the Florida Everglades, the lack of concurrence between soil auger data and the scaled radar imagery was attributed to the highly pitted nature of the underlying limestone bedrock. Variations in the depth to bedrock as great as 43 cm were observed within a 25-cm radius of observation sites (*19*). At each observation site, it was possible for the soil auger to have contacted a residual microhigh or entered a solution cavity. Soil auger measurements often reflect the extreme rather than the average depth to an underlying interface. GPR profiles, based on a composite of scans that have been averaged across the area of radiation beneath the antenna, are influenced less by an irregular subsurface microtopography.

Where sandy soils with low electrical conductivity predominate, conditions are optimum for the use of GPR. To date, the use of GPR has been most successful in Florida. Data obtained with the GPR in Florida have been used to update the soil surveys for Hardee, Hillsborough, Manatee, Orange, Sarasota, and Seminole counties. GPR data were used to statistically document the proportion of soils within map units. This information was presented in both tabular and descriptive formats in soil survey reports to inform users about soil variability.

Ground-penetrating radar techniques, while not used as fully elsewhere as in Florida, have been used successfully in many other states to increase the efficiency of data collection and to improve the quality of soil interpretations.

Extending the Depth of Observation

Ground-penetrating radar can extend the depth of soil characterization and improve the quality of soil information at lower depths. The examination of soil profiles with conventional surveying tools is restricted by the presence of coarse fragments (cobbles, stones, and boulders). Field time and cost increase as conventional surveying tools (augers and shovels) are repeatedly stopped by coarse fragments. In areas containing large amounts of coarse fragments, decisions are often based on a few widely spaced exposures or on assumed soil-landscape relationships.

Overcoming Restrictive Features in Soils

On many uplands, the depth to bedrock is underestimated as a result of coarse fragments. The probability of encountering a rock fragment with a soil auger increases with soil depth and thereby reduces the probability of observing deep (100–150 cm) or very deep (150 cm) soils. At most

sites, it is uncertain whether auger penetration was halted by a rock fragment or by bedrock. In an unpublished study of tills in Maine containing large amounts of coarse fragments, conventional surveying tools could not effectively and consistently probe beyond depths of 75–100 cm. GPR was not restricted by coarse fragments and provided exceptionally high-quality profiles of the underlying bedrock surface (Figure 3). The bedrock contact (highlighted with dark line) is irregular and varies in depth from 30 to 175 cm. In the lower right hand corner of this figure, a vein of dissimilar material or a fracture plane, is apparent within the bedrock. While less pronounced, the contact of ablation till with basal till is evident between depths of 68 and 84 cm.

Very gravelly, stony, or bouldery layers can form restrictive barriers that thwart conventional tools. In a Michigan study, a thin (50 cm), very gravelly (35–60-percent-rock fragments) layer limited the number and depth of auger observations in an area of sandy-skeletal, mixed udorthentic Haploborolls (Alpena series). The time spent excavating this very gravelly layer with a soil auger and pry bar exceeded reasonable limits. Because of time constraints, the inferences made were based on a small number of observations about the underlying materials within the survey area.

To improve the understanding of materials underlying the very gravelly layer, a GPR investigation was conducted. Unlike conventional surveying tools, the GPR provided a continuous record of subsurface conditions and was not restricted by the layers of coarse fragments. In Figure 4, the very gravelly layer is apparent immediately below the surface. Strata within the coarse-textured glacio-lacustrine deposits are evident between depths of 1 to 2 m. The GPR charted the mean and range of thicknesses of sand and gravel deposits, the depth to loamy till, and the occurrence of limestone bedrock.

Determining the Thickness of Sand and Gravel Deposits

Although it may be possible to determine the potential location of sources of sand or gravel from soil survey reports, little information is available concerning the range or average thickness of these deposits. Soils are rated as probable sources of sand and gravel based on properties occurring between depths of 0.25 to 1.5 m.

In many areas, as sand and gravel resources are depleted and the cost of excavation increases, knowledge of the average depth and range in thickness of suitable material will become increasingly important. GPR can be used effectively in coarse-textured materials to determine their potential as sources for sand and gravel.

Estimating Volume of Organic Materials in Peatlands

Soil survey reports provide information concerning the classification and areal extent of organic soil materials. However, these reports do not contain sufficient data for estimating peat volume. To estimate the volume of organic materials, a larger number of measurements to depths beyond the current limits of soil survey investigations may be required. Procedures for estimating the thickness of peat deposits have been established (*27*). However, established methods are time consuming and costly. The speed and continuous subsurface profiling by GPR reduce the cost of data collection and permit sampling of a greater area. With GPR it is possible to quickly assess the volume of peat reserves, estimate the thickness of layers varying in degrees of humification, and profile the topography at the base of the organic materials.

Figure 5 was constructed from data collected from a bog in Wisconsin. Images from the organic-mineral contact

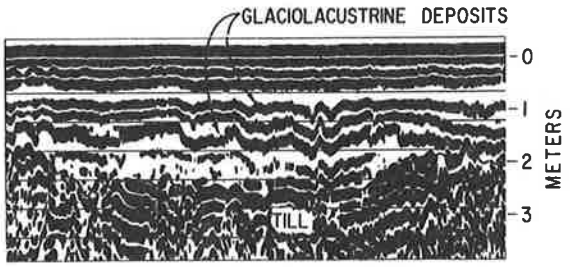

FIGURE 4 A GPR profile of stratified glacio-lacustrine sediments overlying till.

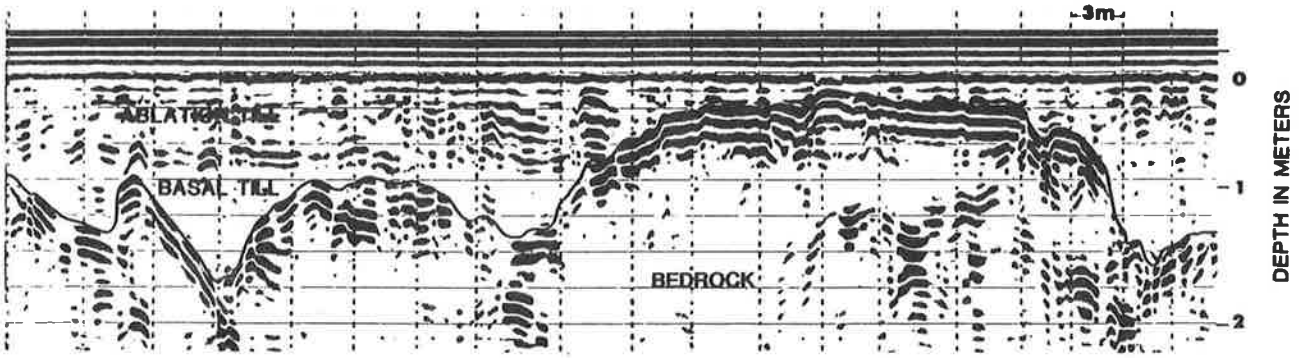

FIGURE 3 A GPR profile of the depth to bedrock.

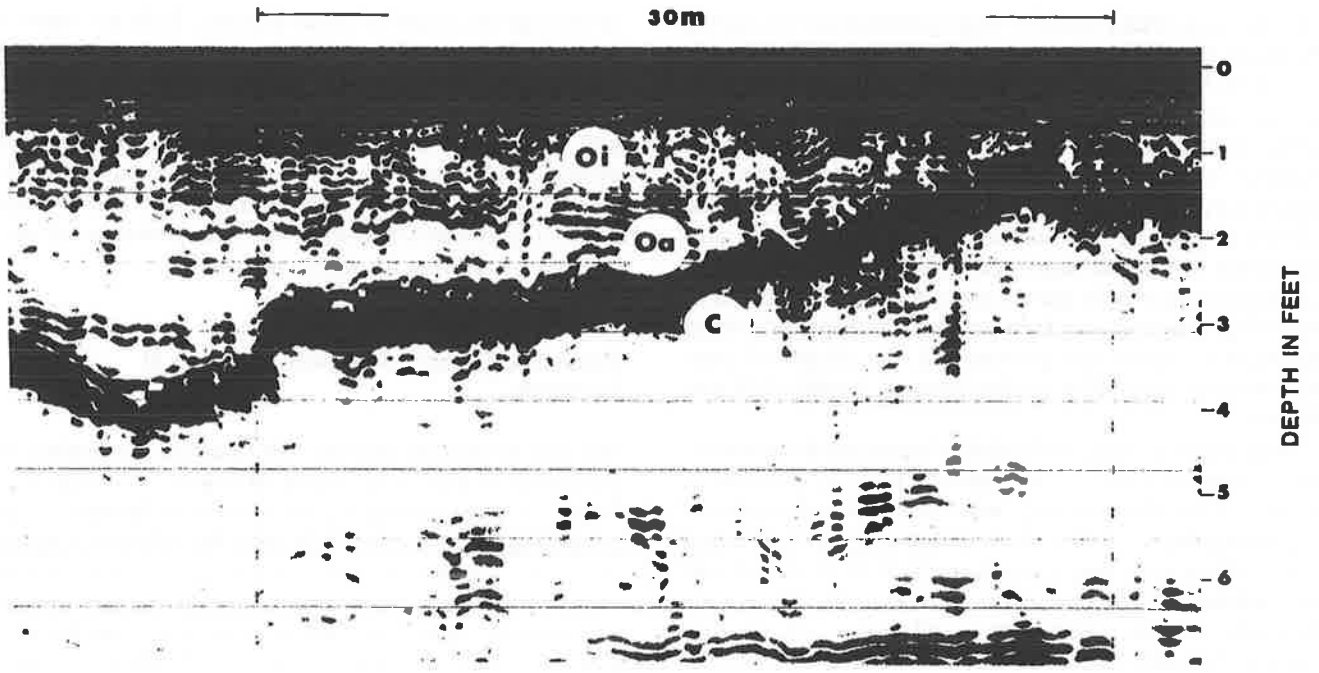

FIGURE 5 A GPR profile of fibric (Oi) and sapric (Oa) organic soil materials and the organic-mineral soil interface (C).

are conspicuous. A contact separating fibric (Oi) from sapric (Oa) organic materials is evident at a depth of 0.5 m. This contact represents a significant change in humification, bulk density, and water content. In the lower part of this figure, strata within the underlying Eau Claire Formation can be seen.

Developing Improved Soil-Landscape Models

As a result of cost and time constraints, soil scientists can not observe profiles from every acre. Observation sites are selected on the basis of soil-landscape relationships and models of soil genesis. Predicting the occurrence and distribution of soils is often based primarily on associations made between soil properties and soil landforms, landscape position, and steepness of slopes. Observation points from which these association models are formulated tend to be limited in number and biased toward the most prominent soils and landscape features (*28*). Unfortunately, as noted by Cline, the predictive value of soil-landscape models is not perfect.

Ground-penetrating radar and computer graphic techniques have been used to produce economical and detailed two- and three-dimensional plots of subsurface conditions. Computer-generated grip maps constructed from data collected by GPR have been used to display soil-landscape relationships (*22, 23*), to characterize the composition of soil map units, and to chart the variability of subsurface horizons and properties (*20*).

In Figure 6, three-dimensional block diagrams of the loess surface and the paleosurface (top of the Pensauken formation) within a 2.52 ha study area in northern Delaware are shown (*23*). Using GPR and computer graphic techniques, it was learned that loess thickness is highly irregular and largely controlled by the underlying paleosurface and cannot be predicted from relief or landform. Documentation of the variability of loess thickness disclosed that the mapping unit names do not properly reflect the composition of the map units. Results from this and other studies underscore the importance of evaluating and improving soil-landscape models and the need for measuring variability in soil properties.

CONCLUSION

Users of soil survey reports are becoming more numerous and diversified. They are requiring more detailed and site-specific information with narrower confidence limits and soil information to depths greater than are presently attained in most modern soil surveys. Ground-penetrating radar has been used to provide accurate and detailed information concerning the characteristics, composition, and variability of soils within map units and to cope with the needs for more intense sampling and detailed and quantitative descriptions of soil variability.

Ground-penetrating radar has been used to increase the accuracy and precision of soil surveys. Compared with conventional surveying methods, GPR techniques provide continuous spatial records of subsurface features, greater depth and areal coverage per unit sampled, and higher levels of confidence in site evaluations. Ground-penetrating radar techniques are also faster, more economical, less likely to overlook subsurface features, and nondestructive.

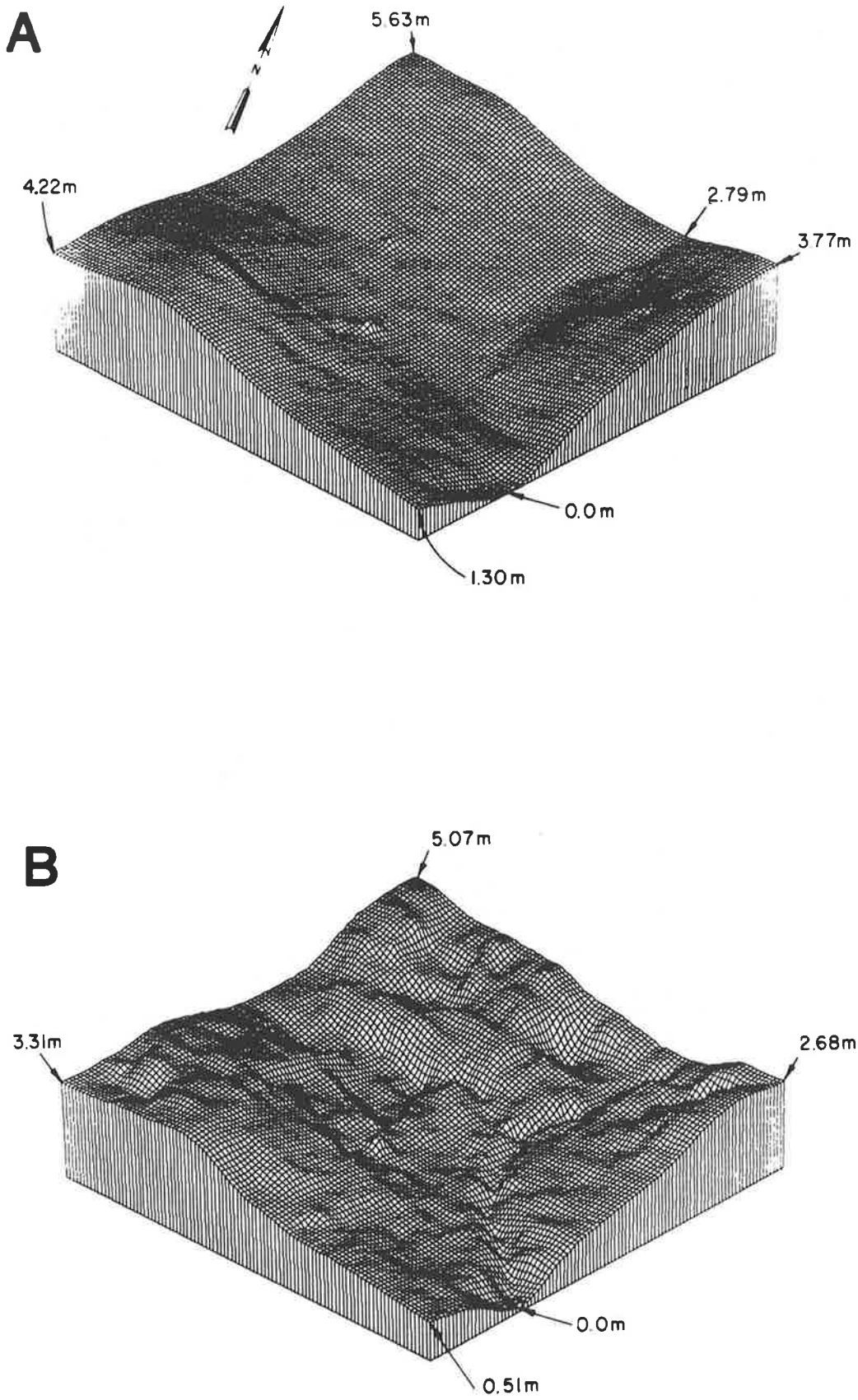

FIGURE 6 Surface net diagrams from GPR profiles showing relative (A) elevation of modern surface and (B) elevation of paleosurface.

Results remain highly site-specific and interpreter-dependent. While it is neither a magic black box nor the panacea to all soil-surveying needs, GPR is a complementary tool that can be used in many areas to increase the quality and quantity of soil data, the depth of observation, and our understanding of soil-landscape relationships.

ACKNOWLEDGMENT

The authors wish to express their appreciation to Douglas Barnes of the Soil Conservation Service.

REFERENCES

1. R.B. Brown. The Need for Continuing Update of Soil Survey. *Proc., Soil Crop Science Society, Fla.*, Vol. 44, 1985, pp. 90–93.
2. F.P. Miller. Soil Survey under Pressure: The Maryland Experience. *Journal of Soil and Water Conservation*, Vol. 33, No. 3, 1978, pp. 104–111.
3. R.W. Johnson, R. Glaccum, and R. Wojtasinski. Application of Ground-Penetrating Radar to Soil Survey. *Proc., Soil Crop Science Society, Fla.*, Vol. 39, 1979, pp. 68–72.
4. J.C. Cook. Radar Exploration through Rock in Advance of Mining. *Transactions of the Society of Mining Engineers*, AIME 254, 1973, pp. 140–146.
5. R. Benson and R. Glaccum. *The Application of Ground-Penetrating Radar to Soil Surveying.* Final Report. NASA, Cape Kennedy Space Center, Technos, Inc., Miami, Fla., 1979.
6. K.G. Blom and J.S. Nelson. *Ground Radar Survey, Peat Deposits, St. Louis County, Minn.* Harding-Lawson Associates, Navato, Calif., 1980.
7. M.E. Collins, G.W. Schellentrager, J.A. Doolittle, and S.F. Shih. Using Ground-Penetrating Radar to Study Changes in Soil Map Unit Composition in Selected Histosols. *Soil Science Society of America Journal*, Vol. 54, 1986, pp. 408–412.
8. S.F. Shih and J.A. Doolittle. Using Radar to Investigate Organic Soil Thickness in the Florida Everglades. *Soil Science Society of America Journal*, Vol. 48, 1984, pp. 651–656.
9. K. Tolonen, A. Rummukainen, M. Toikka, and I. Marttila. Comparison between Conventional Peat Geological and Improved Electronic Methods in Examining Economically Important Peatland Properties. *Proc., 7th International Peat Congress*, Dublin, Ireland, June 1984.
10. C.P. Ulriksen. Investigation of Peat Thickness with Radar. *Proc., 6th International Peat Congress*, Duluth, Minn., Aug. 1980.
11. C.P. Ulriksen. *Application of Impulse Radar to Civil Engineering.* Doctoral thesis. Lund University of Technology, Department of Engineering Geology, Lund, Sweden, 1982, 175 pp.
12. R.D. Worsfold, S.K. Parashar, and T. Perrott. Depth Profiling of Peat Deposits with Impulse Radar. *Canada Geotechnical Journal*, Vol. 23, No. 2, 1986, pp. 142–154.
13. Remotec Applications, Inc. *The Use of Impulse Radar Techniques for Depth Profiling of Peat Deposits.* National Council of Canada, Division of Energy Research and Development, Ottawa, NRCC20982, 1982, 94 pp.
14. J.A. Doolittle. Investigating Histosols with Ground-Penetrating Radar. *Soil Survey Horizons*, Vol. 23, No. 3, 1983, pp. 23–28.
15. L. Bjelm. *Geological Interpretation of SIR Data from a Peat Deposit in Northern Sweden.* Professional paper. Lund Institute of Technology, Department of Engineering Geology, Lund, Sweden, 1980.
16. *Radar Assessment of Peat Resources* (Abstract). Geophysical Survey Systems, Inc., Hudson, N.H., 1979.
17. J.A. Doolittle. Characterizing Soil Map Units with the Ground-Penetrating Radar. *Soil Survey Horizons*, Vol. 22, No. 4, 1982, pp. 3–10.
18. J.A. Doolittle. Using Ground-Penetrating Radar to Increase the Quality and Efficiency of Soil Surveys. In *Soil Survey Techniques*, Soil Science Society of America Special Publication No. 20, 1987, pp. 11–32.
19. S.F. Shih, J.A. Doolittle, D.L. Myhre, and G.W. Schellentrager. Using Radar for Groundwater Investigation. *Journal of Irregular Drainage Engineering*, Vol. 112, 1985, pp. 110–118.
20. M.E. Collins and J.A. Doolittle. Using Ground-Penetrating Radar to Study Soil Microvariability. *Soil Science Society of America Journal*, Vol. 51, 1987, pp. 491–493.
21. C.G. Olson and J.A. Doolittle. Geophysical Techniques for Reconnaissance Investigations of Soils and Surficial Deposits in Mountainous Terrain. *Soil Science Society of America Journal*, Vol. 49, 1985, pp. 1490–1498.
22. W.E. Puckett, M.E. Collins, and G.W. Schellentrager. Evaluating Soil-Landscape Patterns on Karst Using Radar Data. *Agronomy Abstract*, 1986, p. 232.
23. R.A. Rebertus, J.A. Doolittle, and R.L. Hall. Landform and Stratigraphic Influences on Variability of Loess Thickness in Northern Delaware. *Soil Science Society of America Journal*, Vol. 53, 1989, pp. 843–847.
24. S.F. Shih, D.L. Myhre, G.W. Schellentrager, and J.A. Doolittle. *Using Radar to Improve Salinity Management.* Paper No. 85–2611. American Society of Agricultural Engineers, 1985.
25. R.E. Grim. *Clay Mineralogy.* McGraw-Hill Book Company, Inc., New York, 1953, 384 pp.
26. Soil Survey Staff. *Soil Taxonomy: A Basic System of Soil Classification for Making and Interpreting Soil Surveys.* Soil Conservation Service., U.S. Department of Agriculture Handbook 436, 1975, 754 pp.
27. ASTM Committee on Standards. *Standard Practices for Estimating Peat Deposit Thickness.* ASTM D4544–86, Philadelphia, Pa., 1986.
28. M.G. Cline. The Soils We Classify and the Soils We Map. In *Soil Resource Inventories*, Cornell University, Ithaca, N.Y., Agronomy Memo 77–23, 1977, pp. 55–70.

Use of trade names in this report is for identification purposes only and does not constitute endorsement by the authors or USDA-SCS.

Publication of this paper sponsored by Committee on Engineering Geology.

Some Airborne Applications of Subsurface Radar

STEVEN A. ARCONE

The results of several helicopter-borne short pulse radar surveys over frozen and thawed freshwater bodies are discussed. The examples given are geologically simple so that effects of the system could be separated from the complications of wave propagation in the ground. As expected, best performance was achieved using well.isolated and small high-frequency antennas at slow speeds and low altitudes over smooth interfaces defining low loss media. In addition the isolation of the airborne antenna from ground loading permits application of deconvolution filtering based on the known, constant radiated pulse waveform. The major obstacles to deeper earth penetration using high power, low frequency transmitters and antennas are high surface reflectivity and aircraft clutter. Current research is looking at methods to suppress these unwanted effects.

Short pulse radar was originally developed for ground surface applications. The first commercial systems introduced by the Geophysical Survey Systems, Inc. (GSSI) in the early 1970s were airborne over frozen lakes, rivers and seas (*1-5*) within a few years in attempts to measure ice thickness. Simple geologic situations that were easily interpretable were encountered in some of this work, but most of the applications outdistanced the systems used. The more difficult applications required signal processing for dealing with incoherent reflections from inhomogeneous media (e.g., brash ice) and high-power, low-frequency antennas for greater penetration into water or wet soils. These requirements have only begun to be addressed in the last few years.

This paper discusses several ice survey examples and other applications using a system identical in principle to those used in the references mentioned above, and one system that is radically different. The purpose is to introduce the reader to present and future possibilities of airborne short pulse radar. The examples illustrate both great successes and experimental failures. At present helicopter rental rates ($400-600/hour for a Bell Jet Ranger), it is hoped that distinct coherent reflections will appear as soon as the survey site is attained. As the helicopter moves along, it is thought that the time separation of the reflections will vary. All too often, however, within 60 seconds of takeoff, the oscilloscope display is cluttered with coherent events that either remain immobile in the scan or never change their relative position as range or altitude changes. Although exploration geophysicists are generally reluctant to report negative results, some examples of geophysical exploration "garbage" will be given here.

U.S. Army Cold Regions Research and Engineering Laboratory, Hanover, N.H. 03755.

EQUIPMENT: THE RADAR SYSTEM

In short pulse radar the fundamental idea is to connect some sort of discharge device to a very broadband antenna, radiate the resulting pulse, and receive a reflection whose time of propagation can be timed with suitable clocks in a control unit. Common methods of pulse generation are not much more sophisticated in principle than Hertzian spark gap generators, but pulse compression techniques using code modulation are now being developed. The standard commercially available short pulse radar system has been discussed in many articles (*6, 7*). Here the radar system will also be reviewed, but with an eye toward its airborne application.

Transmit and Receive Antenna Units

The antennas are usually resistively loaded dipoles, the design of which seeks to attenuate all oscillations of the current discharge. Such antennas sacrifice all the glamour of conventional radar antennas—high gain, narrow beamwidths, efficiency, excellent front-to-back ratio—in order to achieve this short pulse shape, two of which are shown in Figure 1. To the left in Figure 1 is shown a GSSI Model 101C resistively loaded dipole, vintage 1979. The right side of Figure 1 depicts A-cubed "pulse ekko" low frequency folded dipole, vintage 1985. The waveforms have been modified slightly by filters of a control unit. Range resolution is always at a premium; angular location is presumed to be directly beneath the antenna, lacking any directionality in the beam radiation pattern. Frequency spectra of commercial models are centered between 50 and 1000 MHz, with a few special application antennas as low as 10 MHz.

A short pulse radar antenna placed on the ground will experience ground loading; i.e., excitation of the ground

will induce radiation that slows the flow of current on the antenna. This reaction lowers the frequency content of the pulse and alters its shape depending on ground electrical properties. The ground also causes a curious lobing to the radiation pattern, as energy is divided mainly between the critical angle $\theta_c = \sin^{-1} 1/n$ where, n is the ground index of refraction, and the broadside directions (*8*). An airborne antenna radiates a single broad lobe with minimal pulse width, and guarantees that the transmitted waveform will never vary; an important consideration for deconvolution (i.e., pulse compression) signal processing schemes such as Wiener filters. The major drawback of airborne antennas is the interference of radiation reflected from the aircraft, examples of which will be shown later.

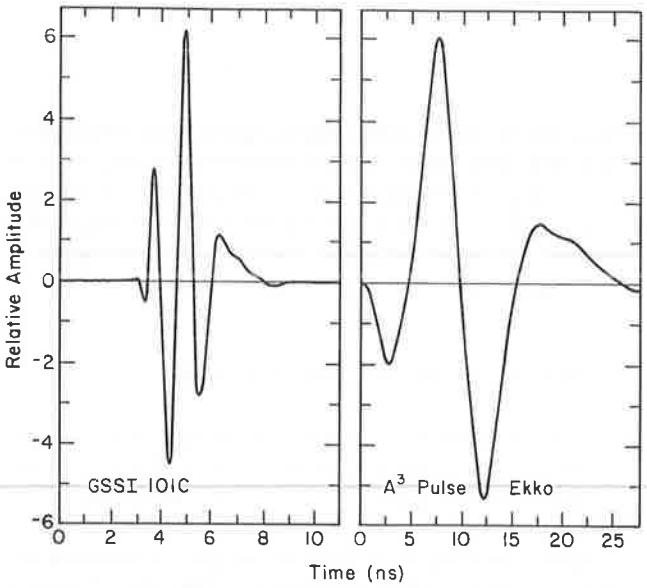

FIGURE 1 Waveform examples in short pulse radar.

The transmitter and most of the receiver electronics are placed at the antenna terminals to reduce noise, and both antennas and electronics are often placed in one package that is shielded to reduce back radiation (Figure 2). Semiconductor discharges are used to generate Gaussian-shaped pulses, peak amplitudes of which are now available at over 1000 volts. The signals received are immediately amplified and then sampled to convert the frequency content into the audio range for tape recording and data display on conventional graphic devices. Real-time digitization is not yet possible, since the frequency bandwidth of the smaller antenna units extends into the low GHz range. The sampled returns are reconstructed into scans extending over time windows ranging generally from about 50 to 2000 ns. The pulse repetition frequency (PRF) of all commercial units is about 50 kHz, so that approximately 6700 pulses go into the construction of 1 scan at a scan rate of about 8/sec: a rather large waste of energy.

Control Unit

A control unit contains the hardware to set the scan rate, time windows, overall gain and the all-important TRG

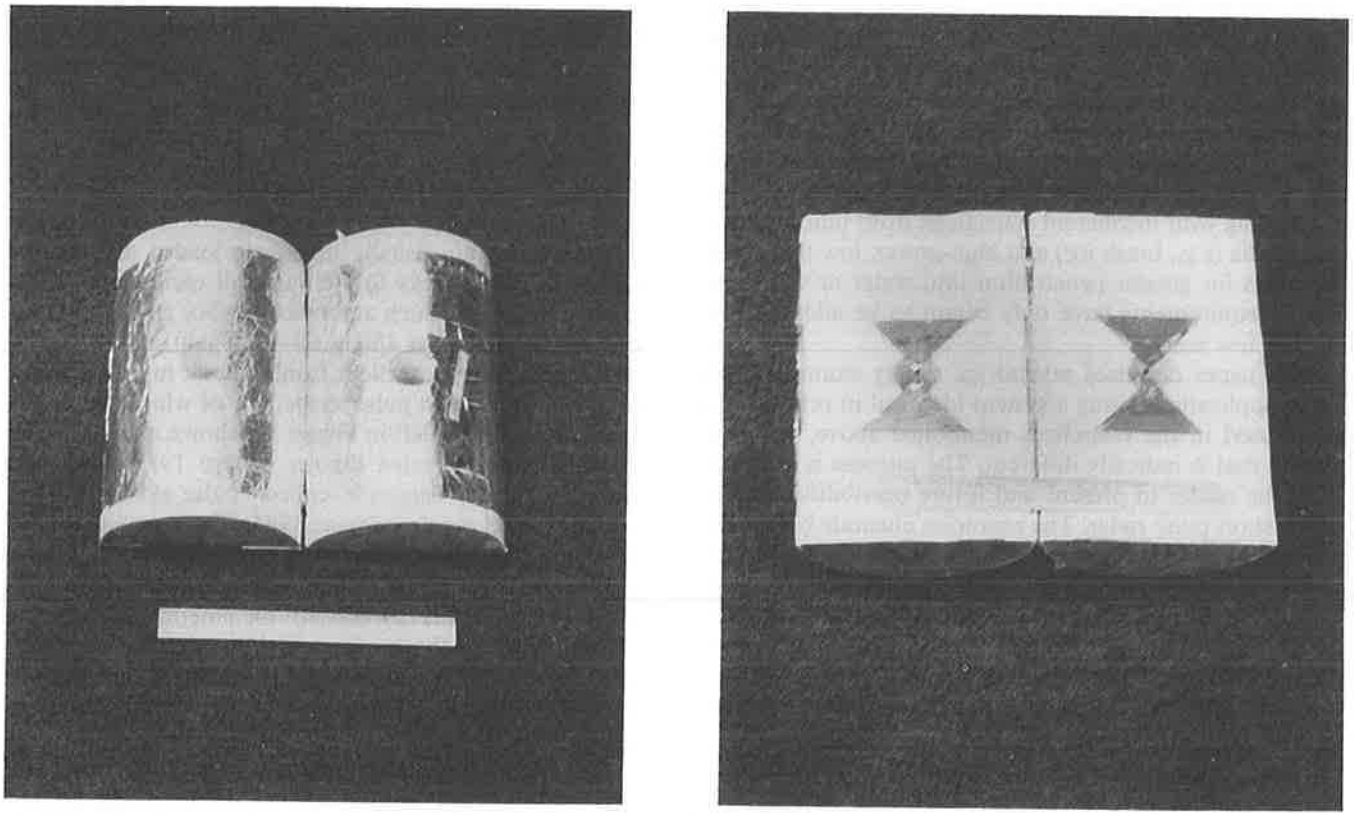

FIGURE 2 Single unit packaging of shielded transmit and receive antennas.

(time range gain) function. This function allows the gain to be varied over the scan to enable suppression of the strong early returns and amplification of the weaker later returns. A small oscilloscope for viewing the scans and a cassette tape recorder are available, along with a variety of high and low pass filter settings to exclude most ambient noise. Some units may include digital circuitry to allow the audio signals to be stacked continuously—an excellent technique for enhancing the signal to noise ratio in the presence of incoherent noise. Unfortunately, the antennas must be kept motionless while this operation is performed. Therefore, the function is of no use in an airborne survey where the aircraft altitude constantly varies, even by tens of centimeters over a 1- or 2-second time span.

A basic rule of ground surveying is to go as slowly as human patience will permit, as this affords the best-quality data. The same holds true in the air; 5 mph or less is best. Data have been successfully recorded at speeds between 5 and 20 mph at 8 scans/second. Higher scan rates are necessary at greater speeds. Table 1 shows the approximate ground area of sensitivity for one scan as a function of speed for the GSSI model 101C antenna (center frequency—900 MHz) operating at 8 scans/sec at an altitude of 3 m. The calculations are based on a measured transmit-receive 3 dB beamwidth of 70 degrees (*9*) in both principal radiation planes. These beamwidths should hold for other antenna units of similar design (e.g., model 3102 at 500 MHz), the dimensions of which scale according to the center frequency of operation.

The necessary time range window is determined by the expected time of return for the deepest reflection (or "event") sought. The free space velocity of electromagnetic waves is 30 cm/ns, so that every meter of altitude adds 6.2 ns to the needed time window. Propagation velocities beneath the earth's surface are much slower, varying from about 17 cm/ns in dry sand to about 3 cm/ns in icy water. Care must be taken that the frequency range of the pulse does not lie in the dispersive and absorptive region for the particular material of interest, or else the distorted pulses that return may hardly be recognizable, much less visible.

Signal Processing and Graphic Displays

The signal processing functions mentioned above, audio conversion, filtering, time range amplification, and stacking are all available in modern, commercially available subsurface radars. Missing are matched filters or deconvolution schemes designed to recognize the reflected wavelets of interest and suppress all other events. Such filtering schemes have been developed by individual organizations (e.g., United States Geological Survey in Denver, Colorado, and U.S. Army Cold Regions Research and Engineering Laboratory, Hanover, New Hampshire), but not for commercial use. At present, data storage, handling, and processing are the major priorities in subsurface radar development.

TABLE 1 AREA OF SENSITIVITY AS A FUNCTION OF ALTITUDE

Altitude (m)	Area (m^2)
3.0	16
4.5	35
6.0	60
7.5	90
9.0	130

NOTE: Approximate ground area of sensitivity as a function of altitude based on the 3 dB beamwidth of the pulse center frequency. Values are good to ±10 percent for scan rates between 8 and 50 sec^{-1} and flight speeds up to 7.5 m sec^{-1}.

The most common method of data display is electric current burning on chemically treated paper. Figure 3 shows a hypothetical radar scan and equivalent graphic display, an ideal model if the radar events were to remain unchanged over a short distance. Darkness is proportional to signal amplitude and the horizontal bands represent the consecutive positive and negative oscillations of the pulse waveform. The chart paper rolls out as fast as the data were recorded on magnetic tape, which means that it takes as long to display data as it does to do a survey. As stacking is impossible in an airborne survey, it is virtually the raw data that are displayed on the graphic. The advantage of this display is that the banding formed by the density of the consecutive scans allows the eye to follow the continuity of various events within a profile with ease. The disadvantage is that individual waveforms cannot be readily examined as in a seismic section, but must be retrieved. Retrieval is not easy unless the waveforms have been digitally recorded and stored (there is one manufacturer who now offers this service).

Aircraft Mounting

The primary consideration for mounting a short pulse radar antenna to an aircraft is minimizing reflections from

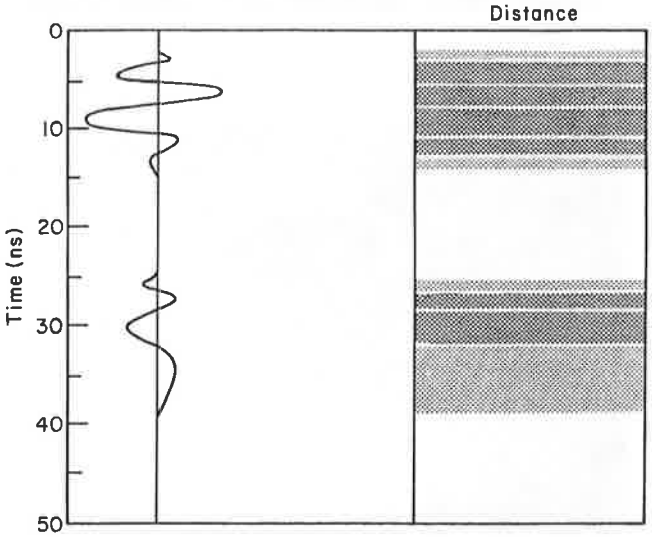

FIGURE 3 Hypothetical radar scan and equivalent graphic display.

the aircraft. This requires either a shielded construction or a remote mounting. Many antenna units now available are metallically backed to confine radiation to one hemisphere. Nevertheless, energy will radiate from the sides of the unit and even leak around the back of the shielding: a front-to-back ratio of about 20 dB is common. Larger antenna units operating below 150 MHz are generally not shielded owing to the added weight of the metallic backing.

Figure 4 shows two experimental mountings for which data will be shown later. Figure 4a shows a GSSI model 3102 "500 MHz" antenna fixed to the skids of a Bell Jet Ranger 206B. The antenna unit weighs about 3 kg and is set about 1 m from the nearest skid. Figure 4b shows a low frequency unit of unshielded antennas slung beneath a helicopter. In both cases, the antennas must be far enough from the nearest reflector (ground or aircraft) to allow the direct transmission to the receiver to clear before any events of interest are received.

EXAMPLE SURVEYS

Sheet Ice: Lakes

There is hardly a geophysical exploration system that does not base its data interpretation upon the theoretical interaction of the energy involved (e.g., seismic or radar waves, d.c. currents) with a model of smoothly layered earth. Such an ideal model is often realized in cold regions where layers of water, ice, and thawed and frozen soils are common, as well as the usual sedimentary layering found everywhere. Most ideal is a frozen lake where motionless water allows even freezing. Somewhat less ideal is a river, where the energy of flowing water produces frazil and brash ice formations which distort the homogeneity and smooth interfaces of the ice sheet.

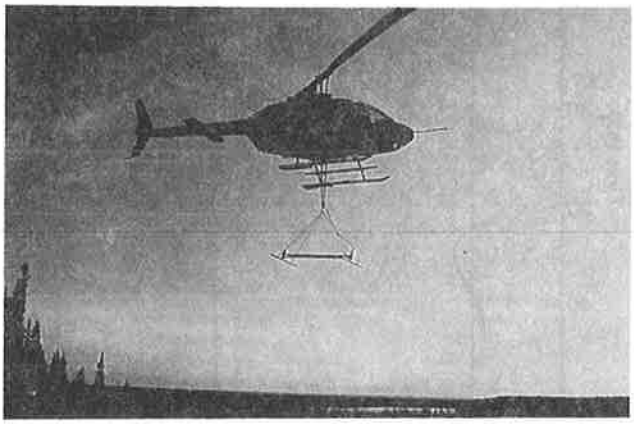

FIGURE 4 Short pulse radar antennas on a Bell Jet Ranger 206.

Figure 5 is a helicopter survey performed in late March 1986 of a lake in interior Alaska, whose ice was just over 1 m thick. The vertical ice thickness scale shown in the figure applies only within the first two reflections. The decibel values given in parentheses refer to the round trip propagation loss for the water and ice multiple events at the points indicated. Portions of some events depicted in this figure may not be visible because the figure has been made light enough to view the signal zero crossings (thin white lines) in the stronger events.

The transmitted pulse was centered near 500 MHz. Helicopter speed was about 18 m/sec, or 40 mph (generally air speed is much less), and the total record is about 4300 m long. The large changes in the vertical position of the reflections are due to wind-aided changes in altitude. The figure demonstrates many aspects of an airborne survey of a simple two-layer medium: direct coupling, helicopter reflections, ice surface and bottom reflections and a faint multiple reflection that occurred between water and the helicopter. Two of the events are labeled with attenuation figures given in decibels (dB). These figures represent the amount of propagation loss calculated to have been suffered by the particular event labeled at the altitude indicated at the arrowhead. These losses are due to geometric spreading of the beam and transmission and reflection losses at the ice-air and ice-water interfaces. All of the ice reflections are coherent: i.e., the banding indicates retention of the transmitted waveform. At 18 m/s airspeed, 10 m altitude, 8 scans/s and a beamwidth of 70 degrees, the antenna has sensed over 170 m^2 of ice while compiling 1 scan. Generally, earth layering over such a large area will not be so uniform as to allow radar returns at 500 MHz to retain this degree of coherency, as is now seen.

Sheet Ice: River

Figure 6 depicts a very low altitude survey of a section of the frozen Yukon River that contained a stretch (approximately 200 m) of open water, with a hanging dam of frazil ice. The transmitted pulse was centered near 900 MHz. Altitude was kept at about 1.5 m and air speed was very slow at about 1.8 m/sec (4 mph). The time scale is only about 25 percent of that of Figure 5, so that the small vertical variations seen most clearly in the surface reflections represent altitude changes of only tens of cm. At the right of the figure are temporally coherent reflections from a smooth cover of sheet ice. The reflections seen beneath open water reflections are multiple bounces between the helicopter and water. Attenuation at 900 MHz in fresh-

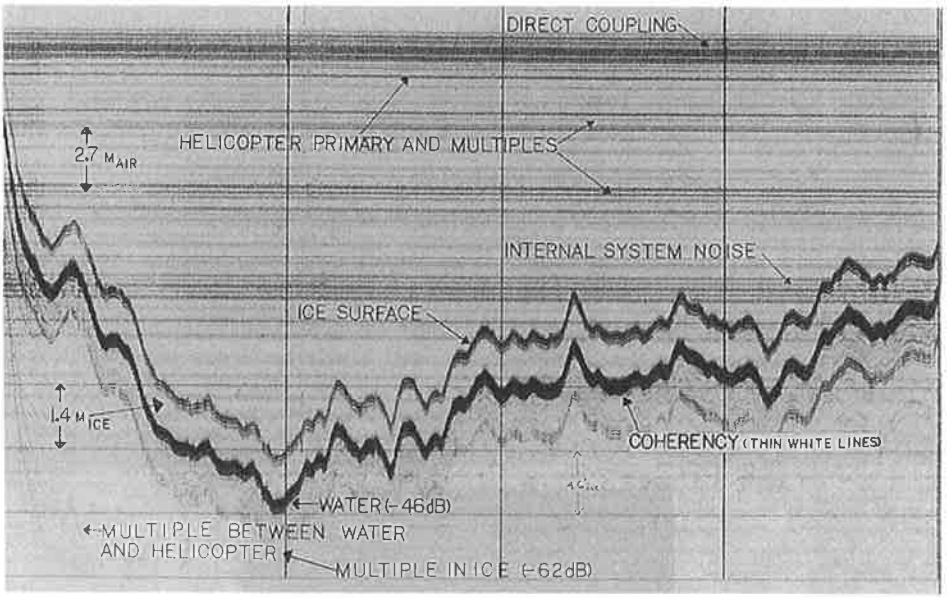

FIGURE 5 Antenna Model 3102 profile of ice thickness over Birch Lake, Alaska.

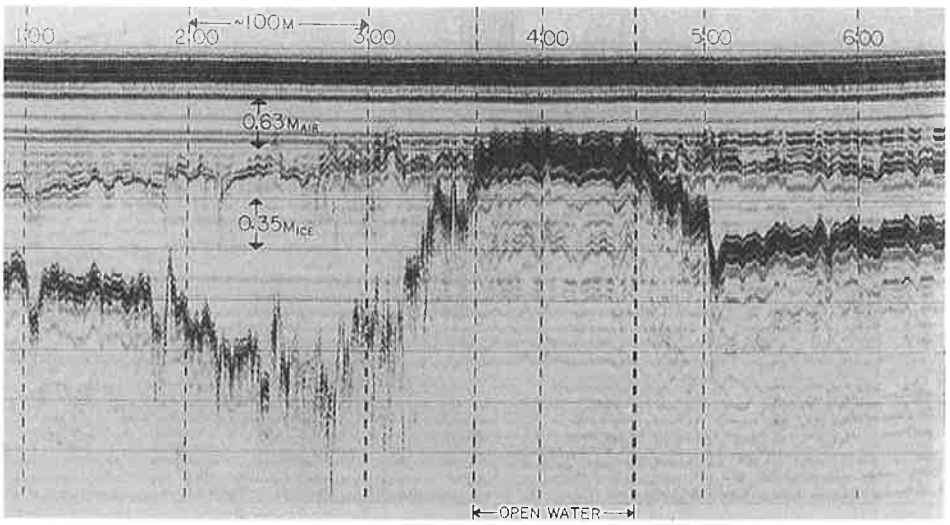

FIGURE 6 Very low altitude (<2 m) model 101c (900 MHz) antenna survey of section of Yukon River.

water at 0°C is over 70 dB/m so there is no chance that this is a subsurface event. Of greatest interest is the large lobe of frazil ice that formed under the sheet ice downstream (to the left) of the open water. The lobe ranges up to 1.7 m thick, which met the criterion for pier fortifications on the Yukon bridge (up to 3 m of ice was detected in a sun-shielded cove farther upstream). Note that the frazil ice reflections consist of coherent and incoherent signals. These returns cry out for some squaring and smoothing to establish a more traceable boundary.

Figure 7 is a survey conducted over the same transition from ice to water seen in Figure 6. The survey was done with the 500 MHz model 3102 antenna at 6 m/sec flight speed and a slightly higher altitude. The detail shown in Figure 6 is degraded in Figure 7, especially over the frazil ice formation. The lower figure shows an expanded section of the data was digitized and deconvolved using a Wiener filter based on a pulse waveform received over the open water. The noise suppression and the time domain pulse compression can be seen, which will enable the thickness of the ice to be measured more easily.

An ability to measure the thickness of thin ice is of interest to the Coast Guard or to municipal agencies responsible for regulating winter activities such as ice fishing, skating festivals, motorcycle races, etc. The minimum resolvable thickness from the raw data of the antenna used in Figure 6 (GSSI model 101C) is about 20 cm, and about 10 cm with deconvolution. Antennas with a broader

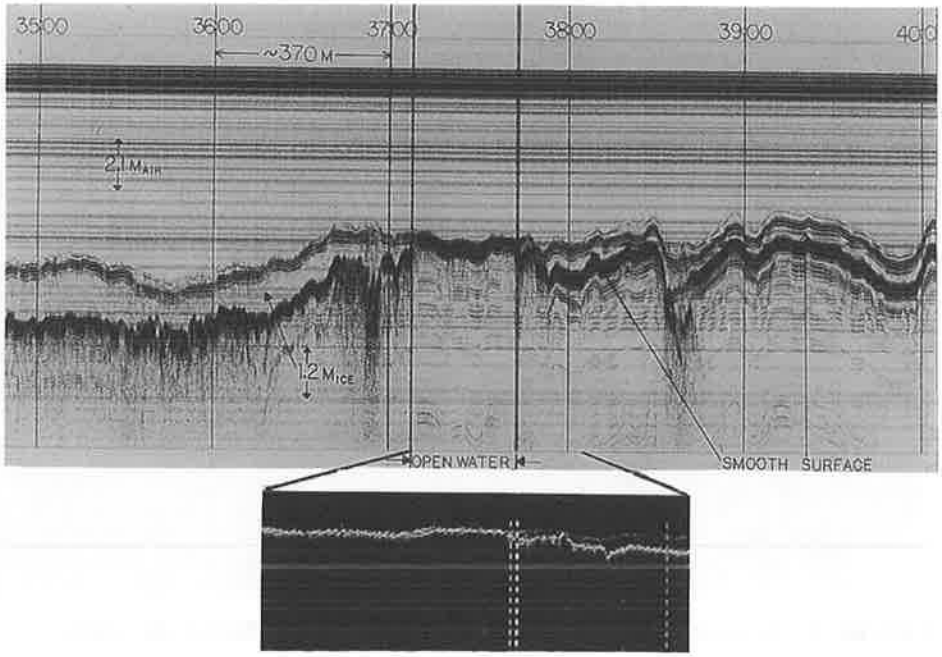

FIGURE 7 Same survey as Figure 6 except at higher altitude and flight speed.

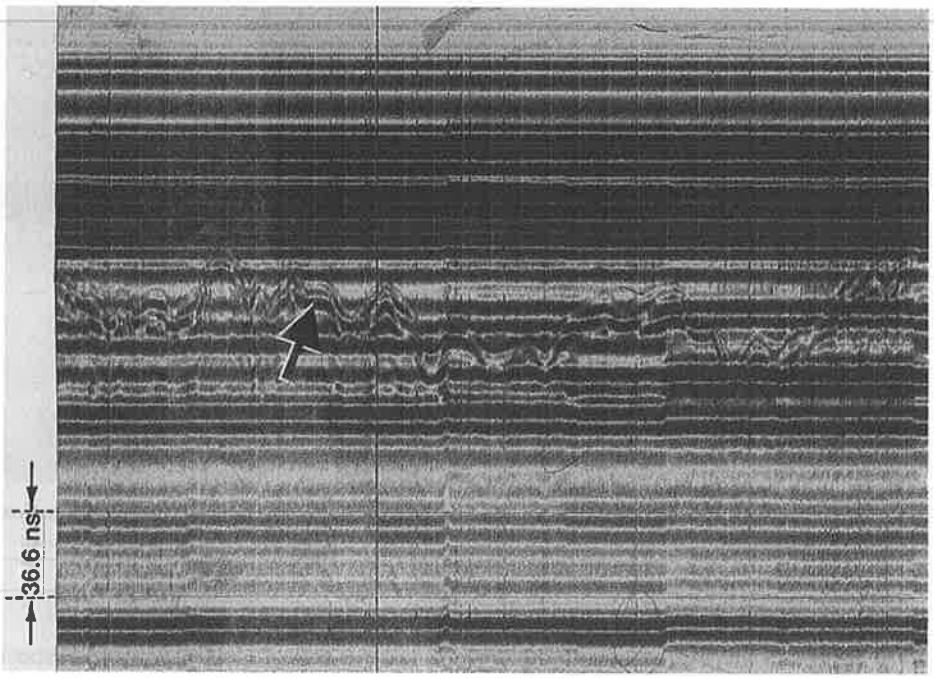

FIGURE 8 Frozen river survey using a GSSI Model 3112 antenna hard mounted between helicopter skids.

bandwidth at the same center frequency, that will reduce these thicknesses to about 10 and 5 cm respectively, will soon be available.

As promised earlier, an example of radar "garbage" is given in Figure 8, which is a profile of a shallow portion of an ice-covered river using a GSSI model 3112 antenna whose pulse was centered near 100 MHz. The antenna was shielded with electromagnetic absorbing material and was hard-mounted between the skids under a Bell Jet Ranger 206B body. The purpose of this survey was to profile the river bottom, hence the use of a lower frequency which gives far less attenuation per meter (see Figure 9, discussed below) than does 500 MHz. In the figure, the ice surface (indicated by an arrow) response is barely visible

among the coherent noise of resonances between helicopter and antenna. Consequently, metallically shielded antennas slung beneath a helicopter have received experimental attention and will be discussed next.

Fresh Warm Water

Penetration of water by remote sensing techniques is required for applications such as dredging bathymetry surveys, and for inspection of bridge pier foundations which may have been improperly emplaced, damaged or which may have caused scouring. This is best done by sonar at the water surface, as its resolution is excellent both vertically and laterally. Radiowaves are also effective in freshwater and may be substituted where turbidity (which can block sound propagation) is high. The prohibitive attenuation rate cited above for cold water at 900 MHz vastly decreases as temperature rises and frequency decreases. Radiowaves are the only possibility for use in rapid, airborne surveys of freshwater bodies, because sound waves cannot penetrate the air-water interface. However, the reflectivity at the air-water interface is still a formidable obstacle to penetration as seen below.

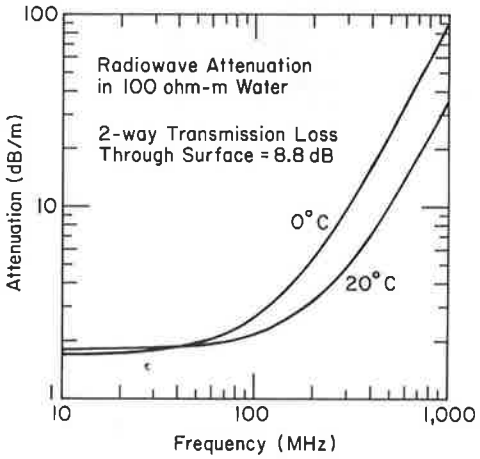

FIGURE 9 Attenuation rate of radiowaves in freshwater.

Figure 9 plots the attenuation rate of 100 MHz radiowaves in fresh water at two temperatures and a conductivity of 0.01 S/m (or 100 ohm-m resistivity; polluted rivers in industrial areas have values closer to 50 ohm-m). Both dielectric dispersion and conductivity contribute to the attenuation rate at this frequency, with dielectric dispersion dominating at cold temperatures. At 100 MHz the attenuation falls to a near-minimal 2 dB/m for warm water. An additional loss of 8.8 dB must be added to any theoretical determination of attenuation to account for losses upon two-way transmission through the air-water interface. Additional losses will occur upon reflection from the bottom. The wavelength in warm water at this frequency is only about 33 cm, so that good resolution of bottom features is possible.

Figure 10 demonstrates the capabilities of surface radar in a fluvial environment. The survey profiled scour holes by the piers of the Buckley Bridge in Hartford, Connecticut; numbered vertical demarcations indicate the positions of the piers. The detail, even of the subsurface sedimentation, nearly rivals the quality of sonar profiles. Unfortunately, this profile was made with a partially submerged, high power antenna towed beside a small boat. The sob-

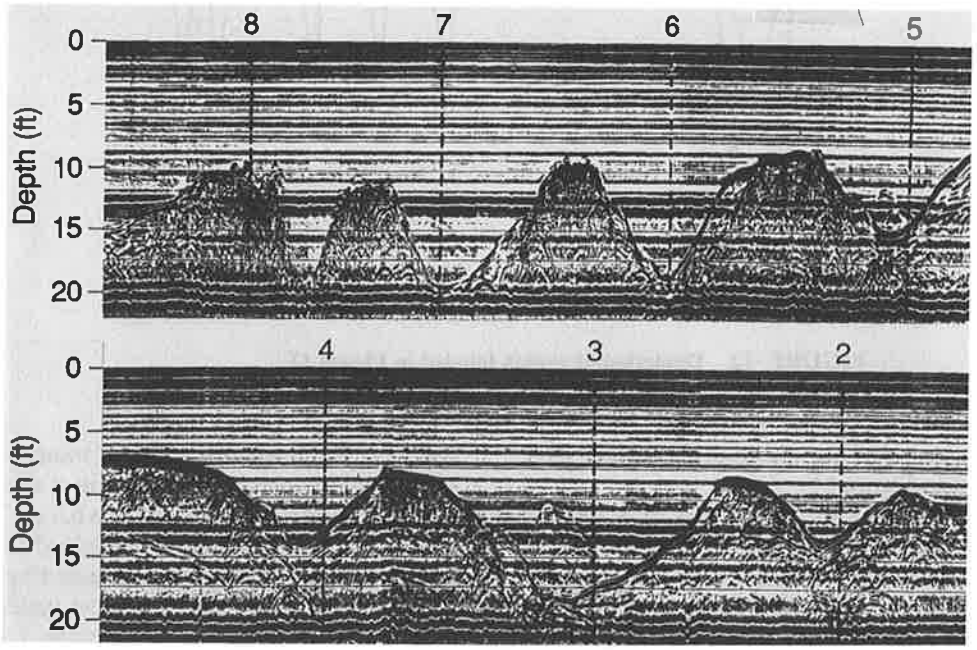

FIGURE 10 Surface radar profile of scour holes on the upstream side of the Buckley Bridge.

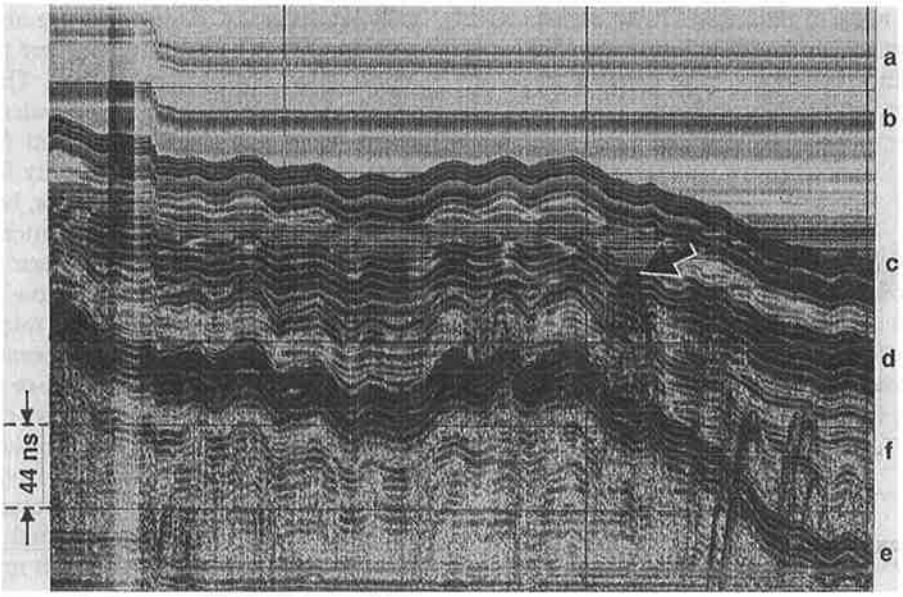

FIGURE 11 Helicopter survey of a shallow reservoir using antennas in a cargo net.

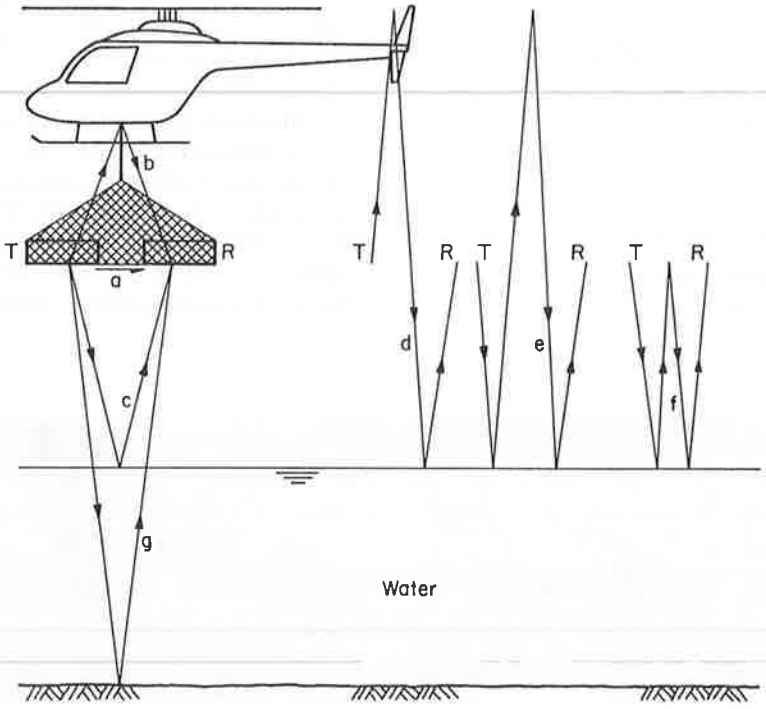

FIGURE 12 Depiction of events labeled in Figure 11.

ering reality of the status of our airborne subsurface river surveying is shown in Figure 11.

Figure 11 is a helicopter survey of part of a shallow reservoir near Hopkinton, New Hampshire, ranging up to 2.5 m depth and 0.0067 S/m conductivity. The reservoir is a flooded valley containing a now submerged concrete road. The antennas used were shielded, resistively loaded dipoles mounted in separate housings (transmit T and receive R in the figure) operating at a center frequency near 250 MHz and using a peak transmitter power of 0.8 kW. The antennas were carried in a sling 4 m below the helicopter and survey altitude was 6.8 m. The major events are labeled by letter and are explained in the depiction of Figure 12. The results are dominated by events c, d, and e, the latter two of which involve helicopter reflections, despite the shielding of the antennas. Event f is believed to be a multiple reflection between the antennas and the water. There is no perceivable bottom reflection which

should occur 140–150 ns beneath the start of event c or about where event e is (event e was followed to the end of the reservoir at depths < 1 m but still remained at – 140 ns delay). However, at least the first hyperbolic reflection at the right of the record is due to the concrete roadway at 0.7 m depth while the other hyperbolas are at 1.5 to 1.8 m depth. Therefore, a very weak bottom reflection coefficient may have contributed to the lack of a bottom profile in this example.

SUMMARY AND RECOMMENDATIONS

Airborne short pulse radar is most successful in the following conditions:

(1) The ground surface is smooth and of low reflectivity; ice sheets and flat dry soils or bedrock exposures are ideal;
(2) Air speed and altitude are low; and
(3) The antennas are shielded.

Areas for further improvement include the following:

(1) Incorporation of a satellite-based positioning system for accurate reconstruction of flight lines.
(2) Fast digitization and storage of the analog data. A helicopter speed of 2 m/sec and a digitization rate of 25 ks/sec would produce 12.5 MB/km. Some units are now commercially available.
(3) Deconvolution software programs built into the system for rapid signal processing. The advantage of deconvolution was seen in Figure 7. Another approach is to use a pulse code modulation scheme that performs pulse compression by the cross-correlation of a transmitted pulse code with a stored, complementary code (*9*).
(4) Incorporation of video graphics display. The present paper chart method takes as long to display as does conducting the survey, and much information regarding the waveforms is lost.
(5) Development of more effective, low frequency, shielded antennas. Frequencies below 50 MHz are advantageous where penetration is as important as resolution, but antenna size and weight increase with decreasing frequency. Almost any size is manageable in a sling, but shielding causes a large increase in weight, especially for separate transmit and receive antennas needed for high-power work. A reasonable weight limit for a 4-seat helicopter would be 50 kg.

Alternatives to shielding are filtering, cross-polarization and circular polarization. Filtering out reverberations is common practice in seismic sub (water) bottom surveys where echoes between a water surface and bottom are clearly defined. In our case, however, there are many waveforms in the helicopter reflections and each would need its own filter design. Cross-polarization involves receiving at a polarization orthogonal to that transmitted. This eliminates reflections from flat surfaces, as only rough surfaces or volume inhomogeneities can cause polarization rotation. Consequently, radar echoes from flat river bottoms also would not be received. The most promising alternative is circular polarization. Water surface echoes will reverse the rotational sense of a circularly polarized wave, but the water bottom should not. Therefore, if an alternative receive mode is used to monitor the antenna height above the water surface, circular polarization may be used to monitor water depth. Broadband logarithmic spiral antennas excited by pulsed waveforms are currently receiving experimental attention.

REFERENCES

1. A. Kovacs and R. M. Morey. Remote Detection of Water under Ice-Covered Lakes on the North Slope of Alaska. *Arctic*, Vol. 31, No. 4, 1978, pp. 448–458.
2. A. M. Dean. *Remote Sensing of Accumulated Frazil and Brash Ice in the St. Lawrence River.* CRREL Report 77-8. U.S. Army Cold Regions Research and Engineering Laboratory, Hanover, N.H., 1977.
3. G. Batson, H. T. Shen, and R. Ruggles. *Investigation of Ice Conditions in the St. Lawrence River, Winter 1981–82.* Final Report No. DTSL55-C-C0085, prepared for U.S. Dept. of Transportation, St. Lawrence Seaway Development Corp., Clarkson College of Technology, Potsdam, N.Y., September 1984.
4. G. Batson, H. T. Shen, and S. Hung. Multi-Year Experience of Remote Sensing of Ice Thickness on the St. Lawrence River. *Proceedings, Eastern Snow Conference*, Vol. 29, 41st Annual Meeting, Washington, D.C., June 7–8, 1984.
5. J. Rossiter, J. Snellen, K. Butt, and T. Ridings. *Multi-Year Ice Thickness Distribution in the Beaufort Sea Determined by Airborne Impulse Radar.* C-CORE Publication No. 80-11. C-CORE, Memorial University, St. John's, Newfoundland, Canada, 1980.
6. A.P. Annan and J. L. Davis. Impulse Radar Sounding in Permafrost. *Radio Science*, Vol. 11, No. 4, 1976, pp. 383–394.
7. S.A. Arcone and A.J. Delaney. Airborne River Ice Thickness Profiling with Helicopter-Borne Short Pulse Radar. *Journal of Glaciology*, Vol. 33, No. 115, 1987, pp. 330–340.
8. N. Engheta, C.H. Papas, and C. Elachi. Radiation Patterns of Interfacial Dipole Antennas. *Radio Science*, Vol. 17, No. 6, 1982, pp. 1557–1566.
9. S.A. Arcone, A.J. Delaney, and R. Perham. *Short Pulse Radar Investigations of Freshwater Ice Sheets and Brash Ice.* CCREL Report 86-6, U.S. Army Cold Regions Research and Engineering Laboratory, Hanover, N.H., 1986.
10. R.H. Wills. A Digital Phase Coded Ground Probing Radar. Ph.D. dissertation. Dartmouth College, Hanover, N.H., 1987.

Publication of this paper sponsored by Committee on Engineering Geology.